EXAMINING THE VASOACTIVE PROPERTIES OF NITRITE IN NORMOXIA AND HYPOXIA

By

Nicholas David Gollop
BSc (Hons), MB BCh, MRCP (UK), PGCert

A Thesis in Fulfilment of the Requirements for the Degree of
Doctor of Philosophy (PhD) in Medicine

Submitted to
Norwich Medical School, University of East Anglia
Date: 16th December 2020

Abstract word count: 299
Thesis word count: 58,501

"This copy of the thesis has been supplied on condition that anyone who consults it is understood to recognise that its copyright rests with the author and that use of any information derived there from must be in accordance with current UK Copyright Law. In addition, any quotation or extract must include full attribution."

STATEMENT 1

This work has not previously been accepted in substance for any degree and is not currently submitted in candidature for any degree.

Signed:  Date: 16th December 2020

STATEMENT 2

This thesis is being submitted in partial fulfilment of the requirements for the degree of PhD.

Signed:  Date: 16th December 2020

STATEMENT 3

This thesis is the result of my own independent work/investigation, except where otherwise stated. Other sources are acknowledged by explicit references.

Signed:  Date: 16th December 2020

ABSTRACT

Introduction: Inorganic nitrite is a nitric oxide-soluble guanylyl cyclase-cyclic guanosine monophosphate-protein kinase G (NO-sGC-cGMP-PKG)-dependent vasodilator, the effects of which are augmented in hypoxia. In normoxia (murine, *ex vivo*), the underlying vasoactive mechanisms may be NO-independent and mediated by multiple intermediates. In humans, this may also apply. It is unknown if the coronary arteries are subject to hypoxia-augmentation of nitrite-mediated vasodilation. Harnessing the vasoactive properties of nitrite could provide novel therapeutic approaches to managing multiple cardiovascular diseases.

Aims: To examine the effect of nitrite on the nitrite-PKG pathway in normoxia (murine, *ex vivo*), on NO-attenuated resistance arteries (humans, *in vivo*), and on epicardial coronary haemodynamics (humans, *in vivo*) in normoxia and hypoxia.

Methods and Results:

Chapter 3**:** Using tension wire-myography, NO scavenging and sGC inhibition in normoxia, we showed that nitrite caused NO-dependent conduit artery vasodilation and NO-independent resistance vasodilation. We identified that NO-independent processes included a novel NO-sGC-independent, PKG1α oxidation pathway, utilising hydrogen peroxide and cysteine/glutathione persulfides.

Chapter 4: In the Haem and Nitrite Study, we showed that intra-brachial nitrite led to dose-dependent increases in forearm blood flow ratio (FBFR). We showed that 30-35-day stored autologous whole blood transfusion led to non-significant increases in subject circulating cell-free haem and NO consumption, but did not change FBFR in normoxia or hypoxia.

Chapter 5: In the Nitrite and Coronary Artery Study, we showed that systemic nitrite administration led to an increase in epicardial coronary artery CSA and a reduction in velocity (hypoxia>normoxia) and flow, associated (probably causally) with a reduction in MAP in normoxia.

Conclusions: *In vitro* nitrite utilises hydrogen peroxide and persulfides to induce tissue-specific vasodilation via PKGIα oxidation in normoxia. *In vivo*, nitrite-mediated FBF is not modified by transfusion of ~500mls of 30-35-day old autologous blood in normoxia or hypoxia, and, nitrite significantly increases epicardial coronary CSA but decreases blood velocity and flow (hypoxia>normoxia).

Access Condition and Agreement

Each deposit in UEA Digital Repository is protected by copyright and other intellectual property rights, and duplication or sale of all or part of any of the Data Collections is not permitted, except that material may be duplicated by you for your research use or for educational purposes in electronic or print form. You must obtain permission from the copyright holder, usually the author, for any other use. Exceptions only apply where a deposit may be explicitly provided under a stated licence, such as a Creative Commons licence or Open Government licence.

Electronic or print copies may not be offered, whether for sale or otherwise to anyone, unless explicitly stated under a Creative Commons or Open Government license. Unauthorised reproduction, editing or reformatting for resale purposes is explicitly prohibited (except where approved by the copyright holder themselves) and UEA reserves the right to take immediate ‘take down’ action on behalf of the copyright and/or rights holder if this Access condition of the UEA Digital Repository is breached. Any material in this database has been supplied on the understanding that it is copyright material and that no quotation from the material may be published without proper acknowledgement.

ABBREVIATIONS

ACE – angiotensin converting enzyme

ACh – acetylcholine

ACS – acute coronary syndrome

AE – adverse event

AMI – acute myocardial infarction

ANOVA – analysis of variance

AO – anhydrase oxidase

ASPA – Animals Scientific Procedures Act

AT – angiotensin

ATP – adenosine triphosphate

AWERB – Animal Welfare and Ethical Review Body

BK – big potassium calcium channel

BP – blood pressure

C57BL/6 – (a common inbred strain of laboratory mouse)

CA – carbonic anhydrase

cAMP – cyclic adenosine monophosphate

CANN – the Cognitive Ageing Nutrition and Neurogenesis trial

cGMP – cyclic guanosine monophosphate

CI – chief investigator

CICR – calcium-induced-calcium-release

CK – creatine kinase

CMR – cardiac magnetic resonance

CO – cardiac output

CONSORT – Consolidated Standards of Reporting Trials

CPTIO – 2-4-carboxyphenyl-4,4,5,5-tetramethylimidazoline-1-oxyl-3-oxide

CRN – clinical research network

CRTU – clinical research and trials unit

CSA – cross-sectional area

CST – clinical support team

CTPIO – 2-4-carboxyphenyl-4,4,5,5-tetramethylimidazoline-1-oxyl-3-oxide

CVD – cardiovascular disease

CVR – coronary vascular resistance

CysSSH – cysteine persulfide

DASH – Dietary Approaches to Stop Hypertension

DBP – diastolic blood pressure

DMT – Danish Myotechnology

EC – effective concentration

ECG – electrocardiogram

ED_{50} – 50% effective dose

EDHF – endothelium-derived hyperpolarizing factor

EDRF – endothelium-derived relaxing factor

ELISA – enzyme-linked immunosorbent assay

eNOS – endothelial nitric oxide synthase

FBF – forearm blood flow

FBFR – forearm blood flow ratio

FDA – Food and Drug Administration

FSH – follicle stimulating hormone

FWHM – full width half maximum

G_6PD – glucose-6-phosphate dehydrogenase

GAPDH – glyceraldehyde 3-phosphate dehydrogenase

GCP – Good Clinical Practice

GSSH – glutathione persulfide

GSNO – S-nitrosoglutathione

GTN – glyceryl trinitrate

GTP – guanosine triphosphate

H2O2 – hydrogen peroxide

Hb – haemoglobin

HbNO – nitrosyl haemoglobin

HCAs – human coronary arterioles

HIF – hypoxia-induced factors

HNO2 – nitrous acid

HPLC – high performance liquid chromatography

HR – heart rate

HSNO – thionitrous acid

IB – intra-brachial

ICE – integrated clinical environment

IMP – investigational medicinal product

IV – intravenous

KCL – potassium chloride

kDa – kilodalton

KHB – Krebs-Henseleit Buffer

KI – knock-in

L-arg – L-arginine

L-NAME – N(gamma)-nitro-*L*-arginine methyl ester

LAD – left anterior descending

LV – left ventricle

LVSD – left ventricular systolic dysfunction

MACE – major adverse cardiac event

MAP – mean arterial pressure

MHRA – Medicines and Healthcare products Regulatory Agency

MLC – myosin light chain

MLCK – myosin light chain kinase

MRC – Medical Research Council

NADH – nicotinamide adenine dinucleotide + hydrogen

NADPH – nicotinamide adenine dinucleotide phosphate + hydrogen

NATO – Norwich Academic Training Office

NEM – N-ethylmaleimide

NHS – National Health Service

NHSBT – National Health Service Blood and Transplant

NNUH – Norfolk and Norwich University Hospital

NO – nitric oxide

NOS – nitric oxide synthase

N2O3 – dinitrogen trioxide

NSTEMI – non-ST elevation myocardial infarction

ODQ – 1H-[1,2,4] oxadiazolo-[4, 3-a]quinoxalin-1-one

PAR – population-attributable risk

PAS – Patient Administration System

PCI – percutaneous coronary intervention

PCR – Polymerase Chain Reaction

PDE – phosphodiesterase

PI – principal investigator

PIS – participant information sheet

PKA – protein kinase A

PKG – protein kinase G

PPM – parts per million

PVR – pressure/volume relationship

PWV – pulse wave velocity

RA – right atria

RAA – renin angiotensin aldosterone

RBC – red blood cell

RBHT – Royal Brompton and Harefield Trust

RCA – right coronary artery

REC – research ethics committee

RGS2 – regulator of g-protein signalling 2

ROI – region of interest

ROS – reactive oxygen species

RSNO – S-nitrosothiols

RXNO – nitroso species

SABRE – Serious Adverse Blood Reactions and Events

SBP – systolic blood pressure

SD – standard deviation

SEM – standard error mean

sGC – soluble guanylyl cyclase

SHOT – Serious Hazards of Transfusion

SNAP – Nitroso-N-acetylpenicillamine

SNO-Hb – S-nitrosohaemoglobin

SR – sarcoplasmic reticulum

STEMI – ST-elevation myocardial infarction

SVR – systemic vascular resistance

U46619 – (a synthetic analogue of the endoperoxide prostaglandin PGH_2)

UEA – University of East Anglia

UK – United Kingdom

USA – United States of America

VASP – vasodilator stimulated phosphoprotein

VDCC – voltage-gated calcium channels

VIP – vasoactive intestinal peptide

VSMC – vascular smooth muscle cell

WHO – World Health Organisation

WIA – wave intensity analysis

WT – wild type

XM – cross-match

XOR – xanthine oxidoreductase

CONTENTS

LIST OF FIGURES, TABLES & APPENDICES

FIGURES

TABLES

APPENDICES

1. Norwich Academic Training Office (NATO) - Excellence in Training Awards 2017
2. Paper: Feelisch et al, 2019. Long-lasting blood pressure lowering effects of nitrite are NO-independent and mediated by hydrogen peroxide (H_2O_2), persulfides and oxidation of protein kinase G 1alpha redox signalling, *Cardiovasc Res*. cvz202.
3. Blood donation documents
    i. Donor health check for new and returning donors form (FRM form 421/6)
    ii. Autologous blood pre-donation assessment form (FRM 1560/4)
    iii. Pre-deposit autologous blood donation memorandum (FRM 1563/1.4 – cross referenced in primary document SOP 3968)
    iv. SOP3968 (Change Control [6422] Process Flow)
4. Blood transfusion documents
    i. The Haem and Nitrite Study – Study specific prescription/drug chart
    ii. Autologous whole blood: pre-transfusion safety checklist
5. NOx sample processing methodology
6. RXNO sample processing methodology
7. The Nitrite and Coronary Artery Study – MRI safety checklist
8. Root cause analysis for blood transfusion incident and corrective actions
9. The Nitrite and Coronary Artery Study – Study specific prescription/drug chart
10. Letter from Supervisor regarding RXNO samples in The Haem and Nitrite Study

ACKNOWLEDGEMENTS

This PhD thesis would not have been possible without the support and guidance of my primary supervisor, Professor Michael Frenneaux. His desire for knowledge enabled me to push scientific boundaries and seek answers to questions that, at the start of this PhD journey, seemed unobtainable. I would also like to thank my secondary supervisor, Dr Vassilios Vassiliou. Vass joined our research team in the second year of the PhD and he immediately added enthusiasm, creativity and momentum. He provided daily support in the set-up and also the delivery of both of the clinical studies. Both supervisors supported me through this PhD journey and I am greatly indebted to them both.

Next, I would like to thank members of our research group including Dr Brodie Loudon, Dr Sathish Parasuraman, Mrs Crystal Lowry, Dr Donnie Cameron, Dr Nathan Proctor, Dr Cristian Militaru and Dr Dave Willis for their insight, experience and support. Requiring special mention is Brodie, who studied his PhD alongside me. Brodie was always incredibly perceptive. He was a great companion to share this experience with. I wish him success in his PhD submission.

During this PhD, I have faced a series of personal and professional challenges and these experiences have pushed me to my limits. Also, sadly, my uncle and my grandmother passed away. During these difficult times, my parents, Dave and Tina provided me with unconditional support, understanding and love. They helped me to regain control and complete this journey. I couldn't have done it without them. I would also like to thank Celina Dietrich, who by a chance encounter at the Bob Champion Research and Education Building at UEA joined me on this journey and has since provided me a constant source of support. When I would drive to Papworth at 5am in the morning for the CABG2 study (not included in this thesis) or when I would catch a 5:30am train to London for the Nitrite and Coronary Artery Study, she would always make sure I had everything I needed, and even drive me to

the station. She is the only person who really knows how hard I have worked on this and she has supported me every step of the way. I can't wait until she also passes her PhD, so we can celebrate together.

I would like to professionally acknowledge the following people/groups for their contribution to the projects presented in this thesis: Chapter 3 - Dr Melanie Madhani, Dr Alessandra Borgognone, Dr Kayleigh Griffiths, Dr Rosie Hayes, Dr Hannah Noordali, Miss Joanna Goodwin, Prof Martin Feelisch (and his team) and Prof Takaaki Akaike (and his team). Chapter 4 – Prof Phil Chowienczyk, Prof Anne-Marie Minihane, Dr Gail Miflin and Dr Suhail Asghar (and the NHSBT operational team), Mrs Patsy Lowson (and the NHSBT donation team), Mrs Debbie Asher (and the NNUH blood bank team), Mr James Goillau (and the BCRE team), Dr Simon Rushbrook (Hepatology Consultant), Dr Simon Fletcher (Critical Care Consultant), Mrs Vanessa Martin (and the CRTU team), Miss Rachel Stebbings (Research Nurse) and Mr Clive Beech (Research Pharmacist). Chapter 5 - Dr Jennifer Rivers, Mr Shafa Ullah, Prof Sanjay Prasad, Prof Jennifer Keegan, Mr Ricardo Wage and Mr Kevin Kirby. Whilst this list is by no means exhaustive, the input of those listed above was critical to the success of the projects presented in this thesis.

Finally, I would like to thank the 523 people who responded to the advertisements for the 2 clinical studies and to the 74 people who gave up a significant amount of their time and energy to participate in my clinical research. Together, we questioned the evidence and we have contributed to science. Thank you.

PERSONAL CONTRIBUTION

I performed all of the basic science and clinical studies presented in this thesis apart from the following:

Chapter 3 – Basic Sciences

i. Protein Kinase G (PKG) 1α "redox dead" mice were a kind gift from Prof Philip Eaton (King's College London)
ii. Maintenance and genotyping of the PKG1α colony was performed by Dr Alessandra Borgognone, Dr Rosie Hayes and Miss Joanna Goodwin (University of Birmingham)
iii. Blood vessel isolation and mounting of blood vessels for vascular myography was conducted by Dr Melanie Madhani (University of Birmingham)
iv. Miss Joanna Goodwin contributed to the resistance vascular myography experiments
v. *In vivo* nitrite treatment for the PKG1α dimerization western blotting experiments were conducted by Dr Alessandra Borgognone and Dr Rosie Hayes (University of Birmingham).

Chapter 4 – The Haem and Nitrite Study

i. Senior on-call support in the Norfolk and Norwich University Hospital (NNUH) was provided by Dr Simon Fletcher (Critical Care Consultant) and Dr Vassilios Vassiliou (Cardiology Consultant)
ii. Senior blood donation process support was provided by Dr Suhail Asghar (Associate Specialist, National Health Service Blood and Transplant [NHSBT])
iii. Blood donation process support was provided by Sister Patsy Lowson (Sister at the Thetford donation team)
iv. Statistical analysis support was provided by Dr Allan Clark (Study statistician, University of East Anglia [UEA])

Chapter 5 – The Nitrite and Coronary Artery Study

i. Senior on-call support was provided by Prof Sanjay Prasad (Cardiology Consultant)

ii. Cardiac magnetic resonance (CMR) image acquisition and analysis was delivered by Prof Jennifer Keegan (Principal Physicist, Royal Brompton and Harefield Trust [RBHT]) and Mr Ricardo Wage

FUNDING

The work presented in this thesis was funded by a Medical Research Council (MRC) programme grant awarded to Professor Michael Frenneaux (PI). I was employed on this grant. This work was also supported by funding from The Norfolk Heart Trust awarded to Professor Michael Frenneaux (investigator) and myself (co-investigator) to fund the salary of a specialist nurse to assist in delivery of The Haem and Nitrite Study.

PRIZE/PRESENTATIONS/PUBLICATIONS

Prize

1. 1st Prize – 'Best Research Proposal/Protocol in PhD/MD category'. Norwich Academic Training Office (NATO) - Excellence in Training Awards 2017. (Appendix 1).

Presentations

1. Gollop, N. D. The effects of cell-free haemoglobin nitric oxide (NO)-blockade on nitrite forearm vessel dilatation under normoxia and hypoxia in healthy volunteers. By invitation to the NHSBT at Colindale, London, April 2016.
2. Gollop, N. D. NO-Independent vasodilatation. Invited research update. Clinical Research Network (CRN) Eastern Cardiovascular Specialty Meeting, Madingley Hall, Cambridge, April 2018.

Publications

1. Loudon, B. L., Noordali, H., Gollop, N. D., Frenneaux, M. P. & Madhani, M. (2016). Present and Future Pharmacotherapeutic Agents in Heart Failure: An Evolving Paradigm. Br J Pharmacol; 173(12): 1911-24.

2. Feelisch, M., Akaike, T., Griffiths, K., Ida, T., Prysyahna, O., Goodwin, J. J., Gollop, N. D., Fernandez, B. O., Minnion, M., Cortese-Krott, M. M., Borgognone, A., Hayes, R. M., Eaton, P., Frenneaux, M. P. & Madhani. M. 2019. 'Long-lasting blood pressure lowering effects of nitrite are NO-independent and mediated by hydrogen peroxide, persulfides and oxidation of protein kinase G 1alpha redox signalling', *Cardiovasc Res*. (Appendix 2).

CHAPTER 1: BACKGROUND

1: Public health problem

Global perspective

The World Health Organisation (WHO) classifies cardiovascular disease (CVD) as coronary artery disease, cerebrovascular disease, peripheral arterial disease, rheumatic heart disease, congenital heart disease, deep vein thrombosis, pulmonary embolism, and others (including heart muscle diseases, heart valve diseases, and disorders of the lining of the heart) (1). CVD is the leading cause of death worldwide (2). Each year, 17.5 million people die from CVD (31% of all deaths worldwide) of which an estimated 7.4 million are due to coronary heart disease and 6.7 million are due to cerebrovascular disease/stroke, figure 1. CVD can also lead to ischaemic cardiomyopathy and subsequent heart failure (3). Over 75% of CVD deaths occur in low- and middle-income countries (4).

The Framingham Study and the INTERHEART Study (5-7) demonstrated that 90-95% of population-attributable risk (PAR) of overt CVD can be determined by nine modifiable risk factors. These include smoking, apolipoprotein B/apolipoprotein A1 ratio, history of hypertension, diabetes, abdominal obesity, psychosocial factors, daily consumption of fruit and vegetables, regular alcohol intake and regular physical activity (8-10). Importantly, psychosocial index accounted for 40% of PAR and alcohol consumption had a large beneficial effect in women but a rather borderline effect in men. People who are at high-risk of developing CVD (due to the presence of risk factors) require early detection and aggressive management using lifestyle counselling and medicines, as appropriate, to minimise their risk of developing CVD (2, 10, 11).

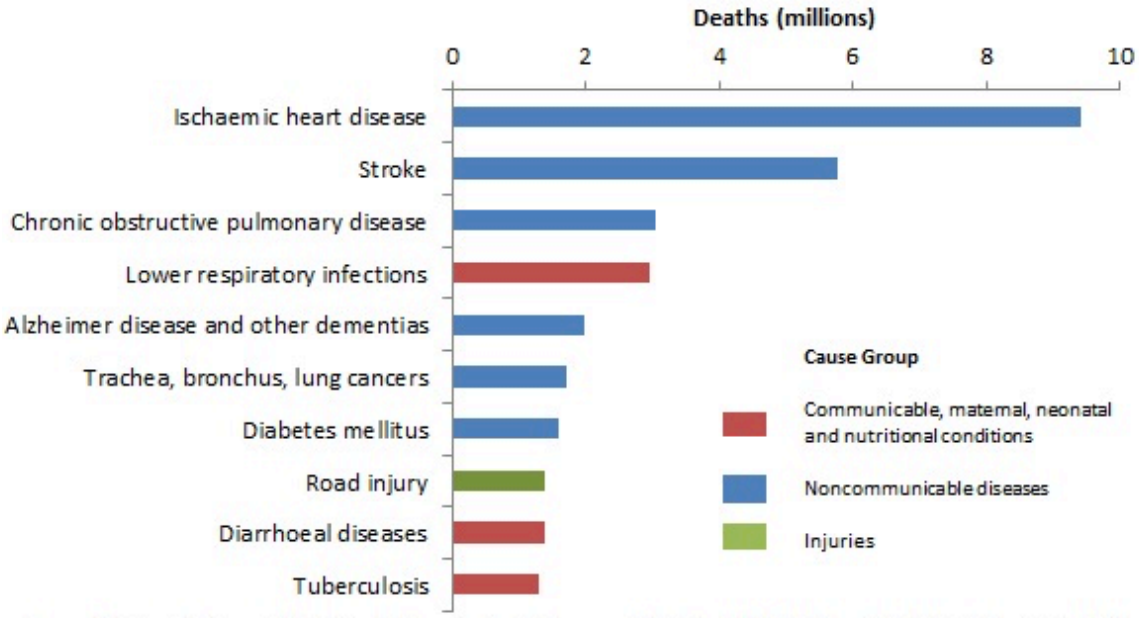

Figure 1: The 10 leading causes of death in the world in 2016. Source: Global Health Estimates 2016. Geneva, (1).

UK perspective

Global rates of CVD are increasing due to an explosion in emerging economies (12). In contrast, in the Western world (including the United Kingdom [UK]), rates of CVD have reduced substantially. Over the last century (between 1915 and 2015) in the UK we have seen major advances in sanitation, nutrition, hygiene, medical science and technology. In 1915, people were predominantly dying of infections (13, 14) such as poliomyelitis, diphtheria, tetanus, and whooping cough (15). In 2015, as is common in most developed global nations, the most common natural causes of death are cancer, heart conditions and dementia, figure 2 (15-17).

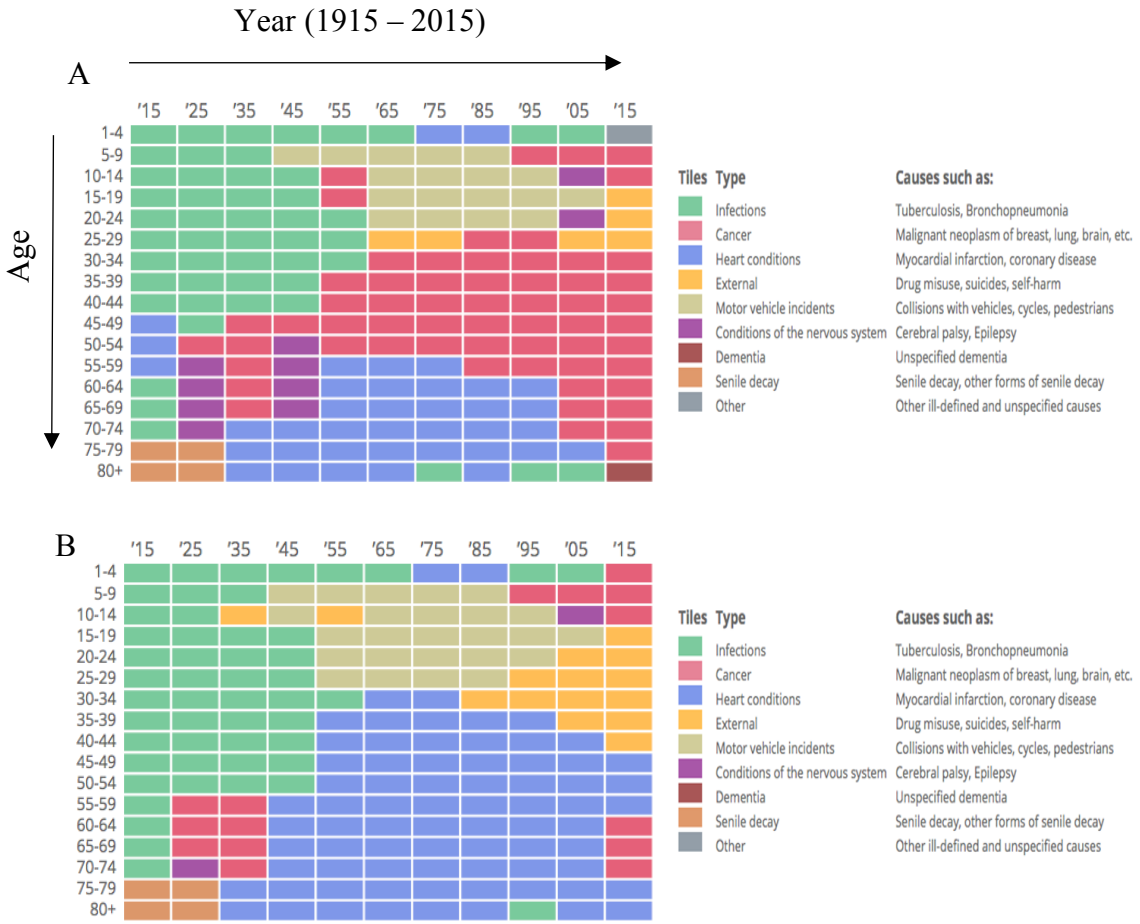

Figure 2: Top causes of death by age and sex, 1915 to 2015 in the UK. Panel A – Women. Panel B – Men. Adapted from 'Deaths registered in England and Wales' (15).

In the UK, CVD death accounts for 26% (160,000) of all deaths each year (18, 19). Of which, ~66,000 are due to coronary artery disease and ~36,000 are due to cerebrovascular disease/stroke (20). There are an estimated 7 million people living with CVD in the UK (3.5 million men and 3.5 million women) (18, 21). In common with the global perspective, the highest rates of CVD mortality are found in areas of socio-economic deprivation (4); in 2012-2014 the cities of Glasgow and Manchester suffered the highest rates in the UK (21). CVD costs the UK economy (including premature death and disability) an estimated £15 billion each year (22).

Despite record levels of obesity, physical inactivity and diabetes, there has been a massive decline in cardiac deaths in developed countries (23, 24). The reasons behind this are not clear. The impact of cardiological procedures such as percutaneous coronary intervention (PCI) on overall cardiac mortality is very small (25) and statins have only had a small-to-moderate impact at a population level (26). Some commentators believe that CVD is a disease of 'industrialization' (27) and this explains the population health trends seen in many nations including the UK, United States of America (USA), Germany, France, Japan, Australia, and Canada.

2: Cardiovascular physiology

Structure and function

Blood vessels can be placed into five distinct functional groups:

1. Large arteries: responsible for the pulsatile component of afterload which is determined by the 'windkessel effect' and by the impact of wave reflection (28, 29)
2. Resistance vessels: small arteries and arterioles, responsible for 'static afterload' (30, 31)
3. Exchange vessels: capillaries and some venules, responsible for gas exchange (32)
4. Capacitance vessels: small veins and venules, which hold 64% of the circulating volume (33)
5. Conduit veins: responsible for the passage of the circulating volume through unidirectional valves, assisted by contraction of surrounding skeletal muscle ('muscle pump') (34, 35).

Arteries and veins have three distinct layers; the tunica intima, tunica media and the tunica externa/adventitia (36), figure 3. The tunica intima is a single layer of squamous endothelial cells held together by a polysaccharide intercellular matrix and surrounded by a thin layer of sub-endothelial connective tissue (37). Useful clinical measurements include aortic and

carotid intima-media thickness (measured by ultrasound) which can be an early life marker of subclinical atherosclerosis (38, 39).

The middle layer is the tunica media and is composed of elastic fibres arranged in a circular pattern, connective tissue and polysaccharide substances (40). The tunica media is rich in vascular smooth muscle cells (VSMCs), which control the calibre of the vessel and the capability of the vessel to contract and relax (41, 42). This is greatest in arteries, least in conduit veins and in moderate supply in the small veins and venules.

Arteries, small veins and venules also have a nerve supply to allow for neural mediation of vasotone, these are termed '*nervi vasorum*' (43). These are mostly sympathetic fibres, capable of causing both vasodilation and vasoconstriction, subject to the nature of the neurotransmitter and receptors located on the target cell (44, 45). The tunica externa/adventitia is the most external of the three layers. It is composed completely of connective tissue (46) and may be a source of mesenchymal stem cells (47).

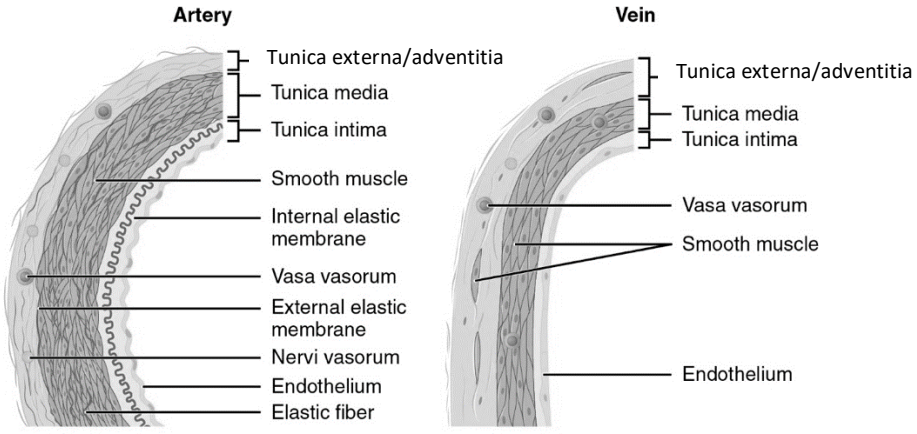

Figure 3: Anatomical overview of arteries and veins. Adapted from: OpenStax College, Anatomy and Physiology (48).

Haemodynamics

The circulatory system is subject to numerous regional and systemic factors that influence the regulation of blood flow (49-52). For example, in the large arteries, pulsatile afterload is determined by:

1. Large artery elastance through the 'windkessel effect' (28, 29)
2. The timing and magnitude of waves returning to the central aorta following reflection at the arterial branch points.

In healthy young people, reflected waves reach the central aorta in diastole, augmenting coronary reperfusion whilst minimising cardiac afterload. Premature arrival of the reflected waves in the central aorta during late-systole augments late-systolic pressure (increasing cardiac afterload and hence myocardial oxygen demand) and simultaneously reduces coronary perfusion pressures. Premature wave reflection can occur due to increased pulse wave velocity (PWV), associated with increased large artery stiffness, higher heart rate, and with shorter path length related to shorter stature. Evidence suggests that being less tall results in early arrival of systolic reflected waves, which leads to increased central aortic late systolic pressure, increased pulsatile load on the left ventricle, and therefore increased work. This may, at least in part, explain the greater prevalence of heart failure with preserved ejection fraction in women, due to their generally shorter height (53).

The small arteries and arterioles (resistance vessels) are the site of 70% of the pressure drop across the vascular tree (30, 31). Systemic vascular resistance (SVR) is subject to three variables; blood viscosity, vessel length and vessel radius, and these are mediated by several mathematical constants. Flow can be explained using the Hagen–Poiseuille equation, figure 4 (54), which takes into account the change in pressure between 2 points (P_1 and P_2) divided by the above calculated resistance. If we assume velocity (distance divided by time) is kept constant, a change in vessel length, cross-sectional surface area (CSA), fluid viscosity or

pressure can lead to a change in flow (55). For example, if velocity is kept constant and a vessel has a blood flow of 100m/s (A), doubling the mean arterial pressure (MAP) will double the flow (D) and doubling the vessel radius will lead to a x16 increase in flow (E), figure 4. It is also important to recall that velocity (V) is flow divided by cross-sectional surface area (CSA), therefore, if flow is kept constant, an increase in CSA would lead to a reduction in velocity.

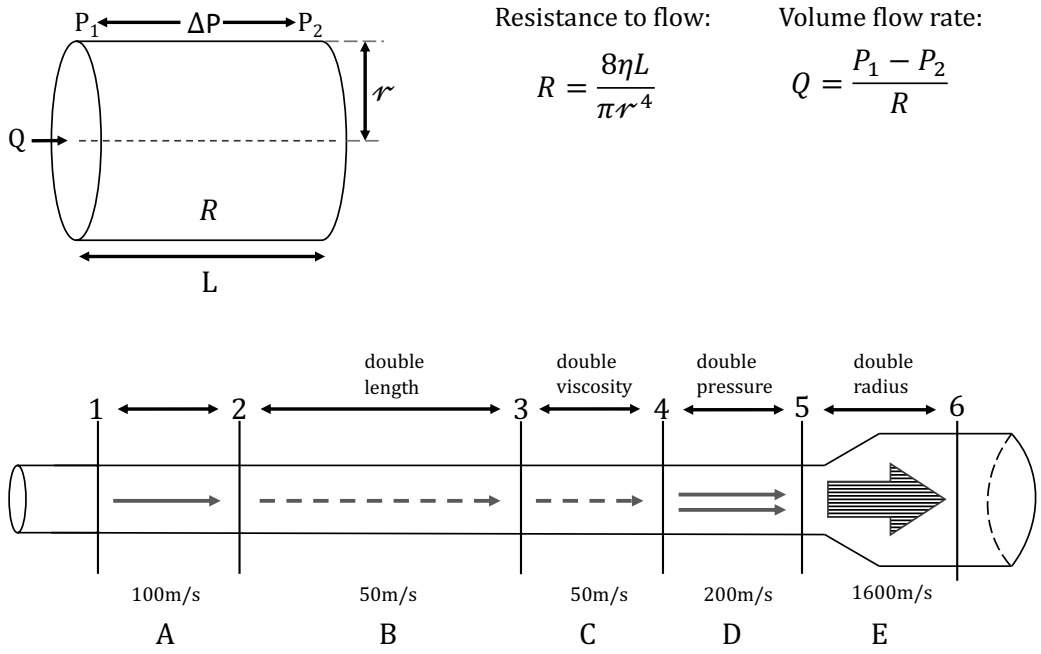

Figure 4: Haemodynamics – the Hagen–Poiseuille equation. Key – Q: flow rate, ΔP: change in pressure, r: radius, η: fluid viscosity, L: length of tube. (54).

The term 'compliance' describes the change in dimension following a change in stress. In venous physiology, compliance is the ratio of the change in volume (ΔV) resulting from a change in transmural distending pressure (ΔP), or ΔV/ΔP. It is the slope of the pressure/volume relationship (PVR). Because venous compliance is very high at low pressures, the slope of the PVR over the physiological pressure range (10-40mmHg) is nearly linear (56).

The term ‘elastance’ describes the vessels ability to recoil and return to its previous dimensions after being stretched. The degree of elastance is due to the amount of elastin fibres present in the tunica media. Elastance is inversely proportional to compliance, so can be expressed as change in pressure (ΔP) divided by the change in volume (ΔV), or ΔP/ΔV. (57). Arteries are more elastic and as described above, this can contribute to the aortic ‘windkessel effect’.

Capillaries are exchange vessels and consist of a single layer of endothelium and occasional connective tissue (58). Capillaries are surrounded by pericytes that may have contractile properties that allow them to regulate blood flow (59, 60). It is also thought that different signalling pathways regulate the constriction of capillaries by pericytes and of arterioles by VSMCs (61). In addition, capillary opening is further influenced by erythrocyte deformability (which is NO-modulated) and the surface charge on the endothelium and erythrocyte (62).

Distensibility of the venous system (capacitance vessels) is physiologically important as it means that significant proportions of the circulating volume can be stored within blood vessels; 84% systemic circulation of which 64% is capacitance vessels (63, 64). The ‘stiffness’ of the capacitance vessels affects the slope of the volume-pressure relation (venous compliance). In contrast, changes in venous tone cause parallel shifts in the venous volume-pressure relation resulting in changes in the ‘venous [unstressed] volume’ (i.e. the venous volume at zero transmural pressure).

Modulation of compliance is also very important with respect to stroke volume. In healthy subjects, during exercise, venoconstriction of the splenic and splanchnic vascular beds translocates blood from the peripheral to the central compartment, increasing LV end

diastolic volume, and hence, via the Frank-Starling mechanism, contributes to the increased force of contraction and increased CO (65-67).

Blood moves through the venous system (conduit veins) via several key mechanisms. In most part, relying on unidirectional valves and contraction of surrounding skeletal muscles (34, 35). Additional less significant factors also contribute, such as negative pressure 'suction' (such as in the thoracic cavity on inspiration) (68), smooth muscle contraction in the tunica media (41, 42) and compliance (57).

3: Cardiovascular pathophysiology

Cardiovascular disease

Atherosclerotic CVD is a condition in which excess fats, calcium deposits, abnormal inflammatory cells and other substances accumulate in the arteries and initially form 'fatty streaks' and later 'intermediate lesions' (69). Fatty streaks and intermediate lesions are usually asymptomatic and occur in the second and third decade of life (70). Over time, these lesions can increase in size and can progressively obstruct the arteries, including the coronary arteries; thereby reducing the oxygen-bound blood supply to the active contracting myocardium during periods of increased exertion (71). The reduced oxygen supply can cause the myocardium to become ischaemic during exertion, resulting in symptoms (usually chest tightness) termed 'stable angina' (72).

Typically, from the fourth decade onwards, plaques that have a thin fibrous cap or a substantial inflammatory infiltrate in the lipid rich core are prone to erode or rupture (73). The inflammatory cells release metalloproteinase enzymes that break down the fibrous cap allowing the highly thrombogenic lipid core to be exposed to the blood stream and resulting in thrombosis, which in the coronary arteries leads to acute coronary syndrome (ACS) (74,

75). In contrast, plaques with a thick fibrous cap and a lesser inflammatory infiltrate are less prone to rupture but may progress to cause flow-limiting stenosis (76). Further consequences of atherosclerotic disease can include vascular remodelling (77) leading to aneurysms (78) and deposition of calcium leading to valvular dysfunction (79).

Preventing and managing CVD

At the forefront of the clinical management of CVD is effective primary prevention (80, 81). Major CVD risk factors are well-defined and understood, as are the evidence-based and widely recommended preventative measures that can be taken in order to reduce morbidity and mortality (80-83). Despite this, the long-term uptake of effective measures including a healthy diet, regular exercise, smoking cessation, statins and anti-hypertensive therapies, remains inadequate across populations with CVD morbidity and mortality remains unacceptably high (84).

Early detection of CVD risk factors together with effective implementation of pragmatic primary preventative measures can significantly reduce the burden of CVD in society. The UK National Institute for Healthcare and Clinical Excellence (85) guidelines for lipid modification recommend reducing the 10-year CVD risk threshold from ≥20% down to ≥10% for implementation of statin therapy, which will result in a significant increase in the numbers of individuals eligible for these drugs. Importantly, age remains the strongest predictor of intermediate to long-term CVD risk and often younger individuals with adverse CVD risk profiles have relatively low 10-year CVD risk scores (86). Reducing the threshold for implementation of cost-effective therapies should lead to a greater proportion of younger at-risk subjects receiving effective preventive therapies (87).

Acute myocardial infarction, if extensive, can result in severe left ventricular systolic dysfunction (LVSD) associated with pulmonary oedema and can lead to cardiogenic shock

and death (88, 89). Lesser degrees of acute damage may also progress (over weeks to years) to severe LVSD and heart failure, a process known as 'remodelling' (90). This progression is mediated in part through activation of the circulating and local (tissue) renin angiotensin aldosterone (RAA) systems and the sympathetic nervous system (91, 92). A wealth of clinical trials have demonstrated the efficacy of agents that block the RAA system (angiotensin-converting enzyme [ACE] inhibitors, angiotensin [AT] receptor blocker [+/- neprilysin inhibitor], eplerenone and spironolactone) (92) and the adrenergic nervous system in both treating established heart failure and in preventing the remodelling process (93-95).

Myocardial ischaemia (as for example, in effort-induced ischaemia) may result in transient LV systolic and diastolic dysfunction (a phenomenon known as 'stunning') (96). Recurrent episodes of stunning may eventually result in sustained regional LV systolic dysfunction (LVSD) in the affected territory, such that it appears on echocardiography as if it were infarcted (a phenomenon known as 'hibernation') (97). It is important to recognise hibernation in patients with heart failure and LVSD since correction of flow limiting stenosis can result in complete recovery of LV function (98). Viability is most accurately assessed using CMR (or positron emission tomography [PET] if available) but can also be assessed by dobutamine stress echocardiography and nuclear scintigraphy (99).

4: Principles of vasoactivity

At a cellular level, VSMCs are arranged in a fusiform shape (40). Each myocyte contains many molecules of myosin (predominantly myosin class II in smooth muscle, 'heavy chains') (100) and actin (predominantly α-actin in smooth muscle, 'light chains') (101), which together interact resulting in excitation-contraction coupling (102). Key proteins involved in VSMC contraction include calmodulin (which regulates smooth muscle contraction), caldesmon (which enhances contraction and tension maintenance) and

calponin (which maintains continual load bearing) (103). Key tensile structures involved include vimentin, desmin, dense bodies and adherens junctions (102).

VSMC contraction and relaxation

VSMCs contract when the following sequence ensues. An initial stimulus (mechanical, electrical, chemical or VSMC passive stretch) (104) creates a rise in intracellular calcium. Calcium can be released from internal stores (via production of inositol triphosphate and release from the sarcoplasmic reticulum [SR]) (105) or by increased influx. Elevated calcium binds calmodulin (forming the calcium-calmodulin complex) (106) which activates myosin light chain kinase (MLCK), which in turn phosphorylates myosin light chains (MLCs) in the presence of adenosine triphosphate (ATP), resulting in cross-bridge formation and subsequent VSMC contraction (107). This process repeats creating a continual unidirectional movement termed 'cross-bridge cycling', resulting in increased tension along the length of the tensile structures, resulting in smooth muscle contraction (108).

VSMCs relax when the MLC is no longer phosphorylated (102). This can result from:

1. Reduced calcium induced calcium release (CICR) from SR or reduced influx (109)
2. Inhibition of MLCK by increased intracellular cyclic adenosine monophosphate (cAMP) (110)
3. Phosphatase-activated MLC dephosphorylation (111)

Coronary vasoactivity

The vasomotor response of the coronary arteries is thought to be very similar to that of the peripheral vasculature. In 1995, Anderson and colleagues assessed patients with known coronary artery endothelial dysfunction and healthy controls. The group showed that those with coronary artery disease manifested as vasoconstriction in response to acetylcholine

(ACh) and had significantly impaired flow-mediated vasodilation in the brachial artery compared with that of patients with normal coronary endothelial function (112).

5: Vasoactive substances

Vasoconstrictors

Vascular tone determines SVR and therefore regulates MAP/blood pressure (BP) (113). Mathematically, SVR is the dependent variable; however, physiologically, SVR and CO are normally the independent variables and MAP is the dependent variable (114). Thus, if the heart is required to pump against increased resistance, blood pressure increases and CO remains normal (assuming the heart is not failing) (115).

Muscarinic agonists (including ACh) can mediate vasodilation in the presence of an intact endothelium via NO-release (116). Interestingly, if the endothelium is no longer intact, ACh can lead to vasoconstriction by binding to and increasing the activity of the muscarinic receptor M2. This results in reduced cAMP and reduced protein kinase A (PKA) activity leading to MLC phosphorylation and subsequent vasoconstriction (117).

Additional important endogenous vasoconstrictors have been described, including thromboxane, neuropeptide Y, angiotensin II, anti-diuretic hormone (vasopressin), asymmetric dimethylarginine, thrombin, and insulin, to name a few. The mechanisms of these vary, but they all act to either decrease endothelin, decrease NO, or increase intracellular calcium (116). Physiologically, adaptive mechanisms also exist to regulate vasotone. Increased cutaneous vessel tone is a hypothermic preventative mechanism; blood is removed from cold extremities, minimising avoidable heat loss and maintaining adequate temperatures centrally (118).

Vasodilators

The study of vasodilating agents has evolved over the last 50 years (119) with several key papers defining our current knowledge. In 1976, Moncada and colleagues published their discovery of a vasodilatory prostaglandin synthesised and released by the vessel. In the following year, the same group showed that the endothelium in the most abundant source of prostacyclin (120). In the following decade, a series of papers demonstrated that NO and nitrocompounds activated guanylate cyclase (121), and that endothelium-dependent hyperpolarisation resulted in smooth muscle relaxation (122), and that the predominant endothelium-derived relation factor (EDRF) was NO (123). The synthesis of NO was further characterised when L-arginine was identified as the precursor in the so-called 'endogenous L-arginine/NO-synthase pathway' (124). Interestingly, towards the end of the 1980's, the focus began to shift away from defining single vasodilatory pathways to trying to understand these various factors collectively. Whilst NO and prostaglandin had been well-characterised vasodilators at the level of the arteries (110) increasing evidence for other endothelium-derived vasodilating factors, known as the 'endothelium-derived hyperpolarizing factor' (EDHF) began to accumulate (125, 126).

Current evidence suggests that the term EDHF should represent a mechanism rather than a specific factor. EDHF-mediated vasorelaxation seems to be heterogenous depending on various factors (such as vessel size, vascular bed, oxidative stress, hypoxic demand, etc) (127). It has been postulated that EDHF-mediated vasorelaxation may utilise a range of different endothelial mediators/processes (including arachidonic acid derivatives, hydrogen peroxide [H2O2], potassium ions flux, C-type natriuretic peptide, gap-junction-mediated processes, etc) (127) (119) working simultaneously (or being able to substitute) providing a back-up when NO-mediated vasodilation is compromised (119, 126). Recent work has shown that EDHF may also have a tissue-specific distribution, with endothelium-dependent vasodilation in human conduit arteries being mediated mainly by NO, whereas vasodilation

in resistance arteries is mediated by a combination of NO, prostaglandins and EDHF together (42).

Whilst the role of EDHF in small resistance arteries is now more clearly defined, we still have not fully characterised which hyperpolarizing factors represent the EDHF. Previously viewed as a cytotoxic ROS, H_2O_2 is now thought to play a central role in cell signalling and nitrite reduction (128). It was suggested that H_2O_2 had a role in regulating vasomotion through modulation of the adventitial layer (129), and that H_2O_2 generation from the mitochondrial electron transport chain in the perivascular adipose tissue contributes directly to the modulation of aortic muscle contraction (130). Most recently, we identified that nitrite administration caused H_2O_2 generation and consecutive production of persulfide species (CysSSH and GSSH) in mesenteric resistance vessels, leading to oxidative activation of PKG1α (131).

Next to NO, prostacyclins and H_2O_2, several other important vasodilators exist and function with varying potency, depending on local oxygen concentrations. For example, adenosine, which is known to bind to A1, A2a and A2b receptors on VSMCs (132), leading to increased ATP-sensitive potassium channel activity, VSMC hyperpolarization and reduced intracellular calcium (117), may be augmented in hypoxia (133). Evidence also suggests that in hypoxia, adenosine exerts an array of pleiotropic effects including proliferation and migration of endothelial cells (134), reduction of vascular leak (135) and downregulating immune responses (136). Other additional endogenous vasodilators have been described with varying potency in hypoxia vs normoxia, including histamine (137) vasoactive intestinal peptide (VIP) (138), L-arginine (139), bradykinin (140) substance P (141), natriuretic peptides and heparin (142). In the most part, these vasodilators are potentiated in hypoxia, providing a 'protective' ischaemic response mechanism. Whilst exact mechanisms

vary, they all act to either increase endothelin, increase NO, or decrease intracellular calcium (116).

Pathophysiological conditions can also result in vasodilation, such as hypoxia, hypercapnia, acidosis and hyperkalaemia. These conditions all lead to a decrease in intracellular calcium, resulting in VSMC relaxation and subsequent vasodilatation (111). Interestingly, systemic epinephrine (adrenaline) acts via both α- and β-adrenoreceptors, causing vasoconstriction and vasodilation, respectively. Its effect is dose-dependent; at low concentrations the dominant effect is via β-adrenoreceptors and at high concentrations the dominant effect is via α-adrenoreceptors (143, 144). The response is the opposite in the coronary arteries, where β2 response is greater than that of α1, resulting in overall dilation with increased sympathetic stimulation (145).

6: Nitrate and nitrite metabolism

Inorganic nitrite (and nitrate) are abundant in the circulation and tissues, with nitrite being capable of acting as a storage pool for bioavailable NO. In resting, non-fasted humans, various values have been reported for plasma nitrate and nitrite, with values falling within the ranges of 20 – 50 μmol and 0.1 - 0.5 μmol respectively (146, 147) (148-150). Nitrite concentrations also differ from cell, to vessel, to organ. In Wistar rats, for example, the RBC compartment had more than two-fold higher nitrite than plasma (680 ± 60 nmol vs 290 ± 50 nmol) (151). A similar magnitude of difference was also observed in humans (288 nmol vs 121 nmol) (150) with a notable artery-to-vein nitrite gradient (arterial 176 ± 10 nmol vs venous 143 ± 7nm) (150). In Wistar rats, nitrite content of the lung, kidney, heart and liver was 0.5 – 0.8 μmol whereas the brain (1.7 ± 0.3 μmol) and specifically aorta (22 ± 9 μmol) had much higher levels (151). In humans, a wide range of factors can significantly affect nitrite levels, such as dietary habits, infection, living at altitude and pregnancy (152) (153, 154).

Essentially, there are two major sources of inorganic nitrate: i) the endogenous L-arginine/NO-synthase pathway and, ii) the diet (such as in fresh leafy vegetables and beetroot – as commonly found in the Mediterranean diet) (155). Endogenous nitric oxide synthases (NOS) release NO molecules from L-arginine with the consumption of 1.5 NADPH equivalents and two oxygen molecules per NO formed. This is an aerobic process and requires calcium–calmodulin and tetrahydrobiopterin (BH_4) as cofactors (156). Whilst eNOS is able to function down to oxygen levels of ~10 μmol (157) below this level, a series of anoxic 'alternate mechanisms' are activated to enable NO production at the oxygenase domain (158).

Once NO is produced, it binds to haemoglobin with very high affinity (159) and is quickly oxidized to nitrite and nitrate (160). Non-enzymatic auto-oxidation of NO to nitrite is very slow, but greatly increases if catalysed by caeruloplasmin. The vascular endothelium is both a target as well as a production source of NO due to its membrane bound endothelial nitric oxide synthase (eNOS) (161). Endothelial sheer stress caused by increased blood flow during exercise can also increase eNOS expression and its activity, resulting in increased NO levels (162). Inducible NOS (iNOS), usually present in very low levels is strongly upregulated by systemic inflammation (163). In contrast, patients with endothelial dysfunction are known to have lower eNOS activity and reduced nitrite plasma levels, which correlate closely with cardiovascular risk factors (164). NOSs catalyse conversion of L-arginine to NO and citrulline and this reaction can only occur in the presence of oxygen. NO can then diffuse into VSMCs where it binds to the haem centre and activates sGC, which converts guanosine triphosphate (GTP) to cyclic guanosine monophosphate (cGMP). This sequence activates PKG leading to low-grade phosphorylation of downstream targets (165). This process is very slow and only yields low levels of NO and therefore minimal systemic vasodilation (166).

The second major source of circulating nitrite is dietary intake of nitrate and nitrite. Green leafy vegetables and beetroot contribute to daily nitrate intake significantly. Certain foods, such as cured meats also contain high levels of nitrite (167). For example, a plate of green leafy vegetables can provide more nitrate than is formed endogenously over a full day by all nitric oxide synthases (168). Interestingly, beetroot juice has been used in several human studies to investigate the effects of oral nitrate supplementation. The average European diet has a nitrate intake of 50-150 mg per day (UK 95 mg) from food and a further 50 mg from drinking water (169), however specialised targeted diets have been developed, such as the Dietary Approaches to Stop Hypertension (DASH) diet, which provide up to 1222 mg nitrate intake a day (169).

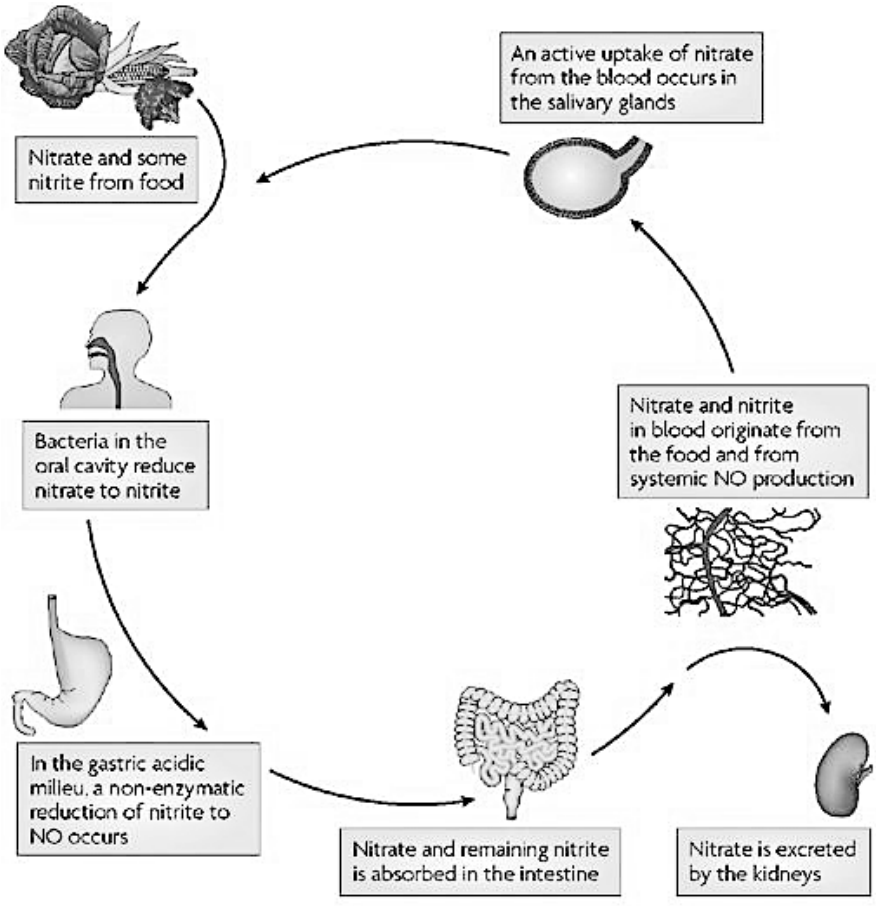

Figure 5: The entero-salivary circulation (168)

The 'entero-salivary circulation' relies heavily on a unique set of bacterial nitrate reductases possessed by specific bacterial populations in the mammalian mouth and gut (168). The

process begins by the ingestion of dietary nitrate (and nitrite), of which, 5-7% is reduced to nitrite by bacterial nitrate reductases in the mouth. In the low stomach pH 1-2, nitrite is protonated to HNO_2 and further to N_2O_3 which is then reduced to NO (via acid disproportionation) (170). Interestingly this NO production is thought to play an important role in gastric mucosa blood flow regulation and anti-bacterial non-specific immunity protection such as from helicobacter pylori infection (171). Around 75% of the excess nitrate in the bloodstream is excreted by the kidneys. The remaining nitrate (and some nitrite) is then absorbed across the gastric mucosa into the bloodstream where at the level of the venules and capillaries it is oxidised to nitrite which is more stable (172). As discussed before, NO can also be oxidised back to nitrite and nitrate by eNOS at the vascular endothelium via non-enzymatic auto-oxidation. Next, the remaining 25% of the circulating nitrate and nitrite can also be actively taken up in the salivary glands and is concentrated 10- to 20-fold and then secreted into the mouth cavity where it is swallowed into the stomach and re-enters the cycle. Baseline levels of nitrite vary in healthy people, but according to values published, appear to exist in the range of 0.13 μmol/L - 0.25 μmol/L (173-175).

The importance of the 'entero-salivary circulation' and the role of bacterial reductases have been highlighted by animal and human experiments using anti-septic mouth washes or spitting out of saliva, both of which prevent effective plasma nitrite rise following inorganic nitrate ingestion and abolish its biological effects (176, 177).

7: Pharmacokinetics of nitrate and nitrite metabolism

Nitrates and nitrites exist in two main forms. Inorganic nitrates/nitrites are small, water soluble ions that exist in the diet and are also endogenously produced via oxidation of NO (as discussed above) and organic nitrates/nitrites are synthesized and structurally more complex, with the exception of ethyl nitrite, are all medicinally synthesised products (178). These chemical differences result in distinct pharmacokinetic and pharmacodynamic properties, bioavailabilities and metabolic profiles. As alluded to in figure 5, the route of

administration plays an important role in nitrite metabolism. Inorganic nitrates/nitrites do not undergo first pass metabolism and rely on the entero-salivary circulation for absorption and also to buffer against toxic levels of nitrite prolong beneficial effects, whereas organic nitrates do not. As a result of this, inorganic nitrates/nitrites have a delay of ~3 hour to nitrite plasma peak levels (179, 180), whereas organic nitrate/nitrite have a rapid blood level rise and onset of action within 1-3 minutes (181). As shown by Pannala and colleagues in 2003, consumption of a high-nitrate meal (221.7 ± 10.8 mg) led to a rapid increase in salivary (baseline ~249-483 μmol/L vs 2h post: 2.6 mmol/L, $p<0.001$), urinary (baseline: 53 mg vs 24-collection: 223 mg, $p<0.001$) and plasma (baseline: 26 mg vs 1h post: 179 mg, $p<0.001$) nitrate levels, with increased levels of nitrite in the saliva (baseline 204-302 μmol/L vs 2h post: 1.8 mmol/L, $p<0.001$), sustained for at least 5h post-nitrate ingestion (182).

In a study by Rix in 2015, they demonstrated that with increasing doses of nebulised nitrite, there was a progressive increase in C_{max} (maximum plasma concentration), AUC (area under the curve plasma concentration-time curve from time zero to end time point), CL/*F* (apparent clearance), V_{ss}/F (apparent steady state volume of distribution) and $t_{½}$ (half-life), indicating that nebulised sodium nitrite is capable of producing dose-proportional plasma pharmacokinetics. The group also showed that the $t_{1/2}$ of nitrite in plasma at 4°C was ~30 minutes, which was comparable with that reported following intra-arterial (0.7 h) (173) or intravenous (0.5 h) (179) and (0.8 h) (175) administration in other healthy subject studies, providing additional insight into how nitrite in metabolised and distributed (183).

Also, as will be discussed in greater detail later, metabolism of organic nitrate/nitrite is partly regulated by reductase systems and local oxygen tension, and able to lead to significant vasodilation, whereas inorganic nitrites have a far subtler effect on vasodilation (184-186). Specifically, in the context of ischaemia-reperfusion injury, inorganic nitrate/nitrite has important cytoprotective effects, whereas repeated use of organic nitrates may increase

injury (158, 187). Differences also exist in efficacy. For example, in chronic use, organic nitrates are known to be associated with tolerance and endothelial dysfunction, whereas inorganic nitrite does not appear to induce tolerance (173).

Finally, as discussed previously, the mode of excretion differs, with inorganic nitrates/nitrites being subject to renal clearance (figure 5) (168) whereas organic nitrates/nitrites are not (188). Therefore, all of these factors taken together, it is very important to separate the pharmacokinetics of these two forms of nitrates/nitrites when considering their use in clinical research (178).

In a detailed review article by James et al, 2015, the discordances in data from inorganic nitrate supplementation studies were discussed. They highlighted the importance of knowing whether the individual variation of nitrate/nitrite/NO metabolism may be greater than the effect being tested (189). As discussed above, whilst data exists, they highlighted the importance of the source of nitrate or nitrite (inorganic vs organic), route of administration, study cohort kinetic profile, and timing of bolus/serial dose/infusion, as each potentially influences the success of any given study. Interestingly, the group also highlighted the need for more research to help understand at what stage in the nitrate-nitrite-NO pathway 'non-responders' are being limited in their response. They called for future work to examine this inter-individual variability, by assessing nitrate pharmacokinetics, comparing different sources and routes of administration of nitrate in the same individual(s) in a carefully controlled crossover study (189).

8: Nitrite-mediated vasodilation

Nitrite in normoxia

Over the years, several groups have demonstrated that nitrite can also induce significant vasodilation and systemic BP changes during normoxia in specific physiological conditions

(146, 177, 190-192). This observation is not adequately explained, as nitrite is predominantly reduced to NO in the venules and capillaries, yet for flow to increase and MAP to fall there must be significant relaxation of the resistance vessels upstream. The mechanism(s) underlying this are unclear. Various hypotheses have been proposed including electrochemical retrograde transmission of hyperpolarisation via gap junctions (193, 194) and vascular looping resulting in proximal NO donation from capillaries and venules (195). To date, no consensus has been reached.

Understanding how nitrite can cause vasodilation in resistance vessels in normoxia has significant therapeutic importance. It is this gap in the knowledge that led our group to examine this mechanism. As a terminal point in the well-described NO-sGC-cGMP-PKG pathway and the gatekeeper to downstream target phosphorylation, a plausible candidate of particular interest is PKG. PKG exists as two isoforms; type 1 (75kDa) and type 2 (85kDa). Both isoforms are homodimeric and share similar quaternary structures. PKG1 is predominantly expressed in the cardiovascular system and has two splice variants; PKG1α (heart, lungs, cerebellum) and PKG1β (platelets and hippocampal neurons) (196). PKG1α has 11 cysteine residues within its structure, five of which are sensitive to redox oxidation. Disulphide bond formation is a cysteine modification able to form in signalling kinases and influence enzymatic activity (197).

Nitrite-mediated PKG1α dimerization

In 2007, Burgoyne and colleagues from the Eaton group, King's College, UK showed that PKG1α can operate as a 'redox sensor' and can also dimerize via inter-protein disulphide bonding after exposure to exogenous H_2O_2 in rats (198). This mechanism was further explored by the same group in 2010. They showed that oxidising agents acted on low pKa cysteine thiols (Cysteine 42) to generate disulphide bonds between adjacent cysteine

residues, resulting in PKG1α dimerization. They proposed that PKG1α can function via monomeric activation and oxidative dimerization simultaneously.

Until 2012, this hypothesis was very difficult to study, until a significant paper by Eaton and colleagues, presented a transgenic knock-in (KI) mouse model that was unable to form PKG1α dimers through oxidation (referred to as being 'redox dead') (199). These mice were created by a single-atom change (an oxygen atom replacing a sulphur atom), leading to an amino acid substitution (Cysteine, position 42, replaced with Serine) as a result, they could not form disulphide bonds between cysteine residues and thus prevented oxidative dimerization of PKG1α. In 2012, the group showed that PKG1α KI mice developed hypertension, which further drew attention to the role of PKG1α dimerization in vasodilation and maintenance of healthy vascular tone (199).

Also, in 2012, Eaton and colleagues observed that when cGMP formation by sGC was blocked with ODQ, PKG1α dimer formation increased from 13 ± 2% to 29 ± 4% of total PKG1α in aorta and mesenteries, respectively. This, at the time, seemed unusual, as the higher levels of NO were detected in the aorta (conduit vessel) and therefore it was expected that ODQ blockade would induce a compensatory response and therefore greater levels of disulphide bond formation at this site (the conduit vessel). Even more unexpectedly, ODQ induced constriction in aorta, but not in mesenteries. This data was interesting because it suggested that once PKG1α is bound to cGMP, it is not able to form disulfide bonds, indicating that these two processes may in fact be mutually exclusive (later described in more detail by the Kass group, 2018). It also suggested that there may be a difference in the mechanism driving the vasodilatory response, with conduit vessels vasodilating in response to monomeric PKG1α and resistance vessels vasodilating in response to PKG1α oxidative dimerization (199).

With the advent of the redox-dead mouse, several groups took an interest in PKG1α dimerization, in the context of cardiovascular physiology. In 2012, Zhang and colleagues attempted to explain the mechanisms by which H_2O_2 dilates human coronary arterioles. The group showed that H_2O_2 induced dose-dependent and reversible PKG1α oxidative dimerization, which resulted in big potassium (BK)-calcium channel opening, potassium efflux, hyperpolarisation and subsequent reduced calcium influx, preventing VSMC contraction (200). This finding was very interesting as it appeared to show a mechanism for H_2O_2-dependent, PKG1α-dimer mediated coronary artery vasodilation in normoxia. The group suggested that the hydrogen sulphide system mediated oxidation at the cysteine residues, leading to dimerization.

Later in 2012, Eaton and colleagues studied the vasoactive mechanisms of glyceryl trinitrate (GTN). The group showed that in the redox-dead KI mouse there were substantive deficiencies in hypotensive response to GTN as measured by radiotelemetry. When the same was performed in wild-type littermates, GTN caused PKG1α oxidative dimerization via disulfide formation and induced a significant hypotensive response. The group showed that resistance blood vessels from KIs were markedly less sensitive to GTN-induced vasodilation than the wild-types (WTs) (201). This work showed that GTN directly induced disulfide bond formation and subsequent PKG1α dimerization in the resistance vessels.

In 2013, it was suggested by Eaton and colleagues that not only does PKG1α dimerization play an important physiological role in resistance vessel tone and BP maintenance, it is also implicated in serious pathological processes, such as sepsis. The group showed that in conditions where vasodilation and increased vascular permeability are cardinal features, PKG1α dimerization may be a key underlying finding (202). This observation raised the notion that PKG1α oxidative dimerization often follows an oxidative surge, which is uncommonly seen in normal physiology but can occur during sepsis in normoxia. The group

proposed that in a high reactive oxygen species (ROS) state (such as sepsis), PKG1α oxidative dimerization can take place resulting in profound vasodilation in normoxia.

In 2016, the Eaton group demonstrated that the PKG1α dimer is able to regulate cardiac diastolic relaxation and plays an important role in fine-tuning the Frank-Starling response. Using phosphoproteomics, they showed that PKG1α can dimerize in response to oxidants generated by diastolic mechanical filling stress. Once dimerized, PKG1α can selectively phosphorylate cardiac phospholamban Ser16, a site important for diastolic relaxation. When the redox-dead KI model underwent the same protocol, these mice developed diastolic dysfunction and diminished ventricular filling (203). This finding highlighted that in heart failure, PKG1α oxidative dimerization may result from increased ROS production, which further supported the previous work by Rudyk and colleagues in 2013.

In 2017, the Eaton group sought to bring the therapeutic potential of PKG1α dimerization to the forefront. The group developed an assay and screened for electrophilic drugs that activate PKGIα disulfide bond formation by selectively targeting Cysteine 42, resulting in vasodilation and BP lowering effects. The group identified a novel compound, which they called 'G1', which displayed antihypertensive effects in an angiotensin II-induced hypertension mouse model (204). Using the redox-dead KI mouse the group revealed that these anti-hypertensive effects were attenuated, validating PKGIα C42 as the target of G1, as well as providing proof-of-principle for a new class of antihypertensive drugs that have potential for further development for clinical use in humans (204).

In 2018, the Kass group, John Hopkins, USA showed that in cardiac myocyte, localisation of PKG1α is subject to whether it is in its monomeric or homodimeric form. The activated monomer is membrane-bound whereas oxidative dimerization leads to it becoming released into the cytosolic compartment. As sGC is membrane-bound and phosphodiesterase (PDE) is cytosolic, the location of activated PKG1α is very important when considering how to

target it for therapeutic intervention (either by stimulation of sGC or inhibition of PDE5) (205).

Alternative mechanisms for nitrite-mediated vasodilation

Persulfides

A separate body of literature also supports the belief that hydrogen sulphide can reduce nitrite to NO and/or promote nitrite reduction via XOR or porphyrins (206). Persulfides have been implicated in nitrite reduction via polysulfide and perthionitrite intermediate formation (207). In 2016, the Feelisch group, UK, suggested that nitrosopersulfide could also generate polysulfides and NO, which could in turn activate the classical NO-sGC-cGMP-PKG pathway (208). These observations indicate that either persulfide intermediates and/or high ROS may be important in the direct oxidation of PKG1α cysteine residues.

S-nitrosothiols (RNSO)

S-nitrosothiols (RNSOs) were originally thought to serve as intermediates in the action of organic nitrates (209) and endogenous RSNOs were shown to represent a main source of NO bioactivity *in vivo* (210). In recent years, RSNOs have emerged as having a central role in the modulation of NO bioavailability and subsequent vasotone in the presence of haem proteins (as will be discussed in later) (211-213) and through the redox modulation of sGC thiol groups (specifically nitrosylation of cysteine), leading to the generation of bioavailable NO (214).

RSNOs have also been shown to be an important post-translational protein modification in cardiovascular signalling (215, 216) and cardioprotection (217) including in the context of thiol protection from oxidative modification on reperfusion protection during ischaemia-reperfusion injury (218, 219). In 2008, Sayed and colleagues made the link between S-nitrosylation of sGC and vasoactivity by showing that GTN treatment of primary aortic smooth muscle cells induced S-nitrosylation of sGC and that this was reversed when GTN

was stopped (220). This concept was challenged by Sun and colleagues in 2013 who used Langendorff-perfused mouse hearts to show that ODQ and KT5823 inhibition (sGC and PKG inhibitors, respectively) did not abolish ischaemic preconditioning (IPC)-induced acute protection. They postulated that a sGC/cGMP/PKG-independent signalling pathway, via RSNOs, was responsible for NO-mediated cardioprotection during acute IPC.

Whilst the exact roles of RSNOs in nitrite-mediated vasodilation require further characterisation, emerging evidence continues to indicate the RSNOs have an important role to play, with potentially thousands of RSNOs (including S-nitrosoglutathione [GSNO], thionitrous acid [HSNO] and S-Nitroso-N-acetylpenicillamine [SNAP]), regulated by many denitrosylases and nitrosylases are capable of functioning as both targets and transducers of S-nitrosylation (221, 222).

Due to the meticulous work over the last decade by the Eaton group and others (197-208), the following observations have been made:

1. Nitrite can induce NO-independent PKG1α oxidative dimerization in normoxia
2. PKG1α oxidative dimerization is a tissue-specific phenomenon seen in the resistance vasculature and this is important in the maintenance of MAP
3. High ROS, persulfide intermediates and the hydrogen sulphide system may be implicated in direct oxidation of the cysteine residues.

These observations are of great interest to our group scientifically and therapeutically. In an attempt to unravel the story further we examined the mechanisms mediating PKG1α oxidative dimerization in normoxia with respect to NO-dependency, vessel-type variations, ROS and persulfide intermediates, figure 6. Accordingly, in Chapter 3 we examined the mechanisms of nitrite-mediated vasodilation in normoxia in a murine *ex vivo* model.

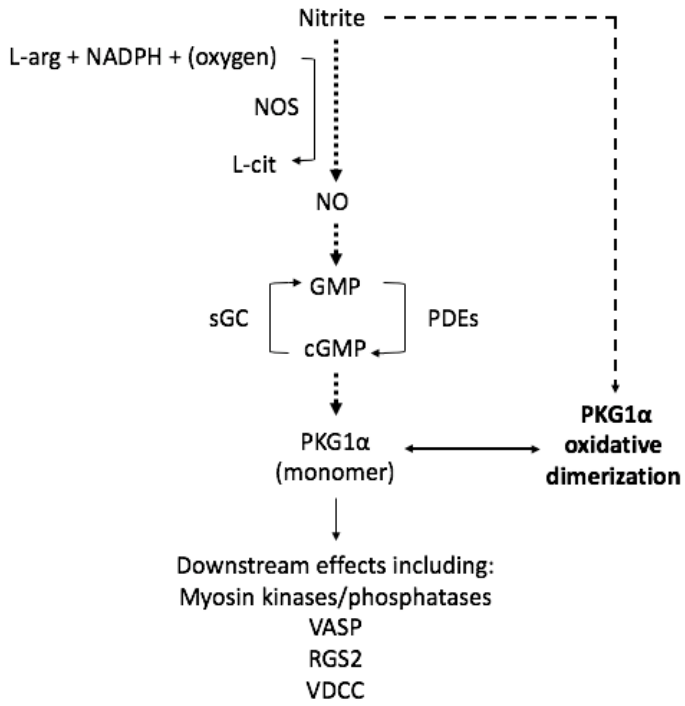

Figure 6: Can nitrite mediate NO-independent vasodilation in murine resistance arteries in normoxia *ex vivo?* (via PKG oxidation/dimerization or associated intermediates or via alternative non-PKG intermediates such as hydrogen sulphide or RSNOs). Key XOR – xanthine oxidoreductase, L-arg: L-arginine, NADPH: nicotinamide adenine dinucleotide phosphate, NOS: nitric oxide synthase, NO: nitric oxide, sGC: soluble guanylate cyclase, GMP: guanylate monophosphate, cGMP: cyclic guanosine monophosphate, PDE: phosphodiesterase, PKG1α: protein kinase G1 alpha, VASP: vasodilator stimulated phosphoprotein, RGS2: regulator of g-protein signalling 2, VDCC: voltage-gated calcium channels.

Nitrite in hypoxia

In the context of the clinical studies we performed in this thesis, we first need to define what the term 'hypoxia' means and what this represents both physiologically and pathologically. We also need to understand how nitrite interacts with different reductase systems in hypoxia, with a specific focus on changing oxygen gradients across different vascular beds and tissues

(168, 223-225). In healthy physiology, arterial blood has a free oxygen concentration of ~100-130 μmol (pO_2 15-100 mmHg), venous blood has 35-40 μmol (pO_2 1.5-15 mmHg), perivenous tissues have 20-30 μmol, and mitochondrial respiration is compromised when free oxygen is <2 μmol (pO_2 <1.5 mmHg). We can assign hyperoxia as being >130 μmol, normoxia as the interval spanned by arterial blood and perivenous tissues (130-20 μmol), hypoxia as the interval spanned between perivenous tissues and mitochondrial respiration compromise (20-2 μmol), and anoxia being <2 μmol (229).

As alluded to above, it is also important to also point out that oxygen gradients vary significantly across vascular beds and tissues, due in part to differential degrees of oxygen consumption. Several studies report a wide range of human and animal partial oxygen pressures measured across various tissues in normoxia. Values vary significantly between adult mammal species (for example, rat liver pO_2 70-77 mmHg vs pig liver pO_2 20 mmHg) (230) vascular beds (pig arterial blood pO_2 75 mmHg vs human arterial blood pO_2 90 mmHg) (229, 230) and between organs (rat renal cortex pO_2 50 mmHg vs mouse renal cortex pO_2 23 mmHg) (231-233). It is important to consider that across the human vascular tree, sharp oxygen gradients exist, especially when we consider the gradient span between normoxic arterial blood (130 μmol) through to active muscularised capillaries (25 μmol) (234) and that these differences in partial oxygen pressures directly influence nitrite reductase systems and the degree to which nitrite is reduced to NO.

Whilst it is not possible to study the effects of hypoxia (in the strictest sense; 20-2 μmol [pO_2 1.5 – 15 mmHg]) on arterial vasoactivity in healthy human volunteers *in vivo*, it is possible to study nitrite in a 'reduced oxygen condition' of 62.5 – 72.5 μmol (pO_2=47.5 to 55 mmHg) achieved by subjects breathing 12% oxygen / 88% nitrogen in order to achieve an oxygen saturation of 83-88%, as a surrogate for clinical hypoxia (235), as might be seen in patients suffering with established cardiovascular disease, sepsis, or established respiratory disease,

etc. (236). The 'reduced oxygen' *in vivo* human model has been used by several groups to study vascular physiology and disease (174, 235, 237-241). For clarity, we refer to the reduced oxygen condition as 'hypoxia' throughout this thesis to differentiate it to the condition of normoxia (21% oxygen) which is also studied.

Nitrite reductases

Nitrite reduction is ubiquitous throughout biology. In bacteria and Archaea, denitrification in the major mechanism by which fixed nitrogen returns to the atmosphere from soil and water (242). In humans, as discussed, nitrite can be either i) synthesised via the endogenous L-arginine/NO-synthase pathway, or ii) can be generated by reduction of inorganic nitrate by facultative anaerobic bacteria in the mouth and stomach (149, 168). As described, humans do not innately possess nitrate reductase enzymes, so this symbiosis is essential in the metabolism of nitrate to nitrite. Nitrite reduction in turn generates NO enabling a wide range of important downstream pleiotropic effects (168, 243). Nitrite reduction (equation 1) is the process in which a protein donates an electron to nitrite in the presence of a proton source to form NO, becoming oxidized in the process (244):

$$(1)\ NO_2^- + H^+ + \text{Nitrite reductase}^{n+} \rightarrow NO + OH^- + \text{Nitrite reducatase}^{(n+1)+}$$

In contrast to the NOS pathway (described previously) which is strictly oxygen-dependent, NO production from nitrite reduction is greatly facilitated by hypoxia (245, 246), such as those that commonly occur in hypoxic vasodilation of cardiovascular systems (247) muscle tissue during extensive exercise (248) and ischemic tissues (249). Unlike NOS, nitrite reductases can produce NO via oxygen-independent processes, suggesting the potential contribution of NO in mediating hypoxic signalling-dependent cellular responses (250).

Reduction is significantly potentiated by hypoxia and acidosis, and is catalysed by a variety of reductases. It is important to emphasise that different nitrite reductase systems are activate

at different partial oxygen pressures, therefore the degree to which nitrite is reduced to NO will depend on the changing oxygen gradients across different vascular beds and tissues (168, 223-225). This is an important observation, as several studies that have looked at the effect of blocking any one of these reductases *in vivo* have frequently failed to show an effect on NO generation, indicating a degree of redundancy, thereby ensuring NO production in situations for which the oxygen-dependent NO-synthase enzyme activities are compromised (168, 229). For example, Cytochrome *c* (251), cytochrome *bc1* (245, 252) and cytochrome *c* oxidase (Cco) (246, 252) of the mitochondrial electron transport chain, have been reported to generate NO via nitrite reductase-dependent catalysis at very low oxygen concentrations (229). Interestingly, nitrite is able to enter the cell and access the mitochondria due to nitrite anion. In addition, as previously mentioned, eNOS is also able to function down to oxygen levels of ~10 μmol (157) to reduce nitrite to NO (161, 253), however below this level, a series of anoxic 'alternate mechanisms' are activated to enable NO production at the oxygenase domain (158).

Another important class of nitrite reducing metalloproteins are the molybdopterins. These molybdenum-based proteins include xanthine oxidoreductase (XOR), aldehyde oxidase (AO), sulfite oxidase (SO), and the mitochondrial amidoxime reducing components (mARCs) (249, 254). XOR, which is a nicotinamide adenine dinucleotide + hydrogen (NADH)-dependant reductase that has been shown to be most potent during hypoxia (255). XOR is seen in mammalian cells and is involved in catabolism of purines and pyrimidines, oxidizing hypoxanthine to xanthine and xanthine to uric acid. It can also reduce oxygen to superoxide and H2O2. Interestingly, XOR-mediated NO production can operate in hypoxia (O_2 <2 μmol) via 'process I' and also in all oxygen conditions from hypoxia to hyperoxia (O_2 <2 - >130 μmol) via 'process II' (229). In normoxia, dose-dependent XOR has been shown to reduce MAP/BP in N(gamma)-nitro-L-arginine methyl ester (L-NAME) induced

hypertensive rats and this effect was abolished when the mice were treated with allopurinol (a XOR inhibitor) (256).

Aldehyde oxidase (AO) is another molybdenum containing flavoenzyme which has a high sequential homology with XOR (86% conserved) (254). AO contributes significantly to anoxic reduction of nitrite in rat tissue homogenates (254). Other reductase systems to briefly mention are i) carbonic anhydrase (CA), which due to the biochemical similarity between nitrite and bicarbonate, also readily reduces nitrite to NO in both normoxia and hypoxia (241), and ii) myoglobin, which has been shown to be a potent hypoxia-dependent nitrite reductase (O_2 ~4 μmol) (257) and this effect has also been shown at supra-physiological levels (258).

Another key mechanism that allows nitrite reduction to NO is via 'acid disproportionation' which is a slow non-enzymatic conversion which takes place under profoundly acidotic conditions (259). This process takes place in the stomach, but also in ischaemic tissues where the local pH is low (equation 2):

$$(2)\ NO_2^- + H^+ \leftrightharpoons HNO_2 \text{ - - - > } 2HNO_2 \leftrightharpoons H_2O + N_2O_3 \text{ - - -> } N_2O_3 \rightarrow NO + NO_2$$

<u>Haem proteins in normoxia and hypoxia</u>

In normoxia, one of the discoveries that identified NO as the EDRF was that its activity is inhibited by haemoglobin (209) as oxyHb reacts with NO to form metHb and nitrate, figure 7, equation 3:

$$(3)\ Fe^{2+}O_2Hb + NO \rightarrow Fe^{3+}Hb + NO_3^-$$

'NO dioxygenation' is a near diffusion-limited fast reaction ($k = 10^7 - 10^8\ M^{-1}s^{-1}$), is irreversible and inactivates NO in blood (260). It leads to the reduction in NO signalling,

however this effect is problematic from a theoretical perspective. Modelling of NO generation has shown that NO should only have a half-life of 1 μs and should only be able to diffuse 0.1 μm before being consumed by haemoglobin within the erythrocyte (148) yet, NO still appears to escape the erythrocyte and reach the vascular endothelium, where it has its vasodilatory effects (261). A plausible explanation is the formation of intermediates such as dinitrogen trioxide (N_2O_3) or RSNOs on protein surfaces (212). Several mechanisms adopting the use of intermediates have been proposed, figure 7. The ß93 cysteine residue in haemoglobin has been shown to be a site for RSNO formation and NO export (211). N_2O_3 is a promising candidate as it is highly reactive, rapidly able to disproportionate to NO, has a longer half-life (vs NO) and is diffusible.

In hypoxia, haem-binding proteins, such as haemoglobin, myoglobin, cytoglobin, neuroglobin, and the non-mammalian globin X are the most well-documented haem-based nitrite reductases (262). Of particular note, haemoglobin (263) has been shown to play an important role in nitrite reduction. At levels near the lower end of normoxia (O_2 ~30 μM), deoxyHb can reduce nitrite. In hypoxia, the fraction of deoxyHb rises and accelerates the release of NO from the RBC (229). The process requires the haem iron to be in the ferrous state (Fe^{2+}) and without a bound ligand (i.e deoxyHb) (262). The reduction of nitrite to NO takes place via an electron transport reaction at the haem iron (equation 4):

$$(4)\ NO_2^- + H^+ + HbFe^{2+} \rightarrow NO + OH^- + HbFe^{3+}$$

Also, in hypoxia, haemoglobin can generate N_2O_3 via a 'nitrite anhydrase reaction', in which nitrite reacts with deoxyHb forming a Fe^{3+} nitrosyl intermediate which can then react with a second nitrite molecule to form N_2O_3 (264, 265) (equation 5):

$$(5)\ NO_2^- + H^+ + HbFe^{2+} \rightarrow (HbFe^{3+} - NO \leftrightarrow HbFe^{2+} - NO^+) + OH^+$$

$$(\mathrm{HbFe^{3+} - NO \leftrightarrow HbFe^{2+} - NO^{+}}) + \mathrm{NO_2^-} \rightarrow \mathrm{HbFe^{2+}} + \mathrm{N_2O_3}$$

Taking all of the potential NO liberating mechanisms together, as shown in figure 7, nitrite and oxyHb can produce metHb and nitrate. MetHb can react with NO to produce deoxyHb and N_2O_3, which can be exported and converted to NO and nitrite, or it can be used to form RSNOs. Also, deoxyHb can produce NO-bound metHb, which can dissociate, again releasing NO, or this NO can be transferred to a thiol forming SNO-Hb then a nitrosating group to another thiol to generate RSNOs, adapted from (213).

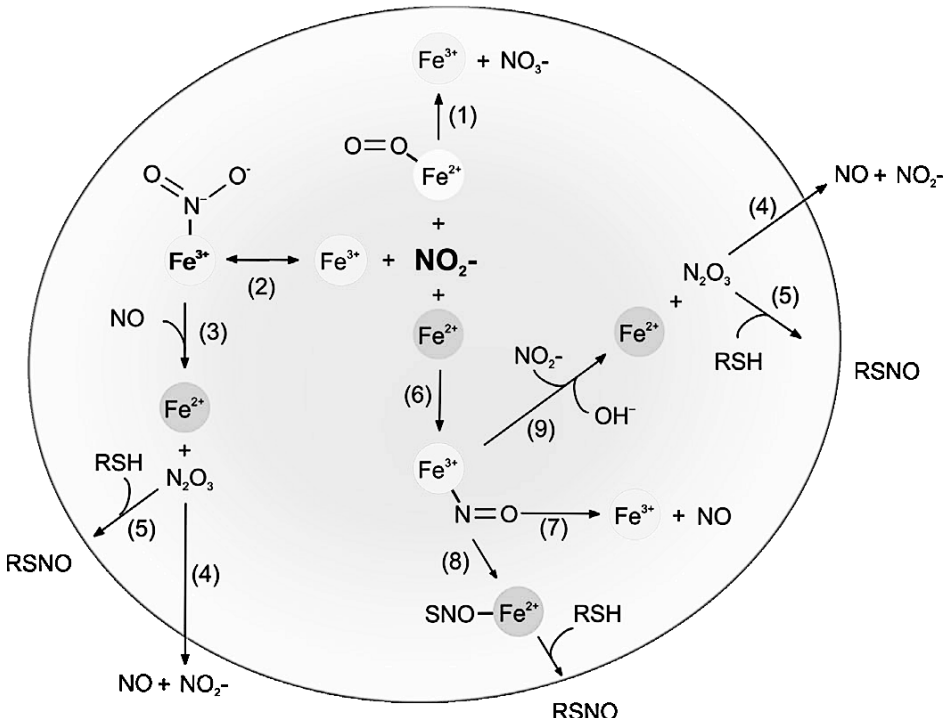

Figure 7: Potential nitrite and Hb interaction within the RBC resulting in NO bioactivation Adapted from (213). Note: White Fe^{2+}: oxyHb, grey Fe^{2+}: deoxyHb, not-circled Fe^{3+}: ferric Hb. Key:

Reaction 1: Nitrite + oxyHb = metHb and nitrate

Reaction 2: MetHb + nitrite = nitrite-bound met

Reaction 3: Nitrite-bound metHb + NO = deoxyHb + N_2O_3

Reaction 4: N_2O_3 → NO + nitrite

Reaction 5: N_2O_3 → RSNOs

Reaction 6: Nitrite + deoxyHb = NO-bound metHb

Reaction 7: NO-bound metHb = metHb + NO

Reaction 8: NO + SNO-Hb → RSNOs

Reaction 9: NO-bound metHb + nitrite + hydroxyl = deoxyHb + N_2O_3 → NO + nitrite or RSNOs.

Whilst haem proteins can reduce nitrite to NO, the physiological role behind this function remains unclear as due to the allosteric nature of the reaction, it is most efficient near the

Hb-P50 (oxygen tension at which haemoglobin is 50% oxygenated) and is thus modulated at considerably reduced oxygen concentrations (253, 266).

In 2002, Joshi and colleagues compared bolus NO addition to NO generated homogeneously throughout solution by using NO donors. Using visible spectroscopy, they showed that multiple haemoglobin species are formed as well as both nitrite and nitrate. They concluded that the reaction of NO with haemoglobin during normoxia resulted in consumption, rather than conservation of NO, highlighting that oxyhaemoglobin is capable of scavenging NO (267). In the same year, Reiter and colleagues hypothesized that decompartmentalization of haemoglobin into plasma could divert nitric oxide from homeostatic vascular function. By studying patients with sickle-cell disease, they showed that plasma contained higher levels of cell-free ferrous haemoglobin and this stoichiometrically consumed micromolar quantities of nitric oxide, abrogating forearm blood flow responses to nitric oxide donor infusions (268).

A study by Cosby and colleagues in 2003 showed that in the presence of a nitrite infusion, NO adducts of haemoglobin are increased, demonstrating that haemoglobin may be functioning as an important nitrite reductase (269). In 2007, Dalsgaard and colleagues observed that nitrite-dependent vasodilation conforms to first-order reaction kinetics with respect to nitrite concentration. Using selective inhibitors during hypoxia, they showed that nitrite-induced vasorelaxation was independent of the main nitrite reductases and importantly was inhibited by oxygenated haemoglobin but not by deoxygenated haemoglobin (270). This observation raised the notion that haem proteins may have different effects on vasoactivity dependent on oxygen tension. In hypoxia, it appears that haemoglobin can sub-serve a number of roles, including nitrite reductase in hypoxia; as an acceptor of the resulting NO (eg, through nitrosyl haemoglobin [HbNO]); and as a donor of NO precisely where it is required, ie, at the site of hypoxia (through S-nitrosohaemoglobin) (237).

In 2008, Gladwin and Kim-Sharpiro, USA presented a host of complex mechanisms underlying the role of haem proteins in hypoxia-mediated nitrite reduction, including allosteric autocatalysis, redox potential ligand accessibility, proton and redox Bohr effect, oxidative denitrosylation, radical-radical reaction pathways, and anaerobic nitrogen trioxide generation (263). Whilst other groups have been unable to corroborate these proposed mechanisms, importantly this commentary did raise useful questions around the exact role of haem proteins with respect to NO bioavailability. In the same year, the same group presented the argument that during normoxia, cell free-haem proteins can also avidly scavenge, bind and attenuate NO (271). They ascribed this to blood degradation whilst in storage, a process they named the 'storage lesion' effect (272). The group postulated that this storage lesion effect could overcome the compartmentalisation barrier and accounted for the ability of haem to bind NO, leading to a reactive vasoconstriction. The group promoted that nitroxyl-derived salts could counteract the vasoconstrictive effects of elevated plasma haemoglobin when administered with stored blood (273).

Donadee and colleagues examined the rate at which stored blood haemolyses and showed that the degree of haemolysis and haemoglobin release in blood stored in standard conditions increases significantly and exponentially over time vs baseline; from baseline 4-day plasma Hb (11.6±2.5 μmol/L) to 39-day plasma Hb (81.0±18.4 μmol/L). They showed that with haemolysis, cell-free haem accumulation is coupled with microparticle encapsulated haemoglobin accumulation, which despite prolonged storage largely remains in the ferrous oxyhaemoglobin state. They showed that cell-free haem increases are directly proportional to NO consumption, $p < 0.001$, via the classic deoxygenation reaction (equation 3 page 59) at a 1:1 reaction stoichiometry and that microparticles also inactivate NO at similar rates. This is very interesting, given microparticles are continuously released after transfusion and are not known to be cleared by haptoglobin, so may be an ongoing source of NO bioactivation (274).

Taken together, it is now clearer than ever that the role of haem proteins in nitrite metabolism (and NO liberation) is a complex process relying on a multitude of factors, including oxygen tension, haem compartmentalization within the RBC (213) and possibly within exocytosed microparticles (274). As described, the ability of haem proteins to perform both nitrite reduction and NO dioxygenation allows haem proteins to both increase and decrease NO levels and NO signalling depending on local oxygen tension and pH, although this may be mediated by RBC membrane integrity, figure 7 (213). In addition, the formation of N_2O_3 or RSNOs from the Hb/nitrite reaction may be the key to nitrite-mediated NO activity export from intact red blood cells, but these mechanisms still remain a matter of debate. It is also unclear if a meaningful difference exists in the metabolism of nitrite (and release of NO) in the presence of circulating (intact) blood vs stored blood (as used in blood transfusion).

Clinical blood transfusion and vasoconstriction

Whilst allogenic blood transfusion has well-defined associated risks (virus transmission, acute lung injury due to increased pulmonary artery pressure, haemolytic reactions and sepsis, to name a few) (275), it is thought to be a relatively safe clinical intervention if processed, administered and monitored correctly. Despite this, a series of clinical studies have also shown that packed red cell transfusions which have been stored for prolonged periods are associated to increased mortality in critically ill patients (276-278). Whilst the rationale behind this association is not fully understood, increasing evidence suggests that this may be due to deleterious effects of stored blood.

In 2014, Berra et al showed that in 40-day stored packed red cell transfusions, subjects with endothelial dysregulation experienced elevated pulmonary artery pressures ($p<0.05$) and that this could be attenuated by breathing nebulised nitric oxide (80 parts per million [ppm]). In 2015, the Gladwin group showed that intra-arterial infusion of stored blood attenuated

endothelial NO bioavailability, resulting in reduced forearm blood flow (measured by strain gauge plethysmography) (260). Whilst this study was logical, their work did create uncertainty. For example, they administered a brachial artery blood transfusion and waited 4-minutes before assessing endothelial integrity with ACh. The local concentration of free haem would have fallen over this period and would have equilibrated across the circulation. Also, they only administered <200mls of blood, which may have had negligible effects due to volume of distribution effects.

Despite these limitations, their study did present the notion that stored blood with uncompartmentalized haemoglobin can be used in the context of clinical research to attenuate endothelial NO bioavailability (which had previously not been possible *in vivo*, as compounds such as CTPIO are not licensed for human use). Using this 'healthy volunteer NO-blockade model' we designed a study to test the effect of nitrite on resistance artery vasodilation in normoxia and hypoxia in the healthy vascular endothelium and, and to our knowledge, for the first time, in the NO-reduced environment in humans. This comparison enabled our group to test in Chapter 4 if nitrite was able to mediate vasodilation via NO-independent processes, such as via PKG oxidation/dimerization or associated intermediates (as studied from a mechanistic perspective in Chapter 3), or via alternative non-PKG intermediates such as hydrogen sulphide or RSNOs, in humans *in vivo*, figure 8.

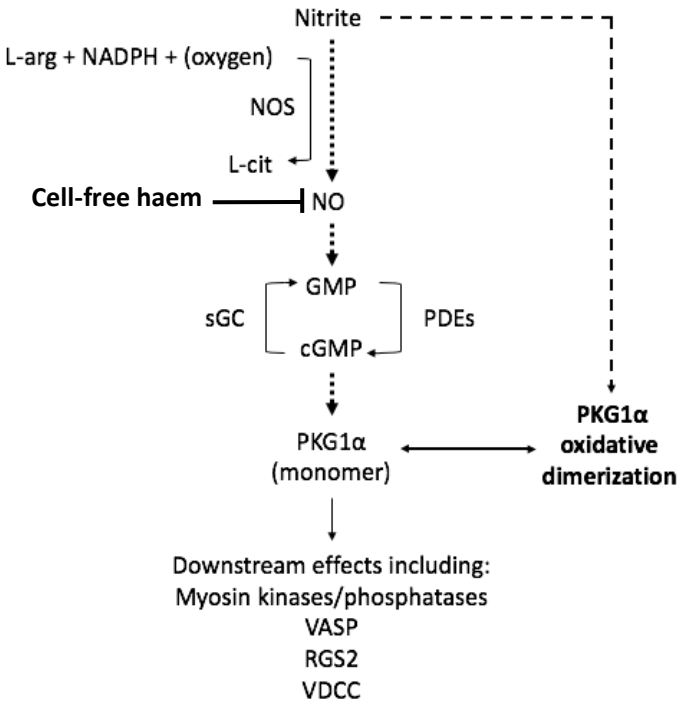

Figure 8: Can nitrite mediate NO-independent vasodilation in human resistance arteries in normoxia *in vivo?* (via PKG oxidation/dimerization or associated intermediates [as studied from a mechanistic perspective in Chapter 3], or via alternative non-PKG intermediates such as hydrogen sulphide or RSNOs). Key – XOR: xanthine oxidoreductase, AO: aldehyde oxidase, CA: carbonic anhydrase, eNOS: endothelial nitric oxide synthase, NO: nitric oxide, sGC: soluble guanylate cyclase, GMP: guanylate monophosphate, cGMP: cyclic guanosine monophosphate, PDEs: phosphodiesterase's, PKG1α: protein kinase G1α, VASP: vasodilator stimulated phosphoprotein, RGS2: regulator of g-protein signalling 2, VDCC: voltage-gated calcium channels.

Nitrite in the coronary arteries

The coronary arteries are physiologically similar to the peripheral arteries with respect to vasomotor activity (112, 279) and are most similar to conduit vessels in their function (126, 280). Consistent with systemic conduit arteries, a body of work exists which highlights that healthy coronary arteries do not exert significant resistance to flow (281, 282). In 2016, Raphael and colleagues showed that coronary flow can also be profoundly influenced by a

variety of cardiac factors (with vascular compression during systole resulting in backward travelling compression waves, and left ventricular relaxation resulting in backward travelling expansion waves – the latter resulting in forward flow by suction) (283).

Historical evidence exists, albeit very limited, suggests that organic nitrites such as amyl nitrite can increase velocity and flow within the coronary arteries. In 1972, Benchimol and colleagues presented a study in which 21 subjects had instantaneous coronary arterial phasic blood flow measurements immediately after amyl nitrite inhalation. In all subjects, the group reported appreciable diastolic coronary arterial phasic blood flow and flow velocity increasing by up to 216% (284). In 1977, the same group presented a second study in which phasic instantaneous aortocoronary saphenous vein bypass graft blood velocity was continuously measured during the inhalation of amyl nitrite in 20 closed-chest conscious subjects. Amyl nitrite inhalation resulted in an 84% rise in velocity. These findings suggested that amyl nitrite could increase cross-sectional area of the studied vessels and also blood velocity in parallel (285). Whilst of interest, it is also noted that amyl nitrite does have different vasoactive properties to inorganic nitrite and may not be directly comparable.

In 2015, Keegan and colleagues validated a non-invasive high temporal spiral phase velocity mapping technique using CMR. The group showed that compared with invasive doppler guidewire measures, spiral phase velocity mapping showed a strong linear relationship with a slope close to unity (0.89 and 0.90 for right and left arteries respectively). This advancement enabled accurate assessment of the temporal patterns of blood flow in the coronary arteries (286).

In a study by O'Gallagher and colleagues in 2018, 9 patients undergoing diagnostic angiography had a coronary doppler wire placed in the proximal artery and average peak velocity (APV) was measured following 5-minute infusion of saline, nitrite 2.6 μmol/min,

nitrite 26 μmol/min and GTN 1μg/min. The group also measured vessel diameter changes and calculated coronary blood flow and coronary resistance. The group showed that the higher dose of nitrite and the GTN significantly dilated the coronary artery vs saline (with a change of +8.9%, $p = 0.01$ and +10.8%, $p = 0.03$, respectively). They showed no significant difference between the vasodilator effects of higher dose nitrite and GTN, $p = 0.45$. There was also no effect of the lower dose of nitrite on coronary artery CSA, +3.9%, $p = 0.30$. They also showed that GTN increased coronary blood flow vs baseline, +23.9%, $p = 0.02$ and lowered coronary resistance, -29.3%, $p = 0.02$. Whereas both low and high doses of nitrite did not significantly affect coronary blood flow or coronary resistance, $p > 0.05$. They also did not show any significant differences in SBP, DBP, or MAP in any of the interventions, $p > 0.05$. Thus, the group had demonstrated that nitrite dosing led to selective and dose-dependent epicardial coronary vasodilation in normoxia and postulated that systemic nitrite could act as a normoxia-dependent selective resistance vessel dilator (287). Whilst this study only had 9 subjects, these findings suggest that nitrite is capable of mimicking the effects of NO in the epicardial arteries, without changing coronary artery blood flow.

The O'Gallagher study was published during the 'Nitrite and Coronary Artery Study' (Chapter 5) and the findings informed our work and validated the scientific need to characterise whether the nitrite had vasoactive properties in the coronary arteries analogous to that seen in the systemic conduit arteries, figure 6. We also took the opportunity to test whether this mechanism was NO-dependent by testing in both normoxia and hypoxia (expecting NO-dependence to lead to greater vasodilation in hypoxia). Finally, as a proof of concept, we attempted to answer our scientific question using non-invasive CMR technology (namely temporal spiral phase velocity mapping) to show that the vasoactive properties of the coronary arteries can be examined in normoxia and hypoxia, safely and non-invasively, *in vivo* (Chapter 5).

9: Clinical applications of nitrite

Historically, organic nitrates have been used routinely in clinical medicine for centuries (288). As far back as 1847, the discovery of nitroglycerin and its ability to be rapidly converted to NO, led to a surge in scientific discovery, not only in explosives and propellants, but also in cardiovascular medicine. In Europe, by the 1860s, organic amyl nitrite was being used for its anti-anginal and vasodilatory properties, which led to studies of oral inorganic nitrite and recognition of its ability to cause sustained hypotension, to alter oxygen carrying capacity of blood and change its appearance (224). Organic nitrates (including sodium and potassium nitrate) were also used to treat angina pectoris until the mid-20th century, but became less favoured due to the appearance of case reports of methaemoglobinaemia caused by ammonium nitrate. Whilst these cases were rare and often had plausible explanations, their use declined nonetheless (224, 289).

Whilst dietary inorganic nitrate is generally safe, high dietary nitrite can be associated with methaemoglobinaemia, especially in people with glucose-6-phosphate dehydrogenase deficiency (G6PD deficiency) (290, 291). The G6PD enzyme is the terminal part of the Pentose Phosphate Pathway and if deficient this leads to reduced levels of 6-phosphoglucono-δ-lactone, NADPH and glutathione, which leads to accumulation of free radicals and increased oxidative stress and haemolysis. The G6PD / NADPH pathway is the only source of reduced glutathione in RBCs, therefore, in patients with G6PD deficiency, red cells are vulnerable to oxidation of haemoglobin and oxidant injury of the red cell membrane, resulting in significant haemolysis, which manifests as Heinz bodies in the blood film. Similarly, the inherited metabolic disorder, pyruvate kinase deficiency (the terminal enzyme in the glycolytic pathway) can also lead to RBC haemolysis as failure to complete glycolysis leads to deficient ATP, and as mature RBCs do not have mitochondria, they depend on anaerobic generation of ATP for most of their energy requirements (292).

A more generally applicable public health concern associated with high consumption of inorganic nitrites is the risk of carcinogenesis by nitrosamines. Nitrosamines are formed by reaction of secondary or tertiary amines with a nitrosating agent (usually nitrous anhydride, formed from nitrite in acidic, aqueous solution). Ascorbic acid (vitamin c) and sulfur dioxide are used to inhibit nitrosamine formation in foods (293). Foods which have been shown to contain volatile nitrosamines include cured meats, primarily cooked bacon, beer, some cheeses, non-fat dry milk and sometimes fish (293, 294). Whilst the evidence base supports a clear link between nitrosamine formation and human cancer (295-298), the association between nitrite consumption and human cancer is less clear.

Whilst a large systematic review, analysing 61 studies between 1985 - 2005 identified an association between nitrite and nitrosamine ingestion and gastric cancer (299) more recent reviews have specifically identified that in the absence of co-administration of a carcinogenic nitrosamine precursor, there is no evidence for nitrite consumption leading to gastrointestinal carcinogenesis (300). Interestingly, whilst the nitrate rich Mediterranean diet is supported by convincing data from large long-term cohort studies showing that higher level of adherence to the Mediterranean diet were associated with reduced risk of gastric cancer (301, 302), it also exceeds the WHO recommended maximum daily nitrate intake (3.7 mg/kg) by ~550% (169).

Indeed, it appears the association with cancer is more complex than nitrite ingestion alone. In a study assessing high intake of nitrite and nitrates in a cohort of people in Mexico City, Hernández-Ramírez and colleagues showed that these people were at a significantly increased risk of stomach cancer, but concomitant high intake of polyphenols (pears, mangos, beans, carrots, squash and legumes) protected from the development of gastric cancer (303). Taken together, the evidence suggests that the carcinogenicity of

nitrates/nitrites are subject to a variety of co-factors which determine the amount of nitrosamines and nitrosamides produced.

With over 130 years of medical experience, organic nitrate-based therapies can still be found in various forms in contemporary medicine and can be used to treat a wide range of cardiovascular conditions. Common applications include modified-release isosorbide mononitrate (ISMN) for stable angina and GTN infusions for acute LVSD. However, an important limitation to the use of organic nitrates, is that they are associated with tolerance and endothelial dysfunction (173). The exact mechanisms of this phenomena are not fully understood but are considered to be multifactorial and associated with vascular biochemical changes, physiological compensation, and possibly receptor regulation (304). The presence of less-favourable characteristics (such as tolerance and resistance) creates the need for an alternative therapy to either replace or work as an adjunct alongside nitrates in selected individuals.

In 2008, Maher and colleagues showed that inorganic nitrite promoted vasodilation in forearm resistance and capacitance vessels and that this process was augmented in resistance vessels during hypoxia (237). Also, in 2018, Webb and colleagues showed that dietary supplementation of nitrate (using beetroot juice) could substantially reduce MAP/BP. They also showed that the dietary nitrate load also prevented endothelial dysfunction induced by an acute ischemic insult on the human forearm (177). Both studies showed that nitrite has clear therapeutic potential (as both a vasodilator and an anti-hypertensive).

In 2013, Ingram and colleagues showed that during dobutamine stress echocardiography of subjects with inducible myocardial ischaemia, low-dose inorganic nitrite (1.5 μmol/min^{-1} for 20 minutes) improved functional responses in ischemic myocardium. They also demonstrated that when testing healthy subjects, nitrite could protect against vascular

ischaemia reperfusion injury when measuring forearm flow-mediated dilation during whole-arm ischaemia-reperfusion (305).

In 2014, Siddiqi and colleagues published a phase-2 study investigating the potential therapeutic role of intravenous nitrite in the management of acute myocardial infarction. The study was a double-blind, randomized, placebo-controlled trial of 229 patients, receiving intravenous administration of sodium nitrite (70 μmol, 5 min infusion) immediately before the reperfusion phase as a form of peri-conditioning in ST-elevation myocardial infarction (STEMI) patients. They showed that there were no significant changes in the infarct size (assessed by CMR) both 6-8 days and 6 months post-event (306), or in the areas under the curves for Creatine Kinase and Troponin. Whilst being a negative study, benefit was observed in diabetic patients in a post-hoc analysis, raising interest in the role of nitrite in those with endothelial dysfunction.

In 2015, Omar and colleagues showed that nitrite selectively dilates conduit arteries at supra-physiological and near-physiological concentrations of oxygen via a normoxia-dependent mechanism that is associated with cGMP production and is enhanced by acetazolamide and raloxifene. They showed that this effect was abolished during hypoxia and hyperoxia (280). In the same year, Jones and colleagues published a phase-2 study investigating the effects of intracoronary infusion of sodium nitrite (1.8 μmol) or matched sodium chloride placebo prior to balloon dilatation in 80 STEMI patients. They reported no change in infarct size (as determined by MRI) or CK or troponin T levels. However, they did show an improvement in myocardial salvage index and a lower number of major adverse cardiac events (MACEs) recorded 1-year post-procedure (307). However, these were post-hoc analyses and must be considered hypothesis generating. To date, other groups have been unable to corroborate the findings in this study.

Considering the historical perspective and weighing up the discussed evidence with respect to safety and clinical efficacy, nitrite presents itself as a unique compound with therapeutic potential. Defining the underlying mechanisms of action of nitrite-mediated vasodilation in normoxia could help us to understand the capabilities of nitrite as a potential therapeutic option (131, 308-310).

10: Overall hypotheses

Chapter 3:

i. In normoxia, inorganic nitrite will induce PKG1α dimerization/oxidation via a NO-independent mechanism and initiate vasodilation predominantly in the resistance vessels.

Chapter 4:

i. In normoxia, we hypothesise that nitrite may be operating largely via a NO-independent process (as demonstrated *in vitro* in Chapter 3), therefore we expect that the addition of autologous whole blood will have a much lesser effect on inorganic nitrite-induced forearm vasodilation

ii. In hypoxia, given that nitrite-mediated vasodilation is known to be augmented and thought to be mainly due to NO release, we expect that the addition of autologous whole blood will reduce the degree of inorganic nitrite-induced forearm vasodilation.

Chapter 5:

i. In normoxia, inorganic nitrite will increase epicardial (conduit) coronary artery CSA and assuming flow is constant, this will lead to a reduction in velocity (according to the Hagen–Poiseuille equation)

ii. In hypoxia, hypoxic-augmentation of inorganic nitrite-mediated vasodilation in the epicardial coronary arteries will lead to increased effects on CSA and velocity vs normoxia.

CHAPTER 2: METHODS

1: Basic sciences

Animal welfare

The work described was completed using an animal licence (number PPL 30/2797) registered to Dr Melanie Madhani. All experimental procedures were reviewed and approved by the local Animal Welfare and Ethical Review Body (AWERB) and the UK Home Office. The study was conducted according to the Animals (Scientific Procedures) Act 1986 (ASPA) and European Commission guidelines. DNA from mouse ear clippings were extracted, amplified using polymerase chain reaction (PCR) and separation through electrophoresis. Genotyping ensured all mice used in this study were correctly identified as either homozygous PKG1α WT or homozygous C42S PKG1α KI.

Tension wire myography

Tension wire myography was performed using a four chamber multi-myograph 610M (Danish Myotechnology, Denmark [DMT]), connected to PowerLab 4/35 (AD Instruments, UK). Data was collected with LabChart Pro Software (AD Instruments, UK), which included the DMT Normalization Module, enabling determination and setup of pre-experimental conditions for the tissue. The methodology for performing tension wire myography is summarized in the flow chart below, figure 9.

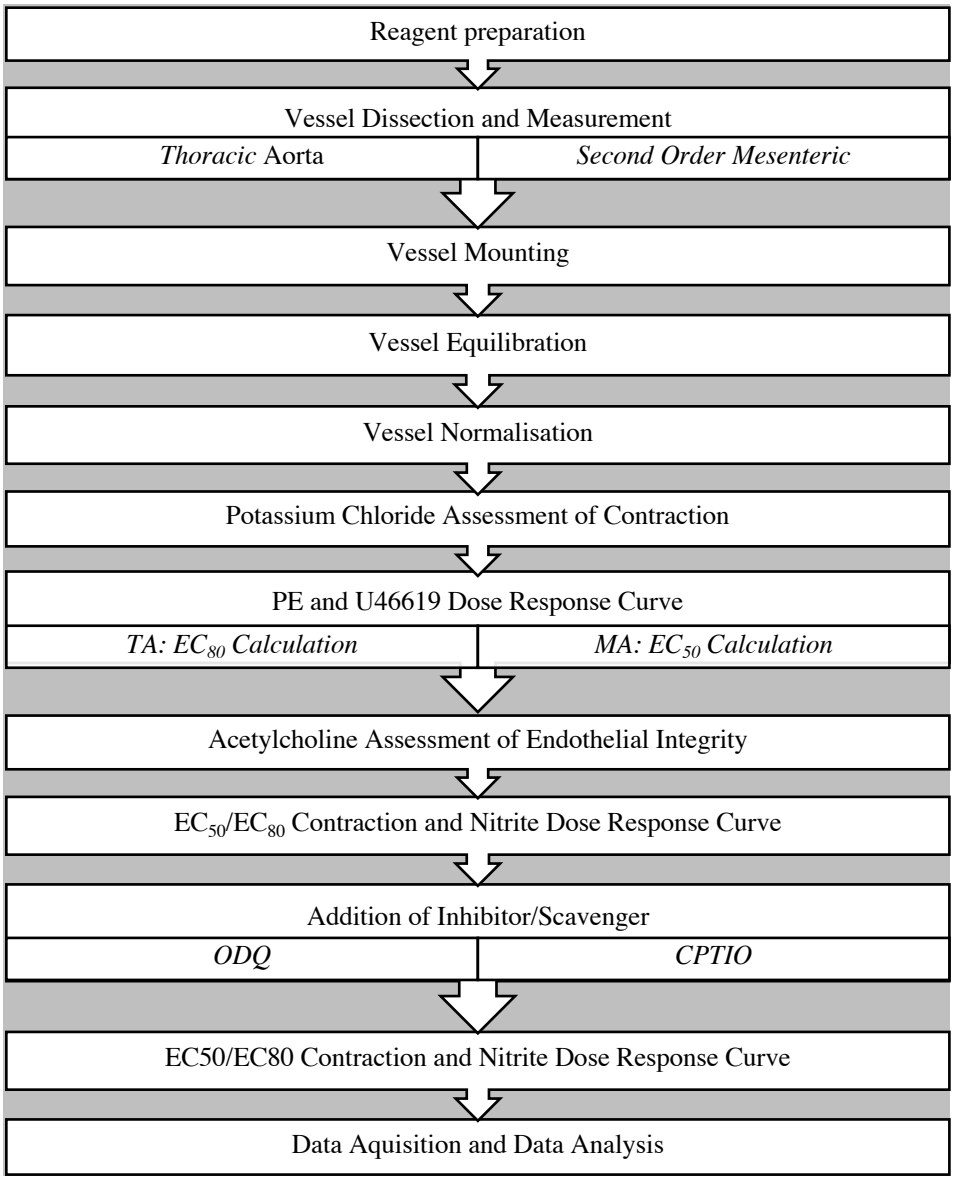

Figure 9: Tension wire myography methodology flow chart

Preparation of Krebs-Henseleit Buffer (KHB)

KHB was prepared each morning as previously described (311). Reagents required (table 1) were added in succession to distilled water and the solution was gassed with 95% O_2 / 5% CO_2 for 15-minutes prior to addition of $CaCl_2$.

Table 1: Concentrations (mM) of reagents used to make standard KHB

Reagent	Concentration (mM)
NaCl	118.5
$NaHCO_3$	25
KCl	4.7
KH_2PO_4	1.2
$MgSO_4$	1.2
Glucose	11
$CaCl_2$	1.4

NaCl: sodium chloride, $NaHCO_3$: sodium bicarbonate, KCl: potassium chloride, KH_2PO_4: potassium phosphate, $MgSO_4$: magnesium sulfate, $CaCl_2$: calcium chloride

Vessel dissection, mounting and measurement

Adult male Cys42Ser PKG1α WT and KI mice (25-30 g) were anaesthetized via an intraperitoneal (IP) injection of sodium pentobarbital (100 mg/kg) and heparin (100 mg/kg) in a 50:50 ratio. Conduit vessel (thoracic aorta) and second-order mesenteric resistance arteries were carefully isolated and extracted from the mice and immediately transferred into ice-cold, freshly gassed KHB. Vessels were cleaned from adhering connective tissue and cut into 2-3 segments (1-2 mm in length), in preparation for mounting. In thoracic aorta, 2 x 40 μm diameter stainless steel wires were passed through the vessel lumen. Both ends of the threaded wire were attached to the jaws of the myograph. For second-order mesenteric resistance vessels, a wire with a diameter of 25 μm was used. Once the vessel was attached to the jaws of the chamber, the KHB was exchanged and the chamber placed on the myograph. Vessel length was calculated by multiplying the observed divisions on a microscope reticule lens by the lens objection. Normoxia was replicated by applying 95% oxygen/5% carbon dioxide at a rate of 2 litres/min^{-1}. The temperature of all chambers was maintained at 37^{o}C throughout the study protocol.

Vessel equilibration and normalisation

Each vessel underwent a 40-minute equilibration period. During this time, the KHB was exchanged and the resting tension was reset to zero every 2-3 minutes. Tension was initially set upon mounting and reset in a step-wise fashion at chosen intervals on the micromillimeter scale using DMT normalization module on LabChart in order to stretch the vessels to optimal lumen diameter and therefore active tension. An exponential curve was plotted to fit the internal circumference pressure data to allow the stretch of the vessel to calculated (312). Following normalisation, another 20-minute equilibration period was set.

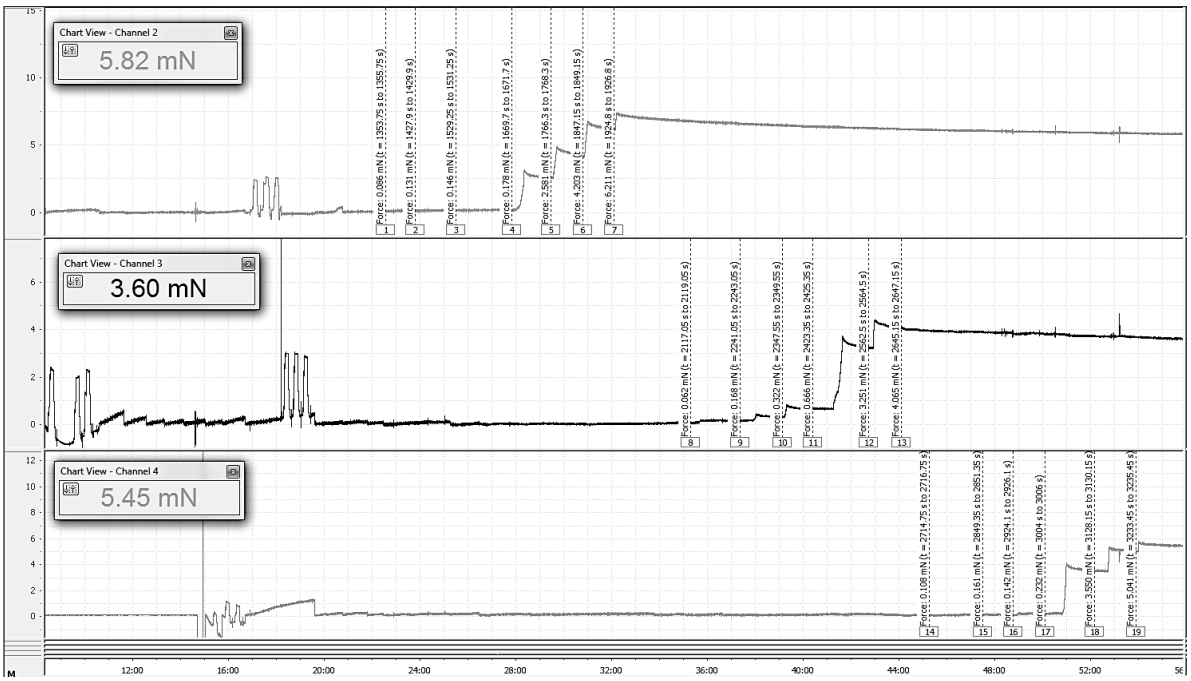

Figure 10: Vessel normalisation showing basal tension and incremental contraction to target optimal passive tension in 3 vessels, measured using LabChart Pro Software (AD Instruments)

Potassium chloride (KCl) assessment of contraction

Following 20-minute equilibration, the vessels were primed with 4.8 mmol potassium chloride (KCl) to stimulate smooth muscle contraction. A positive plateau demonstrated that the studied vessel was vasoactive and therefore suitable for further assessment. If no

response was observed, the vessel was repeatedly washed with KHB and challenged with KCl. If after the second test no contraction was observed, the vessel was excluded from further assessment.

Dose response curves

Cumulative concentrations of phenylephrine PE (thoracic aorta) or thromboxane mimetic U46619 (mesenteric resistance arteries), were added to the baths to construct a concentration response curve (10^{-9} to 10^{3*-6} M). This enabled the calculation of PE 80% maximum contraction (EC_{80}) or U46619 50% maximum contraction EC_{50} (Pinder and James, 2009).

Acetylcholine (ACh) assessment of endothelial integrity

Vascular tissue was then washed three times with fresh KHB and equilibrated for a further 30-minutes until basal tone was reached. The vessels were then contracted to either $EC_{80/50}$, and 5 μl of ACh (concentration 10^{-5} M) was added to each bath to assess integrity of endothelium of vessels. If relaxations elicited by ACh were <50% the tissue preparation was discarded.

Contraction (EC50/80) followed by nitrite dose response curve

PKG1α WT vessels were then washed again with KHB before increasing cumulative concentration of PE or U46619 were added to enable vasoconstriction to either $EC_{80/50}$. Once the response was stable, under normoxic conditions, a cumulative concentration response curve to sodium nitrite was constructed (10^{-9}-10^{-4} M). The vessel reached a negative stable plateau before adding the next cumulative concentration. We also tested vessels with the NO donor, Spermine NONOate (data not shown) to assess NO-mediated vasoactive effects, as per previous work (199, 311, 313), however this work was focused on investigating nitrite-mediated vasodilation in normoxia, specifically NO-dependency, so work with this NO donor was not pursued. Incubation was performed with a sGC inhibitor (1H-

[1,2,4]oxadiazolo-[4, 3-a]quinoxalin-1-one (ODQ); 10μM; (184) and a NO scavenger (2-4-carboxyphenyl-4,4,5,5-tetramethylimidazoline-1-oxyl-3-oxide (CPTIO); 1μM; (184). To evaluate the role of PKG1α oxidation, vascular myography was repeated in the Cys42Ser PKG1α KI mice. Nitrite concentration response curves were constructed in both the conduit and mesenteric resistance vessels (131).

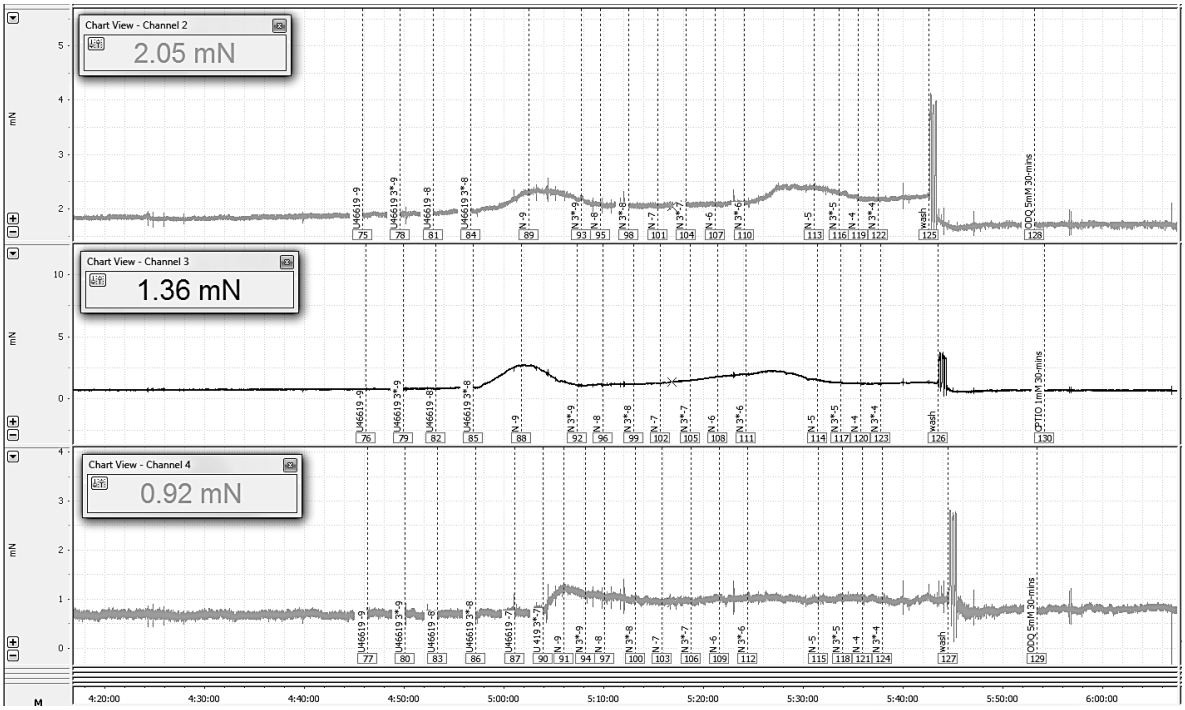

Figure 11: Contraction (EC50/80) followed by Nitrite dose response curve, measured using LabChart Pro Software (AD Instruments)

Data capture and myograph close down procedure

After data was recorded using LabChart Pro Software (AD Instruments, UK). Data was securely saved to the University of Birmingham shared drive. Chambers were repeatedly cleaned with 5ml 5% hydrochloric acid.

Statistical analysis

All data shown as mean (±SEM). Curves were plotted in log [M] form. To assess % relaxation, treatment conditions (e.g. WT or KI +/- CPTIO or ODQ) were analysed using

two-way ANOVA followed by Bonferonni post-hoc tests, in which the significance level was $p<0.05$. Statistical analysis was undertaken using Prism (GraphPad software San Diego, CA, USA).

Additional methods

Additional methods including western blotting and IP nitrite administration were completed by researchers within the Madhani research group to complete the research presented in Chapter 3 and in the associated publication (Appendix 2) (131). Briefly, to translate the myography work into the *in vivo* setting, WT C57BL/6 mice underwent IP injection with either placebo, nitrite 0.1mg/kg, nitrite 1mg/kg, or nitrite 10mg/kg. To minimise chronobiological variation, the mice were culled either at 1-hour or at 24-hours after the IP injection and aortic conduit and mesenteric resistance vessels were extracted, snap frozen and western blotted for Glyceraldehyde 3-phosphate dehydrogenase (GAPDH) (loading control) and PKG. Plasma samples were also taken to show the plasma concentration of nitrite at each of the dosing conditions. As shown the associated publication (131), nitrite plasma levels at 1 hour and 24 hours were ~1M in the placebo, nitrite 0.1mg/kg, and nitrite 1mg/kg dosing conditions. Whereas, in the nitrite 10mg/kg dosing condition at 1 hour, nitrite plasma levels were ~5M. At 24 hours, this value had returned to near baseline despite persistent BP reduction. These data were consistent with work by Bryan and Perlman, who each showed that IP nitrite administration in rats led to rapid increases in plasma nitrite levels, which returned close to baseline values at ~1 hour but also led to major, long-term perturbation of cardiac redox tone (314, 315).

Importantly, the plasma nitrite concentrations reported in the associated publication (131) were very similar to the concentrations achieved during the myography experiments, figures 21 – 23, therefore the data presented in figure 24 can be directly compared to figures 21 – 23 with respect to the concentration of nitrite present and the timing of PKG1α dimer

formation. The PKG monomer band was located at 75kDa and PKG dimer band was located at 150 kilodalton (kDa). Additional details of these methods can be found in the publication associated with Chapter 3 (131) (Appendix 2). The study results and discussion are presented in Chapter 3.

2: The Haem and Nitrite Study

Study design

This study was a single-centre, pharmacodynamic, random order, cross-over trial investigating the physiological vasoactive effects of an intra-arterial inorganic nitrite infusion following a 30-35-day stored autologous whole blood transfusion in normoxia and hypoxia. This study took place at the Norfolk and Norwich University Hospital (NNUH), Norwich, UK. The Haem and Nitrite Study flow chart is summarised below, figure 12.

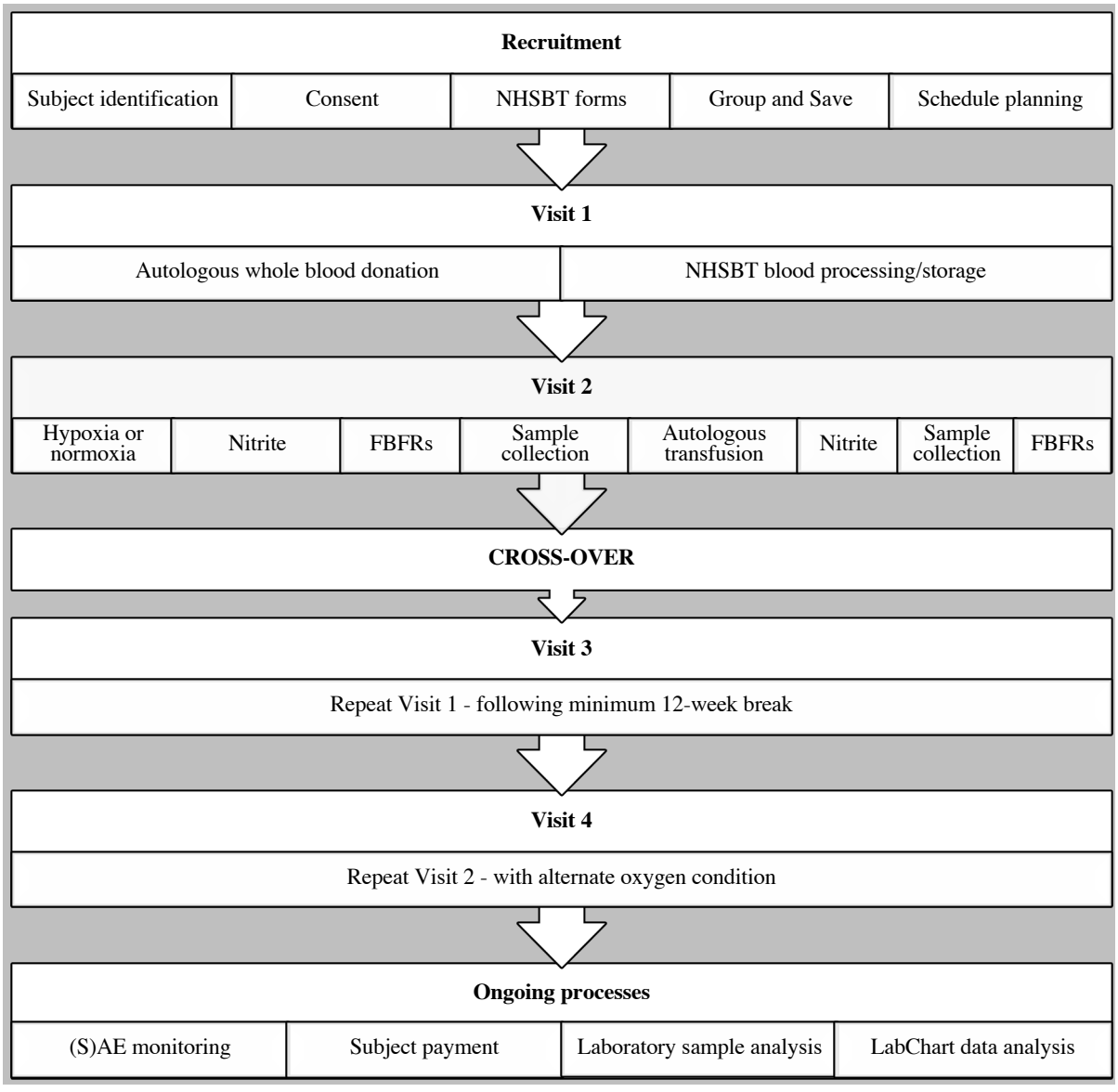

Figure 12: The Haem and Nitrite Study - General study schematic

Power calculations

Applying the assumed mean and standard deviations from previous published works (237, 260) it was calculated that to achieve 80% power, statistical significance of 10% (one-sided 5%, as only interested in one direction of effect, i.e. increase in FBFR) and effect size of 0.40, we would require 41 participants to complete the study (Stata 14). The primary endpoint was change in FBFR during intra-brachial nitrite and haemolysed blood co-infusion in normoxia versus hypoxia. Due to the complexity of the study, we anticipated attrition rates of up to ~40% and recruited 60 healthy subjects.

Regulatory and ethical processes

The protocol was submitted to the Medicines and Healthcare products Regulatory Agency (MHRA) on 23rd September 2015. On 30th September 2015, we were notified that the study was not a Clinical Trial of an Investigational Medicinal Product (non-CTIMP) as defined by the EU Directive 2001/20/EC and therefore no submission to the Clinical Trials Unit at the MHRA was required.

The University of East Anglia (UEA) was the study sponsor. A full suite of documents was submitted for initial Research Ethics Committee (REC) consideration on 21st April 2016. I attended the REC meeting on 5th May 2016 (East of England – Essex REC). The REC requested additional information on 9th August 2016. Additional information was provided to the REC on 15th August 2016. On 5th September the REC provided favourable opinion. Three substantial amendments followed between October 2016 and July 2018 adding a senior clinical team member, clarifying a technical detail in the protocol and increasing our recruitment pool. The REC sub-committee gave a favourable ethical opinion on the basis of each described notice. The study was registered on the clinicaltrials.gov website: NCT03077763.

Recruitment

Subject identification

Recruitment was via the UEA e-Bulletin systems distributed to the School of Medicine staff, followed by 'all-schools' (to both staff and students). Recruitment was also via the NNUH in-house 'This Week' bulletin. Lastly, we approached research-active subjects via the UEA's Cognitive Ageing Nutrition and Neurogenesis (CANN) trial research database led by Professor Anne-Marie Minihane.

Once the clinical research team had received contact from an interested participant, we completed an assessment of eligibility and distributed the participant information sheet (PIS). If the subject chose to proceed, key information was collected to identify the individuals National Health Service (NHS) hospital records. If a record did not exist, an NHS number was allocated and a record created using the Patient Administration System (PAS). All records were kept pseudo-anonymously and the owner of records was known only to the lead research fellow. All processes were documented in the participants NHS clinical notes, as per Good Clinical Practice (GCP) Guidelines (316).

Inclusion and exclusion criteria

No exceptions to the stated eligibility criteria were permitted. If in any doubt the Chief Investigator (CI) was asked to provide advice about inclusion/exclusion in the study.

Inclusion criteria

1. Male or female, aged ≥18-years - If between 18-20 years of age, calculated total blood volume should be more than >3.5L (317)
2. Female subjects must be of non-childbearing potential, defined as follows: postmenopausal females who have had at least 12-months of spontaneous amenorrhea or 6-months of spontaneous amenorrhoea with serum follicle stimulating hormone

(FSH) >40mIU/ml or females who have had a hysterectomy, bilateral salpingectomy or bilateral oophorectomy at least 6-weeks prior to enrolment

3. Body weight >50kg weight (8 stone 12lbs)
4. Not known to have any significant past medical history (assessed by research team) and not having regular follow up
5. Baseline observations (BP and heart rate) within normal parameters and pulse oximetry saturations above 94%
6. Willing to provide blood donation and receive autologous whole blood transfusion
7. After assessment for eligibility - pass all blood donor eligibility criteria
8. Able to provide informed written consent
9. Should inform overseas travel plan during study period (Check Geographical Disease Risk Index on www.transfusionguidelines.org.uk/dsg/gdri) e.g. unable to donate blood for 6 months if travel in a malaria endemic country. Similar guidelines for West Nile virus and T. Cruzi endemic countries.

Exclusion criteria

1. Significant medical, surgical or psychiatric disease that in the opinion of the lead research fellow would affect subject safety or significantly impact his/her ability to comply with follow-up (including any known clotting disorders)
2. Known allergy or intolerance to nitrites
3. Known glucose-6-phosphate dehydrogenase (G6PD) deficiency or G6PD deficiency measured at screening in males of African, Asian or Mediterranean decent
4. Receipt of an investigational drug or biological agent within the 4-weeks prior to study entry or 5-times the drug half-life, whichever is longer
5. Predisposed to acute on chronic limb ischemia evident from a history of claudication or known peripheral arterial disease
6. Past history of significant adverse events post-blood donation.

Consent, NHSBT donation forms, group and save and study scheduling

If participants were suitable for inclusion, they were invited to a face-to-face assessment at the NNUH clinical research and trials unit (CRTU) which included completion of fully informed written consent, completion of the 'Donor health check for new and returning donors' form (FRM form 421/6, Appendix 3i) and the 'Autologous blood pre-donation assessment' form (FRM 1560/4, Appendix 3ii), and completion of the first group and save blood test. A group and save blood test was processed by the NNUH laboratories and results were provided to the blood bank and the research team.

After the assessment clinic, the 'Pre-deposit autologous blood donation memorandum' (FRM 1563/1.4 – cross referenced in primary document SOP 3968, Appendix 3iii) was completed and was sent to the NHSBT clinical support team (CST). The NHSBT CST was notified and the subject was registered and scheduled for autologous donation.

Study visit 1

Autologous whole blood donation

The clinical research team and the NHSBT CST ensured all involved staff were trained according to SOP3968 which was uniquely created for this study (Appendix 3iv - Change Control [6422] Process Flow). The research/NHSBT team performed a clinical risk assessment and the following actions were implemented throughout this study to minimise the risk of clinical harm:

1. A separate panel was set up and these donors were registered as autologous donors so that the product had a different product code
2. The pre-attached pack label detailing the patients name was completed by session staff and adjudicated by the study participant
3. Autologous pre-donation form was completed by session staff and packed with the donation in a separate transport box/bag

4. The autologous donation was quarantined in a locked container whilst in transit
5. Only identified supervising NHSBT and NNUH staff were permitted access to handle the autologous donation at any time.

All donations were collected at two pre-determined NHSBT blood donation sites (Fakenham Community Centre and Wymondham Village Hall) both of which were under the supervision of Sister Patsy Lowson (NHSBT, Thetford Donation Team), figure 13. Donations followed all standard practices to ensure safety throughout.

Figure 13: Healthy volunteer undergoing autologous whole blood donation. Images produced with permission of the participant.

NHSBT blood processing and storage

Operational aspects of this study were implemented with expert guidance of Dr Suhail Asghar (NHSBT, Associate Specialist). Processing took place at the NHSBT Filton site and storage at NHSBT Cambridge site. Blood was requested 3-4 days before use via the NNUH blood bank using the 'non-standard product request form'. Blood was delivered on the next

routine transport to the NNUH blood bank. Blood was stored, separated from normal supply chain units in the NNUH blood bank until it was issued by a designated member of the NNUH blood bank staff to the research team. Enrolled participants were advised to follow a nitrate/nitrite low diet for 2 days prior to visits 2 and 4. Participants were provided with an information sheet detailing the foods they should avoid.

Study visit 2

On visits 2 and 4 of the study, each subject underwent a structured clinical study protocol, figure 14. In the given study. We elected to use 2 x 30-minute intra-arterial nitrite infusions, at 2 different doses (depending on oxygen condition being studied), rather than a continuous infusion throughout the study. There were several considerations that enforced this decision. Firstly, we had a fixed number of 'time-limited' CRTU slots per month (because the facility was supporting a host of other studies). As such, each clinical visit was time-limited and we were not able to wait the amount of time required (reported by some to take ~12 hours) (175) (318) to gain a steady-state of plasma nitrite.

Next, we decided to test each subject's response to nitrite at full dose, before starting blood, as we recognised from previous work studying FBFRs in normoxia that there is significant inter-subject variability (237) and collecting FBFR data in the absence of blood was important to enable us to answer our scientific hypothesis (with respect to NO-dependency). Therefore, in this situation, the two alternative options would have been to run a single, longer steady-state infusion, or 2 separate steady-state infusions, which as discussed above, would have further extended the clinical schedule beyond what was possible.

A final but central consideration in our decision making was that whilst our clinical schedule was planned to last ~3hours, we realistically (and correctly) recognised that these sessions would last much longer, due to factors associated with performing complex clinical research

as a sole researcher in a busy NHS environment. For example, it could take up to 1 hour for the pharmacy to dispense the study drug (but this was only possible for research prescriptions between 10am-3pm) and it could take >3 hours for the blood bank to cross-match and release the autologous unit (based on clinical service demand) – which was often the case. Most study visits lasted >5 hours and subjects were simply not able to tolerate any extension to this duration. The clinical schedule was already long and highly invasive for healthy volunteers, with subjects being bed-bound for the duration (and unable to use the bathroom), so we did not feel it was appropriate or ethical to extend the duration of visits unless absolutely critical.

We recognised that given that the half-life of nitrite in plasma is reported to be between ~35-45 minutes (319-321) and even shorter in whole blood (322), if we administered a 30-minute infusion, as shown as infusion 1 (N1 or H1) below, we would expect to see between 12.5-25% carry over and elevation in the baseline measurements of NOx/RXNO at the point of initiating infusion 2 (N2 or H) (taking into account the 10-minute period [in which saline was infused at 1 ml/min to keep the arterial line patent and equilibrate the vessel] and the first 90-minutes of the 120-minute blood transfusion). Whilst a continuous steady-state infusion may have avoided this, we recognised that if we repeated NOx/RXNO levels at sample collection 3, we could statistically correct the baseline, when comparing the results in infusions 1 and infusions 2. The correction was performed as described in the 'Statistical analysis' section below. We accepted that this post-hoc adjustment was an acceptable trade-off, and this is the rationale for the clinical schedule as shown in figure 14.

Given the complexity of the study design, to aid explanation of results and discussion, the following figure adopts labels for nitrite infusions (N1, N2, H1, H2), key sample collections (Normoxia/Hypoxia 1-4), and also FBFR time points (T0-T30) to enable clear comparations and discussion, figure 14. These labels will be used throughout the results and discussion.

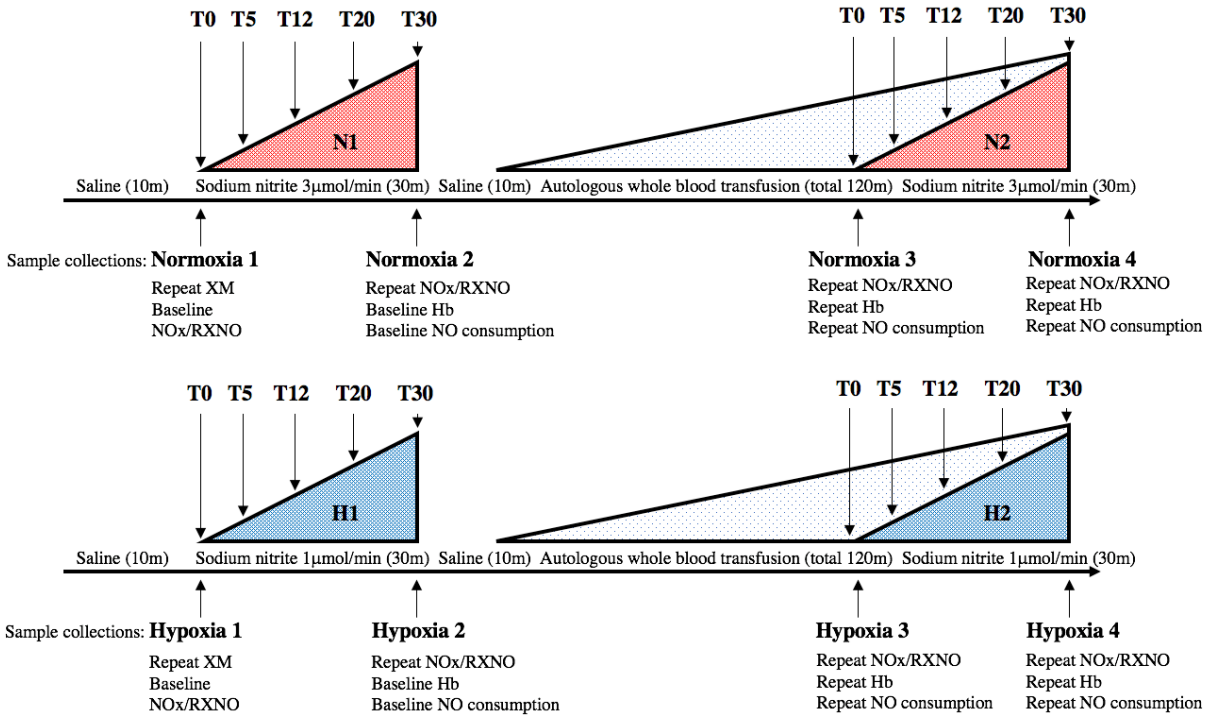

Figure 14: The Haem and Nitrite Study – Clinical intervention schematic. Note: time durations of each stage shown in brackets. Key - N1: first nitrite infusion in normoxia, N2: second nitrite infusion in normoxia, H1: first nitrite infusion in hypoxia, H2: second nitrite infusion in hypoxia, T0: plethysmography FBFR at time 0 mins, T5: FBFR at 5 mins, T12: FBFR at 12 mins, T20: FBFR at 20 mins, T30: FBFR at 30 mins. Normoxia 1: first sample collection timepoint in normoxia (baseline), Normoxia 2: second samples collection timepoint in normoxia (repeat), Normoxia 3: third samples collection timepoint in normoxia (repeat), Normoxia 4: forth samples collection timepoint in normoxia (repeat), Hypoxia 1: first sample collection timepoint in hypoxia (baseline), Hypoxia 2: second samples collection timepoint in hypoxia (repeat), Hypoxia 3: third samples collection timepoint in hypoxia (repeat), Hypoxia 4: forth samples collection timepoint in hypoxia (repeat).

Equipment preparation and subject preparation

All equipment was prepared in advance and maintained by the research team. One hundred 27-gauge needles were individually autoclaved (55 autoclave series, Tuttnauer, UK), then

individually attached to a sterile epidural catheter (Portex®, Smith's Medical, UK) using sterile dental wax (Kemdent, Swindon, UK) and an open flame (Fireboy, Intergra UK and CV 470 plus Butan/Propan) maintaining sterility throughout.

The participant was admitted to the NNUH CRTU using PAS, enabling the research team to access acute medical support in the case of a medical emergency and also to utilise the Integrated Clinical Environment (ICE) system to send the cross-match and order the autologous whole blood unit from the NNUH blood bank. All plethysmography sessions were performed in the NNUH CRTU providing a quiet, temperature-monitored environment (optimally maintained between 22-26°C) to ensure consistency and reduce variation of forearm blood flow due to extremes of temperature.

On arrival, subjects were interviewed and a focused clinical history was taken (to ensure they remained eligible), they were issued with an identification wristband (used later for blood tracking) and had a second cross-match blood test sent in-line with the research protocol. Participants were asked to lie at a slight incline and they had their forearm width measured to allow for the correct strain-gauge to be selected. The participant had a Hokanson SC5 tourniquet cuff (Hokanson, UK) attached around each wrist. Participants also had a Hokanson SC10 straight segmental cuff (Hokanson, UK) attached around each upper arm. A 20-gauge cannula was placed in either the basilic or cephalic vein at the level of the antecubital fossa of the dominant arm (used for blood-letting and administration of the autologous whole blood transfusion).

The antecubital fossa of the non-dominant arm was palpated carefully to locate the brachial artery and the best point for puncture. The selected site was anaesthetised with 2-3mls of 1% lidocaine and the 27-gauge needle was placed into the lumen of the brachial artery, figure 15. This needle was kept patent by the continuous infusion of clinical grade 0.9% sodium

chloride at a rate of 1 ml/min^{-1}. Brachial artery cannulation was performed by the lead clinical research fellow throughout the study. Comprehensive training in brachial artery cannulation had been provided by Professor Phil Chowienczyk's team at the St Thomas' Department of Clinical Pharmacology, London.

The brachial needle site was left exposed (no dressing) so that the site could be observed throughout the experiment, reducing the risk of unintentional removal or disconnection. In the event of difficulties gaining arterial access senior support was available from Dr Simon Fletcher (Critical Care Consultant) and Dr Vassilios Vassiliou (Cardiology Consultant).

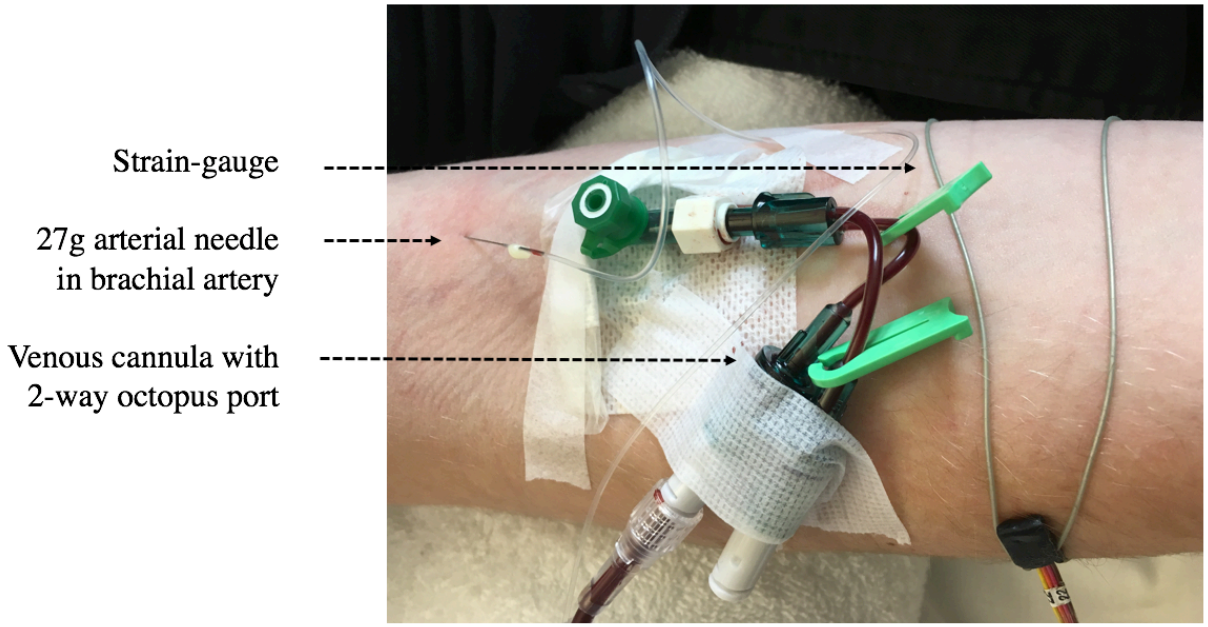

Figure 15: Brachial artery cannulation. Note: the 27-gauge arterial needle was located in the dominant arm at the request of the participant, thus the venous cannula can also be seen located in the basilic vein. Images produced with permission of the participant.

Study drug administration

The study drug was inorganic sodium nitrite 100 µmols in 0.9% sodium chloride 10 mls and was supplied by Tayside Pharmaceuticals (Ninewells Hospital & Medical School, Dundee, UK). Intra-brachial nitrite infusions were administered at a rate of 3 µmol/min^{-1} for 30-

minutes in the normoxic group and a rate of 1 μmol/min^{-1} for 30-minutes in the hypoxic group. This was based on 50% effective dose (ED_{50}) values, taken from previous work, conducted by a previous clinical research fellow of the primary supervisor (237, 323). In this paper, Maher showed that 3.14 μmol intra-brachial nitrite infusion over 20-minutes led to an increase in FBFR x 1.8. He showed that when he gave a higher dose (7.84 μmol) that this effect was reduced (FBFR x 1.6). Maher and colleagues also showed that nitrite in hypoxia (12% oxygen/88% nitrogen) led to ~ x 3 increase in FBFR. The selected doses allowed us to compare percentage change in each oxygen condition as both doses were operating in the middle of the dose response relation.

On each study day, the lead clinical research fellow prescribed the study drug, autologous whole blood transfusion unit and 250 mls of clinical grade 0.9% sodium chloride on the study specific prescription chart (Appendix 4i). If subjects were <70 kg, we adjusted the dose according to weight. Before the infusion, a 10-minute period of saline (1 ml/min) was completed. This was firstly to keep the line patent, as the 27-gauge arterial needle would have occluded if we had not done this (324). Secondly, it provided a short equilibration period as arterial injury (such as puncture) would be expected to be associated with a transient increase in local NO (325), so this period allowed the vessel to return to basal tone, without undue extension of the study schedule.

During the infusion, forearm blood flow (FBF) was measured at baseline, 5, 12 and 20 and 30-minutes in both arms simultaneously to calculate the FBFR. A second intra-brachial nitrite infusion was commenced after 90-minutes (of the 2-hour) autologous whole blood transfusion and was given in exactly the same way as the first infusion. The timing of the second infusion coincided with the completion of the autologous blood transfusion. The FBFR recording schedule was identical to the first nitrite infusion.

Medical gas: 12% oxygen/88% nitrogen

The medical gas used to achieve hypoxia during the hypoxic experiments in this study was a composition of 12% oxygen/88% nitrogen (BOC, The Linde Group, UK). Stock control and ordering of these study specific cylinders was managed by the research team. The study specific cylinders were clearly labelled and when not in use, securely locked in the CRTU facility. During hypoxic experiments, medical gas was prescribed on the study-specific prescription chart (Appendix 4i) and administered via a simple face mask, attached to gas flow regulator (Therapy Equipment Ltd, UK) and attached to the study-specific cylinders. During hypoxic experiments, oxygen saturations were monitored via pulse oximetry (Nellcor N-180, Nellcor, Pleasanton, Calif) and the flow rate was adjusted (range 0L/min^{-1} to 15L/min^{-1}) to maintain target saturations of between 83-88% O_2 (estimated pO_2=47.5 to 55 mmHg, based on Severinghaus' equation) (326). If after 5-minutes target saturations could not be achieved (235), hypoxia measurements continued as per protocol (and subjects were identified as compensating). If hypoxia was not well-tolerated, 100% high-flow oxygen was available to be administered to reverse hypoxia.

Autologous whole blood transfusion

Participants received autologous whole blood transfusion (volume ~500 mls) via the intravenous cannula situated in the antecubital vein in the dominant arm (NNUH Trust guidelines CA4029 v3, CA1026 v10, CA1027 v10, CA2057 v5, Care Domain 4 v2.1). The unit was transfused over a 2-hour period and was administered exactly according to Trust procedures in-line with the study protocol. Each transfusion unit was checked carefully using a detailed checklist before transfusion (Appendix 4ii). Participants underwent bedside observations (tympanic temperature recording and haemodynamic measurements) during the transfusion in-line with Trust procedures. The overall experimental set-up for the Haem and Nitrite study can be seen in figure 16.

Figure 16: The Haem and Nitrite Study - Experimental set up. Key – A: Arterial infusion pump, B: 12%oxygen/88%nitrogen cylinder with tubing and mask, C: SC10 cuff, D: 27g brachial arterial needle, E: SC5 cuff, F: Autologous whole blood transfusion, G: Blood pump, H: Plethysmography recording stack (PC/laptop, EC6 Plethymograph x 2, PowerLab, E20 Rapid Cuff Inflator x 2), I: Observation stack. Images produced with permission of the participant.

Blood sample collection

Throughout the 'clinical intervention schematic', Figure 14, blood was taken from the intravenous cannula in the non-dominant arm at 4 time points:

Sample collection 1:

1. Repeat group and save
2. Baseline NOx and RXNO levels

Sample collection 2:

1. Baseline cell-free haemoglobin levels

2. Baseline nitric oxide consumption levels
3. Repeat NOx and RXNO levels

Sample collection 3:

1. Repeat cell-free haemoglobin levels
2. Repeat nitric oxide consumption levels
3. Repeat NOx and RXNO levels

Sample collection 4:

1. Repeat cell-free haemoglobin levels
2. Repeat nitric oxide consumption levels
3. Repeat NOx and RXNO levels

Venous NOx and RXNO levels were taken into 4ml EDTA tubes, supplemented with N-Ethylmaleimide (NEM, 1 mM final concentration) and immediately centrifuged (2000 rpm for 10-minutes at 4°C) and snap frozen using liquid nitrogen. Samples were stored at -80°C. Cell-free haem and NO consumption assay samples were collected into 4ml EDTA tubes, not supplemented with NEM.

Strain-gauge plethysmography: forearm blood flow ratios (FBFRs)

FBF was measured in both arms using standardised practices which are validated and described in detail in the literature (327-329). The ratio of FBF in the infused arm vs. control arm was expressed as 'FBFR'. The main processes are summarised as follows. Bilateral Hokanson SC5 tourniquet cuffs (Hokanson, UK) were inflated to supra-systolic pressures during measurements to exclude the hand circulation (typically, 150-170 mmHg). Bilateral Hokanson SC10 straight segmental cuffs (Hokanson, UK) were inflated above the elbow to ~40 mmHg to occlude venous flow out of the limb at the time of measurement while not changing the rate of arterial inflow (327-329). Mercury-silastic strain gauges were placed on the widest part of the forearm bilaterally, as shown in Figure 16. A change in arm

circumference in response to infusion of drug or blood resulted in a change in strain gauge length and this was proportional to changes in forearm blood flow. Upper arm cuffs were inflated for approximately 10-seconds and deflated for 5-seconds and the flow measurements were recorded for 5 completed curves and the average of these was calculated. Measurements were simultaneously performed on both arms of each subject to allow for calculation of FBFR. These measurements were performed at the start of the study drug infusion, then at 5, 12, 20 and 30-minutes.

Data was visualised using LabChart 7.0 Life Science Data Analysis Software (AD Instruments, UK), Figure 17. As shown in Figure 14, subjects underwent 2 x 30-minute intra-arterial infusions per study visit. Whilst we recognise that the half-life of nitrite in plasma is reported to be between ~35-45 minutes (319-321) and even shorter in whole blood (322), given that we were administering the study drug at a steady state (either 3 μmol/min or 1 μmol/min), we would not expect to see pharmacological decay leading to any perceptible changes in forearm blood flow (figure 17). In addition, strain-gauge plethysmography paired with intra-brachial drug infusions are a well-established method, for measuring FBFR and it would not be expected for the operator to observe effects of decay, beyond that of the study drug half-life, on the LabChart trace (324, 329).

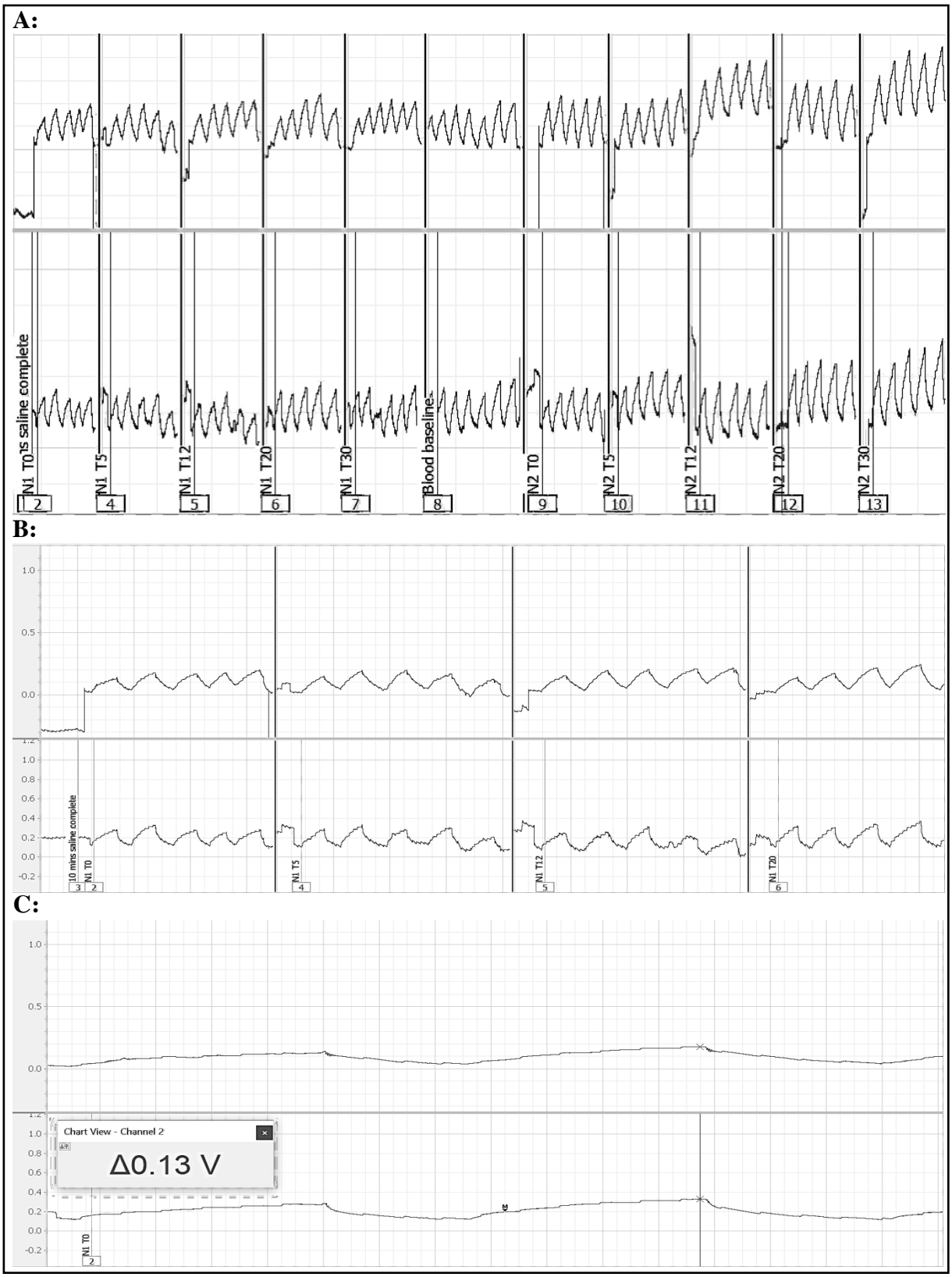

Figure 17: Example plethysmography trace (Channel 1: top trace, right arm, control, and Channel 2: bottom trace, left arm, intervention) during the normoxia study (Panel A), scaled to show multiple measurements taken at each time point to enable post-hoc calculation of mean FBFRs (Panel B). Note: All values were manually extracted (delta voltage, V) from

both arms simultaneously and care was taken to avoid 'inflation artefact' (Panel C). Taken from subject 27.

Study visit 3 & 4

Study visits 3 and 4 were identical to study visits 1 and 2 respectively.

Formalised discharge processes

A discharge checklist was used to assess several key aspects to promote safety and best practice, including reviewing puncture sites, haemodynamics and overall wellbeing at the end of the study visit. Participants were financially reimbursed for their time and travel. A fixed value of £50 was offered for attendance at visit 1 and completion of visit 2, and a further fixed value of £150 was offered for attendance at visit 3 and completion of visit 4. A maximum of £50 was offered for travelling to the donation and study sites (values to match train receipt/mileage).

S(AE) monitoring

Safety reporting was a continuous process and all adverse events were reviewed by the CI either at the point of identification or as soon thereafter as practicable. Definitions of harm of the EU Directive 2001/20/EC Article 2 based on the principles of ICH GCP applied to this study. Definitions of adverse events (AEs) are outlined in the study protocol. All adverse events associated to the use of autologous whole blood transfusion were reported to the Serious Hazards of Transfusion (SHOT) haemovigilance scheme (www.shotuk.org) and to the Serious Adverse Blood Reactions and Events (SABRE) scheme (www.aic.mhra.gov.uk) by the research team.

Sample and data analysis

Sample analysis was performed by Drs Magda Minnion and Bernie Fernandez, under the supervision of Prof Martin Feelisch at the University of Southampton, UK.

Laboratory sample analysis

Plasma nitrate and nitrite species via High Performance Liquid Chromatography [HPLC])

Nitrate and nitrite levels were determined by the method of combining a diazo coupling reaction (Griess reaction) with HPLC. These methods are described in detail in Appendix 5.

In brief, the appropriately pre-treated sample is injected onto the HPLC system and the sample is first filtered through the pre-column and then the NO_2^- and NO_3^- are separated on the analytical column, with NO_3^- being retained longer than NO_2^-. From the (analytical) separation column NO_2^- and NO_3^- elute into the reduction column and the following occurs:

- NO_2^- passes through the reduction column without any reaction and is then mixed with the reactor solution (Griess reagent) at a three-way joint. NO_2^- reacts with the acidified Griess reagent in the reaction coil and generates diazo compounds which have a pink/red colour. The level of diazo compound is measured by absorbance at 540 nm using a spectrophotometric detector.
- NO_3^- is reduced to NO_2^- by reaction with a cadium/copper alloy. NO_2^- derived from NO_3^- undergoes the same reaction as above.

The response of the detector is transformed to a voltage which it generates at the CPU (analogue output) terminal. The concentrations of NO_2^- and NO_3^- in the sample are measured by assessing the peak area of the absorption and comparing it to the peak of the absorption for the standards of known concentration.

RXNO was not analysed in this study. This decision was taken by the supervisors due to limited resources in the laboratory, further exacerbated by the Covid-19 pandemic. The

student was informed of this decision. For further details please see the letter written by the CI in Appendix 10.

Cell-free haem via enzyme-linked immunosorbent assay [ELISA])

Cell-free haemoglobin levels were determined using a human haemoglobin ELISA kit (Abcam, ab157707) and analysis was performed according to the manufacturer's instructions (https://www.abcam.com/human-hemoglobin-elisa-kit-ab157707.html).

In brief, all reagents are equilibrated to room temperature and prepared according to the manufacturer's instruction. Standard or samples are added to each well and incubated at room temperature. After which, wells are aspirated, washed, and HRP labelled secondary detector antibody is added and incubated at room temperature. The wells are again aspirated and washed. Chromogen substrate is then added to each well and colour recording is started using a GloMax Promega Microplate Reader.

NO consumption levels via ozone-based chemiluminescence

NO consumption levels were measured using previously described methods (274, 330). The only difference being that we used the ECO Physics CLD 77 am sp for NO detection and that the analogue signal was interfaced via an A/D converter to the PowerChrom software (eDAQ version 2.76, US).

In brief, NO was generated using DETA-NO (stock 100 mM ion 10 mM NaOH) in PBS (50 mM, 37°C), which produced stable levels in the range of 50-60 ppb NO. The system was calibrated using the triiodide-mediated reduction of nitrite and (negative) peaks from the NO-scavenging experiments were integrated, without prior inversion to positive peak, using the PowerChrom software (ignoring that the resulting peak areas produce negative numbers). Linearity of the responses was confirmed using oxyHb standards in the range of 1-100 μM.

Sample injection volumes were typically 20 μL, using a Hamilton syringe, with appropriate adjustments as necessary if samples were too hemolytic. 100 μL Antifoam was added to 13 mL of PBS (containing DETA-NONOate) in the reaction chamber to minimise foaming. Control experiments with plasma from three different individuals confirmed that NO scavenging was linearly dependent on sample volume injected into the reaction chamber.

LabChart data analysis

All data was extracted from LabChart 7.0 Life Science Data Analysis Software (AD Instruments, UK) anonymised and analysed using Microsoft Excel, version 18, 2018 (Microsoft Corporation, US). In a small proportion of cases the slopes varied very considerably from one inflation to the next. To increase standardisation and eliminate these highly variable flows in an objective manner, we first visually inspected the FBF traces for consistency across all of the studied patients, as shown in figure 18. For each subject at each timepoint (as described), we calculated the range as a percentage of the mean. We 'binned' these percentages into 20% brackets (e.g.: range is 0-20% of mean value = very low variation, through to 200-220% = very high variation). The majority of values (310/601, 52%) were in the 40-60% range of the mean value. We selected a cut-off at range of >140% of the mean as this was the closest 'bin' to 2 standard deviations from the mean, and represented the highest acceptable variability, without removing unnecessary data points.

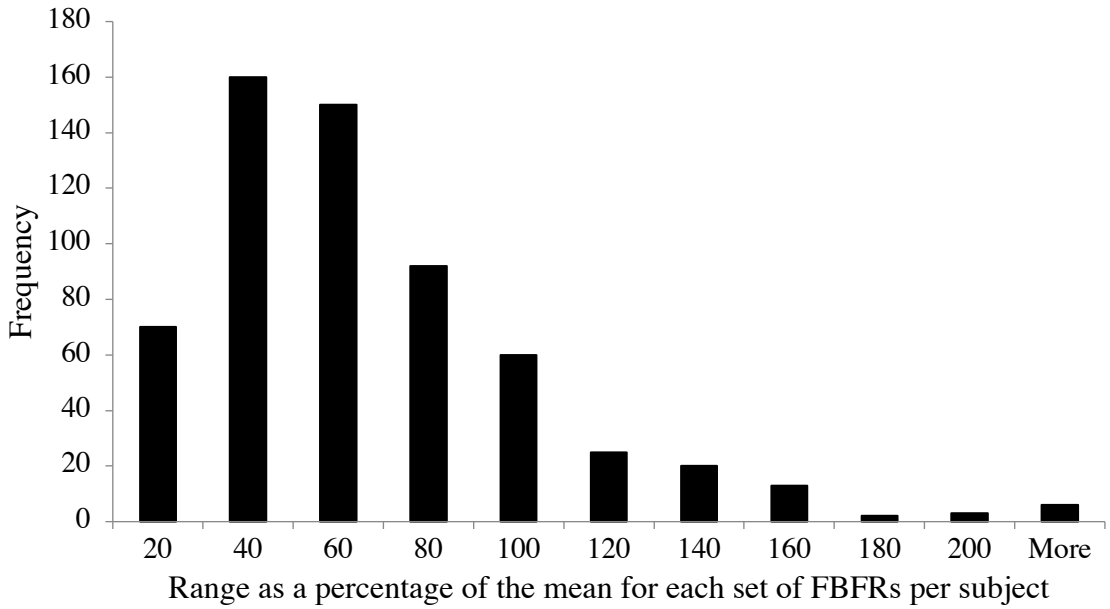

Figure 18: Exclusion of FBFRs >2SD of the mean. Note: In total, 24 sets of measurements were excluded from a total of 601 sets of measurements (3.9%). This process ensured that sets of measurements considered to be 'highly variable' were excluded from the analysis, without bias.

Statistical analysis

The statistical analysis plan was reviewed and agreed by the sponsor and approved by the trial statistician (Dr Allan Clark, UEA). Simple descriptive statistics performed using Microsoft Excel, version 18, 2018 (Microsoft Corporation, US) were used to analyse the baseline characteristics, pulse oximetry and room temperature. Statistical analysis was performed using R statistical software. To assess the change in NOx, unit and subject cell-free haem levels, serial timepoint measurements were analysed using two-way ANOVA followed by Bonferonni post-hoc tests. Effects of nitrite, blood, and oxygen condition were tested for main and interaction effects using a mixed effect linear regression model. All data are expressed as mean (±SEM), unless otherwise stated. Probability values <0.05 were considered statistically significant.

Mixed model (linear regression)

A linear mixed model was fitted to assess the effect of the explanatory variables, including fixed effects for plasma nitrite levels, presence of autologous blood transfusion, oxygen condition, nitrite infusion status and their interactions on FBFRs and random effect for participants to account for the repeated measures:

```
model_1 <-lmer(fbfr~  nitrite_levels
                       + blood
                       + normoxia
                       + time
                      +normoxia*time
                     +blood*normoxia
                     +blood*time
                     +(1|subjectid), data=data.HaNStudy)
summary(model_1)
anova(model_1)
```

The p-values of the regression model itself are conditional on the other factors being at the reference levels and do not tell us if there is a difference between normoxia vs hypoxia or other subgroups of the data. With interaction terms in the model the conditional effect is different from the 'main effect'. Given that the null hypothesis was to test mean FBFR is the same for normoxia and hypoxia after accounting for difference in nitrite levels, blood before/after and time, we present the significance from the model based on the ANOVA structure, due to the interactions. The ANOVA p-values are based on the 'main effects' which are the effects 'averaged' over all the comparisons and represent the average effect accounting for the other factors in the model.

We also included the ‘plasma nitrite levels’ as a variable into the model to ensure that any potential carry-over effect (as discussed earlier) between nitrite infusions was accounted for. ‘Blood condition’ is a dichotomous factor variable contrasting ‘before’ and ‘after’ blood

transfusion. The ‘oxygen condition’ is also a factor variable which either encodes for ‘normoxia’ or ‘hypoxia’. ‘Nitrite infusion status’ was integrated into the model to allow us to distinguish between the effect of nitrite at T0 and T30. To account for the influence of physiological inter-subject variability and to statistically address the repeated cross-over design of the trial, we used subject ID as a random effect in the mixed model. Marginal R^2 shows how much variance in the data was explained by the fixed effects (explanatory variables) in the model, whilst conditional R^2 includes the variance of the data explained by random effect. Estimated effects are used to present the magnitude of effect as indicated by the model. Where interaction effects were non-significant, we used least square means to calculate the estimate, the main effects and the significance.

Model 1 is the overall model for FBFRs. It looks at the effect of plasma nitrite levels, blood condition, oxygen condition, nitrite infusion status, and the interaction between oxygen condition and nitrite infusion status, as well as the interaction between oxygen condition and blood condition on FBFR. Models 2, 3 and 4 assess the effect of plasma nitrite levels, blood condition, nitrite infusion status, and the interaction between nitrite infusion status blood condition on FBFR in normoxia only, hypoxia only, and after blood only, respectively. Model 5 is looking to establish the effect of plasma nitrite levels, blood condition, oxygen condition, nitrite infusion status and two-way interactions between oxygen condition and nitrite infusion status, between oxygen condition and blood condition, and between blood condition and nitrite infusion status on MAP. Model 6 uses the same fixed effects, but investigates their effect on HR.

3: The Nitrite and Coronary Artery Study

Study design

This study was a pharmacodynamic, proof of concept study investigating systemic intravenous infusion of inorganic nitrite on epicardial coronary artery vasodilation, blood velocity and flow using specialised CMR. The study took place at the Royal Brompton and Harefield NHS Trust (RBHT), London, UK. The Nitrite and Coronary Artery Study chart is summarised below, figure 19.

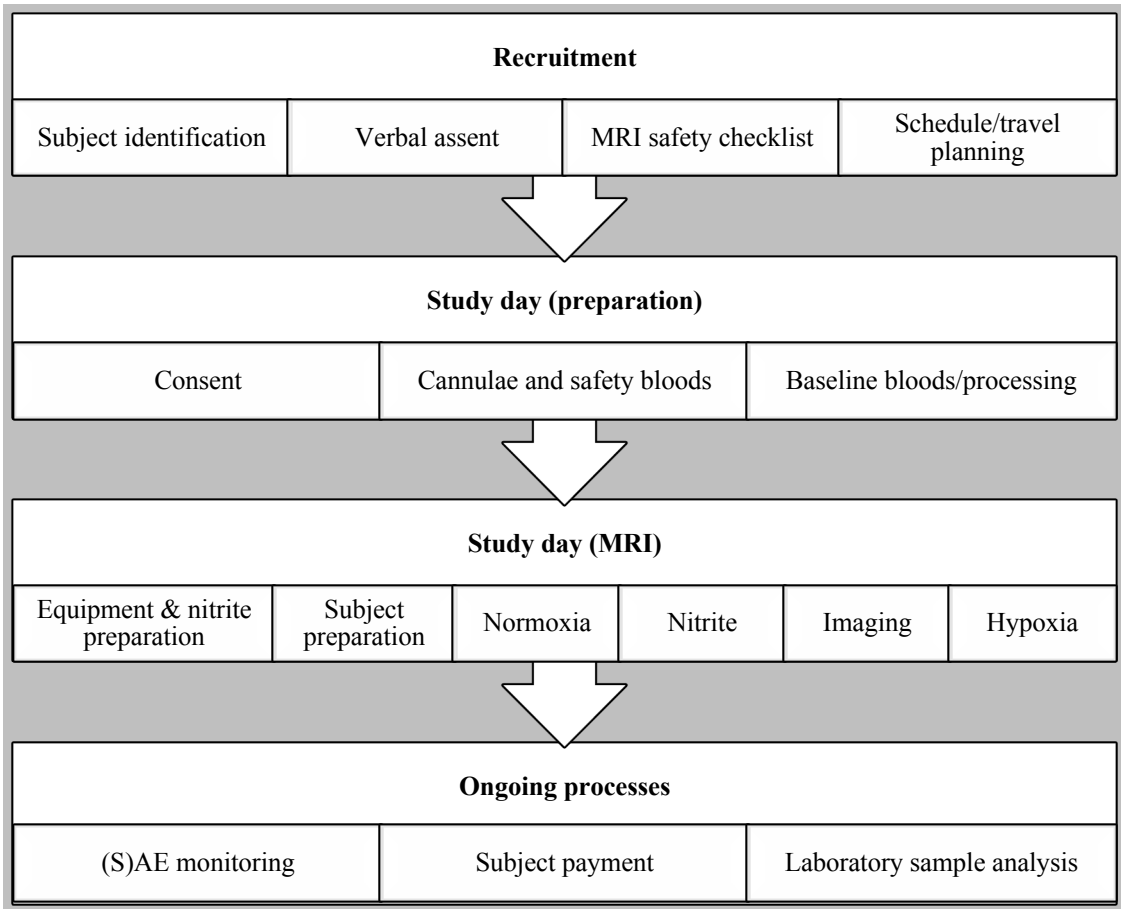

Figure 19: The Nitrite and Coronary - General study schematic

Power calculations

As a proof of concept study only, no formal sample size calculation was performed. We elected to recruit up to 15 subjects.

Regulatory and ethical processes

The protocol was submitted to the MHRA on 3rd July 2017. On 13th July 2017, we were notified that the study was a non-CTIMP as defined by the EU Directive 2001/20/EC and therefore no submission to the Clinical Trials Unit at the MHRA was required. The UEA was the study sponsor. A full suite of documents was submitted for initial REC consideration on 22nd August 2017. I attended the REC meeting on 19th September 2017 (East of England – Cambridge East REC). On 5th January 2018 the REC provided favourable opinion. One substantial amendment was submitted on 29th June 2018 clarifying the study drug dosage. The REC sub-committee gave a favourable ethical opinion on the basis of the described notice. The study was registered at the clinicaltrials.gov website: NCT04354051

Recruitment

Subject identification

The Nitrite and Coronary Artery Study recruited suitable participants from the Haem and Nitrite Study cohort. Recruitment channels were as previously described. Potential participants were advised to contact the research team if they had any questions about the study or if they wished to proceed. As described previously, selected information was collected to identify the individuals National Health Service (NHS) hospital records. If a record did not exist, an NHS number was allocated and a record created using PAS. All records were kept pseudo-anonymously and the owner of records was known only to the lead research fellow. All processes were documented in the participants NHS clinical notes, as per Good Clinical Practice (GCP) Guidelines (316).

Inclusion and exclusion criteria

No exceptions to the stated eligibility criteria were permitted. If in any doubt, the CI was asked to provide advice about inclusion/exclusion in the study.

Inclusion criteria

1. Male or female, aged ≥18 years
2. Not known to have any significant past medical history and not having regular follow-up
3. Able to provide informed written consent

Exclusion criteria

1. Significant medical, surgical or psychiatric disease that in the opinion of the lead research fellow would affect subject safety or significantly impact his/her ability to comply with follow-up
2. Known allergy or intolerance to nitrites
3. Known G6PD deficiency or G6PD deficiency detected at screening in males of African, Asian or Mediterranean decent
4. Female subjects must be of non-childbearing potential, defined as follows: postmenopausal females who have had at least 12 months of spontaneous amenorrhea or 6 months of spontaneous amenorrhoea with serum FSH >40mIU/ml or females who have had a hysterectomy, bilateral salpingectomy or bilateral oophorectomy at least 6-weeks prior to enrolment
5. Receipt of an investigational drug or biological agent within the 4-weeks prior to study entry or 5 times the drug half-life, whichever is the longer
6. Predisposed to acute on chronic limb ischemia evident from a history of claudication or known peripheral arterial disease
7. Any contra-indication to MRI, including the presence of an implanted metal device or suspected metal foreign bodies.

<u>Verbal assent, MRI safety checklist and scheduling</u>

Assented subjects completed the 'MRI Safety Checklist' (Appendix 7) which was reviewed and forwarded to Mr Ricardo Wage, the Chief CMR Radiologist assisting in the study. If

deemed 'MRI safe', subjects were invited to attend a structured clinical study session in the CMR unit at the RBHT, London. After enrolment a suitable CMR study date was arranged. The RBHT CMR unit was notified and the subject was registered and scheduled for imaging. As before, subjects were advised to follow a nitrate/nitrite low diet for 2-days prior to their CMR session.

Study visit

Consent, cannula insertion, safety bloods and sample processing

Preparations included re-assessment of suitability and if confirmed, fully informed written consent. A 20-gauge cannula was placed in either the basilic or cephalic vein at the level of the antecubital fossa of the dominant arm. This was used for blood-letting and study drug administration. A 4 ml venous blood sample was collected to perform safety blood analyses (if indicated. i.e. no renal function results or haemoglobin level in the preceding 12-months) via a bedside haemoglobin (Digital haemoglobin meter, Hangzhou Sejoy Electronics and Instruments Co. Ltd, China) and bedside creatinine test (StatSensor Creatinine, Novo Biomedical, US). Venous blood for nitrite, nitrate and RXNO levels was collected, processed and stored as described in the Haem and Nitrite Study.

Equipment and study drug preparation

All equipment was prepared in advance and maintained by the research team. The study drug was sodium nitrite 17.5 mg in 5 ml 0.9% sodium chloride and was supplied by Tayside Pharmaceuticals (Ninewells Hospital & Medical School, Dundee, UK). The concentrations infused were based on the study published in 2015 by Dr Julian Ormerod (one of Professor Frenneaux's previous clinical research fellows) (258). The group showed that 50 μg/kg/min (equal to sodium nitrite 17.5 mg in a 70 kg subject) was well-tolerated in severe chronic heart failure patients without adverse haemodynamic effects.On each study day, the lead

clinical research fellow prescribed the study drug on the study specific prescription chart (Appendix 9). If subjects were <70 kg, the dose was adjusted according to weight. The study drug was drawn up into a 50 ml syringe and attached to a 5-meter infusion line which was primed with 0.9% saline (volume 3.7 ml). This line was passed through a secure port in the wall of the MRI room and attached to the subject's cannula and clipped to keep the line closed until it was required.

Subject preparation

On arrival to the CMR unit, eligibility was re-confirmed. The subject ensured that they did not have any metallic items in their possession. The subject wore a hospital gown to enable connection of ECG pads to allow for ECG-gated image acquisition. The subject was positioned in the CMR scanner with specific care to ensure correct positioning of the cardiac and spine coils. Next, the gas flow regulator (Therapy Equipment Ltd, UK) was attached to the 12% oxygen/88% nitrogen medical gas cylinder (BOC, The Linde Group, UK) in the CMR control room. A 5-meter length of medical grade oxygen tubing was connected to the gas flow regulator (Therapy Equipment Ltd, UK) and passed through a secure port in the wall between the CMR control room and the 3 Tesla Magnetom Skyra MR scanner (Siemens, Germany). This tubing was then attached to a simple face mask.

Each subject followed a structured clinical study protocol, figure 20. As discussed in 'The Haem and Nitrite Study' clinical intervention schematic, we elected to use a 5-minute IV bolus rather than a continuous infusion throughout the study. In this study, there were several considerations that enforced this decision. Firstly, time available inside the 3 Tesla Magnetom Skyra MR scanner (Siemens, Germany) was incredibly limited and valuable. We had time-limited sessions and were not able to wait the time required (reported by some to take ~12 hours) (175) (318) to gain a steady-state of plasma nitrite, between pre- and post-drug images. Given the half-life of nitrite in plasma is reported to be between ~35-45 minutes

(319-321) and even shorter in whole blood (322) we identified that a bolus regimen with rapid sequential imaging of the post-drug coronaries in normoxia and hypoxia (15-minute sequence), would be an acceptable trade-off, as we would expect to see >75% of the total dose in circulation during hypoxia. An additional point, as will be discussed in depth in the study discussions and limitations, was that the technical complexity of imaging the coronaries meant that any delays in the protocol or small movements of the subject during the study increased the risk of losing the imaging views (as we unfortunately discovered when attempting to measure BP during hypoxia), thus a prolonged protocol was more likely to result to slight unintentional movements. Therefore, whilst appreciating the advantages of a longer protocol, on reflection, keeping the study protocol as short as possible and adopting a bolus administration of nitrite was a necessary to reduce attrition due to poor image quality. However, we also recognise that the bolus nitrite administration method meant that we did not know the exact plasma nitrite level at the point of each image acquisition, and we take this into consideration when interpreting our results.

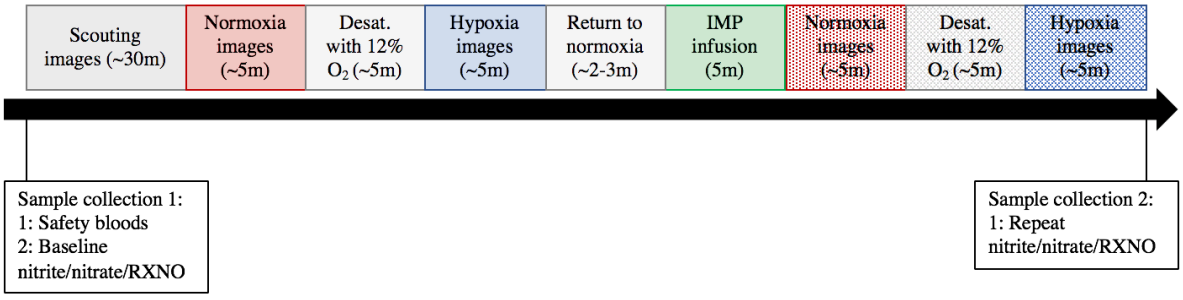

Figure 20: The Nitrite and Coronary Artery Study – Clinical intervention schematic. Key – RXNO: protein-bound NO (RXNO) levels, IMP: sodium nitrite. Note: time durations of each stage shown in brackets.

CMR coronary image acquisitions

The CMR coronary images acquired in this study were overseen by Prof Jennifer Keegan (Principal Physicist and Honorary Senior Lecturer at Royal Brompton and Harefield NHS Trust/Imperial College London). The details of the study methods are identical to those published in papers by Prof Keegan and colleagues (286, 331).

The study used an interleaved spiral phase velocity sequence and which was developed on a 3 Tesla Magnetom Skyra MR scanner (Siemens, Germany). The spiral sequence favoured high temporal resolution acquiring frames every 23 ms. The slice thickness was 8 mm, the spatial resolution was 1.4 × 1.4 mm (reconstructed to 0.7 × 0.7 mm through zero-filling) and the repeat time (acquired temporal resolution) was 19 ms, providing adequate spatial resolution to detect coronary vasodilation (332). Being a spiral phase velocity sequence, data were reconstructed to cartesian format online via a 256 × 256 matrix gridding algorithm (333). Retrospective electrocardiogram (ECG) gating allowed full coverage of the entire cardiac cycle in 50 cine frames, the reconstructed temporal resolution depending on the subjects' heart rates.

The study team targeted the right coronary artery (RCA) due to the preferable anterior anatomical position, locality to the receiver coil and reproducibility (334). The left anterior descending artery (LAD) was less favoured due to posterior location and increased anatomical branches (i.e. limited through-plane acquisition opportunities). The left coronary was however selected if the right was too narrow, tortuous or branching to allow for clear images. Multiple early diastolic breath-hold transverse segmented gradient echo scout acquisitions were acquired in each subject to ascertain the path of the coronary artery of interest, figure 21.

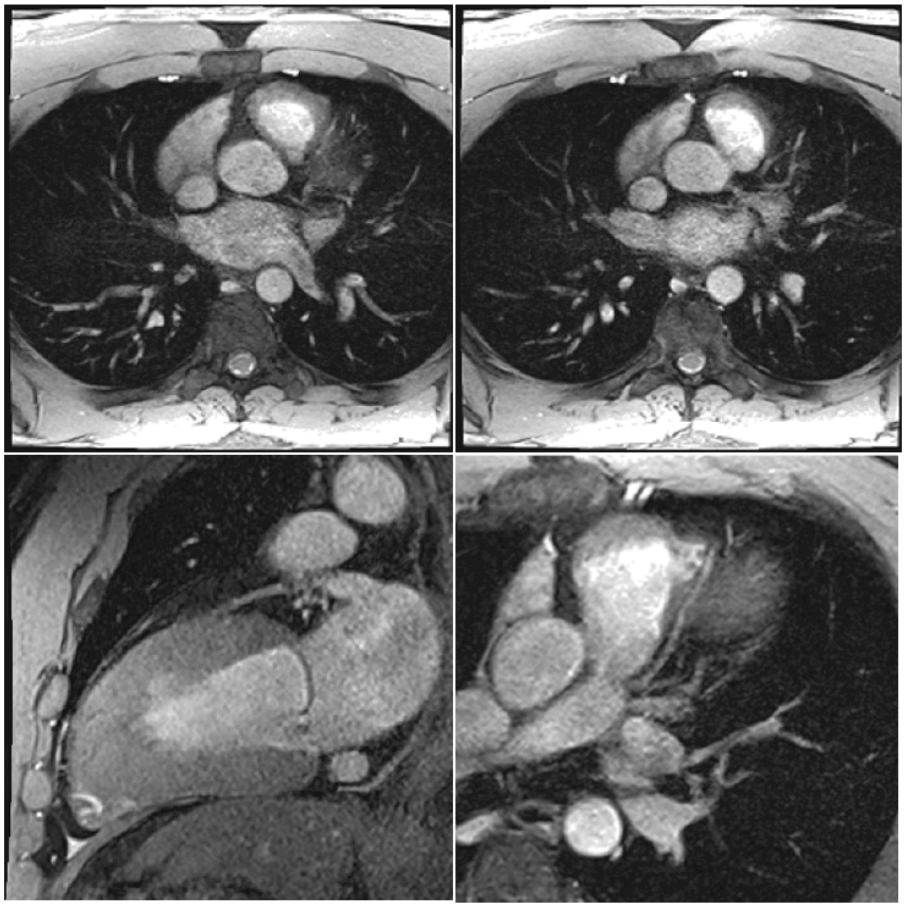

Figure 21: Diastolic transverse-segmented scout acquisitions. Images taken from study subject ID 015.

From these, oblique and double oblique images were acquired showing the path of the artery in-plane, followed by a through-plane acquisition in a straight section of the proximal artery, matched as closely as possible to the location of the invasive measurement, figure 22.

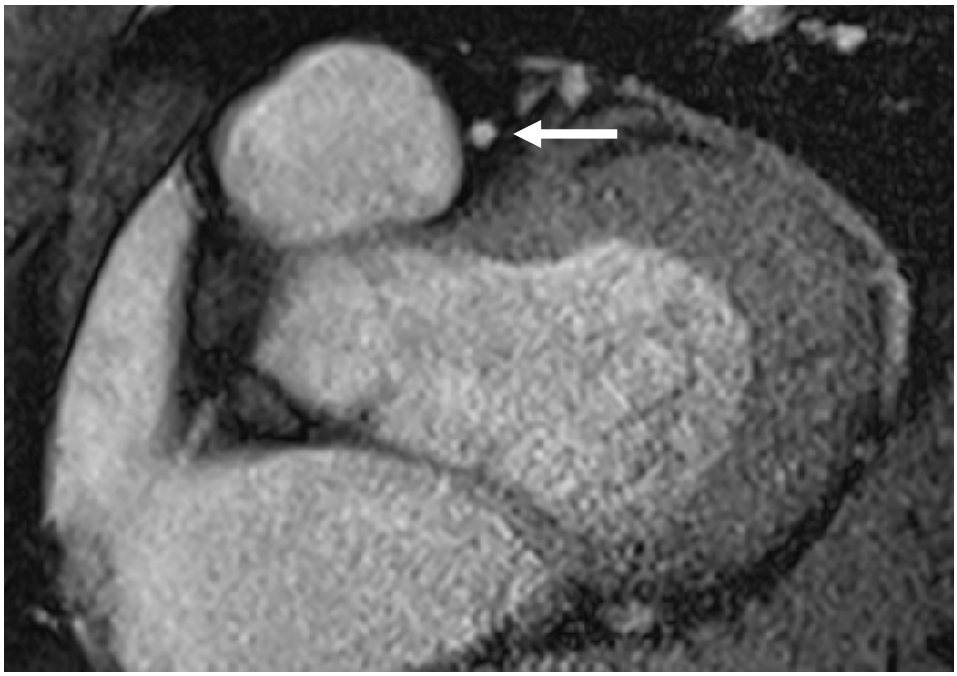

Figure 22: A through-plane acquisition in a straight section of the left anterior descending artery (LAD) (Indicated by white arrow). Image taken from study subject ID 015.

Spiral coronary artery phase velocity maps were then acquired in the same location. Sensitivity to off-resonance was minimised by localised second-order shimming and frequency adjustment based on the signal from a user-defined region of interest (ROI) positioned over the heart. For right coronary studies, an additional breath-hold spiral phase velocity mapping acquisition was performed using fat-excitation (335). This was used to correct the data for the through-plane velocity of the vessel.

Medical gas: 12% oxygen/88% nitrogen

Following acquisition of images during normoxia, subjects were desaturated using a composition of 12% oxygen/88% nitrogen medical gas (BOC, The Linde Group, UK) to enable acquisition of the hypoxia images. The medical gas was the same composition as previously used in The Haem and Nitrite Study.

Desaturation took up to 5-minutes with target saturations of between 83-88% O_2 (estimated pO_2=47.5 to 55mm Hg, based on Severinghaus' equation). During hypoxic experiments, oxygen saturations were monitored via pulse oximetry (Nellcor N-180, Nellcor, Pleasanton, Calif) and the flow rate was adjusted (range 0 L/min^{-1} to 15 L/min^{-1}) to maintain target saturations (326). If after 5-minutes target saturations could not be achieved hypoxia measurements continued as per protocol (and subjects were identified as compensating) (235), If hypoxia was not well-tolerated, 100% high-flow oxygen was available to be administered to reverse hypoxia. After hypoxia images were acquired, the subject was returned to normoxia by breathing room air for a period of 2-3 minutes.

Study drug administration

Inorganic sodium nitrite was infused intravenously at a rate of 50 $\mu g/kg/min^{-1}$ for 5-minutes. The infusion was administered through the in-dwelling venous cannula. Throughout the infusion, repeated haemodynamic measurements were recorded (heart rate and BP). Unfortunately, we discovered during the first run of the study protocol that when we inflated the BP cuff in hypoxia, this caused the subject to move in the MRI scanner and we lost the view of the artery (which had been located in normoxia, after the normoxia BP measurement had been taken). After careful consideration and following discussions, we felt it was more appropriate to increase the chance of imaging the coronary, at the expense of not measuring the BP in hypoxia, so we did not record BP in hypoxia in the given study.

Following administration of the study drug, a second set of coronary CMR images were acquired in both normoxia and hypoxia. These processes were repeated as described previously.

Repeat blood testing and processing

On completion of the studies, venous nitrite, nitrate and RXNO levels were repeated, as described previously.

CMR coronary image analysis

Using a highly specialised CMR sequence meant that coronary image analysis for this study was a complex and specialised task. As such, as an international expert in this field, Prof Jennifer Keegan conducted image acquisition and analyses. The details of the study methods are identical to those published in papers by Prof Keegan and colleagues (286, 331). Importantly, the 2015 publication demonstrated that the method used in the given study provided accurate assessment of temporal patterns of coronary blood flow when compared to peak Doppler values. Specifically, it showed that in individual vessels, plots of CMR velocities at all cardiac phases against corresponding Doppler velocities showed a consistent linear relationship between the two with high R^2 values (mean ±SD: 0.79 +/-0.13) (286) demonstrating validation of this method against Doppler. This method also showed excellent test-retest reproducibility.

As explained step-by-step below, the image analysis process was carefully controlled to reduce variability as defined *a priori*. To reduce observer bias, the operator was blinded to the whether the subject was undergoing normoxia or hypoxia. This was achieved by assessing all images in random order and then linking the subject ID and oxygen condition at the end of the full set of image analysis. To increase inter-observer reproducibility, the method used was semi-automatic. This meant that only 2 decisions had to be made by the operator: i) marking the centre of the vessel and (ii) defining a background region of interest. The rest of the processing was automated, which ensured that variability was kept to a minimum (335). Finally, to increase repeatability, the operator repeated step 4 on several analysed vessels, thus reducing intra-observer variability throughout (336).

Using a semi-automatic in-house MATLAB program, the operator followed a standardised and reproducible process:

1. Manually define background noise region
2. Subtract background noise from detected signal
3. Crop image to 64x64 and interpolate x8
4. Manually mark centre of vessel
5. Take average full width half maximum (FWHM) of radial profile passing through vessel center (exclude poor profiles)
6. Repeat in 16 images (each rotated by 11.25 degrees)
7. Apply mean FWHM (mm) as diameter to $\pi r2$ *t*o calculate cross-sectional surface area (CSA)

This process was repeated in 16 images for each vessel to improve accuracy, figure 23. All data analysis was handled using Microsoft Excel (Microsoft Corporation, US).

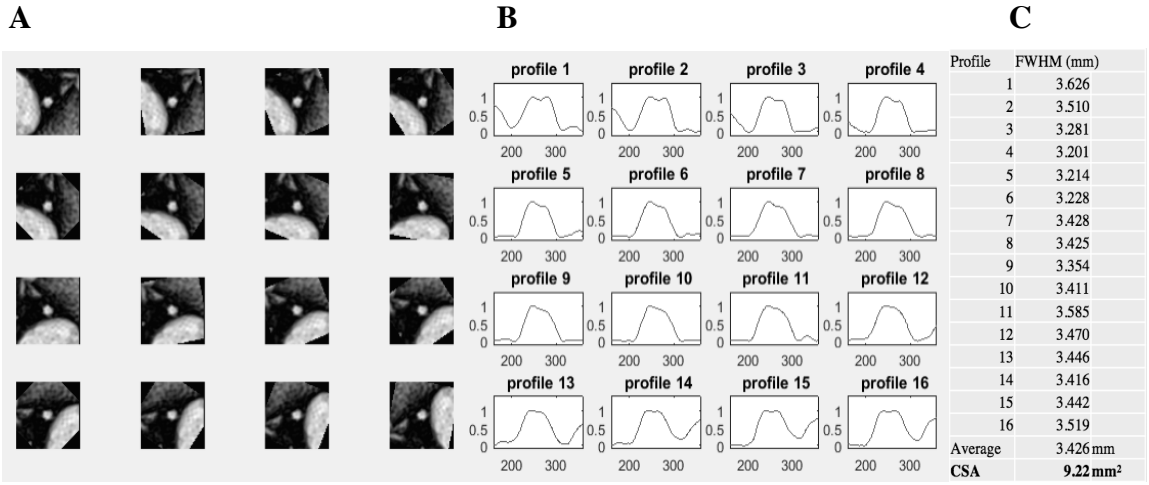

Figure 23: A - Cropped interpolated image centred on LAD (the 16 images are rotated by increments of 11.25deg). B - Horizontal profiles through each rotated image. C - FWHM (mm) of each profile, together with mean FWHM and calculated CSA. Images taken from study subject ID 015.

This enabled the difference in CSA to be calculated between the 4 conditions for each subject, figure 24 and 25.

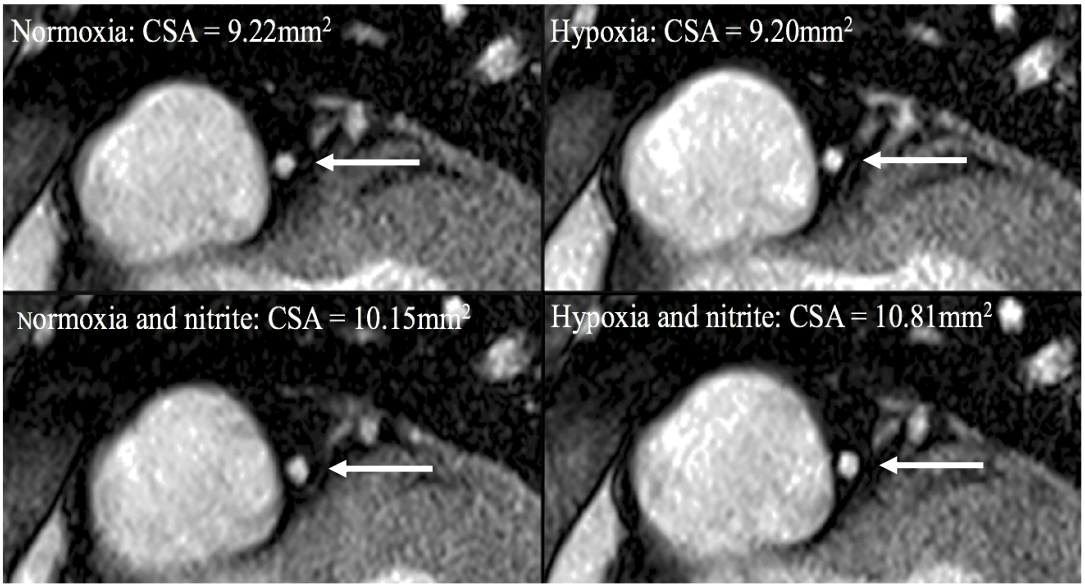

Figure 24: Example transverse images in each of the 4 conditions (normoxia, normoxia and nitrite, hypoxia, hypoxia and nitrite) showing the associated measured CSAs in the LAD (marked with white arrow). Images taken from study subject ID 007.

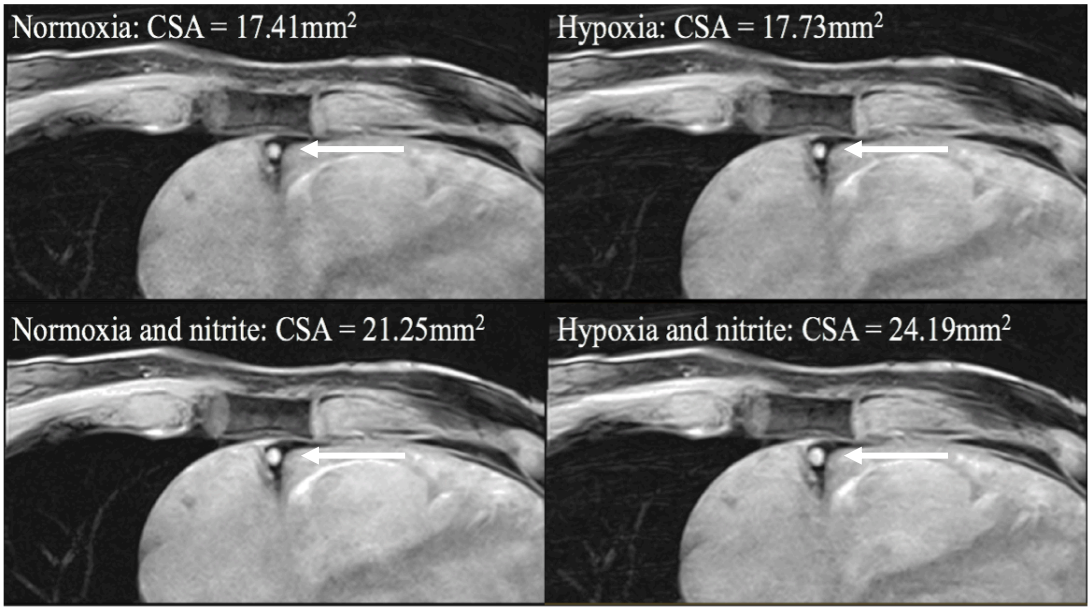

Figure 25: Example oblique images in each of the 4 conditions (normoxia, normoxia and nitrite, hypoxia, hypoxia and nitrite) showing the associated measured CSAs in the RCA (marked with white arrow). Images taken from study subject ID 007.

For breath-hold acquisitions, velocity time curves were generated *post-hoc* for each breath-hold by two independent observers. Using an in-house semi-automatic custom MATLAB program, the operator would follow the described process:

1. Manually mark the centre on the cross-sectional segmented scout image, figure 26A
2. Automatic multi-level thresholding to create a circular ROI around the coronary artery using a modified Hough transform based algorithm, figure 26B; this value was expected to match the CSA values as calculated and were adjusted if needed

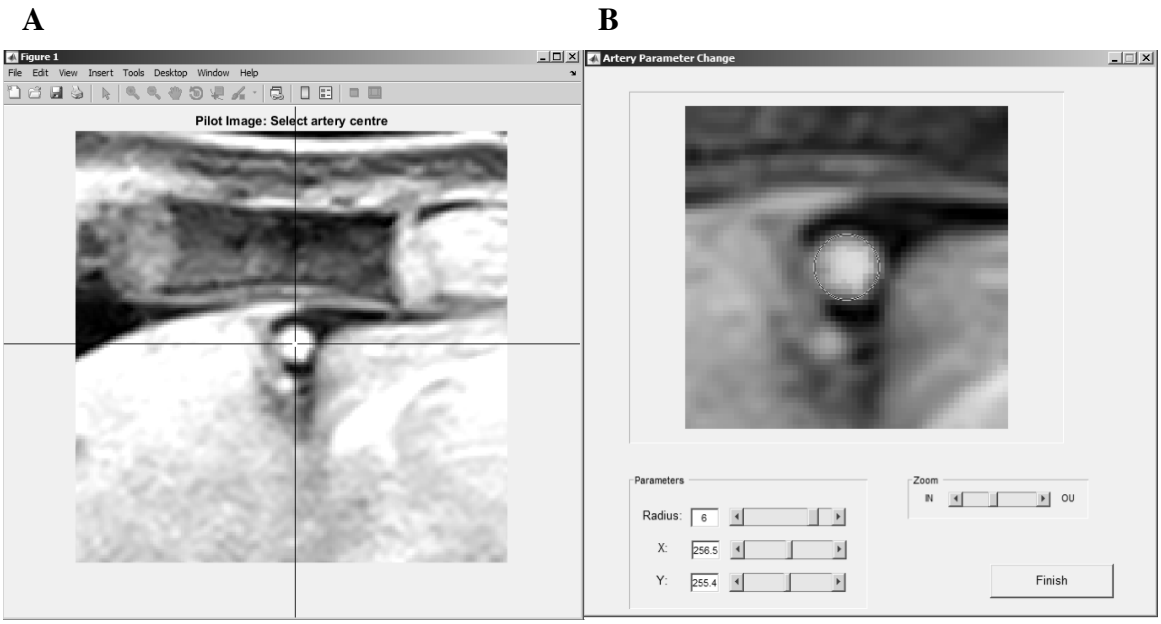

Figure 26: A – Manual marking of centre point of the vessel on the scout image. B - Window level and width automatically set for circular ROI (calculated area from CSA program). Images taken from study subject ID 007.

3. The initial ROI was copied to the first frame of the spiral magnitude dataset which was put through a spatial band pass filter to identify objects of similar size in the next frame in the spiral magnitude dataset, figure 27A
4. The new ROI location was copied throughout the corresponding velocity; automatically tracking the artery from frame to frame of the acquisition, figure 27B

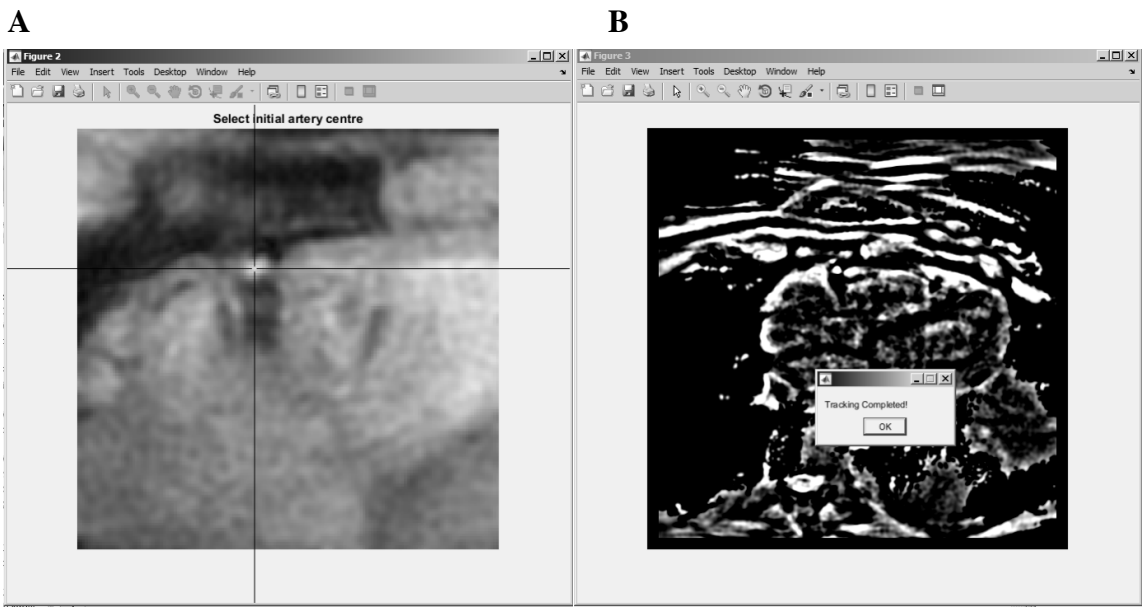

Figure 27: A - Manual marking of centre point of the vessel on first frame of spiral flow study. B - Each cine frame thresh-holded and circular objects with radius of RCA automatically detected and tracked through cardiac cycle. Images taken from study subject ID 007.

5. For each frame, position of automatically detected RCA was checked on magnitude image and velocity maps and a fat ROI was automatically determined – this was used to correct for through-plane motion of the vessel and could be adjusted if needed, figure 28. This however was of less relevance as velocity data was per cardiac cycle and therefore through-plane motion would be expected to equal 0.

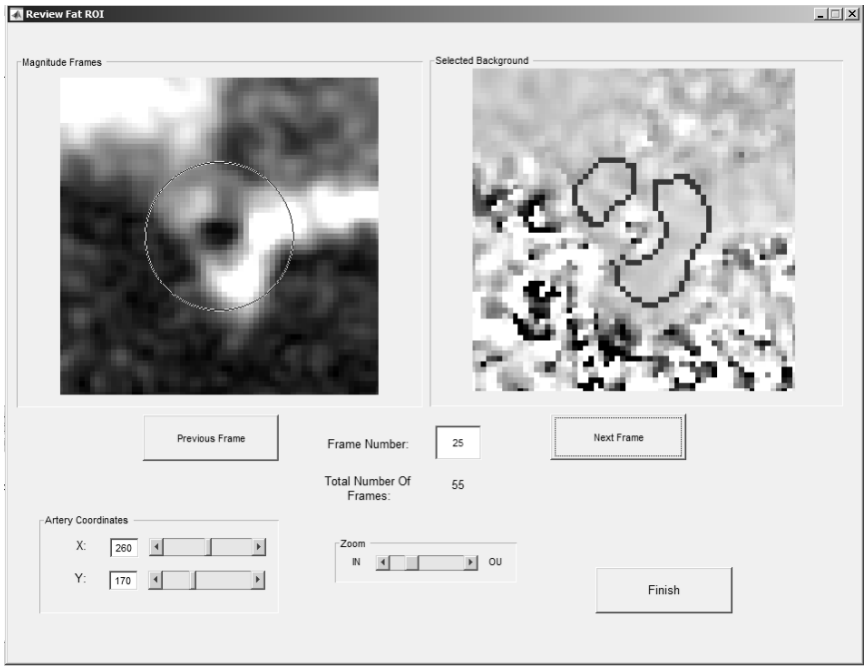

Figure 28: Automatic through-plane motion correction. Images taken from study subject ID 007.

The resulting velocity-time curve is a composite of the uncorrected through-plane velocity of coronary blood and the through-plane velocity of the vessel itself, figure 29. For the LAD, the velocity of a tracked region of nearby myocardium was used as a marker of the through-plane velocity of the vessel (337). For the RCA, surrounding epicardial fat was used instead (335). For each vessel, coronary velocity was calculated as the average velocity through the entire cardiac cycle multiplied by the cross-sectional area. All CMR coronary image analysis data was handled using Microsoft Excel (Microsoft Corporation, US).

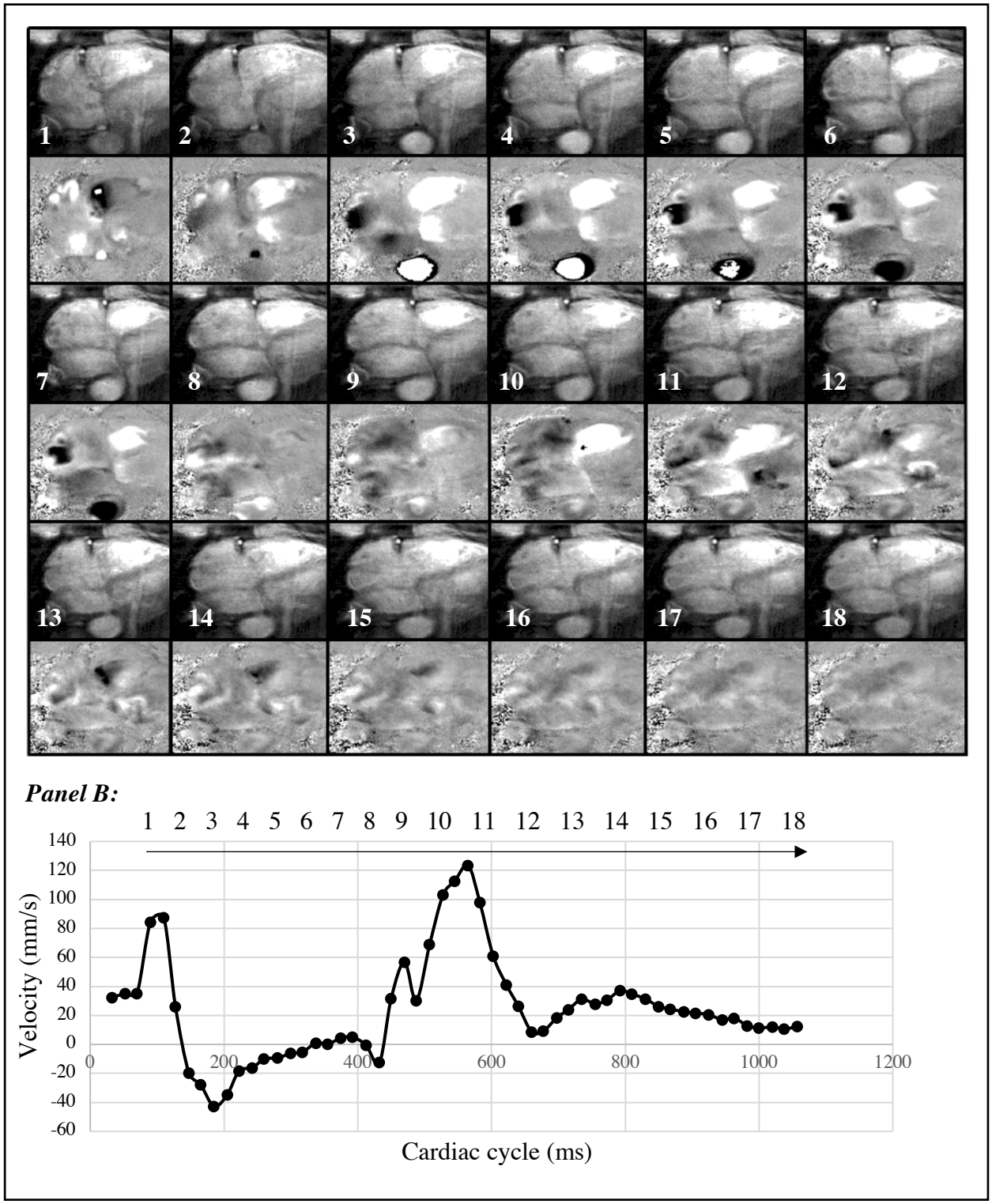

Figure 29: Magnitude images (darker panels, numbered) and paired velocity-time course map (corresponding panels below) on the RCA in normoxia in subject 007. Time course in panels 1-18: 52ms, 110ms, 165ms, 222ms, 280ms, 337ms, 392ms, 450ms, 507ms, 565ms, 622ms, 677ms, 735ms, 792ms, 850ms, 905ms, 962ms, 1020ms. Panel B: Calculated coronary blood velocity (mm/s) vs. time in cardiac cycle (ms) - uncorrected for through-plane motion.

Finally, we calculated mean velocity over the cardiac cycle as follows (equation 6) (286):

$$v = \frac{(v_1t + v_2t + v_3t \ldots + v_{50}t)}{50}$$

Where, v=velocity (mm/s), v_it=velocity at time point 1, etc, divided by 50 cine frames. We also calculated mean coronary blood flow over the cardiac cycle as follows (equation 7) (335):

$$Q = CSA\ x\ (v_1t + v_2t + v_3t \ldots + v_{50}t)\ x\ HR$$

Where, Q=flow (ml/min), CSA=cross-sectional area (mm^2), v_it =velocity time point 1, etc, multiplied by HR=heart rate (bpm). Also, we integrated the velocity-time curve over the cardiac cycle, accounting for pulsatile flow.

Subject payments

Participants were financially reimbursed for their time and travel. A fixed value of £50 was offered for completion of the study day visit and up to £100 was offered for travelling to the study site (value to match train receipt/mileage).

S(AE) monitoring

Safety reporting was a continuous process and all adverse events were reviewed by the CI either at the point of identification or as soon thereafter as practicable. Definitions of harm of the EU Directive 2001/20/EC Article 2 based on the principles of ICH GCP applied to this study. Definitions of AEs are outlined in the study protocol.

Sample and data analysis

Sample analysis was performed by Drs Magda Minnion and Bernie Fernandez, under the supervision of Prof Martin Feelisch at the University of Southampton, UK.

Laboratory sample analysis

Plasma nitrate and nitrite species were measured using HPLC, as previously described in 'The Haem and Nitrite Study' methods (Appendix 5). In addition, RXNO was determined using gas-phase chemiluminescence. These methods are described in detail in Appendix 6.

RXNO levels via gas-phase chemiluminescence

In brief, the amount of total nitroso species (RXNO) is quantified after sample pre-treatment with acidic sulphanilamide. The concentration of RXNOs are determined after reductive cleavage by an iodide/triiodide containing reaction mixture and subsequent determination of the NO released into the gas phase by its chemiluminescent reaction with ozone (O_3). NO reacts with O_3 to form nitrogen dioxide (NO_2). A proportion on NO_2 arises in an electronically excited state (NO_2*), which, on decay to its ground state, emits light in the near-infrared region and is quantified by a photomultiplier. Provided O_3 is present in excess and reaction conditions are kept constant, the intensity of light emitted is directly proportional to NO concentration.

$$NO + O_3 \longrightarrow NO_2^* + O_2$$
$$NO_2^* \longrightarrow NO_2 + h \cdot V$$

Statistical analysis

The statistical analysis plan was reviewed and agreed by the sponsor approved trial statistician (Dr Allan Clark, UEA). Simple descriptive statistics performed using Microsoft Excel, version 16 (2018) were used to analyse the baseline characteristics. Statistical analysis was performed using R statistical software. To assess the change in NOx, RXNO, unit and subject cell-free haem levels, serial timepoint measurements were analysed using two-way ANOVA followed by Bonferonni post-hoc tests. Effects of nitrite and oxygen condition were tested for main and interaction effect using two-way repeated measures ANOVA. All data are expressed as mean (±SEM), unless otherwise stated. Probability values <0.05 were considered statistically significant.

CHAPTER 3: EXAMINING THE MECHANISMS OF NITRITE-MEDIATED VASODILATION IN NORMOXIA IN A MURINE ex vivo MODEL

To examine the mechanisms underlying nitrite-mediated vasodilation in normoxia, the experimental work shown in this chapter was conducted in the Dr Melanie Madhani research laboratory, Institute of Cardiovascular Sciences, University of Birmingham. PKG1α "redox dead" mice were a kind gift from Prof Philip Eaton (King's College London). The maintenance and genotyping of the PKG1α colony was conducted by Dr Alessandra Borgognone, Dr Rosie Hayes and Miss Joanna Goodwin at University of Birmingham. Blood vessel isolation and mounting for vascular myography were conducted by Dr Melanie Madhani. *In vivo* nitrite treatment for the PKG1α dimerization western blotting experiments were conducted by Dr Alessandra Borgognone, Dr Kayleigh Griffiths, and Dr Rosie Hayes. Vascular myography data shown in this chapter was jointly conducted by Miss Joanna Goodwin and myself. My contribution to this work was focused over a 9-month period at the start of the PhD. During this time, I also developed, prepared and initiated the Haem and Nitrite Study (Chapter 4). Once the Haem and Nitrite Study commenced, it was not possible to run this complex clinical study in Norwich and continue the basic science work in Birmingham. Therefore, my positioning in the authorship on the associated publication of the basic science work (Appendix 2) reflects my contribution to the overall basic science programme.

Introduction

Inorganic nitrite is an important systemic vasodilator in humans (190, 191). Nitrite reduction to NO and the subsequent involvement of the NO-sGC-cGMP pathway in hypoxia is well-described (338). Nitrite reduction to NO in normoxia is very slow at physiological pH (339), yet vasorelaxant effects have been described during normoxia, especially in resistance

vessels (146, 177, 190-192). These observations raise the possibility that nitrite-mediated vasodilation in normoxia may be via a NO-independent mechanism.

Direct S-Nitrosylation of the cysteine thiols in PKG1α can result in a wide range of signalling processes (340) and this may include activation of downstream vasoactive targets. NO-independent activation of PKG1α has also been described, involving oxidation of cysteine residues resulting in dimerization. This has been described with H_2O_2 (198), high ROS and the presence of hydrogen sulfide (208).

In addition to the classical NO-sGC-cGMP-PKG pathway, PKG can also be activated by an oxidation mechanism, whereby the homodimer complex forms an interprotein disulfide bond (199). This disulfide bond forms a link in the N-terminus of the two α subunits of PKG1α cys42 residue. Previous studies have shown that PKG oxidation contributes to basal blood pressure as "redox-dead" Cys42Ser PKG1α KI mice have higher blood pressure than their wild-type littermates. Furthermore, various stimuli such as H_2O_2, hydrogen sulfide and GTN have all shown to activate PKG1α and induce vasodilation and lower blood pressure (202-204). In the present study, we sought to investigate whether nitrite-induced vasodilation is mediated by oxidation and/or dimerization of PKG1α.

In the present series of experiments, we examined the vasoactivity of murine thoracic aortae conduit vessels and mesenteric resistance vessels from PKG1α WT and Cys42Ser PKG1αKI ("redox dead") littermates in normoxia following cumulative concentration response to sodium nitrite. To assess whether these effects were nitrite-NO-dependent, we first compared PKG1α WT vessels in the absence and presence of NO scavenger (CPTIO) and sGC inhibitor (ODQ). Next, to evaluate whether nitrite has the ability to mediate vasodilatory effects via the redox pathway, concentration response curves to sodium nitrite were constructed in the PKG1α WT and PKG1α KI mice.

Hypothesis

In normoxia, inorganic nitrite will induce PKG1α oxidation/dimerization via a NO-independent mechanism and initiate vasodilation predominantly in the resistance vessels.

Aims

i. To examine the role of nitrite on the PKG1α oxidation pathway in isolated conduit and resistance blood vessels by using PKG1α WT and KI mice

ii. To examine the time-course of PKG1α dimerization following 1 or 24-hour nitrite pre-treatment.

Results

1: Nitrite regulates vasorelaxation via PKG1α oxidation in the resistance vessels

As shown in figure 30A, concentration-response curve to nitrite (10^{-9}-$10^{-3.5}$ M) in normoxia induced vasodilation in PKG1α WT and KI ('redox-dead') thoracic aortic conduit vessels (n=18). Vasodilation was observed at concentrations of 10^{-5}M and above in both groups. At maximal nitrite dosing (100 μM), both WT and KI littermates showed equal levels of vasodilation (vasodilation recorded at +60% to baseline). The difference in vasodilation between WT and KI littermates was not statistically significant. As shown in figure 30B, concentration response curve to nitrite (10^{-15}-$10^{-3.5}$ M) in normoxia induced dose-dependent vasodilation in mesenteric resistance vessels. This effect was greatest in WT mice (n=19) and was significantly attenuated in PKG1α KI littermates (n=19), $p \leq 0.001$.

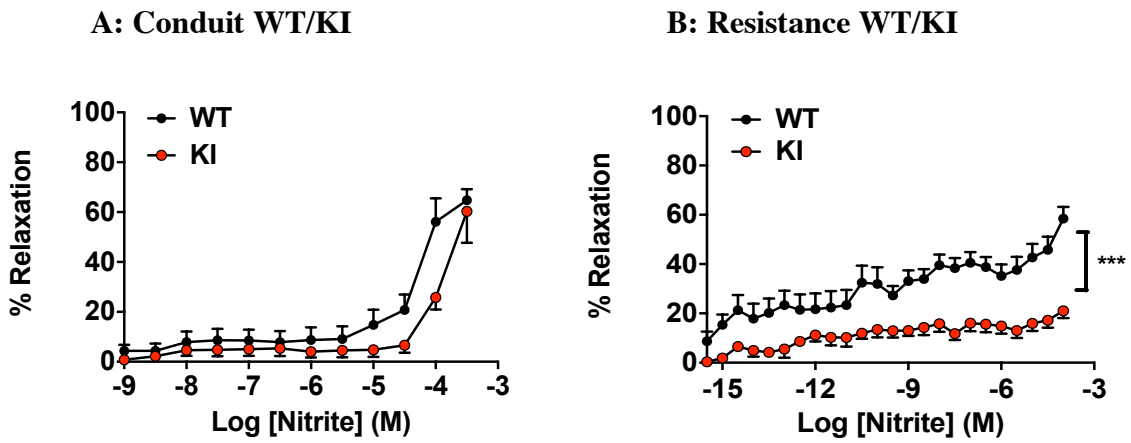

Figure 30: Nitrite-mediated vasodilation in WT and KI conduit (A) and WT resistance vessels, but this effect was significantly reduced in KI littermates (B) Data are presented as mean (±SEM). Panel A. Thoracic conduit (WT n=18, KI n=18). Panel B. Mesenteric resistance (WT n=19, KI n=19). Statistical analysis carried out using one-way ANOVA followed by Bonferroni post-hoc test; *** $p \leq 0.001$.

2: Nitrite regulates vasorelaxation NO-dependently in the conduit vessels during normoxia

As shown in figure 31, cumulative concentration response curve to sodium nitrite (10^{-9}-$10^{-3.5}$ M) in normoxia induced significant vasodilation in WT PKG1α thoracic aortae conduit vessels (n=15). Pre-incubation of WT littermate aortae conduit vessels with the sGC inhibitor, ODQ (10 μM) (figure 31A, n=14) or the NO scavenger, CPTIO (1 mM) (figure 31B, n=15), substantially reduced the vasorelaxant effect of nitrite in normoxia. The difference in observed effect was statistically significant, $p \leq 0.001$. These data suggest that nitrite mediates vasodilation in WT thoracic aortae conduit vessels via a NO-sGC dependent mechanism.

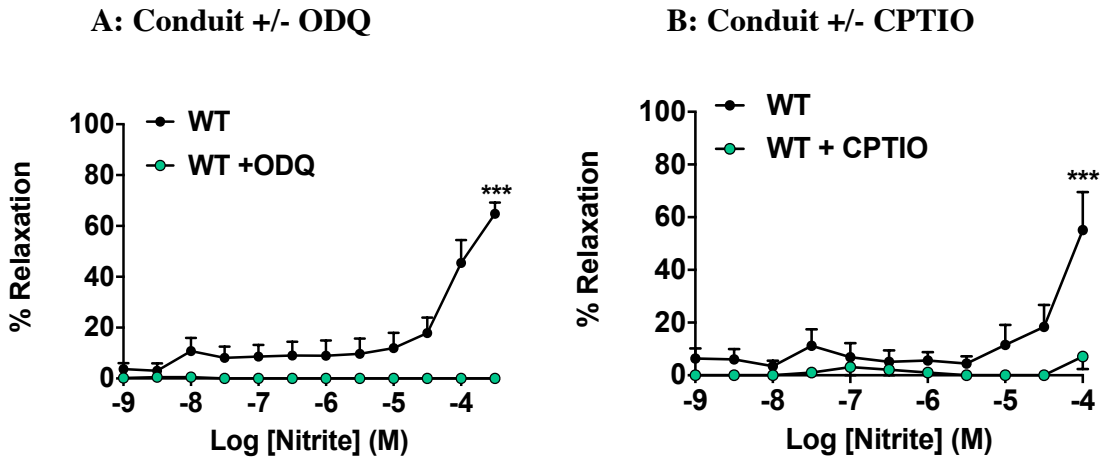

Figure 31: Nitrite-mediated vasodilation in WT conduit vessels is abolished in the presence of ODQ (A) or CPTIO (B). Data are presented as mean (±SEM). Panel A. ODQ (10μM; n=14). Panel B. CPTIO (1mM; n=15). Statistical analysis carried out using one-way ANOVA followed by Bonferroni post-hoc test; *** $p \leq 0.001$.

3: Nitrite-mediated vasodilation in WT mesenteric resistance vessels is mediated via a NO-independent mechanism

As shown in figure 32, the cumulative concentration response curve to nitrite (10^{-15}-$10^{-3.5}$ M) in normoxia demonstrated significant vasodilation in WT PKG1α mesenteric resistance vessels. Pre-incubation of WT littermate mesenteric resistance vessels with the sGC inhibitor, ODQ (10 μM) (figure 32A, n=14) or the NO scavenger, CPTIO (1 mM) (figure 32B, n=15), did not alter the observed effect. These data suggest that nitrite mediates vasodilation in WT mesenteric resistance vessels via a NO-sGC independent mechanism.

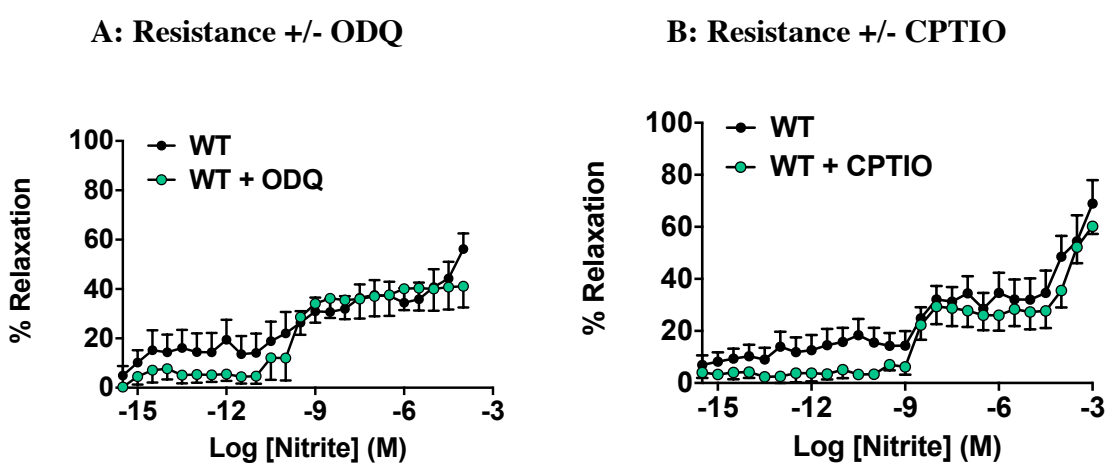

Figure 32: Nitrite-mediated vasodilation in WT resistance vessels is preserved in the presence of ODQ (A) or CPTIO (B). Data are presented as mean (±SEM). Panel A. ODQ (10 μM; n=14). Panel B**.** CPTIO (1 mM; n=15). Statistical analysis carried out using one-way ANOVA followed by Bonferroni post-hoc test.

4: Nitrite-mediated PKG1α oxidative dimerization is a delayed and time-dependent phenomenon in mesenteric resistance vessels

The time course of nitrite-mediated PKG1α dimerization was assessed in C57BL/6 thoracic aortae (conduit vessels) and mesentery (resistance vessels) via western blotting following IP treatment with vehicle control or sodium nitrite for 1 or 24 hours (0.1 mg/kg, 1 mg/kg, and 10 mg/kg), figure 33.

A one-way ANOVA was conducted to explore the effect of increasing doses of nitrite on PKG1α dimer levels in aortae and mesentery at 1 and 24-hours. In the aortae at 1 hour and 24 hours there was no statistical effect of nitrite dosing, $F(3, 16) = 1.056$, $p = 0.395$, and $F(3, 22) = 0.114$, $p = 0.951$, respectively. In the mesentery at 1 hour, there was no statistical effect of nitrite dosing, $F(3, 16) = 0.090$, $p = 0.964$, however, at 24 hours, there was a statistically significant effect for nitrite, $F(3, 20) = 5.194$, $p = 0.008$. Post-hoc comparisons using the Dunnett's Multiple Comparison test indicated that the mean score for placebo, mean (±SD) 19.43 (3.36) was significantly different from 1 mg/kg, 25.47 (4.63), $p < 0.05$)

and 10 mg/kg, 27.57 (2.89), $p < 0.01$), but did not differ significantly from 0.1 mg/kg, 18.96 (2.90), $p > 0.05$.

These findings indicate that nitrite did not induce PKG1α disulfide dimerization in the aorta at 1 or 24-hours (figure 33 A1 and 33 A2). However, nitrite did cause a dose-dependent increase in the PKG1α disulfide dimerization following 24-hours treatment in resistance vessels, $p = 0.008$ but not at 1-hour, $p = 0.964$ (figure 33 B1 and 33 B2). These experiments were conducted in n=5-7 mice per treatment group.

Conduit

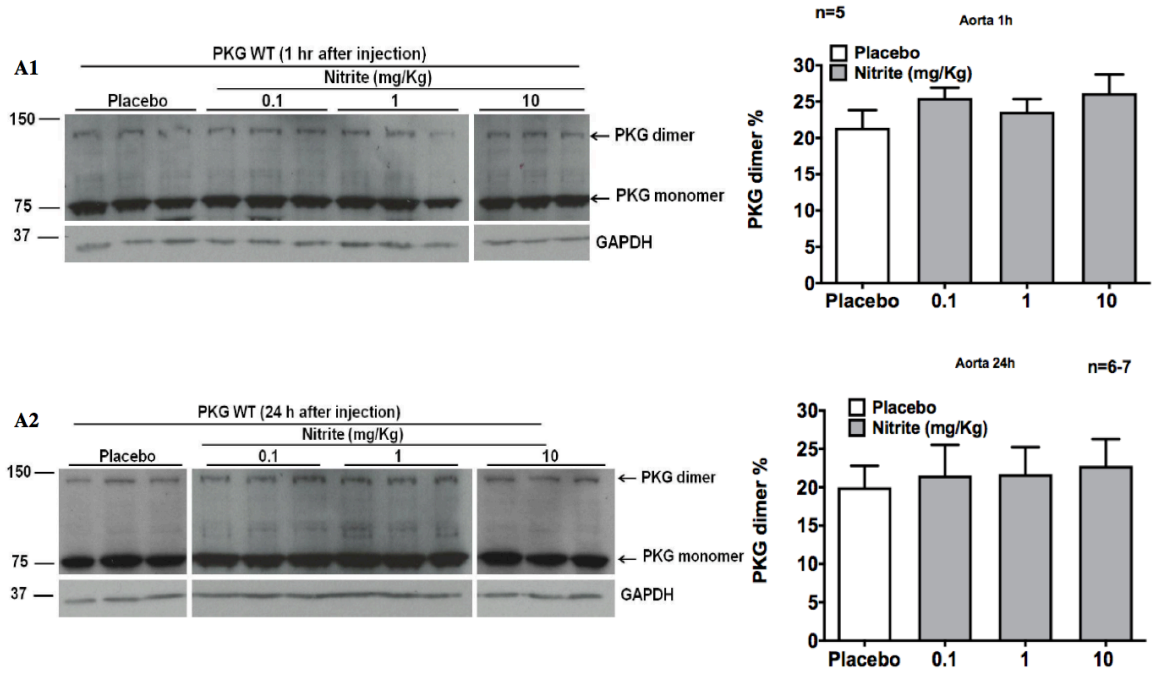

Resistance

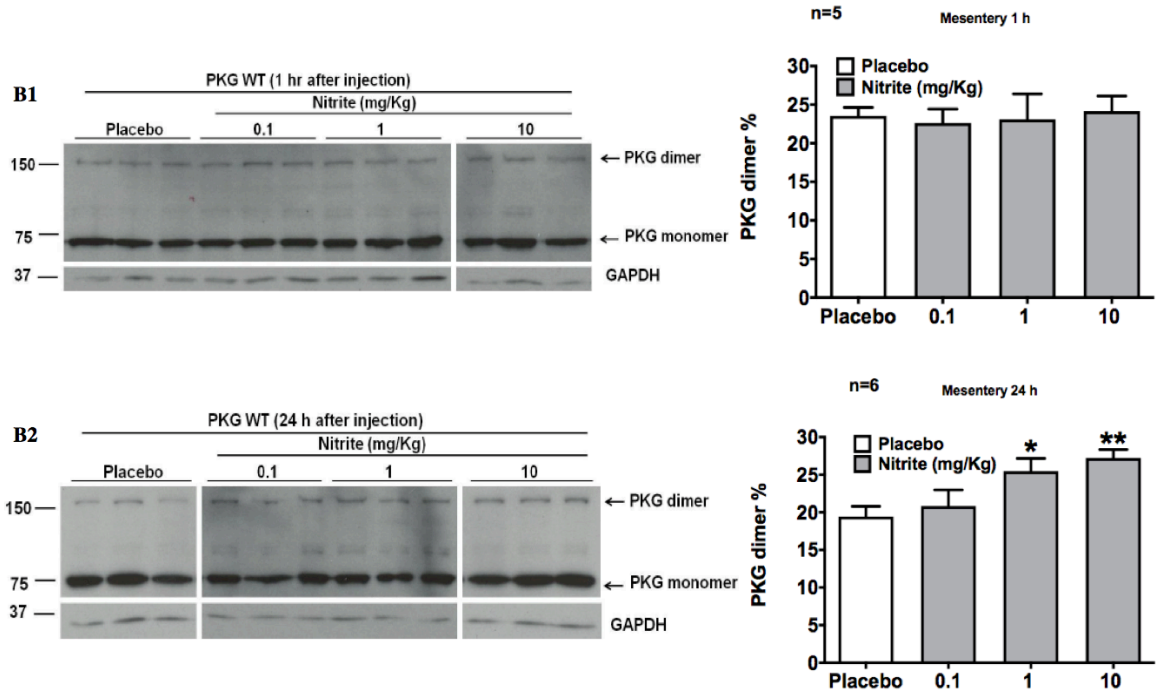

Figure 33: Nitrite-mediated PKG1α oxidative dimerization is a delayed and time-dependent phenomenon in mesenteric resistance vessels. Key – Aortae; conduit vessels – Panel A1: 1-hour exposure to nitrite, n=5, Panel A2: 24-hours exposure to nitrite, n=6-7. Mesenteric; resistance vessels – Panel B1: 1-hour exposure to nitrite, n=5, Panel B2: 24-hours exposure

to nitrite, n=6. Statistical analysis carried out using one-way ANOVA followed by Dunnett's Multiple Comparison post-hoc test; * $p \leq 0.05$, ** $p \leq 0.01$.

In summary, the above experiments showed the following:

1. Nitrite induced vasodilation in the WT and KI conduit vessels (Figure 30A).
2. Nitrite induced vasodilation in the WT resistance vessels, but this effect was significantly attenuated in the KI littermates (Figure 30B).
3. Nitrite-mediated vasodilation in the WT conduit vessels is significantly attenuated in the presence of sGC inhibition and NO-blockage (Figures 31A and 31B),
4. Nitrite-mediated vasodilation in the WT resistance vessels is unaffected by sGC inhibition and NO-blockage (Figures 32A and 32B).
5. Nitrite-mediated PKG1α dimer formation is observed at 24 hours in mesenteric vessels, $F(3, 20) = 5.194$, $p = 0.008$, but not in the conduit vessels, $F(3, 22) = 0.114$, $p = 0.951$ (Figure 33).

Discussion

In the first series of experiments, we demonstrated that during normoxia, nitrite (10^{-9}-$10^{-3.5}$ M) induced vasodilation in WT and KI PKG1α C57BL/6 thoracic aortae conduit vessels (Figure 30A). We also showed that during normoxia, nitrite (10^{-15}-$10^{-3.5}$ M) induced vasodilation in WT PKG1α C57BL/6 mesenteric resistance vessels, but that this effect was not observed in KI littermates (Figure 30B). This finding highlights two important points. Firstly, we showed that during normoxia there is a tissue-specific kinetic differences in vasoactivity, with thoracic aortae conduit vessels vasodilating only at higher concentrations of nitrite (10^{-5}M and above) whereas mesenteric resistance vessels showed a steady dose-dependent response. Secondly, we demonstrated that tissue-specific differences exist with respect to WT vs KI vasoactivity. In figure 30, thoracic aortae conduit vessels appeared to vasodilate equally, irrespective of presence of the transgenic (Cys42Ser) modification,

whereas mesenteric resistance vessels vasodilation was statistically reduced in the presence of the transgenic (Cys42Ser) modification. At the outset, we postulated that a difference may exist in vasoactivity with the transgenic (Cys42Ser) modification KI's being unable to form a PKG1α dimer (199). However, as we will discuss later, the observed difference in vasoactivity between the WT vs the KIs was not due to PKG1α dimer formation as this was observed at 24 hours in mesenteric vessels, but not in the conduit vessels.

In the second series of experiments, we showed that during normoxia, WT PKG1α C57BL/6 thoracic aortae conduit vasoactivity was statistically reduced in the presence of the sGC inhibitor, ODQ (10μM) and the NO inhibitor, CPTIO (1mM) (Figure 31). The loss of vasoactivity in the presence of either inhibitor indicates that WT PKG1α C57BL/6 thoracic aortae conduit vessels require the NO-sGC dependent pathway to induce vasodilation. Whilst this observation has not been previously confirmed at a molecular level, pharmacological experiments with NO scavenger and sGC inhibitors support this finding.

In the third series of experiments, we showed that during normoxia, WT PKG1α C57BL/6 mesenteric resistance vessel vasoactivity was preserved in the presence of the sGC inhibitor, ODQ (10μM) and the NO scavenger, CPTIO (1mM) (Figure 32). This finding suggests that WT mesenteric resistance vessels do not require the NO-sGC pathway to induce vasodilation and that vasodilation is taking place via a nitrite-mediated, NO-sGC-independent process in normoxia. This observation raises the question as to the relevance and the role of PKG1α dimerization in this equation. The literature suggests that PKG1α oxidation is more likely to take place in mesenteric vessels via NO-sGC independent mechanisms (341). Eaton's group have further demonstrated that PKG1α oxidation plays an essential role in the regulation of MAP/BP (201) but can be harmful in dysregulated activation states, such as sepsis (202).

In the fourth set of experiments, we showed that the formation of PKG1α dimer is a delayed and time-dependent phenomenon which takes place at 24-hours incubation in mesenteric vessels, $p = 0.008$. We also showed that even after 24-hours incubation, dimer was not present in conduit vessels (vs placebo), $p = 0.951$ (Figure 33). This finding indicated that our previous observations were not due to PKG1α dimer formation.

Taken together, our results support the notion that elevated vasoactivity in the WT PKG1α C57BL/6 mesenteric resistance vessels was likely due to a novel, nitrite-mediated, NO-sGC independent process which took place in the absence of PKG1α dimerization. Possible explanations for the reduced vasoactivity observed in the KIs may include off-target' effect of the transgenic KI process or some other complex tissue-specific differences.

In view of the nitrite-mediated NO-sGC-independent effect observed in mesenteric resistance vessels and the absence of PKG1α dimer formation before 24-hours incubation, we set about investigating the underlying mechanisms in more detail. We recognised that nitrite must be driving vasodilation in normoxia using a novel pathway, either via modification of nitrite, or by nitrite modifying the oxidative environment, resulting in a shift in the oxidative equipoise. The literature suggested that H_2O_2 (198), hydrogen sulphide (200), high ROS (202), polysulfer species (342), RSNOs (211), N_2O_3 (264, 265), and/or other intermediates (212-214) may all be capable of triggering oxidation of key downstream vasoactive targets driving PKG1α dimerization. Nitrite has also previously been shown to inhibit catalase (343). Our group therefore proposed that wheras nitrite usually acts as a reducing agent, by inhibiting catalase and thereby increasing H_2O_2, it may also indirectly act as an oxidant and be capable of dimerizing PKGIα through a NO-independent mechanism. Indeed, it has also been reported that PKG1α is subject to redox regulation such that the presence of oxidants can result in inter-protein disulfide formation, which translates into an increase in enzyme activity without change in cGMP concentration (198, 199). Thus, species

such as H_2O_2 that are capable of causing thiol to disulfide oxidation, can elicit VSMC relaxation and therefore lead to vasodilation via oxidative activation of PKG1α in a NO-independent fashion. Unlike H_2O_2, however, nitrite does not directly oxidize thiols to disulfides. Thus, the mechanism by which nitrite elicits a NO-independent and prolonged vasorelaxation is not likely to be via direct oxidation of PKG1α thiols triggering dimerization, but via an intermediate (131).

Our group continued to work on this project beyond the laboratory science component of this PhD. The extended research team showed in complementary work that nitrite is capable of inhibiting catalase activity in hepatic tissue *in vitro,* thus inhibiting the degradation of H_2O_2, consistent with pre-existing research (343, 344). These findings were confirmed in resistance arteries harvested 1 and 24-hours after nitrite pre-treatment *in vivo,* with a significant and similar increase in steady-state concentrations of H_2O_2 in mesenteric resistance vessels with both 1 and 10 mg/kg nitrite at - hour, which persisted at 24-hours, $p<0.05$. Next, to confirm the hypothesis that polysulfur species intermediates existed, we treated WT C57BL/6 mice with bolus IP administration of vehicle control or sodium nitrite (0.1, 1, and 10 mg/kg) for 1 or 24 h. Using LC-ESI-MS/MS following derivation with β-(4-hydroxyphenyl)ethyliodoacetamide (HPE-IAM) we showed dose-dependent increases in CysSSH, $p = 0.005$, and GSSH, $p = 0.0001$, in the resistance vessels (131).

Taken together, this work led us to propose that the delayed vasoactive properties of nitrite in mesenteric resistance vessels in normoxia are mediated via the generation of H_2O_2, with subsequent production of persulfide species including cysteine persuflide (CysSSH) and glutathione persulfide (GSSH), oxidatively activating PKG1α. This explains how administration of nitrite (that usually acts as a reducing agent) results in oxidation. We believe that polysulfur species are capable of modifying the local oxidative environment, leading to subsequent activation of key downstream vasoactive phosphoprotein targets,

independent of the PKG1α dimer. We also propose that with extended exposure, this oxidative balance drives PKG1α monomer to dimerize (in WT variants) and over a period of approximately 24-hours and this creates major vasodilation in systemic resistance vasculature, figure 33. This would explain clinical syndromes such as sepsis, for example (202) as this is characterised by a delayed and time-dependent processes which can result in major reductions in MAP (potentially mediated by PKG1α dimer formation). Whilst we have identified and described the association between nitrite, H_2O_2, and persulfide species, we do not exclude the possibility that other intermediates, such as RSNOs (including GSNO, HSNO and SNAP), other NONOates, N_2O_3, and others may also have a role to play in PKG1α oxidation/dimerization (131, 212-214).

These findings warrant further investigation to address the significance of this redox pathway in hypertensive and other cardiovascular disease models. This animal work could be extended to studying other dilators as described above, to see whether they also utilise similar pathways. Beyond animal work, it would also be important to examine whether a NO-independent mechanism plays a role in human vascular tone.

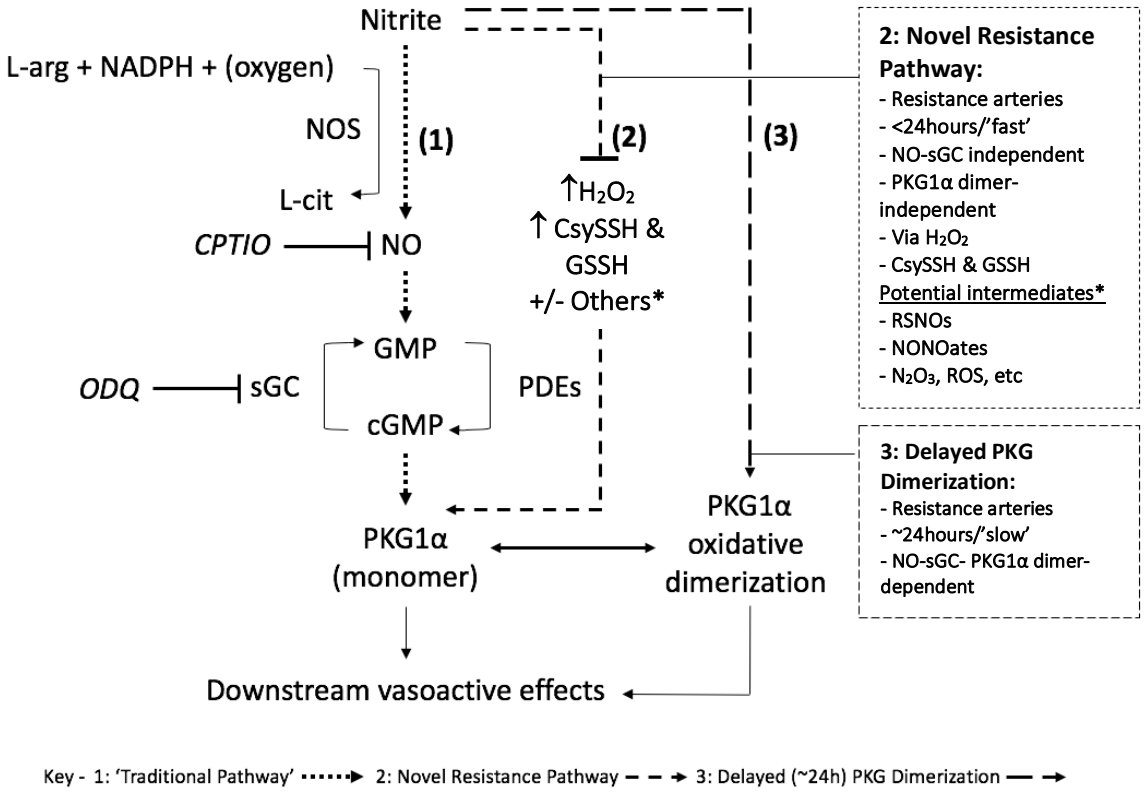

Figure 34: Proposed nitrite-mediated pathways in murine thoracic aortae conduit vessels and mesenteric resistance vessels in normoxia. Key – arg: L-arginine, NADPH: nicotinamide adenine dinucleotide phosphate, NOS: nitric oxide synthase, NO: nitric oxide, sGC: soluble guanylate cyclase, GMP: guanylate monophosphate, cGMP: cyclic guanosine monophosphate, N_2O_3: dinitrogen trioxide, PDEs: phosphodiesterase's, PKG: protein kinase G, CysSSH: cysteine persuflide, GSSH: glutathione persulfide, RSNO: S-nitrosothiols, ROS: reactive oxygen species.

Pathway 1: Traditional NO-sGC-cGMP-PKG pathway (310, 338)

Pathway 2: Novel Resistance pathway, 'fast', NO-sGC-independent, PKG1α dimer independent, mediated via H_2O_2 and/or cysteine hydropersulfide and glutathione persulfide (131) and/or RSNOs, NONOates, N_2O_3, other intermediates (212, 214)

Pathway 3: ~24h delayed PKG1α oxidative dimerization (198, 202, 203, 207, 208)

CHAPTER 4: EXAMINING THE VASOACTIVE PROPERTIES OF INTRA-BRACHIAL NITRITE INFUSION IN THE PRESENCE OF STORED AUTOLOGOUS WHOLE BLOOD IN NORMOXIA AND HYPOXIA in vivo

To examine the interaction effects of intra-brachial nitrite and intravenous autologous whole blood in both normoxia and hypoxia on forearm resistance artery vasodilation, the clinical study shown in this chapter was conducted in the NNUH with the support of the NHSBT service. Blood donation processes were supported by Dr Suhail Asghar (Associate Specialist, NHSBT) and Sister Patsy Lowson (Senior Sister at the Thetford donation team). NNUH blood bank management processes were supported by Dr Hamish Lyall and Mrs Debbie Asher. Senior on-call clinical support was provided by Dr Simon Fletcher (Critical Care Consultant) and Dr Vassilios Vassiliou (Cardiology Consultant). Nursing support was provided by Miss Rachel Stebbings and Mrs Vanessa Martin. Management of medical gases was supported by Mr Clive Beech. Statistical analysis was completed independently by Dr Allan Clark (Study statistician, UEA). Plasma sample analysis was completed by Dr Magda Minnion, Dr Bernie Fernandez and Prof Martin Feelisch. All remaining aspects of this study were conducted by myself.

Introduction

As previously discussed in Chapter 1, several clinical studies have showed that packed red cell transfusions which have been stored for prolonged periods are associated to increased mortality in critically ill patients (276-278). In 2008, the Gladwin group first showed that in normoxia, haem proteins could avidly scavenge, bind and attenuate NO (271) and then later associated this mechanism to blood degradation whilst in storage (272). In combination, these publications created the notion that stored blood with uncompartmentalized haemoglobin can be used in context of clinical research to reduce NO bioavailability and therefore as an alternative to the NO blocker CTPIO that is used in experimental studies but

which is not used in humans. Using this 'healthy volunteer NO-blockade model' we designed a study to test the effect of nitrite on resistance artery vasodilation in normoxia and hypoxia in healthy subjects and in the NO-reduced environment in humans. This comparison enabled our group to assess and compare the NO-dependent component of nitrite-mediated vasodilation during normoxia vs hypoxia.

Hypotheses

i. In hypoxia, given that nitrite-mediated vasodilation is known to be augmented and thought to be mainly due to NO release, we expected that the addition of autologous whole blood will reduce the degree of forearm vasodilation.

ii. In normoxia, we hypothesised that nitrite may be operating via a NO-independent process/es (as demonstrated *in vitro* in Chapter 3), therefore we expected that the addition of autologous whole blood will have a much lesser effect on nitrite induced forearm vasodilation.

Aim

To examine the effect of intra-brachial nitrite in the presence of cell-free haem on forearm resistance artery vasodilation in normoxia and hypoxia via strain gauge plethysmography.

Results

Recruitment

Recruitment for the Haem and Nitrite Study followed the processes outlined in Chapter 2 – Methods. We were contacted by 473 interested individuals and after screening each for suitability, 257 were invited to review the PIS. Following this, 75 wished to proceed to the face-to-face recruitment assessment, of which 60 were successfully recruited onto the study. During the study, 29 subjects discontinued: 14 of these withdrawals were due to personal

reasons, 9 were due to system failures (NHSBT and/or NNUH problems) and 4 were due to technical/plethysmography failures, figure 35. Overall, 31 subjects completed the entire cross-over study. The recruitment sample size target was 41 subjects (80% power, statistical significance of 10% (one-sided 5%), effect size of 0.40), but attrition of 48% far-exceeded expectations. The study consort diagram is shown in figure 35.

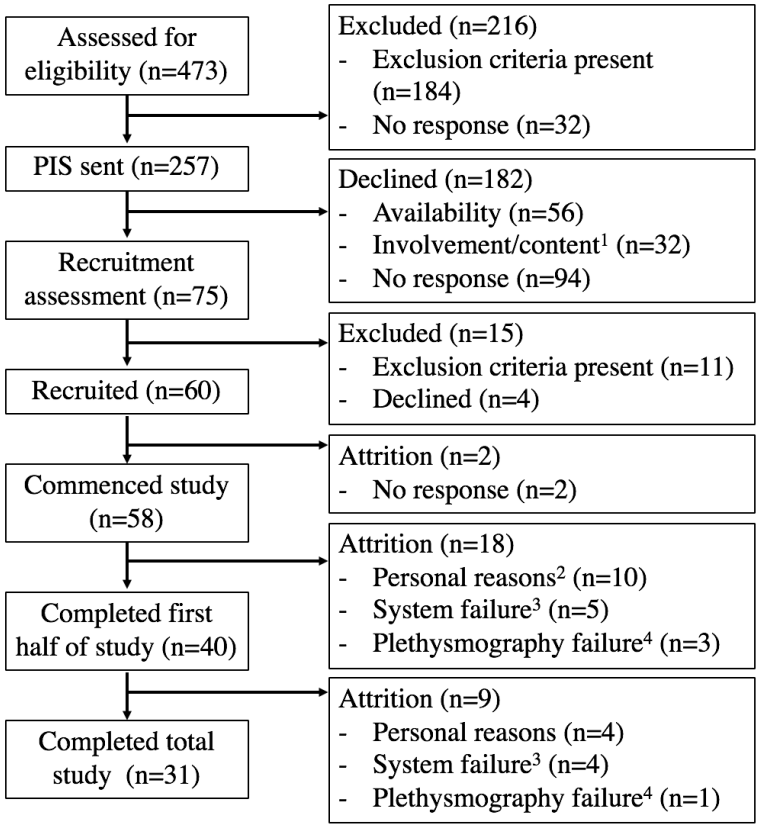

Figure 35: The Haem and Nitrite Study CONSORT diagram

[1] – Involvement/content: declined due to degree of involvement required to participate, level of commitment required, and invasive nature of the study

[2] – Personal reasons: attrition due to changes in occupation or residential location, family commitments, wellbeing and health status, non-defined attrition

[3] – System failure: NHSBT donation slot limitations, NHSBT donation failures, NHSBT processing error, NNUH facility failure, NNUH equipment failure

[4] – Plethysmography failure: autologous whole blood unit provision failure, plethysmography equipment failure, technical failure (inability to gain arterial access).

Population

The study cohort was mostly male (74%) and generally young to middle-aged (mean 43.4 years), table 2. Subjects had no history of active smoking, hypertension, diabetes mellitus, hypercholesterolaemia and no family history of premature ischaemic heart disease. All subjects had a normal cardiovascular examination and normal bedside clinical observations. The study was approved by the East of England – Essex REC. Investigations took place at the NNUH in the CRTU with subjects having had a light breakfast and having abstained from caffeine-containing drinks for at least 6-hours.

Baseline characteristics

This was a healthy volunteer study. As detailed in Chapter 2 – Methods, clear inclusion and exclusion criteria were pre-defined and subjects who did not satisfy the criteria were not selected to participate. Baseline characteristics and haemodynamics were recorded, table 2.

Table 2: Baseline characteristics for healthy volunteers in the Haem and Nitrite study

Characteristic	Subject (n=31)
Sex	
Male (%)	23 (74%)
Female (%)	8 (26%)
Age	
Mean (range)	43.4 (20-73)
Systolic blood pressure (mmHg)	
Mean (±SD)	124.1 (11.7)
Diastolic blood pressure (mmHg)	
Mean (±SD)	75.4 (8.4)
Heart rate (bpm)	
Mean (±SD)	59.6 (10.6)

Safety reporting: adverse events and serious adverse events

In the present study we administrated 3 μmol/min in normoxia and 1 μmol in hypoxia via an intra-brachial line over the 30-minute period (total does, 90 μmol and 30 μmol

respectively). As discussed in Chapter 2, the concentration infused was taken from the study published in 2008 by Dr Abdul Maher in our group (345). Their work showed that 7.84 μmol/min over a 20-minute infusion period (total dose 156.8 μmol) could be administrated safely and was well-tolerated in healthy volunteers. We selected the ED_{50} value of 3 $\mu mol/min^{-1}$ in normoxia and 1 $\mu mol/min^{-1}$ in hypoxia over a 30-minute infusion period. Discussion of the study drug dose and administration regimen is discussed in further detail later.

During the course of the study, we had 3 adverse events (AEs) that were identified as not being associated with nitrite (an episode of sudden-onset anxiety preceding any study intervention, mild swelling of the non-infused arm during the autologous whole blood transfusion and mild neck swelling which clinically presented like a swollen parotid gland ~6 hours after the study visit completed). We also had 1 serious adverse event (SAE) which was related to transfusion of non-autologous blood (but not the study drug). This was rapidly escalated to my supervising team and subsequently reported to the sponsor, REC, SHOT, and SABRE reporting schemes in-line with the study protocol, details of which are presented in Appendix 8.

Pulse oximetry and room temperature

During infusions in normoxia, the mean (±SD) oxygen saturation recorded by pulse oximetry for all subjects was 98.1% ± 1.6%. During the infusions in hypoxia, the mean (±SD) oxygen saturation for all subjects was 87.4% ± 2.8%. The target range during hypoxia was 84-88% and this was achieved in 28/31 studies (93.3%). The remaining 3 hypoxia studies did not achieve oxygen saturations <88% despite extended exposure to the 12% oxygen/88% nitrogen gas, at high flow ($15L/min^{-1}$), representing variability in intra-subject hypoxic ventilatory responses (235). The CRTU room temperature was recorded throughout each study in order to maintain optimum ambient temperatures (22-26^{o}C). The mean (±SD)

room temperature for all studies was 22.7°C ± 3.8°C. The target ambient temperature was maintained throughout the study day on 52/62 occasions (83.9%). On the remaining 10 days, temperatures either fell below 22°C (in the winter months) or rose above 26°C (in the summer months), such that the optimum study temperature was not maintained throughout the study day. The study facility did not have integrated air-conditioning and we were not permitted to use free-standing air-conditioning or heating units (as this was not allowed by the hospital site management team). Therefore, we managed the ambient room temperature to the best of our ability using free-standing oscillating fans.

As discussed, all data was visually inspected for consistency across all of the studied patients and as shown in figure 18, highly variable flows and outliers were excluded. Given the very high study participant attrition, in order to have as much interpretable data as possible, we did not systemically exclude those whose ambient study temperature or hypoxic oxygen saturations were not achieved or maintained during the study day and instead we reviewed all data equally and all non-excluded data was included for analysis.

Blood analysis

Plasma nitrite levels

Blood was collected for analysis before and after each nitrite infusion. Samples were analysed for nitrite and nitrate levels. Samples were not analysed for RXNO levels and this limitation is noted in the methods and the discussion chapters. Descriptive statistics revealed the following. In normoxia, before blood transfusions (sample collection normoxia timepoint 1, Figure 14) baseline nitrite was 0.14 μmol (± 0.03 μmol) and after nitrite infusion (sample collection normoxia timepoint 2) was 0.72 μmol (± 0.27 μmol). After blood transfusion, baseline nitrite (sample collection normoxia timepoint 3) was 0.43 μmol (± 0.23 μmol) and after infusion (sample collection normoxia timepoint 4) was 1.21 μmol (± 0.39

μmol). In hypoxia, nitrite levels were 0.15 μmol (± 0.04 μmol), 0.40 μmol (± 0.10 μmol), 0.19 μmol (± 0.09 μmol) and 0.82 μmol (± 0.28 μmol) at each of these timepoints.

A one-way repeated measures ANOVA was conducted to compare plasma nitrite levels before and after each nitrite infusion, as measured by HPLC. There was a statistically significant main effect for nitrite in each of the 4 study conditions. Before blood in normoxia: plasma nitrite levels $F(1, 30) = 4.567$, $p = 0.041$, partial eta squared = 0.132. After blood in normoxia: plasma nitrite levels $F(1, 29) = 4.377$, $p = 0.045$, partial eta squared = 0.131. Before blood in hypoxia: plasma nitrite levels $F(1, 30) = 6.821$, $p = 0.014$, partial eta squared = 0.185. After blood in hypoxia: plasma nitrite levels $F(1, 30) = 5.628$, $p = 0.024$, partial eta squared = 0.158. These findings indicate that the addition of nitrite led to an increase in plasma nitrite levels in each of the 4 conditions studied, figure 36.

Plasma nitrate levels

Descriptive statistics revealed the following: In normoxia, before blood transfusions (sample collection normoxia timepoint 1, Figure 14), baseline nitrate was 35.62 μmol (± 2.22 μmol) and after infusion (sample collection normoxia timepoint 2) was 37.03 μmol (± 2.55 μmol). After blood transfusion, baseline nitrate (sample collection normoxia timepoint 3) was 34.15 μmol (± 1.88 μmol) and after infusion (sample collection normoxia timepoint 4) was 36.77 μmol (± 2.07 μmol). In hypoxia, nitrate levels were 41.45 μmol (± 3.12 μmol), 38.64 μmol (± 3.05 μmol), 35.31 μmol (± 2.49 μmol) and 36.44 μmol (± 2.56 μmol) at each of these timepoints.

A one-way repeated measures ANOVA was conducted to compare plasma nitrate levels before and after each nitrite infusion, as measured by HPLC. There was not a statistically significant main effect for nitrite before blood in normoxia: plasma nitrate levels $F(1, 30) = 0.499$, $p = 0.485$, partial eta squared = 0.016, but there was a statistically significant main

effect for nitrite after blood in normoxia: plasma nitrate levels $F(1, 29) = 4.624$, $p = 0.040$, partial eta squared = 0.138. Whilst in hypoxia, there was a statistically significant main effect for nitrite before blood: plasma nitrate levels $F(1, 29) = 4.624$, $p = 0.040$, partial eta squared = 0.138, but not after blood: plasma nitrate levels $F(1, 30) = 1.808$, $p = 0.189$, partial eta squared = 0.057. These findings indicate that the addition of nitrite led to variable changes to plasma nitrate levels in each of the 4 conditions studied, figure 36.

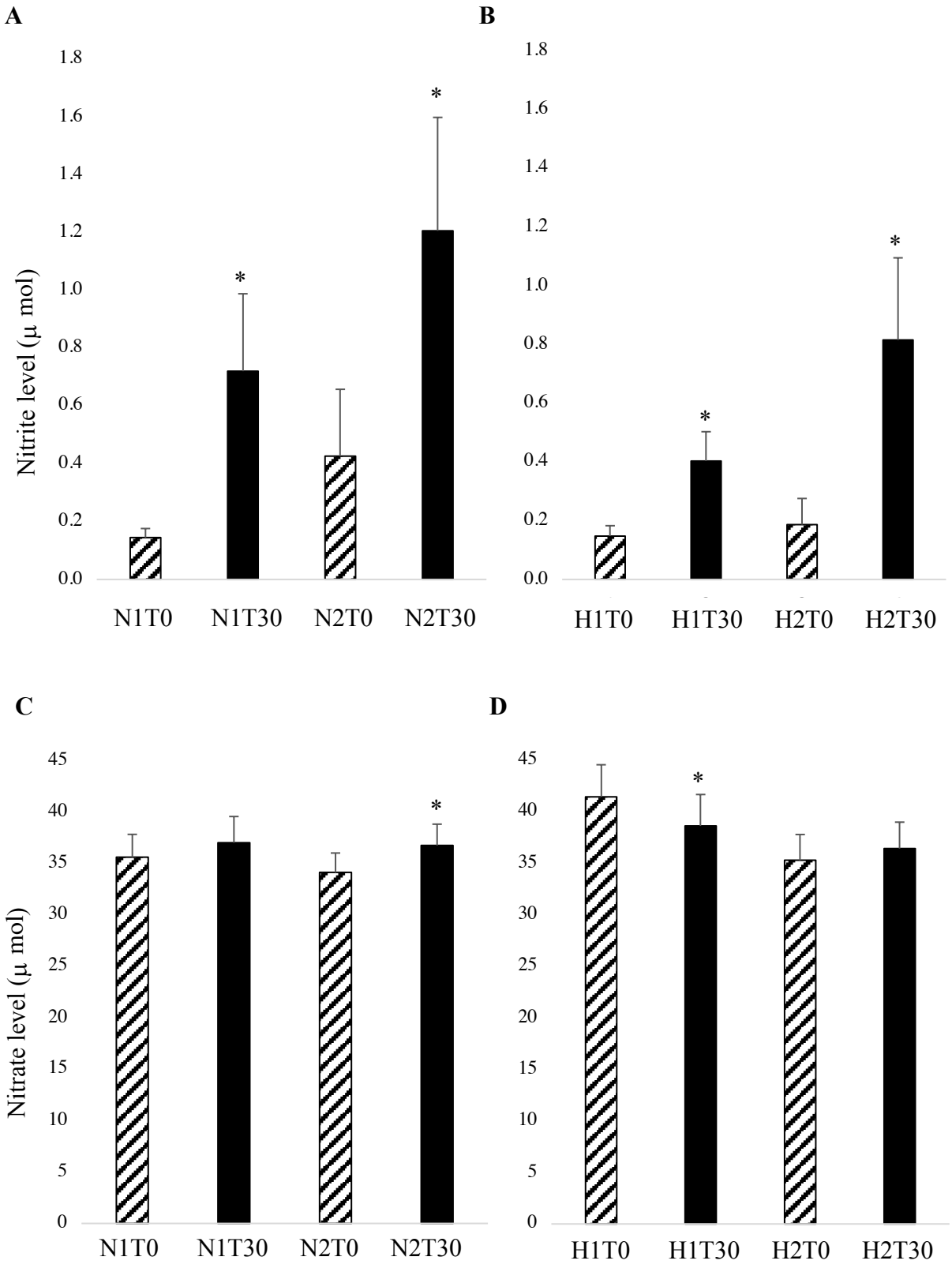

Figure 36: Plasma NOx levels, n = 31. Panel A: Nitrite in normoxia, B: Nitrite in hypoxia, C: Nitrate in normoxia, D: Nitrate in hypoxia. Key (as per figure 14) - N1: first nitrite infusion in normoxia, N2: second nitrite infusion in normoxia, H1: first nitrite infusion in hypoxia, H2: second nitrite infusion in hypoxia, T0: plethysmography FBFR at time 0 mins, T30: FBFR at 30 mins. Values shown as mean (±SEM). Statistical analysis carried out using one-way ANOVA followed by Bonferroni post-hoc test; * $p<0.05$.

Plasma haemoglobin levels

Blood was collected for analysis before, during (at 90-minutes) and after each autologous whole blood transfusion. Samples were analysed for haemoglobin levels. Descriptive statistics revealed that in normoxia (at sample collection normoxia timepoint 2, Figure 14), baseline plasma haemoglobin levels were 71.3 mg/dL (± 12.08 mg/dL), at 90-minutes levels (sample collection normoxia timepoint 3) plasma haemoglobin levels were 96.6 mg/dL (± 17.55 mg/dL) and after the autologous whole blood transfusion (sample collection normoxia timepoint 4) plasma haemoglobin levels were 86.7 mg/dL (± 15.76 mg/dL). In hypoxia, plasma haemoglobin levels were 63.1 mg/dL (± 15.65 mg/dL), 125.3 mg/dL (± 21.38 mg/dL) and 115.8 mg/dL (± 28.78 mg/dL) at each of the respective timepoints.

A one-way repeated measures ANOVA was conducted to compare plasma haemoglobin levels before, during and after each autologous whole blood transfusion, as measured by ELISA (Abcam, UK). There was not a statistically significant main effect for autologous whole blood transfusion on plasma haemoglobin level in normoxia, $F(2,28) = 1.315$, $p = 0.286$, partial eta squared = 0.086, or hypoxia, $F(2, 29) = 2.757$, $p = 0.080$, partial eta squared = 0.160. These findings indicate that the addition of one unit of autologous whole blood does not statistically increase subject plasma haemoglobin levels in normoxia or hypoxia, figure 37.

Autologous whole blood transfusion unit haemoglobin levels

Blood was also collected from a subset of autologous whole blood transfusion units (n = 18) to analyse plasma haemoglobin levels in the stored unit. In those used in the normoxic studies, plasma haemoglobin levels were 289 mg/dL (± 50.30 mg/dL) and in those used in the hypoxic studies, plasma haemoglobin levels were 294.5 mg/dL (± 66.46 mg/dL).

A one-way repeated measures ANOVA was conducted to compare plasma haemoglobin level in the autologous whole blood transfusion unit with the unit donors' baseline level, as measured by ELISA (Abcam, UK). There was a statistically increased level of plasma haemoglobin in the autologous whole blood transfusion unit when compared to the unit donors' baseline plasma haemoglobin level in normoxia, $F(1, 9) = 20.146$, $p = 0.002$, partial eta squared = 0.691, and in hypoxia, $F(1, 7) = 11.416$, $p = 0.012$, partial eta squared = 0.620. These findings indicate that the plasma haemoglobin level in the autologous whole blood units was significantly greater than the plasma haemoglobin level in the respective unit donors, in both normoxia and hypoxia transfusion units, figure 37.

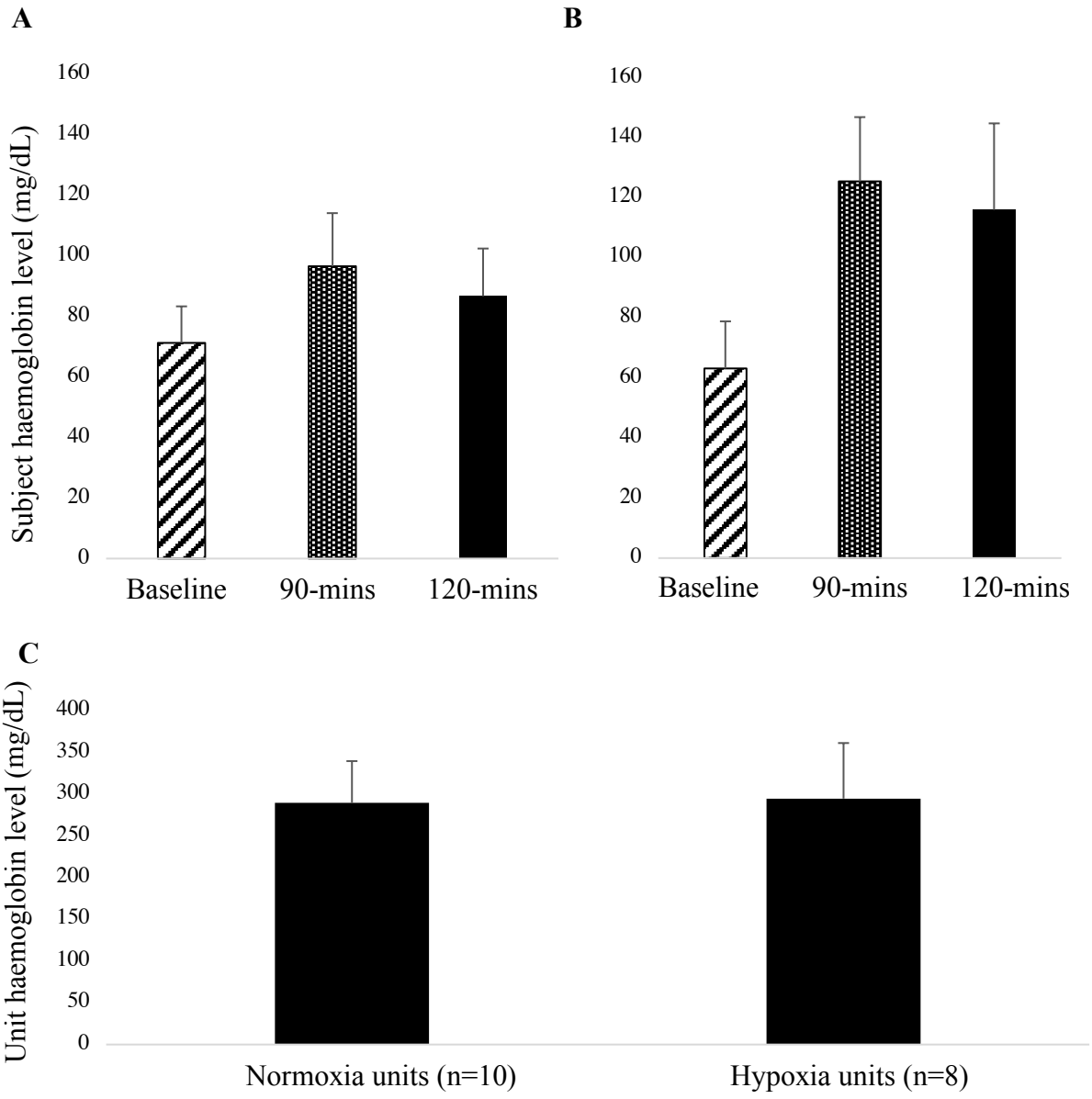

Figure 37: Plasma haemoglobin levels. Panel A: Subject plasma haemoglobin levels in normoxia, n = 31. Panel B: Subject plasma haemoglobin levels in hypoxia, n = 31. Panel C: A subset of autologous whole blood transfusion unit haemoglobin levels in normoxia and hypoxia, n = 18. Values shown as mean (±SEM). Statistical analysis carried out using one-way ANOVA followed by Bonferroni post-hoc test; p=ns.

NO consumption levels

Descriptive statistics revealed that in normoxia, before autologous blood transfusion (at sample collection normoxia timepoint 2, Figure 14), baseline NO consumption level was 92.16 μmol (± 8.97 μmol). At 90-minutes into the autologous blood transfusion (sample

collection normoxia timepoint 3) NO consumption level was 107.07 μmol (± 12.64 μmol). After the transfusion (sample collection normoxia timepoint 4), the NO consumption level was 106.12 μmol (± 10.05 μmol). In hypoxia, NO consumption levels were 104.83 μmol (± 11.44 μmol), 169.23 μmol (± 30.00 μmol) and 153.95 μmol (± 26.23 μmol) and each of the respective timepoints.

A one-way repeated measures ANOVA was conducted to compare NO consumption levels before, during and after each autologous whole blood transfusion, as measured by ozone-based chemiluminescence (274, 330). There was not a statistically significant main effect for autologous whole blood transfusion on plasma haemoglobin level in normoxia, $F(2, 29) = 1.227$, $p = 0.302$, partial eta squared = 0.103, or hypoxia, $F(2, 29) = 2.256$, $p = 0.114$, partial eta squared = 0.180. These findings indicate that the addition of one unit of autologous whole blood does not increase subject NO consumption levels in normoxia or hypoxia, figure 38.

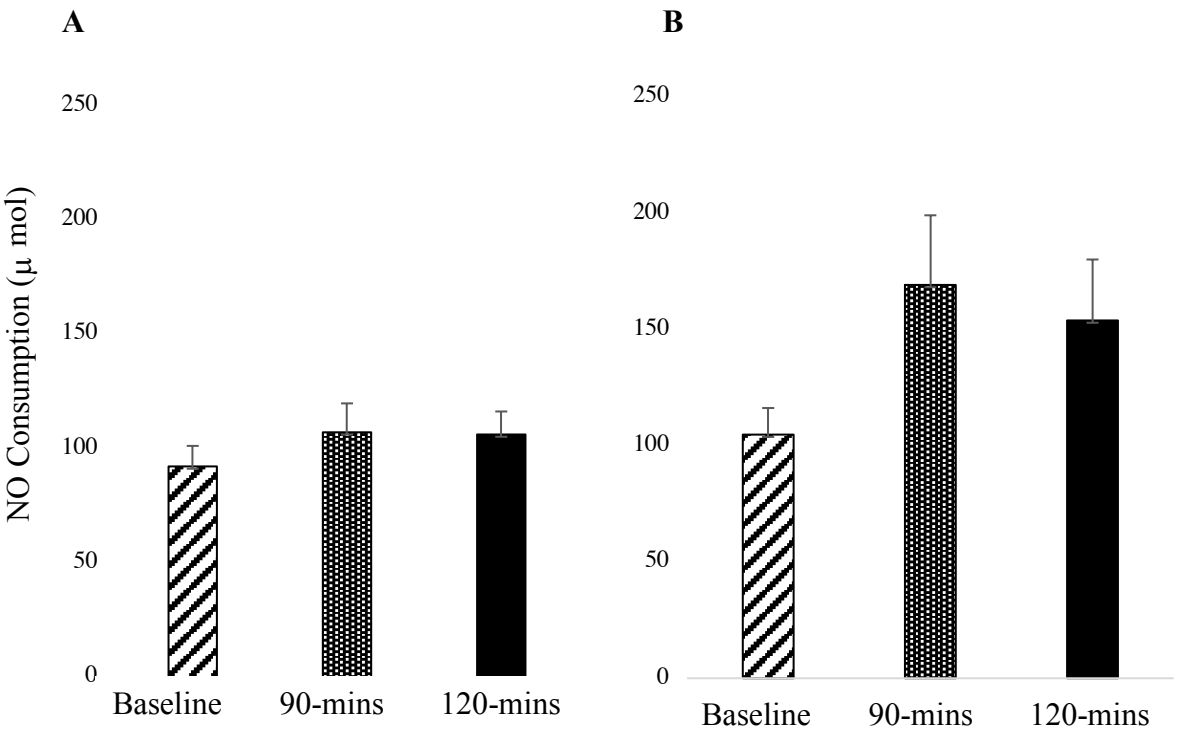

Figure 38: NO consumption levels. Panel A: NO consumption levels in normoxia, n = 31. Panel B: NO consumption levels in hypoxia, n = 31. Values shown as mean (±SEM). Statistical analysis carried out using one-way ANOVA followed by Bonferroni post-hoc test; p=ns.

Mixed effect linear regression model results

Model 1: Effect of nitrite, autologous blood and oxygen condition on FBFR

FBFRs were significantly predicted by nitrite infusion status, $p<0.001$, but not by any other of the main effects or interaction effects (no effect for blood or oxygen condition observed). The FBFR beta-estimate was on average 0.56 higher at T30 than at T0 across both oxygen condition combined and regardless of blood transfusion, table 3. Overall, the fixed effects accounted for 18.3% of the variance in the data (marginal R^2), whilst taking also the random effects into account increased the explanatory power of the model for FBFRs to 38.0% (conditional R^2). This reflects that inter-subject variability was high and thus contributed substantially to the amount of variance that could be explained by the model.

Table 3: Mixed effect linear regression model 1 (effect of nitrite, autologous blood and oxygen condition on FBFR)

Source	**Estimated regression Coefficient**	**Regression Confidence Intervals (CI)†**	**p-value***
Plasma nitrite levels	-0.06	-0.15 – 0.02	0.124
Blood condition	0.03	-0.24 – 0.31	0.592
Oxygen condition	0.11	-0.16 – 0.39	0.050
Nitrite infusion status	0.56	0.28 – 0.84	**<0.001**
Oxygen condition* Nitrite infusion status	0.11	-0.21 – 0.43	0.512
Oxygen condition* Blood condition	-0.01	-0.33 – 0.31	0.966
Blood condition* Nitrite infusion status	0.03	-0.29 – 0.34	0.877
Marginal R^2/ Conditional R^2: 0.183/0.380			

† conditional effects, * averaged effects

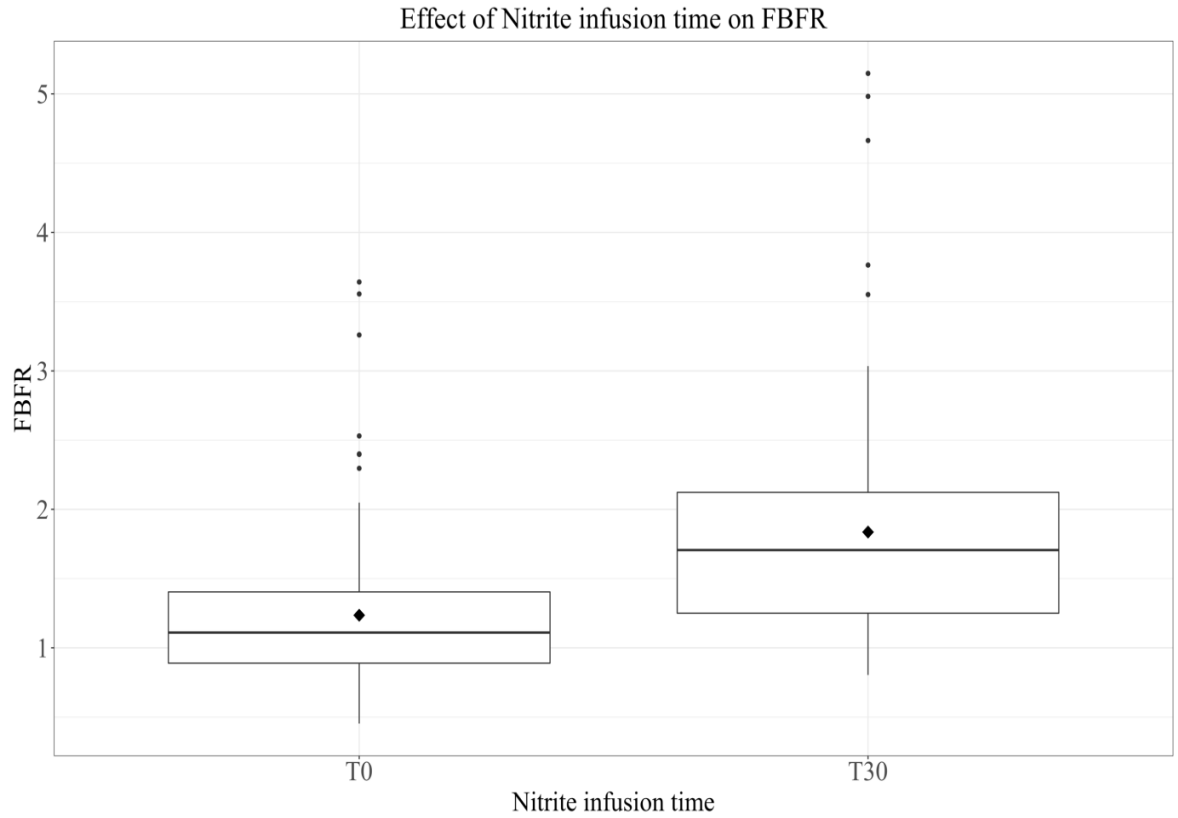

Figure 39: Effect of nitrite infusion status on FBFR in the overall model. Boxes represent interquartile range (IQR), whiskers showing lowest and highest quartile group, middle line denotes median, diamond denotes mean, single dots represent data points >1.5x IQR

Model 2 and 3: Effect of nitrite and autologous blood on FBFR (in normoxia and hypoxia)

To further evaluate whether the observed effect would be present to a similar degree in normoxia and hypoxia, we ran a separate model for each oxygen condition (tables 4 and 5). In normoxia only, model 2, and hypoxia only, model 3, the same findings were observed, with FBFRs only being significantly explained by nitrite infusion status, both $p<0.001$. The FBFR beta-estimate was on average 0.52 in normoxia and 0.64 in hypoxia, Figure 40. The amount of variance explained by the fixed effects only was 18.1% and 15.0% in the normoxia and hypoxia only models, respectively. As before, addition of random effects increased the explanatory power of the models to predict FBFR to 66.8% and 77.2%, respectively.

Table 4: Mixed effect linear regression model 2 (effect of nitrite and autologous blood on FBFR in normoxia only)

Source	**Estimated regression Coefficient**	**Regression Confidence Intervals (CI)†**	**p-value***
Nitrite plasma levels	0.00	-0.07 – 0.07	0.951
Blood condition	0.02	-0.17 – 0.22	0.623
Nitrite infusion status	0.52	0.32 – 0.72	**<0.001**
Blood condition* Nitrite infusion status	0.02	-0.26 – 0.30	0.869
Marginal R^2/ Conditional R^2: 0.181/0.668			

† conditional effects, * averaged effects.

Table 5: Mixed effect linear regression model 3 (effect of nitrite and autologous blood on FBFR in hypoxia only)

Source	**Estimated regression Coefficient**	**Regression Confidence Intervals (CI)†**	**p-value***
Nitrite plasma levels	-0.02	-0.13 – 0.09	0.690
Blood condition	0.00	-0.21 – 0.22	0.859
Nitrite infusion status	0.64	0.43 – 0.85	**<0.001**
Blood condition* Nitrite infusion status	0.02	-0.27 – 0.32	0.876
Marginal R^2/ Conditional R^2: 0.150/0.772			

† conditional effects, * averaged effects.

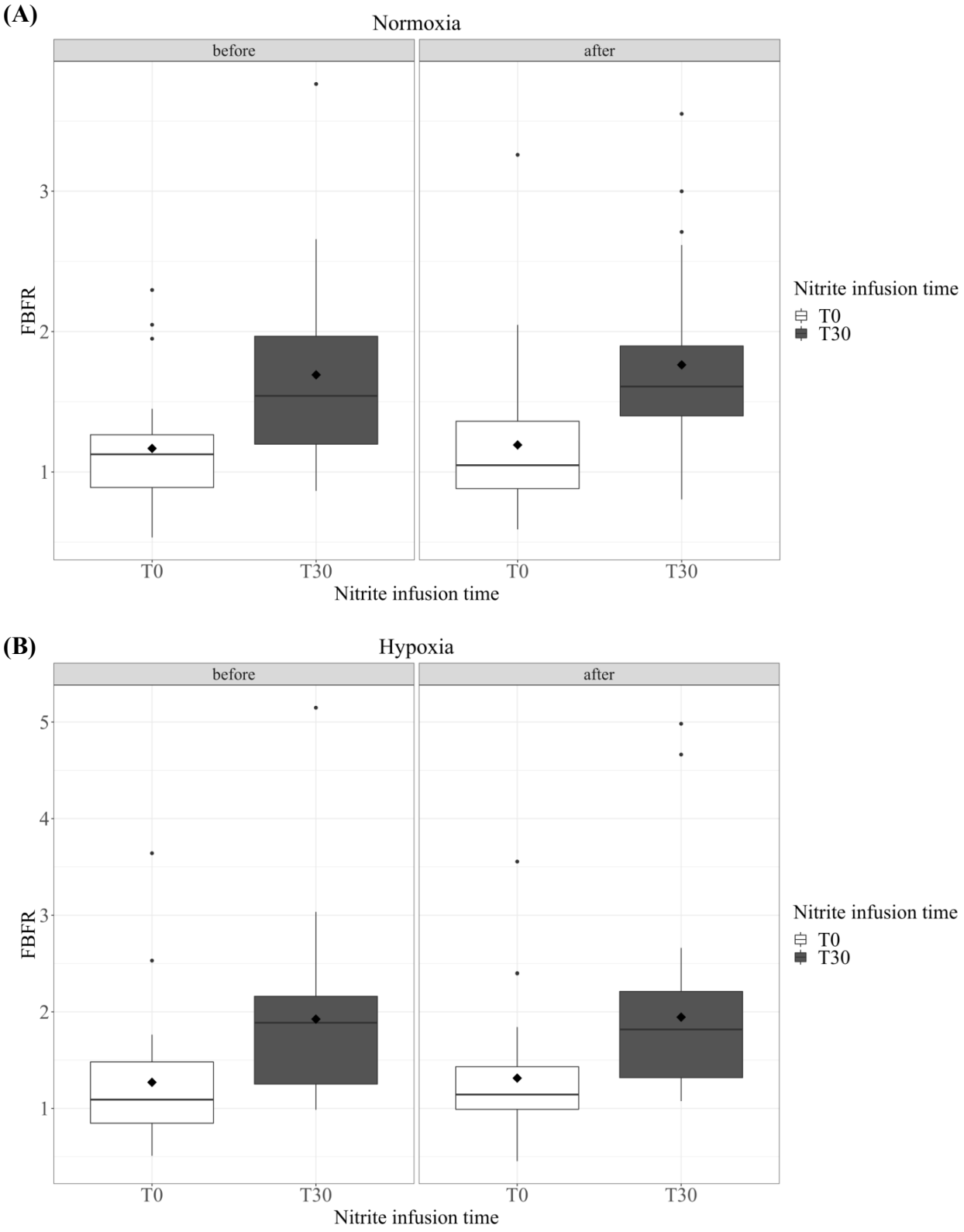

Figure 40: Effect of nitrite infusion status on FBFR in (A) Normoxia and (B) Hypoxia. Left side shows "before" blood transfusion, right side shows "after" blood transfusion. Boxes represent interquartile range (IQR), whiskers showing lowest and highest quartile group, middle line denotes median, diamond denotes mean, single dots represent data points >1.5x IQR.

Model 4: Effect of nitrite and oxygen condition on FBFR (after autologous blood only)

Considering only the data reflecting changes in FBFR once the whole autologous blood transfusion was administered, to test if there was a discernible difference in FBFR after blood in normoxia vs hypoxia, we again showed that only nitrite infusion status. $p<0.001$, had a significant effect on FBFR in the model, table 6, whilst no other main or interaction effects were found to be significant, figure 41. The FBFR beta-estimate was on average 0.61 from T0 to T30.

Table 6: Mixed effect linear regression model 4 (effect of nitrite and oxygen condition on FBFR after autologous blood only)

Source	**Estimated regression Coefficient**	**Regression Confidence Intervals (CI)†**	**p-value***
Nitrite plasma levels	-0.07	-0.18 – 0.04	0.200
Oxygen condition	0.12	-0.24 – 0.47	0.259
Nitrite infusion status	0.61	0.24 – 0.98	**<0.001**
Oxygen condition* Nitrite infusion status	0.07	-0.44 – 0.57	0.802
Marginal R^2/ Conditional R^2: 0.177/0.304			

† conditional effects, * averaged effects.

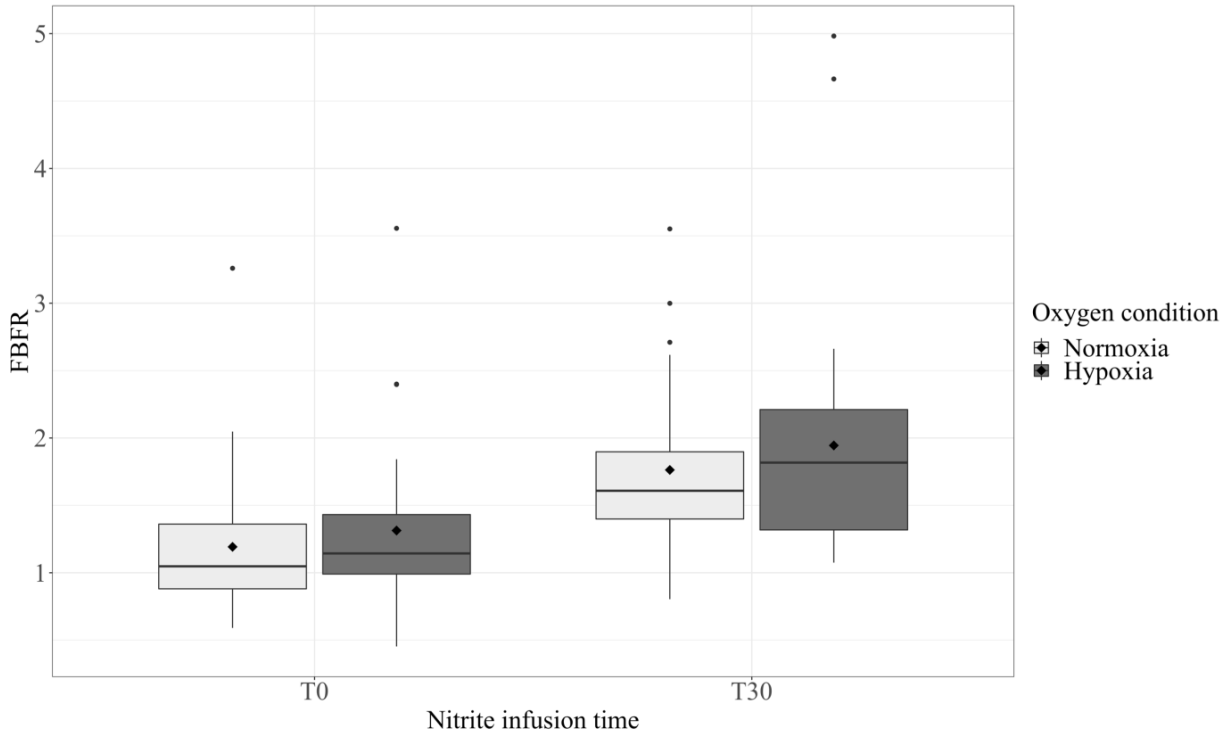

Figure 41: FBFRs after autologous blood transfusion at T0 and T30 by oxygen condition. Normoxia: light grey, Hypoxia: dark grey. Boxes represent interquartile range (IQR), whiskers showing lowest and highest quartile group, middle line denotes median, diamond denotes mean, single dots represent data points >1.5x IQR.

Model 5: Effect of nitrite, autologous blood and oxygen condition on mean arterial pressure

There was a significant effect of 'blood condition', p=0.030, and 'nitrite infusion status', p=0.010, on MAP, but no significant interaction effect between the two, p=0.888. Nor was MAP significantly predicted by any other variables in our model, table 7. Using least square means, we determined that blood condition and nitrite infusion status had opposing effects on MAP. Whilst the administration of whole autologous blood increased MAP by an average of 2.20 mmHg (SE:1.00, 95% CI), the nitrite infusion caused a decrease in MAP by 2.67 mmHg (SE:1.03, 95% CI) when comparing MAP at T0 to T30.

Table 7: Mixed effect linear regression model 5 (effect of nitrite, autologous blood and oxygen condition on mean arterial pressure)

Source	**Estimated regression Coefficient**	**Regression Confidence Intervals (CI)†**	**p-value***
Plasma nitrite levels	0.95	-0.06 – 1.96	0.068
Blood condition	1.02	-2.36 – 4.40	**0.030**
Oxygen condition	-1.34	-4.70 – 2.01	0.602
Nitrite infusion status	-3.08	-6.49 – 0.33	**0.010**
Oxygen condition*Nitrite infusion status	1.10	-2.82 – 5.01	0.584
Oxygen condition*Blood condition	2.65	-1.27 – 6.56	0.187
Blood condition* Nitrite infusion status	-0.28	-4.18 – 3.62	0.888
Marginal R^2/ Conditional R^2: 0.045/0.433			

† conditional effects, * averaged effects.

Model 6: Effect of nitrite, autologous blood and oxygen condition on heart rate

Heart rate (HR) was significantly affected by 'blood condition', $p<0.001$, but we observed no other significant effects, meaning that neither nitrite infusion, nor oxygen condition had a significant impact on participants' HR, table 8. Administration of whole autologous blood transfusion led to an average increase of 3.3 bpm (SE: 0.85, 95% CI).

Table 8: Mixed effect linear regression model 6 (effect of nitrite, autologous blood and oxygen condition on heart rate)

Source	**Estimated regression Coefficient**	**Regression Confidence Intervals (CI)†**	**p-value***
Plasma nitrite levels	0.41	-0.46 – 1.28	0.353
Blood condition	1.21	-1.65 – 4.06	**<0.001**
Oxygen condition	-0.01	-2.85 – 2.83	0.055
Nitrite infusion status	-1.09	-3.98 – 1.80	0.858
Oxygen condition*Nitrite infusion status	0.51	-2.80 – 3.82	0.763
Oxygen condition*Blood condition	2.81	-0.50 – 6.13	0.097
Blood condition* Nitrite infusion status	1.36	-1.94 – 4.65	0.422
Marginal R^2/ Conditional R^2: 0.037/0.683			

† conditional effects, * averaged effects.

In summary, the above study showed the following:

1. NOx: Intra-brachial nitrite infusion led to a significant increase in plasma nitrite levels in all 4 conditions (N1: p = 0.041, N2: p = 0.045, H1: p = 0.014, H2: p = 0.024), all p<0.05
2. Unit cell-free haem: Storage of autologous whole blood for 30-35 days led to an increase in unit cell-free haem of ~410% in normoxia and ~470% in hypoxia
3. Subject cell-free haem and NO consumption: Transfusion of 30-35-days stored autologous whole blood led to non-significant increases in subject cell-free haemoglobin and non-significant increases in subject NO consumption
4. Model 1 showed that there was high inter-subject variability (~20%) and that FBFRs were significantly predicted by nitrite infusion status, p<0.001, but not by any other main effects or interaction effects

5. Models 2-4 confirmed the findings in Model 1: the observed effect was present to a similar degree in normoxia only, $p < 0.001$, hypoxia only $p < 0.001$, and after autologous whole blood transfusion only $p < 0.001$
6. Model 5 showed that autologous whole blood transfusion led to a significant increase in MAP (mean + 2.20 mmHg), p=0.030, whilst nitrite infusion led to a significant reduction in MAP (mean - 2.67 mmHg), p=0.010, but there was no interaction between these two factors
7. Model 6 showed that HR was significantly increased (mean + 3.3 bpm) following autologous whole blood transfusion, $p<0.001$.

Discussion

The main findings in this healthy volunteer cross-over study were that intra-brachial nitrite infusions (N1, N2, H1 and H2) led to significant increases in plasma nitrite (figure 36) which in-turn led to significant increases in FBFRs in all four study conditions (Model 1). Maher showed that intra-brachial nitrite dosed at 3.14 μmol/min over a 20-minute infusion period led to a significant increase in plasma nitrite in the infused arm vs the control arm (nitrite +4 μmol, p=0.0001) which resulted in an increased FBFR of ~x1.8 in normoxia (237). We too showed that nitrite led to significant increases in plasma nitrite in all four studied conditions. As detailed in Chapter 2, the normoxia and hypoxia doses were based on 50% effective dose (ED_{50}) values, taken from previous work, conducted by a previous clinical research fellow of the primary supervisor (237, 323). Using these doses allowed us to compare percentage change in each oxygen condition as for both doses were operating in the middle of the dose response relation.

In the given study, we showed that the selected nitrite doses led to comparable and significant rises in plasma nitrite and FBFR in all four study conditions. However, on

reflection, the choice to have two different doses increased the complexity of the statistical analysis and also meant that we could only make indirect comparison between the normoxia and hypoxia groups. As will be discussed in the study limitations, unfortunately RXNO was not analysed in this study. This was a decision made by the supervising team (Appendix 10). As discussed in Chapter 1, we recognise that RSNOs can be generated from the haemoglobin/nitrite reaction, and that this may play an important role in nitrite-mediated NO activity export from intact red blood cells (213), however in the absence of RXNO levels, we are not able to comment on this further in the given study.

The next main finding was that 30-35 day NHSBT-stored autologous whole blood led to a 4-5-fold increase in unit cell-free haem (Figure 37C) and that once this was transfused, this led to a non-significant increase in subject circulating cell free haem of +35.5% in the normoxia group and +98.8% in the hypoxia group (at 90-minutes) (Figure 37 A and B) and a non-significant increase in NO consumption of +16.2% in normoxia and +61.4% in hypoxia (at 90-minutes) (Figure 38 A and B). As discussed throughout, we modelled our study on the work by Risbano in 2015. As shown in their study, 42-day storage of blood resulted in an approximate 4-fold increase in unit cell-free haem vs fresh blood and after transfusion, subject cell-free haem was increased from 7.9 uM to 10.8 uM (which represents a ~30% increase). They also showed that stored blood (with increased cell-free haem) was statistically correlated with an increase in NO consumption (260). In the given study, we too showed that storage of autologous whole blood for 30-35 days led to a numerical but non-significant 4-5-fold increase in unit cell-free haem, a 35%+ increase in subject circulating cell-free haem and this was associated with an increase in NO consumption. Taken together, these consistent findings demonstrate that the methodological approach we adopted (NSHBT 30-35-day stored autologous whole blood via IV infusion) led to a similar NO-blockade as previously shown by Risbano, Gladwin and colleagues in 2015, although our findings did not reach statistical significance.

There is substantial body of non-clinical evidence investigating the capability of haemoglobin to abrogate NO. In 2002, Joshi and colleagues compared bolus NO addition to NO generated homogeneously throughout solution by using NO donors. Using visible spectroscopy, they showed that multiple haemoglobin species are formed as well as both nitrite and nitrate. They concluded that the reaction of NO with haemoglobin during normoxia resulted in consumption, rather than conservation of NO, highlighting the efficient NO scavenging capability of oxyhaemoglobin (267). In the same year, Reiter and colleagues hypothesized that decompartmentalization of haemoglobin into plasma would divert NO from homeostatic vascular function. By studying patients with sickle-cell disease, they showed that plasma contained higher levels of cell-free haemoglobin and this stoichiometrically consumed micromolar quantities of NO, abrogating forearm blood flow responses to NO donor infusions (268).

In 2011, Donadee, Gladwin and colleagues examined the rate at which stored blood haemolyses. They showed that the degree of haemolysis and haemoglobin release in blood stored in standard conditions increases significantly over time vs baseline; from baseline 4-day plasma haemoglobin (11.6±2.5 μmol/L) to 39-day plasma haemoglobin (81.0±18.4 μmol/L). In addition, they also showed that with haemolysis, cell-free haem accumulation is coupled with microparticle encapsulated haemoglobin accumulation, which despite prolonged storage largely remains in the ferrous oxyhaemoglobin state. They also showed that cell-free haem increases are directly proportional (with a linear relationship) to NO consumption, $p<0.001$, via the classic deoxygenation reaction (as discussed in Chapter 1). Our work showed the same relationship between increasing subject cell-free haem and NO consumption levels, figures 37 and 38, and we also showed that with prolonged storage (30-35-days), donated blood haemolyses and releases cell-free haem, which is capable of binding to and consuming nitrite-derived (and to a lesser extent endothelium-derived) NO *in vivo*.

Whilst there was a notable increase in subject circulating cell-free haem and increase in NO consumption levels, these increases did not reach statistical significance.

Next, using mixed effect linear regression modelling, we showed that following intra-brachial nitrite infusion there was high inter-subject variability and that FBFRs were predicted by nitrite infusion status only (and not by any other main effect or interaction effect) (table 3, figure 39). There is a wealth of evidence stating that as nitrite increases, so too does flow-mediated dilation (346). Yet, despite this seemingly simple correlation, many clinical studies have reported inconsistent results when examining the vasoactive effects of nitrite on peripheral resistance vessels. Cosby and colleagues presented a detailed study in 2003, which examined how nitrite reduction to NO by deoxyhaemoglobin can vasodilate the human circulation. They showed that even a very low dose nitrite infusion (400 nmol/ml over 5 minutes) could lead to significant increases in plasma nitrite levels (176 to 2564 nmol after 5-minute infusion), which was also associated with significant increases in FBF (3.49 to 4.51ml/min per 100ml of tissue, $p = 0.0006$) (269). Yet by contrast, Lauer and colleagues reported that basal plasma nitrite levels were found to be 227-428 nmol/L), however following eNOS stimulation with ACh, plasma nitrite levels increased to 550nmol/L and were associated with a 4-fold increase in FBF, yet when intra-brachial nitrite was administrated as doses up to 36 μmol/min, they showed no increase in FBFs (347).

When considering these studies and our own, it is unclear why such variations exists in the reported vasoactive effect of nitrite in humans. These discrepancies may reflect differences in the subjects and experimental protocols, although such differences are not obvious from the study publications, with the preparation of nitrite and its infusion being similar in the studies described. It is possible that these differences may be subject to a biphasic response to nitrite (with effects being seen at very low and also high doses predominantly), although there is no literature at present that strongly supports this notion. It is more likely that these

differences reflect variations in inter-subject vascular physiology and/or vasoreactivity. As shown in the given study, the level of inter-subject variability was high (with a conditional R^2 of 38.0%), therefore it is probable that inter-subject variability is associated with the differences observed across the presented studies. The reason for the high level of inter-subject variability is not clear, however, as all of the presented studies examined young to middle-aged healthy subjects (in the absence of obesity, smoking, known vascular disease or diabetes), and it is therefore unlikely that the subjects differed significantly with respect to endothelial function (348) or sympathetic stimulation (349). A final consideration is that there may also be notable heterogeneity in the metabolic handling of nitrite between subjects and that this is still an area of need for future research as discussed in Chapter 1 (178, 189).

In Model 2 and 3, we tested whether the observed effect in Model 1 was present to a similar degree in normoxia only and hypoxia only. Interestingly, we observed that the FBFR beta-estimate was on average 0.52 in normoxia and 0.64 in hypoxia, indicating that despite the hypoxia nitrite dose being 1/3 of the normoxia dose, a greater degree of vasodilation took place in hypoxia.

According to the literature, deoxyhaemoglobin has been shown to augment hypoxic vasodilation (262). As shown by Maher in 2008, nitrite-mediated vasodilation of peripheral small resistance arterioles was augmented in the presence of mild hypoxia vs normoxia *in vivo* (237). However in the given study, the oxygen saturations of 83-88% (O_2 = 62.5 – 72.5 μmol), would not have been low enough to cause haemoglobin to act as a nitrite reductase (which is really only possible in lower end of normoxia (O_2 ~30 μmol) (229) (253, 266). A more likely explanation for the observed hypoxic-augmentation of nitrite-mediated vasodilation is that during mild hypoxia, modest vasodilation takes place systemically either via direct effects (inadequate oxygen to sustain smooth muscle contraction) or indirect via effects (223, 229, 235, 240), including the production of vasodilator metabolites (350).

In 2001, Thomas and colleagues reported that hypoxia-induced vasodilatory responses may be due to lowered oxygen tension alone, independent of haemoglobin (as NO survives longer with decreased oxygen due to decreased cellular consumption leading to an increased NO concentration in the tissue) (351). In 2013, Umbrello and colleagues discussed the consequences of supply and demand mismatch and the physiological requirement for hypoxic vasodilation as a mechanism for restoration of oxygen supply. They also discussed the vital role that NO plays in this process as a major signalling and effector molecule by mediating the body's response to hypoxia, given its unique characteristics of vasodilation and modulation of energetic metabolism (reducing oxygen consumption and promoting utilization of alternative pathways) (352).

A similar and very interesting concept was put forward by Jessica Dada in her PhD thesis (unpublished) under the supervision of Prof James, UK, which showed that pre-constricted hypoxic rabbit thoracic aortae rings and porcine LAD vasodilated in response to oxygenated Krebs buffer (in a similar manner to oxygenated Hb) suggesting that delivery of a small oxygen package itself, was able to vasodilate hypoxic vascular tissue. They showed that this process took place in the presence of NOS inhibition, and that the activity of sGC-cGMP pathway could be enhanced in the presence of haem, indicating a NO/endothelium-independent mechanism, using sGC and haem capable of reversing vasoconstriction in hypoxia. This is thought-provoking, as it may be that such processes explain historical data suggesting NO-independent pathways in normoxia in *ex-vivo* and potentially *in-vivo* models. It is most likely that both reductase and NO-donor mechanisms co-exist to a certain degree in strict hypoxia.

Model 4 addressed the vasodilatory effect of nitrite on FBFR in a 'NO-reduced' local environment. This model tested the main study hypothesis, that nitrite-mediated vasodilation is modulated by a NO-dependent mechanism in hypoxia and a NO-independent mechanism

in normoxia (as shown in murine models in Chapter 3). Model 4 showed that after autologous whole blood transfusion, FBFR was only predicted by nitrite infusion status and not by oxygen condition.

As described in detail in Chapter 1, there is a large body of evidence that suggest that nitrite-mediated PKG1α oxidative dimerization may lead to resistance vessel vasodilation (199, 201). Additional intermediates, such as H_2O_2 (200), ROS (202, 203), persulfides (208), RSNOs (210-214), have also been proposed to play an important role in modulation of NO bioavailability and subsequent vasotone. In the work presented in Chapter 3, we showed that in normoxia, nitrite administration to mesenteric vessels led to the generation of H_2O_2, persulfide intermediates (CysSSH and GSSH), which oxidatively activated PKG1α (131). Whilst it is not possible to use pharmacological NO-inhibitors in humans *in vivo*, we attempted to block nitrite-derived NO using cell-free haem, with the aim to show vasodilation in normoxia in the absence of NO, thereby demonstrating one or more NO-independent pathways. However, as already described throughout Chapter 4, whilst 30-35-day stored blood transfusion did lead to a numerical increase in subject circulating free haem and NO consumption, these changes were not statistically significant. Consequently, we did not create a NO-reduced environment in our study subjects, and therefore we were not able to show a difference in NO-dependency in the two oxygen conditions, meaning that based on these results, we reject our study hypothesis.

Further modelling was completed to analyse the safety considerations and the broader haemodynamic effects of the variables on HR and MAP. Model 5 showed that autologous whole blood transfusion led to a significant increase in MAP, whilst nitrite infusion led to a significant reduction in MAP, however there was no interaction between these two factors. The association of NOx and MAP remains an area of considerable research. Whilst Maher did not report MAP in his study, the dose he chose was the same as the dose used by Arif

and colleagues in 2005 (7.84 μmol/min) who showed that this dose resulted in a significant reduction in MAP of ~4 mmHg in normoxia. We too showed a similar result, with Model 5 demonstrating that nitrite infusion across both oxygen conditions led to a significant reduction in MAP with a mean beta-estimate of - 2.67 mmHg. The observed reduction in MAP was likely due to the systemic vasoactive effect of nitrite on resistance vasculature, as already discussed in depth (146, 177, 190-192). Also, given that a total dose of 90 μmol was used in normoxia and 30 μmol was used in hypoxia, these results support the pre-existing observations of hypoxic-augmentation of nitrite-mediated vasodilation in systemic resistance arteries (174, 237). A further observation made during the clinical study sessions and also through modelling was that as the autologous whole blood transfusion was administered, the MAP increased. We showed that ~500 mls of blood led to a significant increase in MAP of + 2.20 mmHg. Therefore, we note that the nitrite dose may be considered as being high as it reduced MAP, but in combination, these two interventions resulted in a stable MAP throughout the study sessions.

Lastly, we also assessed HR-response, given that a clinically meaningful decrease in MAP may have triggered a neurally-mediated compensatory chronotropic response leading to an increase in HR (353). Model 6 showed that HR was significantly increased (mean + 3.3 bpm) following autologous whole blood transfusion, but not due to nitrite infusion status. This finding reflected that as circulating volume increases, HR needs to increase to meet the increased CO, and that the amount of nitrite used did not trigger a compensatory chronotropic response.

When we consider the totality of the results from this study, we can summarise that whilst we showed nitrite-mediated vasodilation that was augmented in hypoxia, it is probable that we used doses that were too high, given the reduction in MAP (albeit not associated with a compensatory chronotropic response). In addition, we also showed that 30-35-day NHSBT-

stored whole blood leads to non-significant increases in unit and subject cell-free haem, and that this is associated with non-significant increases in nitrite-derived (and to a lesser extent endothelium-derived) NO consumption levels. It is possible that the study design prevented us from adding sufficient cell-free haem (either by volume or route), to statistically uncover whether nitrite was using a NO-independent process to mediate vasodilation in resistance arteries in normoxia *in vivo*. However, the increase in cell free haem was very similar in magnitude to that observed in the study by the Gladwin group which showed attenuation of ACh-mediated forearm vasodilation, therefore from this work we are not able to answer the given hypotheses. It is also possible that (given the high study drug dose) the strong vasoactive effect of nitrite subjugated a modest NO-binding effect of autologous whole blood, and that the net observed effect was of no difference between normoxia and hypoxia.

However, this work does carry significant value. This was the second ever study to use autologous whole blood in clinical research in the UK (via the NHSBT) (with the first being a very small oncology study using only a few units). Throughout this study, we set-up multiple new processes (donation, transportation, testing, storage, blood bank management, etc.) and integrated these processes into the complex NHS environment. Next, it should be noted that this is the first study to actually test all three of the independent variables together in humans *in vivo,* which is even more surprising given that it was completed by a sole researcher in the setting of a busy, service-driven NHS hospital (and not in a specialised research facility by a team). This work represents a proof of concept which provides rich insight to guide future similar work.

Limitations

The study recruited 60 subjects to meet the requirement of 41 'completers' to achieve statistical power, however only 31 completed the study, representing a 48% attrition rate. This was driven by study duration, complexity and tolerance. As such, the study data need

to be interpreted with caution. We considered performing a post-hoc power calculation using the acquired data to assess if the study was sufficiently powered, however after careful review of the literature and detailed discussions with the study statistician, we recognised that such a calculation may be considered logically invalid and practically misleading (354, 355). Instead, based on the data we do have, which includes wide confidence intervals, high inter- and intra-subject variability and no evidence of statistically significant differences in the main endpoints, we conclude that the study was underpowered to show the main effects and that this is a limitation of the study (356, 357).

An additional point regarding the data that should be noted, was that we decided to include data from subjects whose oxygen saturations and ambient room temperature recordings deviated from the pre-set 'optimum' values during the study day. We did this because we did not want to exclude data that appeared acceptable and could still be analysed. Whilst these deviations were small and few, and the actual significance of these is not known, inclusion of these results may have reduced the quality of the presented data.

Firstly, given that we planned to use 30-35-day NHSBT-stored autologous whole blood (rather than 42-day stored leukoreduced blood, as used by Risbano), in hindsight, we should modelled the increase in cell-free haem in the unit over time before we started the study. Whilst we did identify this as a prudent step at the time, we had not factored this into our study ethics submission and so we did not pursue this, as we did not want to delay the study initiation by submitting an amendment. Also, following detailed research on storage methods, we felt relatively confident that NHSBT and FDA blood storage processes should lead to a comparable degree of RBC haemolysis and cell-free haem accumulation.

We also faced several limitations with respect to the study set-up from a regulatory perspective. For example, according to NHSBT guidelines, blood donors can donate a

maximum of 1 unit of blood every 12-weeks via the NHSBT, significantly limiting the rate of the study and the amount of blood we could transfuse. Also, leukoreduction of autologous blood was not permissible as it was considered creation of a new 'blood product', therefore we needed to use whole blood, as opposed to packed red cells (which would undergo greater levels of haemolysis and more cell-free haem leakage). Also, according to the NHS REC and also the NNUH NHS clinical guidelines, blood transfusions were not permitted intra-arterially, and could only be administered at a maximum rate of 2-hourly, intravenously, with a maximum volume of 1 unit (in the setting of our study), therefore, we could not replicate the methodology used by Risbano and colleagues. However, given the design of the Risbano study (9-13-minute intra-arterial blood infusion, 30 second rest, 4-minute baseline, followed by 9-minute ACh dose-response curve) they in fact created a systemic dosing model, whereby the stored blood was systemic at the point of ACh administration. Thus, as discussed, their NO-blockade model was almost identical to ours.

Also, the study design was also restricted by several factors. When we designed the study, we acknowledged that 4 separate clinical sessions (i.e. nitrite in normoxia, nitrite in normoxia with blood, nitrite in hypoxia, nitrite in hypoxia with blood) would not have been possible, with respect to very limited NHSBT/NNUH NHS resources and also participant recruitment and tolerance. Therefore, we decided to split this into 2 sessions (a normoxia session and a hypoxia session), as shown in figure 14. However, this design was limited by pre-/post- design, leading to a lower level of evidence vs a randomized element (358). In addition, we also decided to adopt 2 x 30-minute infusions (vs a steady-state infusion, for several reasons as described in Chapter 2), however given the half-life of nitrite and the carry-over effect, this meant that we no longer compared true-NOx baselines, but instead compared two different baselines, albeit statistically accounted for using mixed effect linear regression modelling. A further limitation in this study was that RXNO was not analysed in this study. This decision was taken by the supervisors due to limited resources in the

laboratory, further exacerbated by the Covid-19 pandemic. For further details please see Appendix 10.

A final consideration, and just a point of clarification, was that we intentionally did not use the same dose in the two clinical studies shown in Chapters 4 and 5. The two studies presented in this thesis were not intended to be directly compared as they used two different doses and administration regimens, and addressed two different sets of scientific questions.

Conclusion

In summary, this study did not show a difference in FBFRs between normoxia and hypoxia before or after autologous whole blood transfusion, therefore we are not able to demonstrate whether nitrite uses a NO-independent pathway (or potentially activates PKG1α in human resistance arteries) in normoxia, and consequently we reject our hypotheses. The lack of effect observed was likely due to the high inter- and intra-subject variability recorded during FBF measurements, the limited statistical power due to very high levels of attrition and the high nitrite dose which may have subjugated the modest NO-binding effect of cell-free haem, and that the net observed effect was of no difference between normoxia and hypoxia.

However, within this study we did show that consistent with the literature, blood storage within NHSBT storage limits is subject to increased haemolysis and leakage of cell-free haem and when transfused can lead to numerically increased levels of circulating subject cell-free haem. We showed that this is also associated with an increase in NO consumption (albeit not statistically significant in our study). This work should provide insight into the potential difficulties and also specific opportunities for examining the NO-independent effects of nitrite *in vivo* and we hope that future work will build on this, to further uncover the underlying mechanisms of nitrite-mediated resistance artery vasodilation in normoxia in humans.

CHAPTER 5: EXAMINING THE VASOACTIVE PROPERTIES OF SYSTEMIC NITRITE INFUSION ON THE EPICARDIAL CORONARY ARTERIES DURING NORMOXIA AND HYPOXIA in vivo

To examine the vasoactive properties of systemic inorganic nitrite infusion on the epicardial coronary arteries during normoxia and hypoxia, the clinical study shown in this chapter was conducted in the RBHT, London. Senior clinical support was provided by Prof Sanjay Prasad (Cardiology Consultant). Study day support was provided by Dr Brodie Loudon and Mr Kevin Kirby. CMR scanning was completed by Mr Ricardo Wage. CMR interpretation and CMR statistics were completed by Prof Jennifer Keegan (Principal Physicist, RBHT). Plasma sample analysis was completed by Dr Magda Minnion, Dr Bernie Fernandez and Prof Martin Feelisch. All remaining aspects of this study were completed by myself.

Introduction

It is generally accepted that the epicardial coronary arteries are physiologically similar to the peripheral arteries with respect to vasomotor activity (112, 279), and (except when there is obstructive coronary disease) exert very little resistance to flow (281, 282). The effect of inorganic nitrite on the epicardial coronary arteries, and on the coronary resistance vessels, is not well described. Historically, it has been reported that the organic nitrite amyl nitrite, could increase CSA of saphenous vein grafts in humans and simultaneously increase the coronary artery blood flow (285). Amyl nitrite has also been used as a treatment of angina (224). More recently, O'Gallagher and colleagues showed that intra-coronary inorganic nitrite selectively dilated epicardial coronary arteries under normoxic conditions without any significant changes in SBP, DBP or MAP (287).

Whilst O'Gallagher published their paper prior to the completion of this work, their findings did inform our work and validated the scientific need to characterise whether nitrite had

vasoactive properties in the coronary arteries analogous to that seen in the systemic conduit arteries. Of particular interest, we also took the opportunity to test the hypothesis that hypoxic augmentation of nitrite-mediated vasodilation, as previously shown in the systemic circulation (174, 237) was also present in the epicardial coronary arteries.

Finally, as a proof of concept, we attempted to answer our scientific question using radiation-free, non-invasive CMR technology (namely temporal spiral phase velocity mapping) to show that the vasoactive properties of the coronary arteries can be examined in normoxia and hypoxia safely *in vivo.*

Hypotheses

i. In normoxia, inorganic nitrite will increase epicardial (conduit) coronary artery CSA and assuming flow is constant, this will lead to a reduction in velocity (according to the Hagen–Poiseuille equation).
ii. In hypoxia, hypoxic-augmentation of inorganic nitrite-mediated vasodilation in the epicardial coronary arteries will lead to increased effects on CSA.

Aim

To investigate the effects of nitrite on the epicardial coronary artery CSA, velocity and flow in normoxia and hypoxia via cardiovascular MRI.

Results

Recruitment

Recruitment for the Nitrite and Coronary Artery Study followed the processes outlined in Chapter 2. We identified 50 suitable subjects who had previously agreed to participate in

clinical research from the Haem and Nitrite Study (Chapter 4). Of the 50, 3 subjects had exclusion criteria present (one with prohibitive claustrophobia, one with metal fragments in soft tissue in the face and one with a recent medical diagnosis no-longer considered to be 'healthy' in the opinion of the research team). Following discussion and review of the PIS, a further 33 subjects declined to participate (23 declined due to lack of availability and 10 declined due to difficulties with travelling from Norwich to London), figure 42. The recruitment target for this 'proof of concept' study was 10-15 subjects. As a proof of concept only, this study was not subject to a power calculation. A total of 14 subjects were recruited and we were able to analyse 13 full sets of images (with one set excluded due to inadequate quality for analysis).

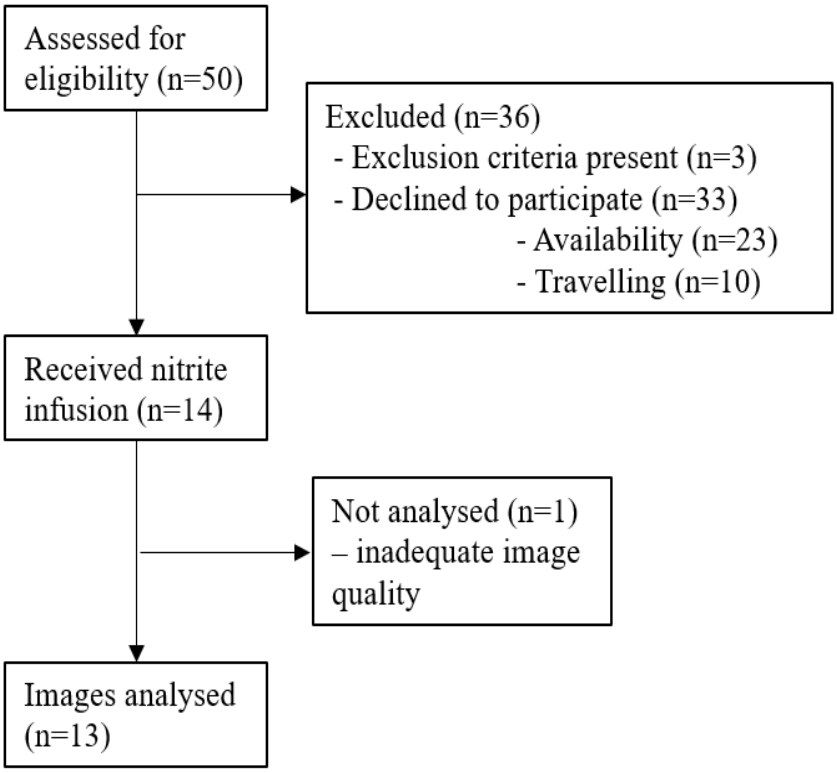

Figure 42: The Nitrite and Coronary Artery Study CONSORT diagram

Population

The study cohort was mostly male (92%) and generally young (mean 37.4 years), table 9. Subjects had no history of active smoking, hypertension, diabetes mellitus,

hypercholesterolaemia and no family history of premature ischaemic heart disease. All subjects had a normal cardiovascular examination and normal bedside clinical observations. The study was approved by the East of England – Cambridge East REC. Investigations took place at the RBHT in the CMR suite with subjects having had a light breakfast and having abstained from caffeine-containing drinks for at least 6-hours.

Baseline characteristics

This was a healthy volunteer study. As detailed in Chapter 2, clear inclusion and exclusion criteria were pre-defined and subjects who did not satisfy the criteria were not selected to participate. Baseline characteristics and haemodynamic measurements were recorded, table 9.

Table 9: Baseline characteristics for the Nitrite and Coronary Artery Study

Characteristic	Subject (n=13)
Sex	
Male (%)	12 (92%)
Female (%)	1 (8%)
Age	
Mean (range)	37.4 (22-71)
Systolic blood pressure (mmHg)	
Mean (±SD)	119.92 (±11)
Diastolic blood pressure (mmHg)	
Mean (±SD)	68.92 (±7.5)
Heart rate (bpm)	
Mean (±SD)	61.4 (±11.6)

Safety reporting: adverse events and serious adverse events

In the present study we administered 50 μg/kg/min^{-1} of sodium nitrite IV over a 5-minute period (254 μmol). As discussed in Chapter 2, the concentration infused was taken from the study published in 2015 by Dr Julian Ormerod in our group (345). This work showed that 50 μg/kg/min^{-1} (equal to sodium nitrite 17.5 mg in a 70 kg subject) was safe and well-tolerated in severe chronic heart failure patients. Discussion of the study drug dose and

administration regimen is discussed in more detail later. Of note, this study did not report any AEs or SAEs.

Arteries imaged and pulse oximetry

During the study we imaged the RCA using oblique views in 8/13 subjects (62%) and the LAD using transverse views in 5/13 subjects (38%). Oblique views were used for the RCAs and transverse views for the LADs as these provided the best images possible. During imaging in normoxia, the mean (±SD) oxygen saturation recorded by pulse oximetry for all subjects was 97.4% ± 1.9%. During the hypoxia acquisitions, the mean (±SD) oxygen saturation for all subjects was 87.2% ± 3.1% representing high variability in intra-subject hypoxic ventilatory responses (235).

Blood analysis

Plasma nitrite, nitrate and RXNO levels

Blood was collected for analysis before the nitrite infusion and ~5-10 minutes after the study imaging protocol was completed. These blood samples were analysed for nitrite, nitrate and RXNO levels. Descriptive statistics revealed that these levels increased after the nitrite infusion, as follows, baseline (sample collection timepoint 1, Figure 20) nitrite 0.34 μmol (± 0.08 μmol) to 231.07 μmol (± 79.15 μmol) after completion of the imaging protocol (sample collection timepoint 2, Figure 20), baseline nitrate 41.79 μmol (± 5.41 μmol) to 169.69 μmol (± 44.49 μmol) following completion of imaging and baseline RXNO 30.89 nmol (± 5.02 nmol) to 226.90 nmol (± 57.66 nmol) following completion of the imaging.

A one-way repeated measures ANOVA was conducted to compare blood levels before and after the nitrite infusion, as measured by HPLC and RXNO determination assays. There was a statistically significant main effect of the nitrite infusion on plasma nitrite levels $F(1, 12) = 8.496$, $p = 0.012$, partial eta squared $= 0.395$. There was also a statistically significant main

effect of the nitrite infusion on plasma nitrate and RXNO levels; plasma nitrate levels $F(1, 12) = 7.680$, $p = 0.016$, partial eta squared = 0.371, and plasma RXNO levels $F(1, 12) = 11.118$, $p = 0.001$, partial eta squared = 0.481. These findings indicate that the nitrite infusion led to an increase in plasma nitrite, nitrate and RXNO.

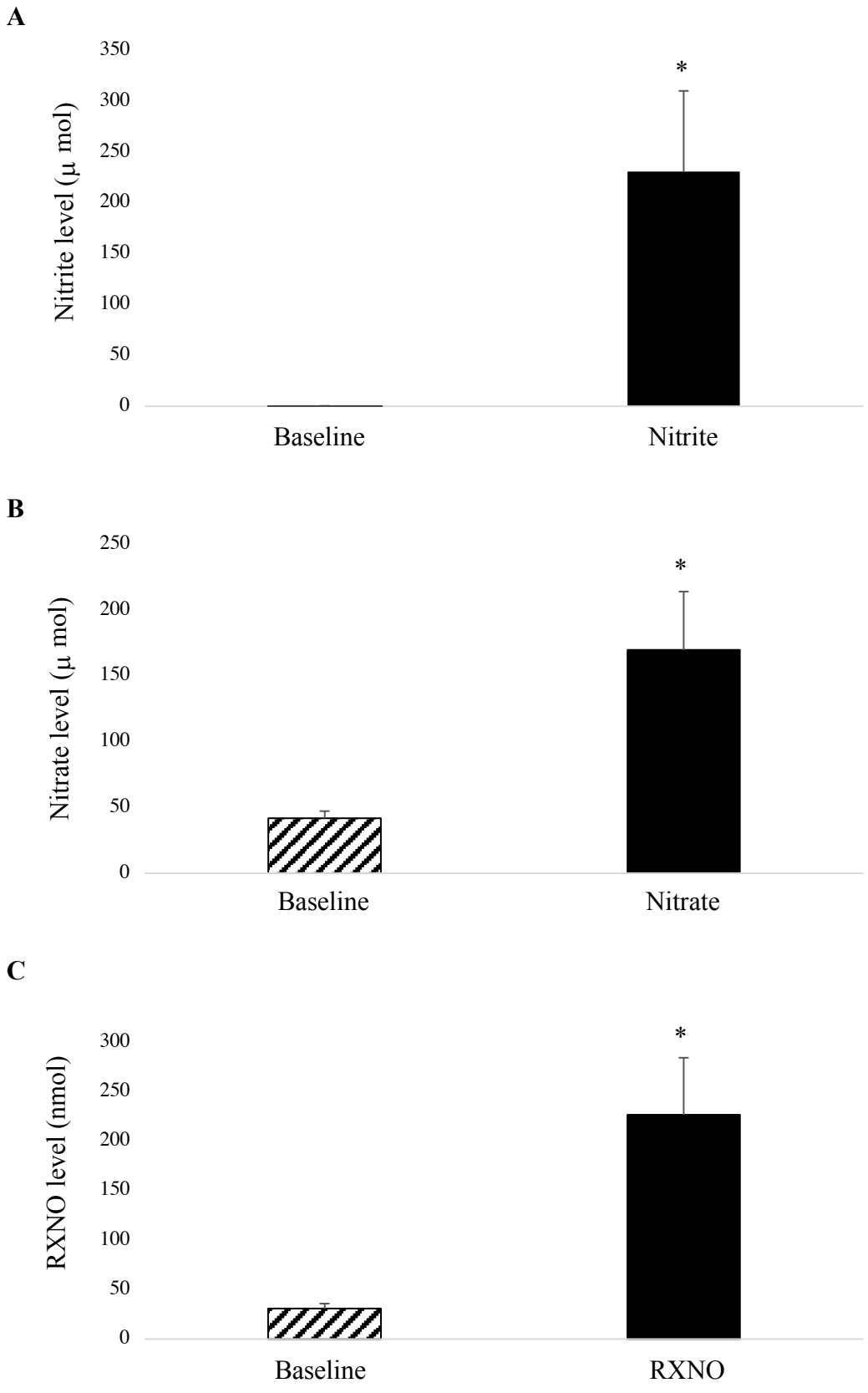

Figure 43: Plasma NOx and RXNO levels. All n = 13. Panel A: Nitrite. Panel B: Nitrate. Panel C: RXNO. Data are presented as mean (±SEM). Statistical analysis carried out using one-way ANOVA followed by Bonferroni post-hoc test, * $p<0.05$.

CMR results

1: Effect of intravenous nitrite infusion and oxygen condition on MAP and HR

As discussed in detail in the methods section (and also the study limitations section), the effect of nitrite on MAP or HR in hypoxia could not be calculated. We did, however measure this in normoxia alone, normoxia and nitrite, and hypoxia and nitrite. Descriptive statistics revealed that these groups had the following MAP means (±SEMs) respectively, 85.92 mmHg (± 2.13 mmHg), 83.31 mmHg (± 2.10 mmHg), and 83.18 mmHg (± 2.59 mmHg), and the following HR means (±SEMs) respectively, 61.38 BPM (± 3.22 BPM), 59.15 BPM (± 3.36 BPM), and 64.15 BPM (± 2.79 BPM).

A one-way repeated measures ANOVA was conducted to compare the impact of intravenous nitrite infusion and normoxia on MAP and HR, as measured by bedside haemodynamic monitoring. There was a statistically significant effect for nitrite on MAP in normoxia, $F(1, 12) = 10.143$, $p = 0.008$, partial eta squared = 0.458, but no statistically significant effect for nitrite on HR in normoxia, $F(1, 12) = 1.724$, $p = 0.214$, partial eta squared = 0.126. These findings indicate that the addition of nitrite in normoxia significantly reduced MAP, but not HR, figure 44.

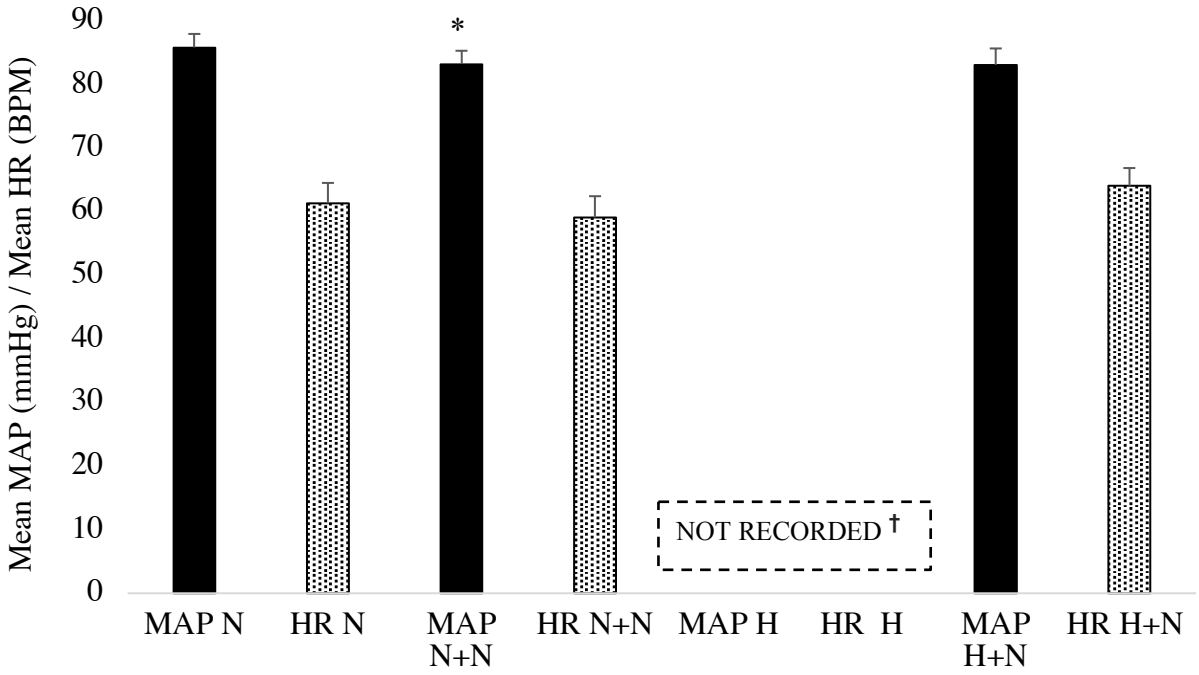

Figure 44: Mean MAP (mmHg) and mean HR (BPM) in each of the 3 conditions recorded, n=13. Data are mean (±SEM). One-way repeated ANOVA followed by Bonferroni post-hoc test, *$p<0.05$. †As described in the methods and in the study limitations, we did not record MAP or HR in hypoxia alone.

2: Effect of intravenous nitrite infusion and oxygen condition on mean epicardial CSA

As described in Chapter 2, mean epicardial CSA was calculated by applying the mean FWHM (mm) as diameter to $\pi r2$, in mm^2. Participants underwent 4 conditions: normoxia alone, normoxia and nitrite, hypoxia alone, and hypoxia and nitrite. Descriptive statistics revealed that these groups had the following means (±SEMs) respectively, 11.14 mm^2 (± 1.16 mm^2), 13.54 mm^2 (± 1.32 mm^2), 11.00 mm^2 (± 1.13 mm^2) and 14.66 mm^2 (± 1.53 mm^2).

A two-way repeated measures ANOVA was conducted to explore the effect of intravenous nitrite infusion and oxygen condition (normoxia or hypoxia) on mean epicardial CSA, as measured by an interleaved spiral phase velocity CMR sequence, developed on a 3 Tesla Magnetom Skyra MR scanner (Siemens, Germany). The interaction effect between nitrite

and oxygen condition was not statistically significant, F (1, 12) = 4.028, p = 0.068. There was however a statistically significant main effect for nitrite, F (1, 12) = 38.971, p <0.0001, with a very large effect size (partial eta squared = 0.765). The main effect for oxygen condition, F (1, 12) = 1.985, p = 0.184, did not reach statistical significance. These findings indicate that the addition of nitrite in normoxia and hypoxia caused a significant increase in CSA, figure 45. Post-hoc pairwise comparisons using a Bonferroni adjusted alpha level of 0.0125 were completed and statistically significant differences were observed between normoxia alone vs normoxia and nitrite, p = 0.004, and hypoxia alone vs hypoxia and nitrite, p < 0.0001.

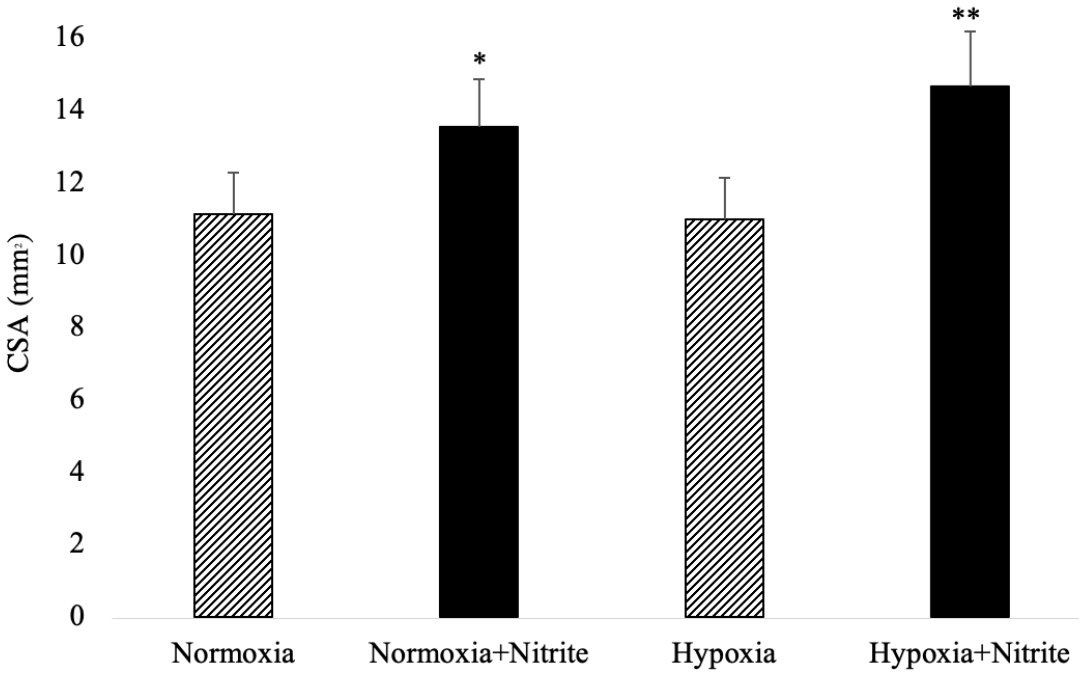

Figure 45: Mean CSA (mm^2) in each of the 4 conditions, n=13. Data are mean (±SEM). Two-way repeated ANOVA followed by Bonferroni post-hoc test, *p<0.05, **p<0.0001.

3: Effect of intravenous nitrite infusion and oxygen condition on mean epicardial blood velocity

As described in Chapter 2, the mean epicardial blood velocity was calculated as being the mean blood velocity in the coronary artery ROI averaged over the cardiac cycle (50-time frames), in mm/s. Participants underwent 4 conditions: normoxia alone, normoxia and nitrite, hypoxia alone, and hypoxia and nitrite. Descriptive statistics revealed that these groups had the following means (±SEMs) respectively, 54.83 mm/s (± 6.84 mm/s), 43.19 mm/s (± 5.71 mm/s), 62.83 mm/s (± 7.61 mm/s) and 43.15 mm/s (± 6.87 mm/s).

A two-way repeated measures ANOVA was conducted to explore the effect of intravenous nitrite infusion and oxygen condition (normoxia or hypoxia) on mean epicardial blood velocity, as measured by an interleaved spiral phase velocity CMR sequence, developed on a 3 Tesla Magnetom Skyra MR scanner (Siemens, Germany). The interaction effect between nitrite and oxygen condition was statistically significant, $F(1, 11) = 5.180$, $p = 0.044$. There was also a statistically significant main effect for nitrite, $F(1, 11) = 64.281$, $p < 0.0001$, with a very large effect size (partial eta squared = 0.854). The main effect for oxygen condition, $F(1, 11) = 1.657$, $p = 0.224$, did not reach statistical significance.

These findings indicate that the combination of nitrite and oxygen condition, and the addition of nitrite alone, caused a significant decrease in mean blood velocity, figure 46. Post-hoc pairwise comparisons using a Bonferroni adjusted alpha level of 0.0125 were completed and statistically significant differences were observed between normoxia alone vs normoxia and nitrite, $p = 0.007$, and hypoxia alone vs hypoxia and nitrite, $p < 0.0001$.

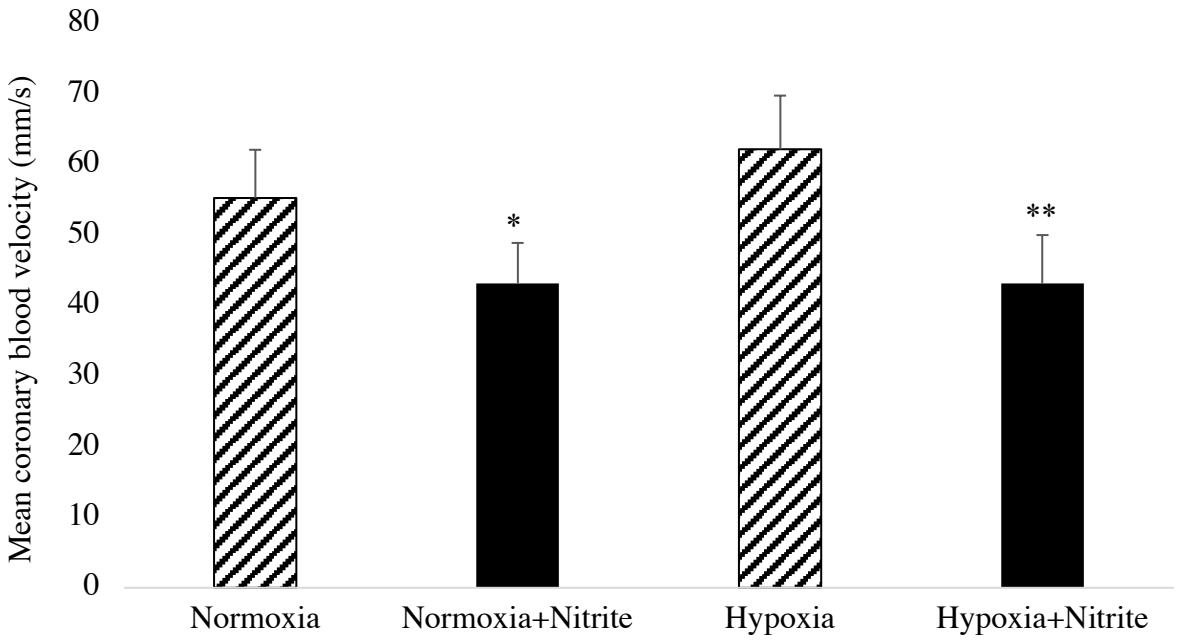

Figure 46: Mean velocity (mm/s) of coronary artery blood in each of the 4 conditions, n=13. Data are mean (±SEM). Two-way repeated ANOVA followed by Bonferroni post-hoc test, *p<0.05, **p<0.0001.

4: Effect of intravenous nitrite infusion and oxygen condition on mean epicardial blood flow

As described in Chapter 2, the mean epicardial blood flow was calculated as the mean blood velocity multiplied by the CSA, in ml/min. Participants underwent 4 conditions: normoxia alone, normoxia and nitrite, hypoxia alone, and hypoxia and nitrite. Descriptive statistics revealed that these groups had the following means (±SEMs) respectively, 31.58 ml/min (± 3.25 ml/min), 30.02 ml/min (± 2.86 ml/min), 35.72 ml/min (± 3.28 ml/min) and 29.94 ml/min (± 2.95 ml/min).

A two-way repeated measures ANOVA was conducted to explore the effect of intravenous nitrite infusion and oxygen condition (normoxia or hypoxia) on mean epicardial blood flow, as measured by an interleaved spiral phase velocity CMR sequence, developed on a 3 Tesla

Magnetom Skyra MR scanner (Siemens, Germany). The interaction effect between nitrite and oxygen condition was statistically significant, F (1, 11) = 7.391, p = 0.020. There was also a statistically significant main effect for nitrite, F (1, 11) = 24.822, p <0.0001, with a large effect size (partial eta squared = 0.693). The main effect for oxygen condition, F (1, 11) = 1.246, p = 0.288, did not reach statistical significance.

These findings indicate that the combination of nitrite and oxygen condition, and the addition of nitrite alone, caused a significant decrease in mean blood flow. Figure 47. Post-hoc pairwise comparisons using a Bonferroni adjusted alpha level of 0.0125 were completed and whilst no difference was observed between normoxia alone vs normoxia and nitrite, p = 0.786, a statistically significant difference was shown in hypoxia alone vs hypoxia and nitrite, p = 0.003.

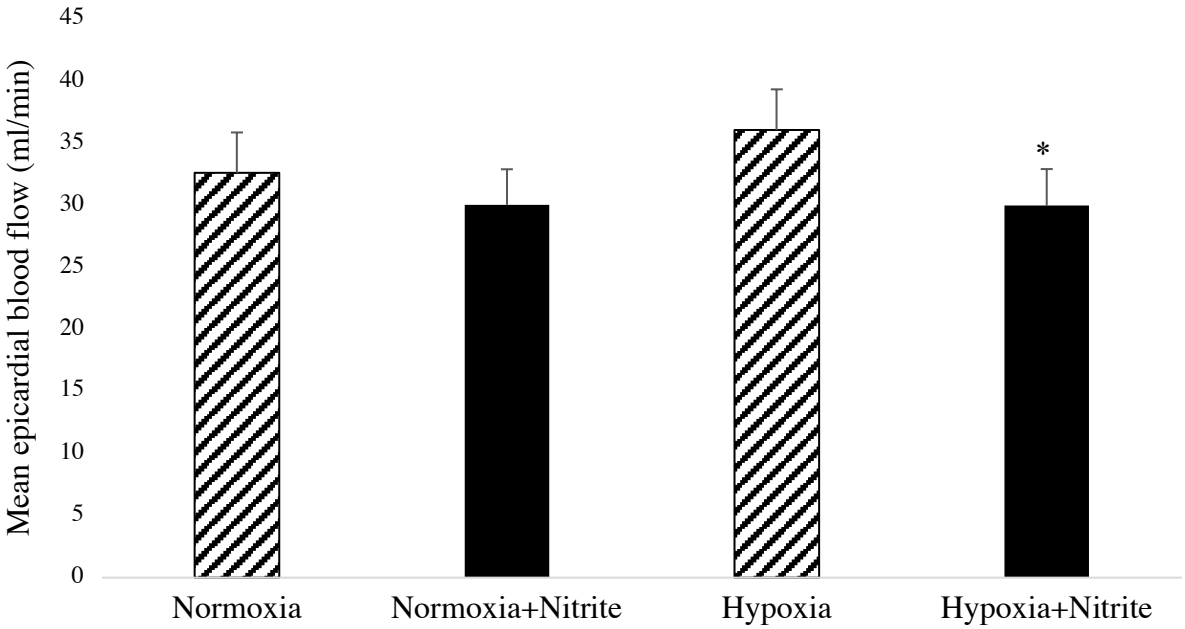

Figure 47: Mean epicardial blood flow (ml/min) in each of the 4 conditions, n=12. Data are mean (±SEM). Two-way repeated ANOVA followed by Bonferroni post-hoc test, *p<0.05.

In summary, the above study showed the following:

1. NOx/RXNO: Intravenous inorganic nitrite infusion led to a significant increase in plasma nitrite levels, $p = 0.012$, plasma nitrate levels, $p = 0.016$ and plasma RXNO levels, $p = 0.001$
2. MAP and HR: Intravenous inorganic nitrite infusion led to a significant decrease in MAP in normoxia, $p = 0.008$, but did not affect HR in normoxia, $p = 0.214$. As noted, BP could not be recorded during hypoxia
3. CSA: There was a significant main effect for nitrite, $p < 0.0001$, but not for oxygen condition, $p = 0.184$, and no significant interaction effect, $p = 0.068$. Post-hoc Bonferroni showed significant effects for nitrite in normoxia, $p = 0.004$ and hypoxia, $p < 0.0001$
4. Velocity: There was a significant main effect for nitrite, $p < 0.0001$, no main effect for oxygen condition, $p = 0.224$, with a significant interaction effect, $p = 0.044$. Post-hoc Bonferroni showed significant effects for nitrite in normoxia, $p = 0.007$ and hypoxia, $p < 0.0001$
5. Flow: There was a statistically significant main effect for nitrite, $p < 0.0001$, no main effect for oxygen condition, $p = 0.288$, with a significant interaction effect, $p = 0.020$. Post-hoc Bonferroni showed a non-significant effect for nitrite in normoxia, $p = 0.786$ but a statistically significant effect in hypoxia, $p = 0.003$.

Discussion

The main findings were that a 5-minute IV nitrite bolus of 50 $\mu g/kg/min^{-1}$ (254 μmol) led to significant rises in plasma NOx and RXNO (figure 41), associated with significant increases in epicardial conduit CSA (figure 43) and significant reductions in velocity in both oxygen conditions (figure 44) and a significant reduction in flow in hypoxia but not normoxia (figure 45). This was associated with a significant reduction in MAP (but not HR) in normoxia

(figure 42), however as noted in Chapter 2 (and will be discussed in the limitations), we were not able to record BP in hypoxia and therefore unable to calculate MAP in hypoxia.

In this study, we wanted to create a 5-minute bolus delivery, to enable rapid administration and visualisation of the effects, given the limited time available on the CMR scanner. With this in mind, we decided to select a dose that we had previously tested and had proven to be safe and systemically efficacious in humans (345). Consistent with Ormerod, who showed that 50 μg/kg/min^{-1} (254 μmol) led to significant increases to all measured NO metabolites vs baseline (nitrite +14.3 μmol, p=0.0001, nitrate +15.6 μmol, p=0.0001, RXNO +27.9 μmol, p=0.0001), we also showed that this dose led to significant increases in plasma nitrite, nitrate and RXNO levels. Also consistent with Ormerod, who showed that the same dose led to a significant reduction in MAP vs baseline (-3mmHg, p=0.004) but no effect on HR vs baseline (-0.8 bpm, p=0.12), we also showed that MAP in normoxia was significantly reduced from 85.92 to 83.31 (-2.61 mmHg) and HR was non-significantly affected, 61.38 to 59.15 (-2.2 bpm).

With the publication of the O'Gallagher study during our study delivery, we learned from their data that our selected dose was comparatively high, given that O'Gallagher showed that significant epicardial coronary artery vasodilation (with a change of +8.9% vs baseline, p = 0.01) could be achieved with a nitrite concentration of just 26 μmol/min over the 5-minute infusion period (total infusion 130 μmol) and without any significant adverse effects on MAP, p>0.05. However, we also observed that at their selected lower dose of 2.6 μmol/min over the 5-minute infusion period (total infusion 13 μmol), O'Gallagher failed to show significant epicardial coronary artery vasodilation (+3.9% vs baseline, p = 0.30). By comparison, in the given study, we used a 5-minute systemic administration of nitrite at 50 μg/kg/min^{-1} (254 μmol) which, even when treated with a Bonferroni adjusted alpha of 0.0125 caused a significant increase in CSA in normoxia vs baseline (11.14 to 13.54, relative

+22%), which was subject to hypoxia-augmentation (11.00 to 14.66, relative +33%). When taken together with O'Gallagher's CSA data, we can confirm that epicardial coronary vasodilation is a dose-dependent response. As mentioned, we also showed a significant reduction in MAP (-2.61mmHg), consistent with Ormerod (345), but in excess of O'Gallagher (287). The clinical relevance of this small reduction in MAP is unknown. We did not observe any associated adverse events in this study and no subject reported being aware of a change in BP during the study. As we reflect on our findings, in the context of O'Gallaghers work, we recommend that future studies undertake a detailed dose-finding study to identify the optimal therapeutic dose of nitrite in the epicardial coronary arteries. Also, if we consider nitrite in a therapeutic setting in the future, preserving MAP will be an important feature as coronary stenosis +/- ischaemia may be associated with haemodynamic instability (72, 89).

As the given work was a proof of concept study, we cannot comment on the underlying mechanisms mediating epicardial conduit vasodilation (in normoxia or hypoxia). We (and others) assume that the coronary arteries are physiologically similar to the peripheral arteries with respect to vasomotor activity (112, 279), yet whether this process is predominated by NO activity, as it is in the systemic conduits (119, 126), remains to be fully determined. What we can ascertain from our work is that the underlying mechanism is subject to hypoxic-augmentation, and given that we were not able to test 'strict hypoxia' (as discussed in detail in Chapter 1), we can assume that these effects were not mediated by reductase activity (237). This observation may hint at the fact that additional intermediates (alongside the traditional sGC-NO pathway) are active and have a role in augmenting vasodilation in the epicardial coronaries arteries in hypoxia. As discussed in Chapter 3, we cannot exclude the possibility that intermediates such as H2O2 (and persulfides), RSNOs, N_2O_3, and PKG1α oxidation (131, 174, 212-214) may have a role to play. Future work should attempt to

examine these intermediates in the context of nitrite-mediated epicardial conduit artery vasodilation.

Historical work by Benchimol and others sowed the seed for this study. Understanding how nitrite-based compounds can affect coronary blood flow has been a topic of enquiry for many years. In the 1960s, the effects of IV nitroglycerin on coronary blood flow in anaesthetized dogs using an open chest model, showed a reduction in MAP and increase in coronary blood flow (359). In an animal (rabbit and dog) study by Grayson and colleagues in 1967, the effects of (inexact quantities) of amyl nitrite inhalation on myocardial blood flow were examined. In rabbits, they showed inhalation for 3-5 minutes led to a mean reduction in BP of 59% and a reduction in coronary blood flow of -17% (associated with a reduction in vascular resistance -46%), whilst in dogs, a mean reduction in BP of 29% and an increase in coronary blood flow of +34% (associated with a reduction in vascular resistance -41%), showing differing coronary blood flow responses to amyl nitrite inhalation in different mammals (360). It is reasonable to speculate that these differences may be driven by multiple factors, including species of animal studied, the relatively limited n-values, the different nitrite-based compounds, and the routes of administration studied/amount of bioavailable drug. The historical mixed results (in animals and man) compelled our group to study whether nitrite could significantly increase CSA, whilst avoiding deleterious effects on velocity and flow in man, and whether this effect would be subject to hypoxic-augmentation, as it is systemically (237).

As outlined in Chapter 2, next to CSA, calculated as FWHM as diameter to $\pi r2$ (in mm^2), we also measured both epicardial conduit artery blood 'velocity' and 'flow'. Blood velocity was calculated as the sum of velocity recordings at 50 time points divided by 50 (in mm/sec). Flow was calculated as the CSA x (sum of velocity recordings at 50 time points) x HR (in mls/min). As discussed in detail in Chapter 2, measures of CSA, velocity and flow had all

been validated by our lead Physicist in a series of peer-reviewed CMR papers, which showed that this method of CMR coronary image acquisition and analysis provided accurate assessment of CSA and temporal patterns of coronary blood velocity and flow when compared to peak Doppler values, with excellent test-retest reproducibility (283, 286). Also, as discussed in Chapter 2, our study was carefully designed to reduce observer bias, increase inter-observer reproducibility and repeatability (336), thus we consider our findings to be accurate and robust.

The study by O'Gallagher indirectly calculated blood flow as CSA x (velocity/2) and coronary resistance (as MAP/flow). They showed that at both studied doses (2.6 μmol/min and 26 μmol/min) there was no appreciable change in coronary blood flow (+12%, p>0.99 and +16.9%, p >0.99, respectively), despite relatively high intra-coronary nitrite concentrations of 73.7 μmol and 705 μmol respectively (287). Yet, in the given study, we showed that in normoxia, an increase in CSA in normoxia (+22%) was coupled with significantly decreased velocity vs baseline (55.27 mm/s to 43.19 mm/s, relative -22%) and a non-significant numerical reduction in flow vs baseline (32.59 to 30.02 ml/min, relative -8%). These effects were augmented and all reached statistical significance in hypoxia vs baseline (62.18 to 43.14 mm/s, relative -31%, and 36.04 to 29.94 ml/min, relative -17%), respectively. Again, these post-hoc pairwise comparisons were conservatively treated with a Bonferroni adjusted alpha of 0.0125.

The combination of findings in this study were rather unexpected in that whilst we expected to observe an increase in epicardial CSA associated with a decrease velocity (consistent with the Hagen–Poiseuille equation) (54, 55), we did not expect to observe a reduction in epicardial coronary flow. In fact, it is widely-accepted that healthy coronary arteries do not exert significant resistance to flow (281, 282), therefore we would have expected the epicardial coronary flow to remain constant in the given study.

From the data collected and the non-mechanistic study design, we cannot provide an exact explanation for the statistical reduction in flow in hypoxia in our study. The reduction in velocity is a function of the increase in CSA, however, given that healthy coronary arteries do not exert significant resistance to flow (281, 282), we expected that flow would remain constant. Whilst the cause of the reduction in flow is not clear from our results, it is possible that the nitrite infusion led to a decrease in aortic BP and this in-turn led to a reduction in intra-coronary pressure. It is also possible that the reduction in MAP activated a baroreflex-mediated sympathetic constriction of the coronary resistance vessels and this too led to a reduction in flow, however as discussed as a limitation of this study, we were not able to record BP in hypoxia and therefore we were not able to calculate MAP or coronary vascular resistance in hypoxia**.** Whilst we recognise subject-specific differences in our study vs O'Gallagher's, specifically with age (37.4 years vs 56 years) and presence of hypertension (0% vs 78%) may account for differences in endothelial dysfunction and reduced vessel elastance, these variations do not explain the differences in flow observed in the two studies.

We could speculate that the observed combination of effects (increased CSA and reduced MAP) may provide a novel therapeutic option for people with atherosclerosis and hypertension, who cannot tolerate or have resistance to, nitrate-based compounds (131, 173, 309, 310). However, the reduction in flow (albeit it in hypoxia only)) may present problems in the context of flow-limiting lesions, as may be present in angina, for example (72), so the therapeutic scope of nitrite in this setting still requires careful consideration in future work, which should be explored in more depth via a detailed dose-finding study.

Lastly, this study was unique on two fronts. Firstly, these are the first data to show that hypoxic-augmentation of nitrite-mediated vasodilation exists in the epicardial conduits vs normoxia (with increased CSA and reduced velocity). Also, this is the first study to use

coronary CMR to examine the vasoactive properties of nitrite on the epicardial coronary arteries in both normoxia and hypoxia *in vivo*. We anticipate this non-invasive, radiation-free methodology will be adopted in future work, to further uncover the therapeutic potential of nitrite in coronary artery disease.

Limitations

The present study was a proof of concept, healthy volunteer study. The cohort was not 'matched' to any specific cardiovascular disease cohort demographic. As discussed in Chapter 2, we took blood samples before and after the imaging protocol (sample collection 1 and 2, figure 20) and used a 5-minute bolus administration of nitrite whilst the subject was in the CMR scanner, so as a result, we did not know the exact plasma nitrite/nitrite/RXNO levels at the exact point of each image acquisition. Therefore, it is possible that the plasma levels were slightly higher in normoxia and slightly lower in hypoxia (given the half-life of nitrite and the order of oxygen conditions). However, the methodology we chose was selected to ensure the subject was kept still once positioned in the CMR scanner and this point does not affect our interpretation of the results. As already identified, future work may adopt a continuous nitrite infusion approach to achieve steady-state NOx/RXNO plasma levels to enable more exact correlations between plasma levels and CMR images.

A further limitation of this study was that we were not able to record BP in hypoxia. This was also due to the technical complexity of imaging the coronaries. Any delays in the protocol or small movements of the subject during the study significantly increased the risk of losing the imaging views (as we unfortunately discovered in the first subject when attempting to measure BP during hypoxia, rendering these results unusable). Therefore, we were not able to calculate MAP or coronary vascular resistance in hypoxia. The addition of this data may have helped us to describe the underlying mechanism contributing to the observed reduction in flow in hypoxia. Future work could consider the use of a finapres

(FMS, Netherlands) or similar to overcome this issue, in order to measure BP throughout, enabling post-hoc vascular resistance calculations.

The final limitation of this study was that, on reflection, the selected dose was comparatively high, especially when compared to the O'Gallagher paper. Future work should complete a dose-finding study to help understand the optimal therapeutic dose of nitrite in the epicardial coronary arteries to allow vasodilation without causing a significant reduction in MAP or flow. As before, a final consideration, and just a point of clarification, was that we intentionally did not use the same dose in the two clinical studies. The two studies presented in this thesis were not intended to be directly compared as they used two different doses and administration regimens, and addressed two different sets of scientific questions.

Conclusion

In summary, these are the first data to show that hypoxic-augmentation of nitrite-mediated vasodilation exists in the epicardial conduit arteries vs normoxia (with increased CSA and reduced velocity). Whilst we identify that the reduction in velocity was due to the increased CSA, we do not have an exact explanation for the reduction in flow in hypoxia. Possible explanations for the reduction in flow in hypoxia may be that the nitrite infusion led to a decrease in aortic BP, or even that the reduction in MAP activated a baroreflex-mediated sympathetic constriction of the coronary resistance vessels, however from the design of this study, we cannot provide an exact answer to the underlying mechanisms of reduced flow in hypoxia. The findings of this study have important implications for our understanding of the therapeutic potential of nitrite in a wide range of cardiovascular diseases, specifically that the epicardial coronary arteries are also subject to the underlying mechanisms mediated by hypoxic-augmentation observed in the systemic vessels. Also, this is the first study to use coronary CMR to examine the vasoactive properties of nitrite on the epicardial coronary arteries in both normoxia and hypoxia *in vivo*. We hope that this radiation-free, non-invasive

methodology will be adopted in future work, to further uncover the therapeutic potential of nitrite in coronary artery physiology and disease.

CHAPTER 6: SUMMARY DISCUSSION, CONCLUSIONSAND FUTURE DIRECTIONS

This MRC-funded PhD thesis presents three quite separate pieces of research, from basic science through to complex clinical and imaging studies. Whilst each area of work addresses a unique set of scientific questions, this work comes together to provide valuable insight into the vasoactive properties of nitrite in normoxia and hypoxia. Below, I will briefly discuss each study in the context of the respective literature, review the main findings, reflect on the limitations and offer suggestions for future work.

Chapter 3: Nitrite can circumvent the NO-sGC pathway via persulfide intermediates to induce tissue-specific vasodilation via PKGIα oxidation in normoxia

Over the past 20 years, the vasoactive properties of nitrite in hypoxia have been well described (161, 258, 269, 361). Nitrite is recognised as a potent vasodilator in humans in hypoxia with a wide range of additional pleiotropic properties (147). Whilst nitrite-mediated vasodilation in strict hypoxic (20-2 μmol) via reductase systems is relatively well understood (229, 269) and hypoxic-augmentation of nitrite-mediated vasodilation has been described (174, 237), the process underlying nitrite-mediated vasodilation in normoxia is subject to opposing views (237, 280, 362). During normoxia, the rate of bioconversion of nitrite to NO is slow, yet several groups have reported that in normoxia, in specific physiological conditions, such as sepsis, heart failure and hypertension, nitrite is capable of mediating significant vasodilation and systemic BP changes (200, 202-204).

Since the development of the 'redox-dead' (KI) mouse model incapable of PKGIα dimerization, by Prysyazhna, Rudyk, and Eaton in 2012, a great deal of work has followed investigating the physiological role of PKGIα dimerization (199). Since, it has been shown

that PKGIα-oxidation-mediated dimerization preferentially effects resistance vasculature (341) and several oxidants are capable of dimerizing PKGIα, including H_2O_2 (200), high ROS (202), and persulfides (208). This work provides an excellent basis to examine potential mechanisms in more detail and this led to our first presented study.

In Chapter 3, using the described transgenic knock-in (KI) mouse model (199), our group examined the mechanisms underlying nitrite-mediated vasodilation in normoxia. Using sGC and NO blockade, we showed that nitrite-mediated vasodilation was NO-dependent in thoracic aortae conduit vessels and was NO-independent in mesenteric resistance vessels. The wider team went on to show that nitrite-mediated BP-lowering was observed in WT mice ~4 hours after IP nitrite injection and this persisted for 24-hours, but this was not seen in redox-dead mice, consistent with the notion that nitrite can elicit persistent hypotension by oxidatively dimerizing PKG1α. Next, the group demonstrated that nitrite significantly increased steady-state concentrations of H_2O_2 in mesenteric resistance vessels at 1-hour and this persisted for 24-hours, whilst in aortae, the rise at 1-hour had returned to normal at 24-hours, revealing a difference in H_2O_2 handling between the two vessel types. We had surmised that the intermediate link driving nitrite-mediated PKG1α oxidative dimerization was via the generation of polysulfur species. This was tested in *vivo,* and we showed dose-dependent increases in CysSSH and GSSH in the resistance vessels, whilst there were no changes in CysSSH and GSSH in conduit vessels. Finally, we showed that H_2O_2 is capable of inducing polysulfidation when inorganic sulfide and cysteine are present.

Nitrite has previously been shown to inhibit catalase (343). Our group therefore proposed that wheras nitrite usually acts as a reducing agent, by inhibiting catalase and thereby increasing H_2O_2, it may also indirectly act as an oxidant and be capable of dimerizing PKGIα through a NO-independent mechanism. Our study confirmed this hypothesis and also

demonstrated that the increase in H_2O_2 leads to an increase in persulfides, which oxidize PKGIα (131).

These findings had not been previously shown and describe a novel redox mechanism which helps to explain how nitrite mediates significant vasodilation in normoxia. These findings warrant further investigation to address the significance of this redox pathway in hypertensive and other cardiovascular disease murine models. Beyond animal work, it would be important to examine whether the same redox mechanisms and polysulfur intermediates play a role in human vascular tone. This knowledge could potentially uncover multiple new therapeutic targets and pathways, and lead to the generation of new pharmacological agents. The therapeutic impact of this discovery may include improved clinical outcomes for patients presenting with acute and chronic vascular disorders including ischaemic crises and hypertensive disease states.

Chapter 4: Systemic autologous whole blood transfusion does not affect nitrite-mediated FBF in normoxia or hypoxia

The effect of haemoglobin on vasoactivity is a topic of great interest. Deoxyhaemoglobin is a well-characterised nitrite reductase functioning via an electron transport reaction at the haem iron (262) and oxyhaemoglobin is known to be an effective NO scavenger (260, 274), yet the physiological implications of these properties are not clear. One set of clinical data suggests that packed red cell transfusions which have been stored for prolonged periods are associated with increased mortality in critically ill patients (276-278), whilst another set reports no ill-effects of stored blood transfusion in surgical and ICU patients (363, 364). One observation that advanced this field was that harmful NO scavenging (and subsequent vasoconstriction) appears to be closely linked with blood unit storage duration. As shown by Donadee, then Risbano (both within the Gladwin group), blood stored for beyond 30-

days contained increased levels of cell-free haem, which despite storage, remained in the ferrous oxyhaemoglobin state (260, 274). These findings provided a possible explanation for why stored blood used for clinical transfusion may result in increased NO scavenging and less favourable clinical outcomes.

The work by Risbano, specifically tested the effect of 42-day stored blood (FDA regulations) on forearm resistance artery endothelial function and showed that it led to reduced FBFRs, indicating attenuation of bioavailable endothelial NO. Having gathered momentum in our basic science work as shown in Chapter 3, we were very interested in this, as Risbano had uncovered a method which enabled our group to attenuate NO in humans *in vivo*. We wanted to test whether stored blood could attenuate nitrite-derived NO (as opposed to endothelial-derived NO) and if so, if nitrite was able to mediate resistance artery vasodilation in normoxia via NO-independent processes. In order to do this, we identified that we would need to run the study as a cross-over design (also in hypoxia, to give a NO-dependent comparison) and in the absence and presence of autologous blood (to observe NO-attenuation).

In Chapter 4, we examined the main and interaction effects of nitrite, stored whole autologous blood (NHSBT 30-35-days stored), and oxygen condition on FBFRs in 31 healthy subjects. Study recruitment was a success with 473 people screened and 60 recruited, with a 41 to complete to achieve (80% power, 5% alpha [as we were only interested in one direction of effect]). However, as discussed at length, only 31 completed (48% attrition) highlighting the complexity of the study protocol. The main findings were that nitrite infusions in all conditions (N1, N2, H1 and H2) led to significant rises in plasma NOx (figure 36). Also, after 30-35-day storage, unit cell-free haem levels increased between 4- and 5-fold (figure 37), which led to a non-significant numerical increase in subject circulating cell-free haem (figure 37) and a non-significant numerical increase in nitrite-derived (and to a

lesser extent endothelium-derived) NO consumption (figure 38). Using mixed effect linear regression modelling, we showed that there was high inter-subject variability and that in all conditions, FBFRs were significantly predicted by nitrite infusion status alone (figures 39 and 40, and tables 3 – 5). There was no interaction effect between nitrite and hypoxia before or after blood (figure 41, table 6). We also showed that the dose of nitrite led to a reduction in MAP (table 7) but did not create a compensatory tachycardia (table 8).

As we were not able to show a difference in FBFRs between normoxia and hypoxia before or after autologous whole blood transfusion, we are not able to demonstrate a difference in mechanism for nitrite in the two studied oxygen conditions. As a result, we were unable to conclude whether nitrite uses a NO-independent pathway (or potentially activates PKG1α in human resistance arteries) in normoxia *in vivo*. The lack of effect observed was likely due to the high inter- and intra-subject variability recorded during FBF measurements, the limited statistical power due to very high levels of attrition and the high nitrite doses which may have subjugated the modest NO-binding effect of cell-free haem, such that the net observed effect was of no difference between normoxia and hypoxia.

This study has established multiple new processes in a complex regulatory environment to enable donation and transfusion of autologous whole blood, and for the first time, used it to attenuate NO *in vivo* to examine the vasoactive effects of nitrite in normoxia and hypoxia. Future work should more closely examine if there are any meaningful differences in administering stored blood intravenously vs intra-arterially in the presence of nitrite. For example, is it possible that the intra-arterial route creates a greater degree of localised endothelium-derived NO blockade vs the intravenous route?

In addition, future work should also re-evaluate the study design, given that two nitrite infusions led to degree of study drug carry-over, which meant that 'true' NOx baselines

could not be compared, albeit statistically accounted for. Developing a protocol using a continuous infusion to achieve steady state NOx levels may have negated this issue. As already described, the pre- and post-design of the autologous blood transfusion was unavoidable (as 4 separate clinical sessions was not possible), however this did reduce the level of evidence vs a randomized element (358). In addition, future study protocol development would need to attempt to reduce the very high attrition associated to the protocol being arduous, invasive, and prolonged. An alternative approach would be to use a randomized parallel groups design with propensity matching. This would remove the minimum 12-week wait between blood donations (which was, in fact, often closer to 6 months due to limited NHSBT donation slot availability) and reduce the time/effort burden on each subject, but this would come at the cost of increased confounding covariates.

Future clinical objectives should include examining the interaction effect of nitrite, cell-free haem and oxygen concentration in haemodynamically stable patients who are receiving clinical allogenic blood transfusion. This work may show that systemic nitrite co-infusion is capable of mitigating the detrimental vasoconstrictive effect of cell-free haem present in stored allogenic blood via NO-independent pathways. This hypothesis would need to be tested via a randomized, double-blinded, placebo-controlled study.

Chapter 5: Systemic nitrite significantly increases epicardial artery CSA and reduces blood velocity in normoxia and hypoxia and reduces flow in hypoxia

Until recently, it has not been possible to non-invasively measure epicardial coronary artery CSA, velocity or flow. Whilst it is generally accepted that the coronary arteries are physiologically similar to the peripheral arteries with respect to vasomotor activity (112, 279) the vasoactive properties of nitrite on the coronary arteries in both normoxia and hypoxia is largely undefined. Historically, it was reported that amyl nitrite increased CSA

of saphenous vein graft in humans and simultaneously increased the coronary artery blood flow (285), but due to limited studies, these findings have remained largely unvalidated for decades.

As a result of advancing CMR imaging capabilities, in 2015 Prof Jennifer Keegan and colleagues presented work to show that using an interleaved spiral phase velocity sequence on a 3 Tesla Magnetom Skyra (Siemens, Germany) MR scanner and unique post-hoc MATLAB processing steps, they could accurately record the change in epicardial coronary CSA, velocity and flow in the human heart *in vivo* (286). Whilst completing our study, O'Gallagher and colleagues published a paper that showed (using coronary Doppler wires) that 5-minute infusions of inorganic nitrite 26 μmol/min selectively dilates epicardial coronary arteries in a dose-dependent fashion in normoxia. Their observations aligned with the large body of pre-existing literature that states that nitrite is capable of vasodilating systemic arteries, however, O'Gallagher and colleagues also identified that nitrite appeared to selectively vasodilate large conduit epicardial arteries (instead of resistance vessels) in the metabolically active myocardium (287). These findings were of specific interest as they suggested that the vasoactive properties of nitrite in the coronary arteries may be subject to oxygen tension (as the conduit vessels would be expected to contain blood with a higher oxygen concentration than the resistance arteries) (365). In view of the above study, we aimed to examine the effects of nitrite-mediated epicardial coronary artery vasodilation in normoxia using advanced CMR techniques, and uniquely, extend on this work by investigating these effects in hypoxia for the first time in humans.

In Chapter 5, we examined the main and interaction effects of nitrite and oxygen condition on epicardial conduit artery CSA, velocity and flow in 14 healthy subjects. Study recruitment was successful with 50 people screened, 14 recruited and 13 with a full set of interpretable images. This study was a proof of concept, so no formal power calculation was performed.

The main findings were that a 5-minute IV nitrite bolus of 50 μg/kg/min^{-1} (254 μmol) led to significant rises in plasma NOx and RXNO (figure 41), associated with significant increases in epicardial conduit CSA (figure 43) and significant reductions in velocity in both oxygen conditions (figure 44) and a significant reduction in flow in hypoxia but not normoxia (figure 45). This was associated with a significant reduction in MAP (but not HR) in normoxia (figure 42).

Taken together, our study results differed to an extent from our hypotheses. The combination of findings in this study were rather unexpected in that whilst we expected to observe an increase in epicardial CSA associated with a decrease velocity (per the Hagen–Poiseuille equation) (54, 55), we did not expect to observe a reduction in epicardial coronary flow in hypoxia. Indeed, as it is generally accepted that healthy coronary arteries do not exert significant resistance to flow (281, 282), we expected that epicardial coronary flow would remain constant in the study.

As this study was not mechanistic in nature, we cannot provide the exact mechanism underlying the reductions in flow in hypoxia. However, it is possible that nitrite infusion led to a decrease in aortic BP and this in-turn led to a reduction in intra-coronary pressure. It is also possible that the reduction in MAP activated a baroreflex-mediated sympathetic constriction of the coronary resistance vessels and this too led to a reduction in flow, however as discussed as a limitation of this study, we were not able to record BP in hypoxia and therefore we were not able to calculate MAP or coronary vascular resistance in hypoxia.

These results provide important new knowledge to the field. Firstly, these are the first data to show that hypoxic-augmentation of nitrite-mediated vasodilation exists in the epicardial conduits. Also, this is the first study to use coronary CMR to examine the vasoactive

properties of nitrite on the epicardial coronary arteries in both normoxia and hypoxia *in vivo*, providing a non-invasive radiation-free methodology for future studies.

Similar to the work in Chapter 4, this study design also had a pre- and post-design element, which meant that the plasma concentration of NOx/RXNO would have been lower in hypoxia vs normoxia. Again, future work may look to establish a protocol using a continuous infusion to achieve steady state nitrite levels and this approach may negate this pre- and post-design issue. We noted throughout our results and discussion that the dose of nitrite we used was associated with a reduction in MAP in normoxia. We also recognised that O'Gallagher achieved significant vasodilation using 26 μmol /min over 5-minutes, which was ~1/2 of our dose, indicating that in the given study we used a dose that was potentially too high. Future work should complete a dose-finding study to help understand the optimal therapeutic dose of nitrite in the epicardial coronary arteries. Lastly, as detailed in the methods, we were unable to study BP in hypoxia only due to movement artefacts. Future work should use a finapres or similar to overcome this, as understanding MAP in hypoxia (at lower doses of nitrite) would provide greater understanding into the tissue-specific selectivity of nitrite in the heart and also help explain why a reduction in flow was observed in hypoxia.

Future scientific objectives should include examining whether the epicardial conduit arteries have analogous NO-dependency to systemic conduit arteries, or given that they appear to vasodilate in synchrony with systemic resistance vessels, whether they too are subject to NO-independent processes (as discussed in Chapter 3). Clinically, future work could focus on the safety, efficacy and tolerability of sustained-release nitrite as a daily therapeutic agent in the context of chronic stable angina. Work could also focus on the fast-acting effects of bolus nitrite and could be studied in the acute setting of angioplasty (either via systemic dosing or even via intra-coronary administration) to examine whether a nitrite bolus can improve outcomes or reduce complications following PCI (131, 308-310). Again, future

clinical studies should be conducted as randomized, double-blinded, placebo-controlled trials.

In combination, the work presented in this PhD thesis has shown that in a murine model ex vivo, nitrite is capable of circumventing the NO-sGC pathway via persulfide intermediates to induce tissue-specific vasodilation via PKGIα oxidation in normoxia. In human resistance arteries in vivo, we showed that 30-35-day NHSBT stored systemic autologous whole blood transfusion did not modify nitrite-mediated FBF in normoxia or hypoxia, therefore we were unable to conclude whether nitrite uses a NO-independent pathway in resistance arteries in normoxia. In the epicardial coronary arteries in vivo, we showed that systemic nitrite infusion significantly increased CSA and reduced blood velocity in normoxia and hypoxia, and reduced flow in hypoxia. These observations highlighted that nitrite-mediated vasodilation in the epicardial coronary arteries is subject to hypoxic-augmentation. Taken together, this work provides important new knowledge to the field of nitrite-mediated vasodilation and generates a number of potential hypotheses for future work.

REFERENCES

1. WHO. ICD-11 2018 [Available from: https://www.who.int/classifications/icd/en/.

2. WHO. World Health Organisation. Global status report on noncommunicable diseases 2014. ISBN: 9789241564854. www.who.int/nmh/publications/ncd-status-report-2014/en/. Accessed 28/11/2016. 2014.

3. Briceno N, Schuster A, Lumley M, Perera D. Ischaemic cardiomyopathy: pathophysiology, assessment and the role of revascularisation. Heart (British Cardiac Society). 2016;102(5):397-406.

4. Havranek EP, Mujahid MS, Barr DA, Blair IV, Cohen MS, Cruz-Flores S, et al. Social Determinants of Risk and Outcomes for Cardiovascular Disease: A Scientific Statement From the American Heart Association. Circulation. 2015;132(9):873-98.

5. D'Agostino RB, Russell MW, Huse DM, Ellison RC, Silbershatz H, Wilson PW, et al. Primary and subsequent coronary risk appraisal: new results from the Framingham study. American heart journal. 2000;139(2 Pt 1):272-81.

6. Anand SS, Islam S, Rosengren A, Franzosi MG, Steyn K, Yusufali AH, et al. Risk factors for myocardial infarction in women and men: insights from the INTERHEART study. European heart journal. 2008;29(7):932-40.

7. Yusuf S, Hawken S, Ounpuu S, Dans T, Avezum A, Lanas F, et al. Effect of potentially modifiable risk factors associated with myocardial infarction in 52 countries (the INTERHEART study): case-control study. Lancet (London, England). 2004;364(9438):937-52.

8. Desai MY, Nasir K, Braunstein JB, Rumberger JA, Post WS, Budoff MJ, et al. Underlying risk factors incrementally add to the standard risk estimate in detecting subclinical atherosclerosis in low- and intermediate-risk middle-aged asymptomatic individuals. American heart journal. 2004;148(5):871-7.

9. Hippisley-Cox J, Coupland C, Brindle P. Development and validation of QRISK3 risk prediction algorithms to estimate future risk of cardiovascular disease: prospective cohort study. BMJ (Clinical research ed). 2017;357:j2099.

10. Karmali KN, Persell SD, Perel P, Lloyd-Jones DM, Berendsen MA, Huffman MD. Risk scoring for the primary prevention of cardiovascular disease. The Cochrane database of systematic reviews. 2017;3:Cd006887.

11. Gourgari E, Dabelea D, Rother K. Modifiable Risk Factors for Cardiovascular Disease in Children with Type 1 Diabetes: Can Early Intervention Prevent Future Cardiovascular Events? Current diabetes reports. 2017;17(12):134.

12. Joseph P, Leong D, McKee M, Anand SS, Schwalm JD, Teo K, et al. Reducing the Global Burden of Cardiovascular Disease, Part 1: The Epidemiology and Risk Factors. Circulation research. 2017;121(6):677-94.

13. Mosley WH, Chen LC. An analytical framework for the study of child survival in developing countries. 1984. Bulletin of the World Health Organization. 2003;81(2):140-5.

14. Okurut K, Kulabako RN, Chenoweth J, Charles K. Assessing demand for improved sustainable sanitation in low-income informal settlements of urban areas: a critical review. International journal of environmental health research. 2015;25(1):81-95.

15. ONS. Top causes of death by age and sex, 1915 to 2015 in the UK. Panel A) Women and panel B) Men. 2018 [Top causes of death by age and sex, 1915 to 2015 in the UK. Panel A) Women and panel B) Men.].

16. He C, Liu L, Chu Y, Perin J, Dai L, Li X, et al. National and subnational all-cause and cause-specific child mortality in China, 1996-2015: a systematic analysis with implications for the Sustainable Development Goals. The Lancet Global health. 2017;5(2):e186-e97.

17. Pagan E, Chatenoud L, Rodriguez T, Bosetti C, Levi F, Malvezzi M, et al. Comparison of Trends in Mortality from Coronary Heart and Cerebrovascular Diseases in

North and South America: 1980 to 2013. The American journal of cardiology. 2017;119(6):862-71.

18. BHF. British Heart Foundation. CVD Statistics – BHF UK factsheet, 2015. www.bhf.org.uk/research/heart-statistics. Accessed 28/11/2016. 2015.

19. Townsend N, Nichols M, Scarborough P, Rayner M. Cardiovascular disease in Europe--epidemiological update 2015. European heart journal. 2015;36(40):2696-705.

20. BHF. Key statistics and information on heart and circulatory diseases for the UK 2019 [Available from: https://www.bhf.org.uk/what-we-do/our-research/heart-statistics.

21. Bhatnagar P, Wickramasinghe K, Wilkins E, Townsend N. Trends in the epidemiology of cardiovascular disease in the UK. Heart (British Cardiac Society). 2016;102(24):1945-52.

22. CEBR. The rising cost of CVD 2014 [Available from: https://cebr.com/reports/the-rising-cost-of-cvd/.

23. Starr JM. Dementia overtakes heart disease as the leading cause of death: But does this mean that incidence has increased? Maturitas. 2017;98:51-2.

24. Wu YT, Fratiglioni L, Matthews FE, Lobo A, Breteler MM, Skoog I, et al. Dementia in western Europe: epidemiological evidence and implications for policy making. The Lancet Neurology. 2016;15(1):116-24.

25. Boden WE, O'Rourke RA, Teo KK, Hartigan PM, Maron DJ, Kostuk WJ, et al. Optimal medical therapy with or without PCI for stable coronary disease. The New England journal of medicine. 2007;356(15):1503-16.

26. Mills EJ, Rachlis B, Wu P, Devereaux PJ, Arora P, Perri D. Primary prevention of cardiovascular mortality and events with statin treatments: a network meta-analysis involving more than 65,000 patients. Journal of the American College of Cardiology. 2008;52(22):1769-81.

27. Szreter S. Industrialization and health. British medical bulletin. 2004;69:75-86.

28. Westerhof N, Lankhaar JW, Westerhof BE. The arterial Windkessel. Medical & biological engineering & computing. 2009;47(2):131-41.

29. Belz GG. Elastic properties and Windkessel function of the human aorta. Cardiovascular drugs and therapy. 1995;9(1):73-83.

30. Viau DM, Sala-Mercado JA, Spranger MD, O'Leary DS, Levy PD. The pathophysiology of hypertensive acute heart failure. Heart (British Cardiac Society). 2015;101(23):1861-7.

31. Bergel DH. The static elastic properties of the arterial wall. The Journal of physiology. 1961;156(3):445-57.

32. Weibel ER. Morphological basis of alveolar-capillary gas exchange. Physiological reviews. 1973;53(2):419-95.

33. Mellander S, Johansson B. Control of resistance, exchange, and capacitance functions in the peripheral circulation. Pharmacological reviews. 1968;20(3):117-96.

34. Raffetto JD, Mannello F. Pathophysiology of chronic venous disease. International angiology : a journal of the International Union of Angiology. 2014;33(3):212-21.

35. van Beekvelt MC, van Asten WN, Hopman MT. The effect of electrical stimulation on leg muscle pump activity in spinal cord-injured and able-bodied individuals. European journal of applied physiology. 2000;82(5-6):510-6.

36. Mecham RP, Ramirez F. Extracellular Determinants of Arterial Morphogenesis, Growth, and Homeostasis. Current topics in developmental biology. 2018;130:193-216.

37. Ogeng'o JA, Malek AA, Kiama SG. Structural organisation of tunica intima in the aorta of the goat. Folia morphologica. 2010;69(3):164-9.

38. McCloskey K, Vuillermin P, Ponsonby AL, Cheung M, Skilton MR, Burgner D. Aortic intima-media thickness measured by trans-abdominal ultrasound as an early life marker of subclinical atherosclerosis. Acta paediatrica (Oslo, Norway : 1992). 2014;103(2):124-30.

39. Balta S, Aparci M, Ozturk C, Unlu M, Celik T. Carotid intima media thickness can predict coronary artery disease. International journal of cardiology. 2015;201:331.

40. Mecham S. The vascular smooth muscle cell: molecular and biological responses to the extracellular matrix: Academic Press; 1995.

41. Martinez-Lemus LA. The dynamic structure of arterioles. Basic & clinical pharmacology & toxicology. 2012;110(1):5-11.

42. Jiang J, Zheng JP, Li Y, Gan Z, Jiang Y, Huang D, et al. Differential contribution of endothelium-derived relaxing factors to vascular reactivity in conduit and resistance arteries from normotensive and hypertensive rats. Clinical and experimental hypertension (New York, NY : 1993). 2016;38(4):393-8.

43. Sato S, Suzuki J. Anatomical mapping of the cerebral nervi vasorum in the human brain. Journal of neurosurgery. 1975;43(5):559-68.

44. Dhital K, Lincoln J, Appenzeller O, Burnstock G. Adrenergic innervation of vasa and nervi nervorum of optic, sciatic, vagus and sympathetic nerve trunks in normal and streptozotocin-diabetic rats. Brain research. 1986;367(1-2):39-44.

45. Folkow B, Lewis DH, Lundgren O, Mellander S, Wallentin I. THE EFFECT OF GRADED VASOCONSTRICTOR FIBRE STIMULATION ON THE INTESTINAL RESISTANCE AND CAPACITANCE VESSELS. Acta physiologica Scandinavica. 1964;61:445-57.

46. Smith JF, Canham PB, Starkey J. Orientation of collagen in the tunica adventitia of the human cerebral artery measured with polarized light and the universal stage. Journal of ultrastructure research. 1981;77(2):133-45.

47. Corselli M, Chen CW, Sun B, Yap S, Rubin JP, Peault B. The tunica adventitia of human arteries and veins as a source of mesenchymal stem cells. Stem cells and development. 2012;21(8):1299-308.

48. CNX O. Anatomy of arteries and veins 2019 [Available from: www.cnx.org/contents

49. Brunner F, Bras-Silva C, Cerdeira AS, Leite-Moreira AF. Cardiovascular endothelins: essential regulators of cardiovascular homeostasis. Pharmacology & therapeutics. 2006;111(2):508-31.

50. Dzau VJ. Circulating versus local renin-angiotensin system in cardiovascular homeostasis. Circulation. 1988;77(6 Pt 2):I4-13.

51. Schulz R, Rassaf T, Massion PB, Kelm M, Balligand JL. Recent advances in the understanding of the role of nitric oxide in cardiovascular homeostasis. Pharmacology & therapeutics. 2005;108(3):225-56.

52. Drummond HA, Jernigan NL, Grifoni SC. Sensing tension: epithelial sodium channel/acid-sensing ion channel proteins in cardiovascular homeostasis. Hypertension (Dallas, Tex : 1979). 2008;51(5):1265-71.

53. Smulyan H, Marchais SJ, Pannier B, Guerin AP, Safar ME, London GM. Influence of body height on pulsatile arterial hemodynamic data. Journal of the American College of Cardiology. 1998;31(5):1103-9.

54. Tahmassebi A. Fluid Flow Through Carbon Nanotubes And Graphene Based Nanostructures 2015.

55. Zhang B, Sun Y, Xia L, Gu J. Time-dependent flow velocity measurement using two-dimensional color Doppler flow imaging and evaluation by Hagen-Poiseuille equation. Australasian physical & engineering sciences in medicine. 2015;38(4):755-66.

56. Schmitt M, Blackman DJ, Middleton GW, Cockcroft JR, Frenneaux MP. Assessment of venous capacitance. Radionuclide plethysmography: methodology and research applications. British journal of clinical pharmacology. 2002;54(6):565-76.

57. Chemla D, Antony I, Lecarpentier Y, Nitenberg A. Contribution of systemic vascular resistance and total arterial compliance to effective arterial elastance in humans. American journal of physiology Heart and circulatory physiology. 2003;285(2):H614-20.

58. Bennett HS, Luft JH, Hampton JC. Morphological classifications of vertebrate blood capillaries. The American journal of physiology. 1959;196(2):381-90.

59. Peppiatt CM, Howarth C, Mobbs P, Attwell D. Bidirectional control of CNS capillary diameter by pericytes. Nature. 2006;443(7112):700-4.

60. Hall CN, Reynell C, Gesslein B, Hamilton NB, Mishra A, Sutherland BA, et al. Capillary pericytes regulate cerebral blood flow in health and disease. Nature. 2014;508(7494):55-60.

61. Mishra A, Reynolds JP, Chen Y, Gourine AV, Rusakov DA, Attwell D. Astrocytes mediate neurovascular signaling to capillary pericytes but not to arterioles. Nature neuroscience. 2016;19(12):1619-27.

62. Sutera SP, Seshadri V, Croce PA, Hochmuth RM. Capillary blood flow. II. Deformable model cells in tube flow. Microvascular research. 1970;2(4):420-33.

63. Gascho JA, Fanelli C, Zelis R. Aging reduces venous distensibility and the venodilatory response to nitroglycerin in normal subjects. The American journal of cardiology. 1989;63(17):1267-70.

64. Jeanneret C, Jager KA, Zaugg CE, Hoffmann U. Venous reflux and venous distensibility in varicose and healthy veins. European journal of vascular and endovascular surgery : the official journal of the European Society for Vascular Surgery. 2007;34(2):236-42.

65. Tyberg JV, Grant DA, Kingma I, Moore TD, Sun Y, Smith ER, et al. Effects of positive intrathoracic pressure on pulmonary and systemic hemodynamics. Respiration physiology. 2000;119(2-3):171-9.

66. Plotnick GD, Becker LC, Fisher ML, Gerstenblith G, Renlund DG, Fleg JL, et al. Use of the Frank-Starling mechanism during submaximal versus maximal upright exercise. The American journal of physiology. 1986;251(6 Pt 2):H1101-5.

67. Kitzman DW, Higginbotham MB, Cobb FR, Sheikh KH, Sullivan MJ. Exercise intolerance in patients with heart failure and preserved left ventricular systolic function: failure of the Frank-Starling mechanism. Journal of the American College of Cardiology. 1991;17(5):1065-72.

68. Strohl KP, Scharf SM. Effect of intrathoracic pressure on left-ventricular performance. The New England journal of medicine. 1980;302(4):235-6.

69. Nishimura S, Ehara S, Hasegawa T, Matsumoto K, Yoshikawa J, Shimada K. Cholesterol crystal as a new feature of coronary vulnerable plaques: An optical coherence tomography study. Journal of cardiology. 2017;69(1):253-9.

70. van Lammeren GW, den Ruijter HM, Vrijenhoek JE, van der Laan SW, Velema E, de Vries JP, et al. Time-dependent changes in atherosclerotic plaque composition in patients undergoing carotid surgery. Circulation. 2014;129(22):2269-76.

71. Glass CK, Witztum JL. Atherosclerosis. the road ahead. Cell. 2001;104(4):503-16.

72. Pries AR, Badimon L, Bugiardini R, Camici PG, Dorobantu M, Duncker DJ, et al. Coronary vascular regulation, remodelling, and collateralization: mechanisms and clinical implications on behalf of the working group on coronary pathophysiology and microcirculation. European heart journal. 2015;36(45):3134-46.

73. Libby P, Pasterkamp G. Requiem for the 'vulnerable plaque'. European heart journal. 2015;36(43):2984-7.

74. Johnson JL. Metalloproteinases in atherosclerosis. European journal of pharmacology. 2017;816:93-106.

75. Badimon L, Vilahur G. Thrombosis formation on atherosclerotic lesions and plaque rupture. Journal of internal medicine. 2014;276(6):618-32.

76. Alatorre CI, Hoogwerf BJ, Deeg MA, Nelson DR, Hunter TM, Ng WT, et al. Factors associated with stroke, myocardial infarction, ischemic heart disease, unstable angina, or mortality in patients from real world clinical practice with newly-diagnosed type 2 diabetes and early glycemic control. Current medical research and opinion. 2018;34(2):337-43.

77. Anzai T. Inflammatory Mechanisms of Cardiovascular Remodeling. Circulation journal : official journal of the Japanese Circulation Society. 2018;82(3):629-35.

78. Bailey DM, Evans TG, Thomas KG, White RD, Twine CP, Lewis MH, et al. Intervisceral artery origins in patients with abdominal aortic aneurysmal disease; evidence for systemic vascular remodelling. Experimental physiology. 2016;101(8):1143-53.

79. Baumgartner H, Falk V, Bax JJ, De Bonis M, Hamm C, Holm PJ, et al. 2017 ESC/EACTS Guidelines for the management of valvular heart disease. European heart journal. 2017;38(36):2739-91.

80. Rabar S, Harker M, O'Flynn N, Wierzbicki AS. Lipid modification and cardiovascular risk assessment for the primary and secondary prevention of cardiovascular disease: summary of updated NICE guidance. BMJ (Clinical research ed). 2014;349:g4356.

81. Uthman OA, Hartley L, Rees K, Taylor F, Ebrahim S, Clarke A. Multiple risk factor interventions for primary prevention of cardiovascular disease in low- and middle-income countries. The Cochrane database of systematic reviews. 2015(8):Cd011163.

82. Hippisley-Cox J, Coupland C, Robson J, Brindle P. Derivation, validation, and evaluation of a new QRISK model to estimate lifetime risk of cardiovascular disease: cohort study using QResearch database. BMJ (Clinical research ed). 2010;341:c6624.

83. Stewart J, Manmathan G, Wilkinson P. Primary prevention of cardiovascular disease: A review of contemporary guidance and literature. JRSM cardiovascular disease. 2017;6:2048004016687211.

84. Elisaf M, Tzouvelekis E, Nikas N. Primary prevention of cardiovascular disease in Greece: Greek results of the EURIKA study. Hellenic journal of cardiology : HJC = Hellenike kardiologike epitheorese. 2014;55(3):217-26.

85. NICE. Cardiovascular disease: risk assessment and reduction, including lipid modification 2016 [Available from: https://www.nice.org.uk/guidance/cg181.

86. Nichols M, Townsend N, Scarborough P, Rayner M. Cardiovascular disease in Europe 2014: epidemiological update. European heart journal. 2014;35(42):2950-9.

87. JBS3. The Joint British Societies recommendations on the prevention of Cardiovascular Disease (JBS3) 2014 [Available from: http://www.jbs3risk.com/.

88. van Diepen S, Katz JN, Albert NM, Henry TD, Jacobs AK, Kapur NK, et al. Contemporary Management of Cardiogenic Shock: A Scientific Statement From the American Heart Association. Circulation. 2017;136(16):e232-e68.

89. Dangas G, Guedeney P. Prediction, staging, and outcomes of ischaemic cardiogenic shock after STEMI: a complex clinical interplay. European heart journal. 2018;39(22):2103-5.

90. Wang YT, Popovic ZB, Efimov IR, Cheng Y. Longitudinal study of cardiac remodelling in rabbits following infarction. The Canadian journal of cardiology. 2012;28(2):230-8.

91. Brilla CG, Rupp H, Funck R, Maisch B. The renin-angiotensin-aldosterone system and myocardial collagen matrix remodelling in congestive heart failure. European heart journal. 1995;16 Suppl O:107-9.

92. Ferrario CM. Cardiac remodelling and RAS inhibition. Therapeutic advances in cardiovascular disease. 2016;10(3):162-71.

93. Ouwerkerk W, Voors AA, Anker SD, Cleland JG, Dickstein K, Filippatos G, et al. Determinants and clinical outcome of uptitration of ACE-inhibitors and beta-blockers in patients with heart failure: a prospective European study. European heart journal. 2017;38(24):1883-90.

94. Yancy CW, Jessup M, Bozkurt B, Butler J, Casey DE, Jr., Colvin MM, et al. 2017 ACC/AHA/HFSA Focused Update of the 2013 ACCF/AHA Guideline for the Management of Heart Failure: A Report of the American College of Cardiology/American Heart Association Task Force on Clinical Practice Guidelines and the Heart Failure Society of America. Journal of cardiac failure. 2017;23(8):628-51.

95. Cleland JGF, Bunting KV, Flather MD, Altman DG, Holmes J, Coats AJS, et al. Beta-blockers for heart failure with reduced, mid-range, and preserved ejection fraction: an individual patient-level analysis of double-blind randomized trials. European heart journal. 2018;39(1):26-35.

96. Barnes E, Khan MA. Myocardial stunning in man. Heart failure reviews. 2003;8(2):155-60.

97. Fiechter M, Fuchs TA, Stehli J, Jacobs S, Falk V, Kaufmann PA. Reversible true myocardial hibernation. European heart journal. 2013;34(9):648.

98. Maranta F, Tondi L, Agricola E, Margonato A, Rimoldi O, Camici PG. Ivabradine reduces myocardial stunning in patients with exercise-inducible ischaemia. Basic research in cardiology. 2015;110(6):55.

99. Shah BN, Khattar RS, Senior R. The hibernating myocardium: current concepts, diagnostic dilemmas, and clinical challenges in the post-STICH era. European heart journal. 2013;34(18):1323-36.

100. Matsuoka R, Yoshida MC, Furutani Y, Imamura S, Kanda N, Yanagisawa M, et al. Human smooth muscle myosin heavy chain gene mapped to chromosomal region 16q12. American journal of medical genetics. 1993;46(1):61-7.

101. Perrin BJ, Ervasti JM. The actin gene family: function follows isoform. Cytoskeleton (Hoboken, NJ). 2010;67(10):630-4.

102. Marty I, Faure J. Excitation-Contraction Coupling Alterations in Myopathies. Journal of neuromuscular diseases. 2016;3(4):443-53.

103. Aguilar HN, Mitchell BF. Physiological pathways and molecular mechanisms regulating uterine contractility. Human reproduction update. 2010;16(6):725-44.

104. Kuo IY, Ehrlich BE. Signaling in muscle contraction. Cold Spring Harbor perspectives in biology. 2015;7(2):a006023.

105. Berridge MJ. The Inositol Trisphosphate/Calcium Signaling Pathway in Health and Disease. Physiological reviews. 2016;96(4):1261-96.

106. Somlyo AP, Somlyo AV. Signal transduction and regulation in smooth muscle. Nature. 1994;372(6503):231-6.

107. Adelstein RS, Sellers JR. Effects of calcium on vascular smooth muscle contraction. The American journal of cardiology. 1987;59(3):4b-10b.

108. Debold EP, Fitts RH, Sundberg CW, Nosek TM. Muscle Fatigue from the Perspective of a Single Crossbridge. Medicine and science in sports and exercise. 2016;48(11):2270-80.

109. Niggli E, Lederer WJ. Molecular operations of the sodium-calcium exchanger revealed by conformation currents. Nature. 1991;349(6310):621-4.

110. Liu Z, Khalil RA. Evolving mechanisms of vascular smooth muscle contraction highlight key targets in vascular disease. Biochemical pharmacology. 2018;153:91-122.

111. Mabuchi Y, Mabuchi K, Stafford WF, Grabarek Z. Modular structure of smooth muscle Myosin light chain kinase: hydrodynamic modeling and functional implications. Biochemistry. 2010;49(13):2903-17.

112. Anderson TJ, Uehata A, Gerhard MD, Meredith IT, Knab S, Delagrange D, et al. Close relation of endothelial function in the human coronary and peripheral circulations. Journal of the American College of Cardiology. 1995;26(5):1235-41.

113. Woodrum DA, Brophy CM. The paradox of smooth muscle physiology. Molecular and cellular endocrinology. 2001;177(1-2):135-43.

114. Sesso HD, Stampfer MJ, Rosner B, Hennekens CH, Gaziano JM, Manson JE, et al. Systolic and diastolic blood pressure, pulse pressure, and mean arterial pressure as predictors of cardiovascular disease risk in Men. Hypertension (Dallas, Tex : 1979). 2000;36(5):801-7.

115. Folkow B. Physiological aspects of primary hypertension. Physiological reviews. 1982;62(2):347-504.

116. Dale Ra. Rang & Dale's pharmacology.: Edinburgh: Churchill Livingstone.; 2007.

117. Boron WF. Medical Physiology: A Cellular And Molecular Approach.: Elsevier/Saunders; 2008.

118. Charkoudian N. Mechanisms and modifiers of reflex induced cutaneous vasodilation and vasoconstriction in humans. Journal of applied physiology (Bethesda, Md : 1985). 2010;109(4):1221-8.

119. Nava E, Llorens S. The Local Regulation of Vascular Function: From an Inside-Outside to an Outside-Inside Model. Front Physiol. 2019;10:729.

120. Moncada S, Higgs EA, Vane JR. Human arterial and venous tissues generate prostacyclin (prostaglandin x), a potent inhibitor of platelet aggregation. Lancet (London, England). 1977;1(8001):18-20.

121. Arnold WP, Mittal CK, Katsuki S, Murad F. Nitric oxide activates guanylate cyclase and increases guanosine 3':5'-cyclic monophosphate levels in various tissue preparations. Proceedings of the National Academy of Sciences of the United States of America. 1977;74(8):3203-7.

122. Bolton TB, Lang RJ, Takewaki T. Mechanisms of action of noradrenaline and carbachol on smooth muscle of guinea-pig anterior mesenteric artery. The Journal of physiology. 1984;351:549-72.

123. Palmer RM, Ferrige AG, Moncada S. Nitric oxide release accounts for the biological activity of endothelium-derived relaxing factor. Nature. 1987;327(6122):524-6.

124. Moncada S, Higgs EA. Endogenous nitric oxide: physiology, pathology and clinical relevance. Eur J Clin Invest. 1991;21(4):361-74.

125. McGuire JJ, Ding H, Triggle CR. Endothelium-derived relaxing factors: a focus on endothelium-derived hyperpolarizing factor(s). Can J Physiol Pharmacol. 2001;79(6):443-70.

126. Luksha L, Agewall S, Kublickiene K. Endothelium-derived hyperpolarizing factor in vascular physiology and cardiovascular disease. Atherosclerosis. 2009;202(2):330-44.

127. Busse R, Edwards G, Feletou M, Fleming I, Vanhoutte PM, Weston AH. EDHF: bringing the concepts together. Trends Pharmacol Sci. 2002;23(8):374-80.

128. Rhee SG. Cell signaling. H2O2, a necessary evil for cell signaling. Science (New York, NY). 2006;312(5782):1882-3.

129. Cascino T, Csanyi G, Al Ghouleh I, Montezano AC, Touyz RM, Haurani MJ, et al. Adventitia-derived hydrogen peroxide impairs relaxation of the rat carotid artery via smooth

muscle cell p38 mitogen-activated protein kinase. Antioxidants & redox signaling. 2011;15(6):1507-15.

130. Costa RM, Filgueira FP, Tostes RC, Carvalho MH, Akamine EH, Lobato NS. H2O2 generated from mitochondrial electron transport chain in thoracic perivascular adipose tissue is crucial for modulation of vascular smooth muscle contraction. Vascular pharmacology. 2016;84:28-37.

131. Feelisch M, Akaike T, Griffiths K, Ida T, Prysyahna O, Goodwin JJ, et al. Long-lasting blood pressure lowering effects of nitrite are NO-independent and mediated by hydrogen peroxide, persulfides and oxidation of protein kinase G 1alpha redox signaling. Cardiovascular research. 2019.

132. Hall Ma. Concise Dictionary of Pharmacological Agents: Properties and Synonyms.: Springer Science & Business Media.; 2012.

133. Stowe DF. Vasodilator responses to moderate hypoxia after submaximal adenosine injection or coronary occlusion in isolated perfused guinea pig hearts. Circulation research. 1980;47(3):392-9.

134. Meininger CJ, Schelling ME, Granger HJ. Adenosine and hypoxia stimulate proliferation and migration of endothelial cells. The American journal of physiology. 1988;255(3 Pt 2):H554-62.

135. Eckle T, Faigle M, Grenz A, Laucher S, Thompson LF, Eltzschig HK. A2B adenosine receptor dampens hypoxia-induced vascular leak. Blood. 2008;111(4):2024-35.

136. Sitkovsky MV, Lukashev D, Apasov S, Kojima H, Koshiba M, Caldwell C, et al. Physiological control of immune response and inflammatory tissue damage by hypoxia-inducible factors and adenosine A2A receptors. Annu Rev Immunol. 2004;22:657-82.

137. Glazier JB, Murray JF. Sites of pulmonary vasomotor reactivity in the dog during alveolar hypoxia and serotonin and histamine infusion. J Clin Invest. 1971;50(12):2550-8.

138. Li X, Lu WC, Zhu YJ. [The relation of vasoactive intestinal peptide and acute hypoxia]. Zhonghua Nei Ke Za Zhi. 1990;29(1):8-10, 59.

139. Basile DP, Donohoe DL, Roethe K, Mattson DL. Chronic renal hypoxia after acute ischemic injury: effects of L-arginine on hypoxia and secondary damage. Am J Physiol Renal Physiol. 2003;284(2):F338-48.

140. Garcia-Bonilla L, Brea D, Benakis C, Lane DA, Murphy M, Moore J, et al. Endogenous Protection from Ischemic Brain Injury by Preconditioned Monocytes. J Neurosci. 2018;38(30):6722-36.

141. Chen J, Yan H. [Effect of hypoxia on vasodilation induced by substance P (SP) and calcitonin gene-related peptide (CGRP)]. Zhongguo Yi Xue Ke Xue Yuan Xue Bao. 1992;14(2):114-7.

142. Fuchs C, Ertmer C, Rehberg S. Effects of vasodilators on haemodynamic coherence. Best practice & research Clinical anaesthesiology. 2016;30(4):479-89.

143. Maman SR, Vargas AF, Ahmad TA, Miller AJ, Gao Z, Leuenberger UA, et al. Beta-1 vs. beta-2 adrenergic control of coronary blood flow during isometric handgrip exercise in humans. Journal of applied physiology (Bethesda, Md : 1985). 2017;123(2):337-43.

144. Giovannitti JA, Jr., Thoms SM, Crawford JJ. Alpha-2 adrenergic receptor agonists: a review of current clinical applications. Anesthesia progress. 2015;62(1):31-9.

145. Vargas Pelaez AF, Gao Z, Ahmad TA, Leuenberger UA, Proctor DN, Maman SR, et al. Effect of adrenergic agonists on coronary blood flow: a laboratory study in healthy volunteers. Physiological reports. 2016;4(10).

146. Gladwin MT, Shelhamer JH, Schechter AN, Pease-Fye ME, Waclawiw MA, Panza JA, et al. Role of circulating nitrite and S-nitrosohemoglobin in the regulation of regional blood flow in humans. Proceedings of the National Academy of Sciences of the United States of America. 2000;97(21):11482-7.

147. Lundberg JO, Gladwin MT, Ahluwalia A, Benjamin N, Bryan NS, Butler A, et al. Nitrate and nitrite in biology, nutrition and therapeutics. Nature chemical biology. 2009;5(12):865-9.

148. Rassaf T, Bryan NS, Kelm M, Feelisch M. Concomitant presence of N-nitroso and S-nitroso proteins in human plasma. Free radical biology & medicine. 2002;33(11):1590-6.

149. Lundberg JO, Govoni M. Inorganic nitrate is a possible source for systemic generation of nitric oxide. Free radical biology & medicine. 2004;37(3):395-400.

150. Dejam A, Hunter CJ, Pelletier MM, Hsu LL, Machado RF, Shiva S, et al. Erythrocytes are the major intravascular storage sites of nitrite in human blood. Blood. 2005;106(2):734-9.

151. Bryan NS, Rassaf T, Maloney RE, Rodriguez CM, Saijo F, Rodriguez JR, et al. Cellular targets and mechanisms of nitros(yl)ation: an insight into their nature and kinetics in vivo. Proceedings of the National Academy of Sciences of the United States of America. 2004;101(12):4308-13.

152. Hukkanen M, Hughes FJ, Buttery LD, Gross SS, Evans TJ, Seddon S, et al. Cytokine-stimulated expression of inducible nitric oxide synthase by mouse, rat, and human osteoblast-like cells and its functional role in osteoblast metabolic activity. Endocrinology. 1995;136(12):5445-53.

153. Sikkema JM, van Rijn BB, Franx A, Bruinse HW, de Roos R, Stroes ES, et al. Placental superoxide is increased in pre-eclampsia. Placenta. 2001;22(4):304-8.

154. Erzurum SC, Ghosh S, Janocha AJ, Xu W, Bauer S, Bryan NS, et al. Higher blood flow and circulating NO products offset high-altitude hypoxia among Tibetans. Proceedings of the National Academy of Sciences of the United States of America. 2007;104(45):17593-8.

155. Hezel MP, Weitzberg E. The oral microbiome and nitric oxide homoeostasis. Oral diseases. 2015;21(1):7-16.

156. Govers R, Rabelink TJ. Cellular regulation of endothelial nitric oxide synthase. Am J Physiol Renal Physiol. 2001;280(2):F193-206.

157. Abu-Soud HM, Ichimori K, Presta A, Stuehr DJ. Electron transfer, oxygen binding, and nitric oxide feedback inhibition in endothelial nitric-oxide synthase. The Journal of biological chemistry. 2000;275(23):17349-57.

158. Gautier C, van Faassen E, Mikula I, Martasek P, Slama-Schwok A. Endothelial nitric oxide synthase reduces nitrite anions to NO under anoxia. Biochemical and biophysical research communications. 2006;341(3):816-21.

159. Moncada S, Higgs A. The L-arginine-nitric oxide pathway. The New England journal of medicine. 1993;329(27):2002-12.

160. Yoshida K, Kasama K, Kitabatake M, Okuda M, Imai M. Metabolic fate of nitric oxide. Int Arch Occup Environ Health. 1980;46(1):71-7.

161. Mikula I, Durocher S, Martasek P, Mutus B, Slama-Schwok A. Isoform-specific differences in the nitrite reductase activity of nitric oxide synthases under hypoxia. The Biochemical journal. 2009;418(3):673-82.

162. Green DJ, Maiorana A, O'Driscoll G, Taylor R. Effect of exercise training on endothelium-derived nitric oxide function in humans. The Journal of physiology. 2004;561(Pt 1):1-25.

163. Tinker AC, Wallace AV. Selective inhibitors of inducible nitric oxide synthase: potential agents for the treatment of inflammatory diseases? Curr Top Med Chem. 2006;6(2):77-92.

164. Kleinbongard P, Dejam A, Lauer T, Jax T, Kerber S, Gharini P, et al. Plasma nitrite concentrations reflect the degree of endothelial dysfunction in humans. Free radical biology & medicine. 2006;40(2):295-302.

165. Moncada S, Higgs EA. The discovery of nitric oxide and its role in vascular biology. British journal of pharmacology. 2006;147 Suppl 1:S193-201.

166. Furchgott RF, Bhadrakom S. Reactions of strips of rabbit aorta to epinephrine, isopropylarterenol, sodium nitrite and other drugs. The Journal of pharmacology and experimental therapeutics. 1953;108(2):129-43.

167. Walker R. Nitrates, nitrites and N-nitrosocompounds: a review of the occurrence in food and diet and the toxicological implications. Food Addit Contam. 1990;7(6):717-68.

168. Lundberg JO, Weitzberg E, Gladwin MT. The nitrate-nitrite-nitric oxide pathway in physiology and therapeutics. Nat Rev Drug Discov. 2008;7(2):156-67.

169. Hord NG, Tang Y, Bryan NS. Food sources of nitrates and nitrites: the physiologic context for potential health benefits. Am J Clin Nutr. 2009;90(1):1-10.

170. Qu XM, Wu ZF, Pang BX, Jin LY, Qin LZ, Wang SL. From Nitrate to Nitric Oxide: The Role of Salivary Glands and Oral Bacteria. Journal of dental research. 2016;95(13):1452-6.

171. Cole SP, Kharitonov VF, Guiney DG. Effect of nitric oxide on Helicobacter pylori morphology. J Infect Dis. 1999;180(5):1713-7.

172. Sato EF, Choudhury T, Nishikawa T, Inoue M. Dynamic aspect of reactive oxygen and nitric oxide in oral cavity. Journal of clinical biochemistry and nutrition. 2008;42:8-13.

173. Dejam A, Hunter CJ, Tremonti C, Pluta RM, Hon YY, Grimes G, et al. Nitrite infusion in humans and nonhuman primates: endocrine effects, pharmacokinetics, and tolerance formation. Circulation. 2007;116(16):1821-31.

174. Ingram TE, Pinder AG, Bailey DM, Fraser AG, James PE. Low-dose sodium nitrite vasodilates hypoxic human pulmonary vasculature by a means that is not dependent on a simultaneous elevation in plasma nitrite. American journal of physiology Heart and circulatory physiology. 2010;298(2):H331-9.

175. Pluta RM, Oldfield EH, Bakhtian KD, Fathi AR, Smith RK, Devroom HL, et al. Safety and feasibility of long-term intravenous sodium nitrite infusion in healthy volunteers. PLoS One. 2011;6(1):e14504.

176. Hendgen-Cotta UB, Luedike P, Totzeck M, Kropp M, Schicho A, Stock P, et al. Dietary nitrate supplementation improves revascularization in chronic ischemia. Circulation. 2012;126(16):1983-92.

177. Webb AJ, Patel N, Loukogeorgakis S, Okorie M, Aboud Z, Misra S, et al. Acute blood pressure lowering, vasoprotective, and antiplatelet properties of dietary nitrate via bioconversion to nitrite. Hypertension (Dallas, Tex : 1979). 2008;51(3):784-90.

178. Omar SA, Artime E, Webb AJ. A comparison of organic and inorganic nitrates/nitrites. Nitric oxide : biology and chemistry. 2012;26(4):229-40.

179. Hunault CC, van Velzen AG, Sips AJ, Schothorst RC, Meulenbelt J. Bioavailability of sodium nitrite from an aqueous solution in healthy adults. Toxicol Lett. 2009;190(1):48-53.

180. Gago B, Nystrom T, Cavaleiro C, Rocha BS, Barbosa RM, Laranjinha J, et al. The potent vasodilator ethyl nitrite is formed upon reaction of nitrite and ethanol under gastric conditions. Free radical biology & medicine. 2008;45(4):404-12.

181. Doel JJ, Benjamin N, Hector MP, Rogers M, Allaker RP. Evaluation of bacterial nitrate reduction in the human oral cavity. Eur J Oral Sci. 2005;113(1):14-9.

182. Pannala AS, Mani AR, Spencer JP, Skinner V, Bruckdorfer KR, Moore KP, et al. The effect of dietary nitrate on salivary, plasma, and urinary nitrate metabolism in humans. Free radical biology & medicine. 2003;34(5):576-84.

183. Rix PJ, Vick A, Attkins NJ, Barker GE, Bott AW, Alcorn H, Jr., et al. Pharmacokinetics, pharmacodynamics, safety, and tolerability of nebulized sodium nitrite (AIR001) following repeat-dose inhalation in healthy subjects. Clin Pharmacokinet. 2015;54(3):261-72.

184. Pinder AG, James PE. When does low oxygen become hypoxia? Implications for nitrite reduction. Circulation research. 2009;104(3):e25-6.

185. Cheriyan J, Webb AJ, Sarov-Blat L, Elkhawad M, Wallace SM, Maki-Petaja KM, et al. Inhibition of p38 mitogen-activated protein kinase improves nitric oxide-mediated vasodilatation and reduces inflammation in hypercholesterolemia. Circulation. 2011;123(5):515-23.

186. Dietrich HH, Ellsworth ML, Sprague RS, Dacey RG, Jr. Red blood cell regulation of microvascular tone through adenosine triphosphate. American journal of physiology Heart and circulatory physiology. 2000;278(4):H1294-8.

187. Qiu Y, Rizvi A, Tang XL, Manchikalapudi S, Takano H, Jadoon AK, et al. Nitric oxide triggers late preconditioning against myocardial infarction in conscious rabbits. The American journal of physiology. 1997;273(6):H2931-6.

188. Carlsson S, Wiklund NP, Engstrand L, Weitzberg E, Lundberg JO. Effects of pH, nitrite, and ascorbic acid on nonenzymatic nitric oxide generation and bacterial growth in urine. Nitric oxide : biology and chemistry. 2001;5(6):580-6.

189. James PE, Willis GR, Allen JD, Winyard PG, Jones AM. Nitrate pharmacokinetics: Taking note of the difference. Nitric oxide : biology and chemistry. 2015;48:44-50.

190. Larsen FJ, Ekblom B, Sahlin K, Lundberg JO, Weitzberg E. Effects of dietary nitrate on blood pressure in healthy volunteers. The New England journal of medicine. 2006;355(26):2792-3.

191. Kapil V, Milsom AB, Okorie M, Maleki-Toyserkani S, Akram F, Rehman F, et al. Inorganic nitrate supplementation lowers blood pressure in humans: role for nitrite-derived NO. Hypertension (Dallas, Tex : 1979). 2010;56(2):274-81.

192. Sobko T, Marcus C, Govoni M, Kamiya S. Dietary nitrate in Japanese traditional foods lowers diastolic blood pressure in healthy volunteers. Nitric oxide : biology and chemistry. 2010;22(2):136-40.

193. Markos F, Ruane O'Hora T, Noble MI. What is the mechanism of flow-mediated arterial dilatation. Clinical and experimental pharmacology & physiology. 2013;40(8):489-94.

194. Hasan R, Jaggar JH. KV channel trafficking and control of vascular tone. Microcirculation (New York, NY : 1994). 2018;25(1).

195. Segal SS. Regulation of blood flow in the microcirculation. Microcirculation (New York, NY : 1994). 2005;12(1):33-45.

196. Hanks SK, Hunter T. Protein kinases 6. The eukaryotic protein kinase superfamily: kinase (catalytic) domain structure and classification. FASEB journal : official publication of the Federation of American Societies for Experimental Biology. 1995;9(8):576-96.

197. Cremers CM, Jakob U. Oxidant sensing by reversible disulfide bond formation. The Journal of biological chemistry. 2013;288(37):26489-96.

198. Burgoyne JR, Madhani M, Cuello F, Charles RL, Brennan JP, Schroder E, et al. Cysteine redox sensor in PKGIa enables oxidant-induced activation. Science. 2007;317(5843):1393-7.

199. Prysyazhna O, Rudyk O, Eaton P. Single atom substitution in mouse protein kinase G eliminates oxidant sensing to cause hypertension. Nature medicine. 2012;18(2):286-90.

200. Zhang DX, Borbouse L, Gebremedhin D, Mendoza SA, Zinkevich NS, Li R, et al. H2O2-induced dilation in human coronary arterioles: role of protein kinase G dimerization and large-conductance Ca2+-activated K+ channel activation. Circulation research. 2012;110(3):471-80.

201. Rudyk O, Prysyazhna O, Burgoyne JR, Eaton P. Nitroglycerin fails to lower blood pressure in redox-dead Cys42Ser PKG1alpha knock-in mouse. Circulation. 2012;126(3):287-95.

202. Rudyk O, Phinikaridou A, Prysyazhna O, Burgoyne JR, Botnar RM, Eaton P. Protein kinase G oxidation is a major cause of injury during sepsis. Proceedings of the National Academy of Sciences of the United States of America. 2013;110(24):9909-13.

203. Scotcher J, Prysyazhna O, Boguslavskyi A, Kistamas K, Hadgraft N, Martin ED, et al. Disulfide-activated protein kinase G Ialpha regulates cardiac diastolic relaxation and fine-tunes the Frank-Starling response. Nature communications. 2016;7:13187.

204. Burgoyne JR, Prysyazhna O, Richards DA, Eaton P. Proof of Principle for a Novel Class of Antihypertensives That Target the Oxidative Activation of PKG Ialpha (Protein Kinase G Ialpha). Hypertension (Dallas, Tex : 1979). 2017;70(3):577-86.

205. Nakamura T, Zhu G, Ranek MJ, Kokkonen-Simon K, Zhang M, Kim GE, et al. Prevention of PKG-1alpha Oxidation Suppresses Antihypertrophic/Antifibrotic Effects From PDE5 Inhibition but not sGC Stimulation. Circulation Heart failure. 2018;11(3):e004740.

206. Cortese-Krott MM, Fernandez BO, Kelm M, Butler AR, Feelisch M. On the chemical biology of the nitrite/sulfide interaction. Nitric oxide : biology and chemistry. 2015;46:14-24.

207. Bailey TS, Henthorn HA, Pluth MD. The Intersection of NO and H2S: Persulfides Generate NO from Nitrite through Polysulfide Formation. Inorganic chemistry. 2016;55(24):12618-25.

208. Cortese-Krott MM, Pullmann D, Feelisch M. Nitrosopersulfide (SSNO(-)) targets the Keap-1/Nrf2 redox system. Pharmacological research. 2016;113(Pt A):490-9.

209. Ignarro LJ, Lippton H, Edwards JC, Baricos WH, Hyman AL, Kadowitz PJ, et al. Mechanism of vascular smooth muscle relaxation by organic nitrates, nitrites, nitroprusside and nitric oxide: evidence for the involvement of S-nitrosothiols as active intermediates. The Journal of pharmacology and experimental therapeutics. 1981;218(3):739-49.

210. Stamler JS. Redox signaling: nitrosylation and related target interactions of nitric oxide. Cell. 1994;78(6):931-6.

211. Gow AJ, Stamler JS. Reactions between nitric oxide and haemoglobin under physiological conditions. Nature. 1998;391(6663):169-73.

212. Robinson JM, Lancaster JR, Jr. Hemoglobin-mediated, hypoxia-induced vasodilation via nitric oxide: mechanism(s) and physiologic versus pathophysiologic relevance. Am J Respir Cell Mol Biol. 2005;32(4):257-61.

213. Helms C, Kim-Shapiro DB. Hemoglobin-mediated nitric oxide signaling. Free radical biology & medicine. 2013;61:464-72.

214. Patel D, Lakhkar A, Wolin MS. Redox Mechanisms Influencing cGMP Signaling in Pulmonary Vascular Physiology and Pathophysiology. Adv Exp Med Biol. 2017;967:227-40.

215. Lima B, Forrester MT, Hess DT, Stamler JS. S-nitrosylation in cardiovascular signaling. Circulation research. 2010;106(4):633-46.

216. Schulman IH, Hare JM. Regulation of cardiovascular cellular processes by S-nitrosylation. Biochim Biophys Acta. 2012;1820(6):752-62.

217. Sun J, Steenbergen C, Murphy E. S-nitrosylation: NO-related redox signaling to protect against oxidative stress. Antioxidants & redox signaling. 2006;8(9-10):1693-705.

218. Kohr MJ, Sun J, Aponte A, Wang G, Gucek M, Murphy E, et al. Simultaneous measurement of protein oxidation and S-nitrosylation during preconditioning and ischemia/reperfusion injury with resin-assisted capture. Circulation research. 2011;108(4):418-26.

219. Murphy E, Kohr M, Sun J, Nguyen T, Steenbergen C. S-nitrosylation: a radical way to protect the heart. J Mol Cell Cardiol. 2012;52(3):568-77.

220. Sayed N, Kim DD, Fioramonti X, Iwahashi T, Durán WN, Beuve A. Nitroglycerin-induced S-nitrosylation and desensitization of soluble guanylyl cyclase contribute to nitrate tolerance. Circulation research. 2008;103(6):606-14.

221. Stomberski CT, Hess DT, Stamler JS. Protein S-Nitrosylation: Determinants of Specificity and Enzymatic Regulation of S-Nitrosothiol-Based Signaling. Antioxidants & redox signaling. 2019;30(10):1331-51.

222. Marozkina N, Gaston B. An Update on Thiol Signaling: S-Nitrosothiols, Hydrogen Sulfide and a Putative Role for Thionitrous Acid. Antioxidants (Basel). 2020;9(3).

223. Ward J. Oxygen delivery and demand. Surgery (Oxford). 2006;24(10):354-60.

224. Butler AR, Feelisch M. Therapeutic uses of inorganic nitrite and nitrate: from the past to the future. Circulation. 2008;117(16):2151-9.

225. Mazzone M, Carmeliet P. Drug discovery: a lifeline for suffocating tissues. Nature. 2008;453(7199):1194-5.

226. Kaelin WG, Jr. The von Hippel-Lindau protein, HIF hydroxylation, and oxygen sensing. Biochemical and biophysical research communications. 2005;338(1):627-38.

227. Haase VH. Hypoxia-inducible factors in the kidney. Am J Physiol Renal Physiol. 2006;291(2):F271-81.

228. Khanna S, Roy S, Maurer M, Ratan RR, Sen CK. Oxygen-sensitive reset of hypoxia-inducible factor transactivation response: prolyl hydroxylases tune the biological normoxic set point. Free radical biology & medicine. 2006;40(12):2147-54.

229. van Faassen EE, Bahrami S, Feelisch M, Hogg N, Kelm M, Kim-Shapiro DB, et al. Nitrite as regulator of hypoxic signaling in mammalian physiology. Med Res Rev. 2009;29(5):683-741.

230. Thomas SR, Pratt RG, Millard RW, Samaratunga RC, Shiferaw Y, McGoron AJ, et al. In vivo PO2 imaging in the porcine model with perfluorocarbon F-19 NMR at low field. Magn Reson Imaging. 1996;14(1):103-14.

231. Brezis M, Rosen S. Hypoxia of the renal medulla--its implications for disease. The New England journal of medicine. 1995;332(10):647-55.

232. Li J, French B, Wu Y, Vanketesh R, Montgomery R, Bardag-Gorce F, et al. Liver hypoxia and lack of recovery after reperfusion at high blood alcohol levels in the intragastric feeding model of alcohol liver disease. Exp Mol Pathol. 2004;77(3):184-92.

233. James PE, Bacic G, Grinberg OY, Goda F, Dunn JF, Jackson SK, et al. Endotoxin-induced changes in intrarenal pO2, measured by in vivo electron paramagnetic resonance oximetry and magnetic resonance imaging. Free radical biology & medicine. 1996;21(1):25-34.

234. Tsai AG, Johnson PC, Intaglietta M. Oxygen gradients in the microcirculation. Physiological reviews. 2003;83(3):933-63.

235. Bell M, Thake CD, Wolff CB. Effect of inspiration of 12% O_2 (balance N_2) on cardiac output, respiration, oxygen saturation, and oxygen delivery. Adv Exp Med Biol. 2011;701:327-32.

236. Hellwig-Burgel T, Stiehl DP, Wagner AE, Metzen E, Jelkmann W. Review: hypoxia-inducible factor-1 (HIF-1): a novel transcription factor in immune reactions. J Interferon Cytokine Res. 2005;25(6):297-310.

237. Maher AR, Milsom AB, Gunaruwan P, Abozguia K, Ahmed I, Weaver RA, et al. Hypoxic modulation of exogenous nitrite-induced vasodilation in humans. Circulation. 2008;117(5):670-7.

238. Feigl B, Zele AJ, Stewart IB. Mild systemic hypoxia and photopic visual field sensitivity. Acta Ophthalmol. 2011;89(2):e199-204.

239. Palkovits S, Told R, Schmidl D, Boltz A, Napora KJ, Lasta M, et al. Regulation of retinal oxygen metabolism in humans during graded hypoxia. American journal of physiology Heart and circulatory physiology. 2014;307(10):H1412-8.

240. Keymel S, Schueller B, Sansone R, Wagstaff R, Steiner S, Kelm M, et al. Oxygen dependence of endothelium-dependent vasodilation: importance in chronic obstructive pulmonary disease. Arch Med Sci. 2018;14(2):297-306.

241. Aamand R, Dalsgaard T, Jensen FB, Simonsen U, Roepstorff A, Fago A. Generation of nitric oxide from nitrite by carbonic anhydrase: a possible link between metabolic activity and vasodilation. American journal of physiology Heart and circulatory physiology. 2009;297(6):H2068-74.

242. Philippot L. Denitrifying genes in bacterial and Archaeal genomes. Biochim Biophys Acta. 2002;1577(3):355-76.

243. Zweier JL, Li H, Samouilov A, Liu X. Mechanisms of nitrite reduction to nitric oxide in the heart and vessel wall. Nitric oxide : biology and chemistry. 2010;22(2):83-90.

244. Amdahl MB, DeMartino AW, Gladwin MT. Inorganic nitrite bioactivation and role in physiological signaling and therapeutics. Biol Chem. 2019;401(1):201-11.

245. Nohl H, Staniek K, Sobhian B, Bahrami S, Redl H, Kozlov AV. Mitochondria recycle nitrite back to the bioregulator nitric monoxide. Acta Biochim Pol. 2000;47(4):913-21.

246. Castello PR, David PS, McClure T, Crook Z, Poyton RO. Mitochondrial cytochrome oxidase produces nitric oxide under hypoxic conditions: implications for oxygen sensing and hypoxic signaling in eukaryotes. Cell Metab. 2006;3(4):277-87.

247. Totzeck M, Hendgen-Cotta UB, Luedike P, Berenbrink M, Klare JP, Steinhoff HJ, et al. Nitrite regulates hypoxic vasodilation via myoglobin-dependent nitric oxide generation. Circulation. 2012;126(3):325-34.

248. Larsen FJ, Weitzberg E, Lundberg JO, Ekblom B. Effects of dietary nitrate on oxygen cost during exercise. Acta Physiol (Oxf). 2007;191(1):59-66.

249. Webb A, Bond R, McLean P, Uppal R, Benjamin N, Ahluwalia A. Reduction of nitrite to nitric oxide during ischemia protects against myocardial ischemia-reperfusion damage. Proceedings of the National Academy of Sciences of the United States of America. 2004;101(37):13683-8.

250. Dijkers PF, O'Farrell PH. Dissection of a hypoxia-induced, nitric oxide-mediated signaling cascade. Mol Biol Cell. 2009;20(18):4083-90.

251. Basu S, Azarova NA, Font MD, King SB, Hogg N, Gladwin MT, et al. Nitrite reductase activity of cytochrome c. The Journal of biological chemistry. 2008;283(47):32590-7.

252. Tischner R, Planchet E, Kaiser WM. Mitochondrial electron transport as a source for nitric oxide in the unicellular green alga Chlorella sorokiniana. FEBS Lett. 2004;576(1-2):151-5.

253. Crawford JH, Isbell TS, Huang Z, Shiva S, Chacko BK, Schechter AN, et al. Hypoxia, red blood cells, and nitrite regulate NO-dependent hypoxic vasodilation. Blood. 2006;107(2):566-74.

254. Li H, Cui H, Kundu TK, Alzawahra W, Zweier JL. Nitric oxide production from nitrite occurs primarily in tissues not in the blood: critical role of xanthine oxidase and aldehyde oxidase. The Journal of biological chemistry. 2008;283(26):17855-63.

255. Li H, Samouilov A, Liu X, Zweier JL. Characterization of the effects of oxygen on xanthine oxidase-mediated nitric oxide formation. The Journal of biological chemistry. 2004;279(17):16939-46.

256. Ghosh SM, Kapil V, Fuentes-Calvo I, Bubb KJ, Pearl V, Milsom AB, et al. Enhanced vasodilator activity of nitrite in hypertension: critical role for erythrocytic xanthine oxidoreductase and translational potential. Hypertension (Dallas, Tex : 1979). 2013;61(5):1091-102.

257. Hendgen-Cotta UB, Merx MW, Shiva S, Schmitz J, Becher S, Klare JP, et al. Nitrite reductase activity of myoglobin regulates respiration and cellular viability in myocardial ischemia-reperfusion injury. Proceedings of the National Academy of Sciences of the United States of America. 2008;105(29):10256-61.

258. Ormerod JO, Ashrafian H, Maher AR, Arif S, Steeples V, Born GV, et al. The role of vascular myoglobin in nitrite-mediated blood vessel relaxation. Cardiovascular research. 2011;89(3):560-5.

259. Zweier JL, Wang P, Samouilov A, Kuppusamy P. Enzyme-independent formation of nitric oxide in biological tissues. Nature medicine. 1995;1(8):804-9.

260. Risbano MG, Kanias T, Triulzi D, Donadee C, Barge S, Badlam J, et al. Effects of Aged Stored Autologous Red Blood Cells on Human Endothelial Function. American journal of respiratory and critical care medicine. 2015;192(10):1223-33.

261. Kim-Shapiro DB, Gladwin MT. Mechanisms of nitrite bioactivation. Nitric oxide : biology and chemistry. 2014;38:58-68.

262. Doyle MP, Pickering RA, DeWeert TM, Hoekstra JW, Pater D. Kinetics and mechanism of the oxidation of human deoxyhemoglobin by nitrites. The Journal of biological chemistry. 1981;256(23):12393-8.

263. Gladwin MT, Kim-Shapiro DB. The functional nitrite reductase activity of the heme-globins. Blood. 2008;112(7):2636-47.

264. Nagababu E, Ramasamy S, Rifkind JM. Intermediates detected by visible spectroscopy during the reaction of nitrite with deoxyhemoglobin: the effect of nitrite concentration and diphosphoglycerate. Biochemistry. 2007;46(41):11650-9.

265. Salgado MT, Nagababu E, Rifkind JM. Quantification of intermediates formed during the reduction of nitrite by deoxyhemoglobin. The Journal of biological chemistry. 2009;284(19):12710-8.

266. Huang Z, Shiva S, Kim-Shapiro DB, Patel RP, Ringwood LA, Irby CE, et al. Enzymatic function of hemoglobin as a nitrite reductase that produces NO under allosteric control. J Clin Invest. 2005;115(8):2099-107.

267. Joshi MS, Ferguson TB, Jr., Han TH, Hyduke DR, Liao JC, Rassaf T, et al. Nitric oxide is consumed, rather than conserved, by reaction with oxyhemoglobin under physiological conditions. Proceedings of the National Academy of Sciences of the United States of America. 2002;99(16):10341-6.

268. Reiter CD, Wang X, Tanus-Santos JE, Hogg N, Cannon RO, 3rd, Schechter AN, et al. Cell-free hemoglobin limits nitric oxide bioavailability in sickle-cell disease. Nature medicine. 2002;8(12):1383-9.

269. Cosby K, Partovi KS, Crawford JH, Patel RP, Reiter CD, Martyr S, et al. Nitrite reduction to nitric oxide by deoxyhemoglobin vasodilates the human circulation. Nature medicine. 2003;9(12):1498-505.

270. Dalsgaard T, Simonsen U, Fago A. Nitrite-dependent vasodilation is facilitated by hypoxia and is independent of known NO-generating nitrite reductase activities. American journal of physiology Heart and circulatory physiology. 2007;292(6):H3072-8.

271. He X, Azarov I, Jeffers A, Presley T, Richardson J, King SB, et al. The potential of Angeli's salt to decrease nitric oxide scavenging by plasma hemoglobin. Free radical biology & medicine. 2008;44(7):1420-32.

272. Kim-Shapiro DB, Lee J, Gladwin MT. Storage lesion: role of red blood cell breakdown. Transfusion. 2011;51(4):844-51.

273. Solomon SB, Bellavia L, Sweeney D, Piknova B, Perlegas A, Helms CC, et al. Angeli's salt counteracts the vasoactive effects of elevated plasma hemoglobin. Free radical biology & medicine. 2012;53(12):2229-39.

274. Donadee C, Raat NJ, Kanias T, Tejero J, Lee JS, Kelley EE, et al. Nitric oxide scavenging by red blood cell microparticles and cell-free hemoglobin as a mechanism for the red cell storage lesion. Circulation. 2011;124(4):465-76.

275. Vamvakas EC, Blajchman MA. Transfusion-related mortality: the ongoing risks of allogeneic blood transfusion and the available strategies for their prevention. Blood. 2009;113(15):3406-17.

276. Koch CG, Li L, Sessler DI, Figueroa P, Hoeltge GA, Mihaljevic T, et al. Duration of red-cell storage and complications after cardiac surgery. The New England journal of medicine. 2008;358(12):1229-39.

277. Pettila V, Westbrook AJ, Nichol AD, Bailey MJ, Wood EM, Syres G, et al. Age of red blood cells and mortality in the critically ill. Critical care (London, England). 2011;15(2):R116.

278. Wang D, Sun J, Solomon SB, Klein HG, Natanson C. Transfusion of older stored blood and risk of death: a meta-analysis. Transfusion. 2012;52(6):1184-95.

279. Takase B, Uehata A, Akima T, Nagai T, Nishioka T, Hamabe A, et al. Endothelium-dependent flow-mediated vasodilation in coronary and brachial arteries in suspected coronary artery disease. The American journal of cardiology. 1998;82(12):1535-9, a7-8.

280. Omar SA, Fok H, Tilgner KD, Nair A, Hunt J, Jiang B, et al. Paradoxical normoxia-dependent selective actions of inorganic nitrite in human muscular conduit arteries and related selective actions on central blood pressures. Circulation. 2015;131(4):381-9; discussion 9.

281. Zeiher AM, Drexler H, Wollschläger H, Just H. Endothelial dysfunction of the coronary microvasculature is associated with coronary blood flow regulation in patients with early atherosclerosis. Circulation. 1991;84(5):1984-92.

282. Berne RM. REGULATION OF CORONARY BLOOD FLOW. Physiological reviews. 1964;44:1-29.

283. Raphael CE, Cooper R, Parker KH, Collinson J, Vassiliou V, Pennell DJ, et al. Mechanisms of Myocardial Ischemia in Hypertrophic Cardiomyopathy: Insights From Wave Intensity Analysis and Magnetic Resonance. Journal of the American College of Cardiology. 2016;68(15):1651-60.

284. Benchimol A, Desser KB, Gartlan JL, Jr. Effects of amyl nitrite on coronary arterial blood flow velocity in man. The American journal of cardiology. 1972;30(4):327-33.

285. Benchimol A, Desser KB, Raizada V. Effects of amyl nitrite on phasic aortocoronary bypass graft blood velocity in man. American heart journal. 1977;93(5):592-5.

286. Keegan J, Raphael CE, Parker K, Simpson RM, Strain S, de Silva R, et al. Validation of high temporal resolution spiral phase velocity mapping of temporal patterns of left and right coronary artery blood flow against Doppler guidewire. Journal of cardiovascular magnetic resonance : official journal of the Society for Cardiovascular Magnetic Resonance. 2015;17:85.

287. O'Gallagher K, Khan F, Omar SA, Kalra S, Danson E, Cabaco AR, et al. Inorganic Nitrite Selectively Dilates Epicardial Coronary Arteries. Journal of the American College of Cardiology. 2018;71(3):363-4.

288. Nossaman VE, Nossaman BD, Kadowitz PJ. Nitrates and nitrites in the treatment of ischemic cardiac disease. Cardiology in review. 2010;18(4):190-7.

289. Petersson J, Phillipson M, Jansson EA, Patzak A, Lundberg JO, Holm L. Dietary nitrate increases gastric mucosal blood flow and mucosal defense. Am J Physiol Gastrointest Liver Physiol. 2007;292(3):G718-24.

290. Rosen PJ, Johnson C, McGehee WG, Beutler E. Failure of methylene blue treatment in toxic methemoglobinemia. Association with glucose-6-phosphate dehydrogenase deficiency. Ann Intern Med. 1971;75(1):83-6.

291. Hultquist DE, Xu F, Quandt KS, Shlafer M, Mack CP, Till GO, et al. Evidence that NADPH-dependent methemoglobin reductase and administered riboflavin protect tissues from oxidative injury. Am J Hematol. 1993;42(1):13-8.

292. van Wijk R, van Solinge WW. The energy-less red blood cell is lost: erythrocyte enzyme abnormalities of glycolysis. Blood. 2005;106(13):4034-42.

293. Scanlan RA. Formation and occurrence of nitrosamines in food. Cancer Res. 1983;43(5 Suppl):2435s-40s.

294. Honikel KO. The use and control of nitrate and nitrite for the processing of meat products. Meat Sci. 2008;78(1-2):68-76.

295. Lijinsky W, Epstein SS. Nitrosamines as environmental carcinogens. Nature. 1970;225(5227):21-3.

296. Hill MJ, Hawksworth G, Tattersall G. Bacteria, nitrosamines and cancer of the stomach. Br J Cancer. 1973;28(6):562-7.

297. Bartsch H, Montesano R. Relevance of nitrosamines to human cancer. Carcinogenesis. 1984;5(11):1381-93.

298. Hoffmann D, Hecht SS. Nicotine-derived N-nitrosamines and tobacco-related cancer: current status and future directions. Cancer Res. 1985;45(3):935-44.

299. Jakszyn P, Gonzalez CA. Nitrosamine and related food intake and gastric and oesophageal cancer risk: a systematic review of the epidemiological evidence. World J Gastroenterol. 2006;12(27):4296-303.

300. Bryan NS, Alexander DD, Coughlin JR, Milkowski AL, Boffetta P. Ingested nitrate and nitrite and stomach cancer risk: an updated review. Food Chem Toxicol. 2012;50(10):3646-65.

301. Buckland G, Agudo A, Luján L, Jakszyn P, Bueno-de-Mesquita HB, Palli D, et al. Adherence to a Mediterranean diet and risk of gastric adenocarcinoma within the European Prospective Investigation into Cancer and Nutrition (EPIC) cohort study. Am J Clin Nutr. 2010;91(2):381-90.

302. Praud D, Bertuccio P, Bosetti C, Turati F, Ferraroni M, La Vecchia C. Adherence to the Mediterranean diet and gastric cancer risk in Italy. Int J Cancer. 2014;134(12):2935-41.

303. Hernández-Ramírez RU, Galván-Portillo MV, Ward MH, Agudo A, González CA, Oñate-Ocaña LF, et al. Dietary intake of polyphenols, nitrate and nitrite and gastric cancer risk in Mexico City. Int J Cancer. 2009;125(6):1424-30.

304. Elkayam U, Mehra A, Shotan A, Osprzega E. Possible mechanisms of nitrate tolerance. The American journal of cardiology. 1992;70(17):49G-53G; discussion G-4G.

305. Ingram TE, Fraser AG, Bleasdale RA, Ellins EA, Margulescu AD, Halcox JP, et al. Low-dose sodium nitrite attenuates myocardial ischemia and vascular ischemia-reperfusion injury in human models. Journal of the American College of Cardiology. 2013;61(25):2534-41.

306. Siddiqi N, Neil C, Bruce M, MacLennan G, Cotton S, Papadopoulou S, et al. Intravenous sodium nitrite in acute ST-elevation myocardial infarction: a randomized controlled trial (NIAMI). European heart journal. 2014;35(19):1255-62.

307. Jones DA, Pellaton C, Velmurugan S, Rathod KS, Andiapen M, Antoniou S, et al. Randomized phase 2 trial of intracoronary nitrite during acute myocardial infarction. Circulation research. 2015;116(3):437-47.

308. Dezfulian C, Olsufka M, Fly D, Scruggs S, Do R, Maynard C, et al. Hemodynamic effects of IV sodium nitrite in hospitalized comatose survivors of out of hospital cardiac arrest. Resuscitation. 2018;122:106-12.

309. Munzel T, Daiber A. Inorganic nitrite and nitrate in cardiovascular therapy: A better alternative to organic nitrates as nitric oxide donors? Vascular pharmacology. 2018;102:1-10.

310. DeMartino AW, Kim-Shapiro DB, Patel RP, Gladwin MT. Nitrite and nitrate chemical biology and signalling. British journal of pharmacology. 2019;176(2):228-45.

311. Madhani M, Scotland RS, MacAllister RJ, Hobbs AJ. Vascular natriuretic peptide receptor-linked particulate guanylate cyclases are modulated by nitric oxide-cyclic GMP signalling. British journal of pharmacology. 2003;139(7):1289-96.

312. Arif S, Borgognone A, Lin EL, O'Sullivan AG, Sharma V, Drury NE, et al. Role of aldehyde dehydrogenase in hypoxic vasodilator effects of nitrite in rats and humans. British journal of pharmacology. 2015;172(13):3341-52.

313. Madhani M, Okorie M, Hobbs AJ, MacAllister RJ. Reciprocal regulation of human soluble and particulate guanylate cyclases in vivo. British journal of pharmacology. 2006;149(6):797-801.

314. Bryan NS, Fernandez BO, Bauer SM, Garcia-Saura MF, Milsom AB, Rassaf T, et al. Nitrite is a signaling molecule and regulator of gene expression in mammalian tissues. Nature chemical biology. 2005;1(5):290-7.

315. Perlman DH, Bauer SM, Ashrafian H, Bryan NS, Garcia-Saura MF, Lim CC, et al. Mechanistic insights into nitrite-induced cardioprotection using an integrated metabolomic/proteomic approach. Circulation research. 2009;104(6):796-804.

316. ICH. ICH E6 Good Clinical Practice (GCP) Guideline 2016 [Available from: https://www.ich.org/products/guidelines/efficacy/efficacy-single/article/integrated-addendum-good-clinical-practice.html.

317. NHSBT. Blood donation guidelines 2019 [Available from: https://www.blood.co.uk/who-can-give-blood/.

318. Oldfield EH, Loomba JJ, Monteith SJ, Crowley RW, Medel R, Gress DR, et al. Safety and pharmacokinetics of sodium nitrite in patients with subarachnoid hemorrhage: a phase IIa study. Journal of neurosurgery. 2013;119(3):634-41.

319. Walsh SR, Tang T, Sadat U, Dutka DP, Gaunt ME. Cardioprotection by remote ischaemic preconditioning. Br J Anaesth. 2007;99(5):611-6.

320. Hon YY, Sun H, Dejam A, Gladwin MT. Characterization of erythrocytic uptake and release and disposition pathways of nitrite, nitrate, methemoglobin, and iron-nitrosyl hemoglobin in the human circulation. Drug Metab Dispos. 2010;38(10):1707-13.

321. Donato M, Goyeneche MA, Garces M, Marchini T, Pérez V, Del Mauro J, et al. Myocardial triggers involved in activation of remote ischaemic preconditioning. Experimental physiology. 2016;101(6):708-16.

322. May JM, Qu ZC, Xia L, Cobb CE. Nitrite uptake and metabolism and oxidant stress in human erythrocytes. Am J Physiol Cell Physiol. 2000;279(6):C1946-54.

323. Maher AR, Arif S, Madhani M, Abozguia K, Ahmed I, Fernandez BO, et al. Impact of chronic congestive heart failure on pharmacokinetics and vasomotor effects of infused nitrite. British journal of pharmacology. 2013;169(3):659-70.

324. Benjamin N, Calver A, Collier J, Robinson B, Vallance P, Webb D. Measuring forearm blood flow and interpreting the responses to drugs and mediators. Hypertension (Dallas, Tex : 1979). 1995;25(5):918-23.

325. Kibbe M, Billiar T, Tzeng E. Inducible nitric oxide synthase and vascular injury. Cardiovascular research. 1999;43(3):650-7.

326. Severinghaus JW. Simple, accurate equations for human blood O2 dissociation computations. Journal of applied physiology: respiratory, environmental and exercise physiology. 1979;46(3):599-602.

327. Brakkee AJ, Vendrik AJ. Strain-gauge plethysmography; theoretical and practical notes on a new design. Journal of applied physiology. 1966;21(2):701-4.

328. Wilkinson IB, Webb DJ. Venous occlusion plethysmography in cardiovascular research: methodology and clinical applications. British journal of clinical pharmacology. 2001;52(6):631-46.

329. Sigdell JE. A critical review of the theory of the mercury strain-gauge plethysmograph. Medical & biological engineering. 1969;7(4):365-71.

330. Wang X, Tanus-Santos JE, Reiter CD, Dejam A, Shiva S, Smith RD, et al. Biological activity of nitric oxide in the plasmatic compartment. Proceedings of the National Academy of Sciences of the United States of America. 2004;101(31):11477-82.

331. Raphael CE, Keegan J, Parker KH, Simpson R, Collinson J, Vassiliou V, et al. Feasibility of cardiovascular magnetic resonance derived coronary wave intensity analysis. Journal of cardiovascular magnetic resonance : official journal of the Society for Cardiovascular Magnetic Resonance. 2016;18(1):93.

332. Schar M, Soleimanifard S, Bonanno G, Yerly J, Hays AG, Weiss RG. Precision and accuracy of cross-sectional area measurements used to measure coronary endothelial function with spiral MRI. Magnetic resonance in medicine. 2019;81(1):291-302.

333. Jackson JI, Meyer CH, Nishimura DG, Macovski A. Selection of a convolution function for Fourier inversion using gridding [computerised tomography application]. IEEE transactions on medical imaging. 1991;10(3):473-8.

334. Brandts A, Roes SD, Doornbos J, Weiss RG, de Roos A, Stuber M, et al. Right coronary artery flow velocity and volume assessment with spiral K-space sampled breathhold velocity-encoded MRI at 3 tesla: accuracy and reproducibility. Journal of magnetic resonance imaging : JMRI. 2010;31(5):1215-23.

335. Keegan J, Gatehouse PD, Yang GZ, Firmin DN. Spiral phase velocity mapping of left and right coronary artery blood flow: correction for through-plane motion using selective fat-only excitation. Journal of magnetic resonance imaging : JMRI. 2004;20(6):953-60.

336. Popović ZB, Thomas JD. Assessing observer variability: a user's guide. Cardiovasc Diagn Ther. 2017;7(3):317-24.

337. Sakuma H, Blake LM, Amidon TM, O'Sullivan M, Szolar DH, Furber AP, et al. Coronary flow reserve: noninvasive measurement in humans with breath-hold velocity-encoded cine MR imaging. Radiology. 1996;198(3):745-50.

338. Zhang Z, Naughton D, Winyard PG, Benjamin N, Blake DR, Symons MC. Generation of nitric oxide by a nitrite reductase activity of xanthine oxidase: a potential

pathway for nitric oxide formation in the absence of nitric oxide synthase activity. Biochemical and biophysical research communications. 1998;249(3):767-72.

339. Feelisch M, Fernandez BO, Bryan NS, Garcia-Saura MF, Bauer S, Whitlock DR, et al. Tissue processing of nitrite in hypoxia: an intricate interplay of nitric oxide-generating and -scavenging systems. The Journal of biological chemistry. 2008;283(49):33927-34.

340. Stamler JS, Lamas S, Fang FC. Nitrosylation. the prototypic redox-based signaling mechanism. Cell. 2001;106(6):675-83.

341. Burgoyne JR, Prysyazhna O, Rudyk O, Eaton P. cGMP-dependent activation of protein kinase G precludes disulfide activation: implications for blood pressure control. Hypertension (Dallas, Tex : 1979). 2012;60(5):1301-8.

342. Stubbert D, Prysyazhna O, Rudyk O, Scotcher J, Burgoyne JR, Eaton P. Protein kinase G Iα oxidation paradoxically underlies blood pressure lowering by the reductant hydrogen sulfide. Hypertension (Dallas, Tex : 1979). 2014;64(6):1344-51.

343. Krych-Madej J, Gebicka L. Interactions of nitrite with catalase: Enzyme activity and reaction kinetics studies. J Inorg Biochem. 2017;171:10-7.

344. Titov VY, Petrenko YM. Nitrite-catalase interaction as an important element of nitrite toxicity. Biochemistry (Mosc). 2003;68(6):627-33.

345. Ormerod JO, Arif S, Mukadam M, Evans JD, Beadle R, Fernandez BO, et al. Short-term intravenous sodium nitrite infusion improves cardiac and pulmonary hemodynamics in heart failure patients. Circulation Heart failure. 2015;8(3):565-71.

346. Casey DP, Beck DT, Braith RW. Systemic plasma levels of nitrite/nitrate (NOx) reflect brachial flow-mediated dilation responses in young men and women. Clinical and experimental pharmacology & physiology. 2007;34(12):1291-3.

347. Lauer T, Preik M, Rassaf T, Strauer BE, Deussen A, Feelisch M, et al. Plasma nitrite rather than nitrate reflects regional endothelial nitric oxide synthase activity but lacks intrinsic vasodilator action. Proceedings of the National Academy of Sciences of the United States of America. 2001;98(22):12814-9.

348. Lauer T, Heiss C, Balzer J, Kehmeier E, Mangold S, Leyendecker T, et al. Age-dependent endothelial dysfunction is associated with failure to increase plasma nitrite in response to exercise. Basic research in cardiology. 2008;103(3):291-7.

349. Weisbrod CJ, Eastwood PR, O'Driscoll G, Walsh JH, Best M, Halliwill JR, et al. Vasomotor responses to hypoxia in type 2 diabetes. Diabetes. 2004;53(8):2073-8.

350. Kulandavelu S, Balkan W, Hare JM. Regulation of oxygen delivery to the body via hypoxic vasodilation. Proceedings of the National Academy of Sciences of the United States of America. 2015;112(20):6254-5.

351. Thomas DD, Liu X, Kantrow SP, Lancaster JR, Jr. The biological lifetime of nitric oxide: implications for the perivascular dynamics of NO and O2. Proceedings of the National Academy of Sciences of the United States of America. 2001;98(1):355-60.

352. Umbrello M, Dyson A, Feelisch M, Singer M. The key role of nitric oxide in hypoxia: hypoxic vasodilation and energy supply-demand matching. Antioxidants & redox signaling. 2013;19(14):1690-710.

353. Freeman R, Wieling W, Axelrod FB, Benditt DG, Benarroch E, Biaggioni I, et al. Consensus statement on the definition of orthostatic hypotension, neurally mediated syncope and the postural tachycardia syndrome. Clin Auton Res. 2011;21(2):69-72.

354. Gelman A. Don't Calculate Post-hoc Power Using Observed Estimate of Effect Size. Ann Surg. 2019;269(1):e9-e10.

355. Matcham J, McDermott MP, Lang AE. GDNF in Parkinson's disease: the perils of post-hoc power. J Neurosci Methods. 2007;163(2):193-6.

356. Levine M, Ensom MH. Post hoc power analysis: an idea whose time has passed? Pharmacotherapy. 2001;21(4):405-9.

357. Dziak JJ, Dierker LC, Abar B. The Interpretation of Statistical Power after the Data have been Gathered. Curr Psychol. 2020;39(3):870-7.

358. Bowen DJ, Kreuter M, Spring B, Cofta-Woerpel L, Linnan L, Weiner D, et al. How we design feasibility studies. Am J Prev Med. 2009;36(5):452-7.

359. Marchetti GV, Merlo L, Antognetti RM. THE EFFECTS OF NITROGLYCERIN ON THE CORONARY BLOOD FLOW AND OXYGEN CONSUMPTION OF THE MYOCARDIUM IN ANESTHETIZED DOGS. The American journal of cardiology. 1964;13:51-7.

360. Grayson J, Irvine M, Parratt JR. The effects of amyl nitrite inhalation on myocardial blood flow and metabolic heat production. Br J Pharmacol Chemother. 1967;30(3):488-96.

361. Furchgott RF. Endothelium-derived relaxing factor: discovery, early studies, and identification as nitric oxide. Bioscience reports. 1999;19(4):235-51.

362. Curtis E, Hsu LL, Noguchi AC, Geary L, Shiva S. Oxygen regulates tissue nitrite metabolism. Antioxidants & redox signaling. 2012;17(7):951-61.

363. Steiner ME, Ness PM, Assmann SF, Triulzi DJ, Sloan SR, Delaney M, et al. Effects of red-cell storage duration on patients undergoing cardiac surgery. The New England journal of medicine. 2015;372(15):1419-29.

364. Lacroix J, Hébert PC, Fergusson DA, Tinmouth A, Cook DJ, Marshall JC, et al. Age of transfused blood in critically ill adults. The New England journal of medicine. 2015;372(15):1410-8.

365. Tune JD, Gorman MW, Feigl EO. Matching coronary blood flow to myocardial oxygen consumption. Journal of applied physiology (Bethesda, Md : 1985). 2004;97(1):404-15.

APPENDICES

Appendix 1: 1st Prize – 'Best Research Proposal/Protocol in PhD/MD category'.

Norwich Academic Training Office (NATO) - Excellence in Training Awards 2017

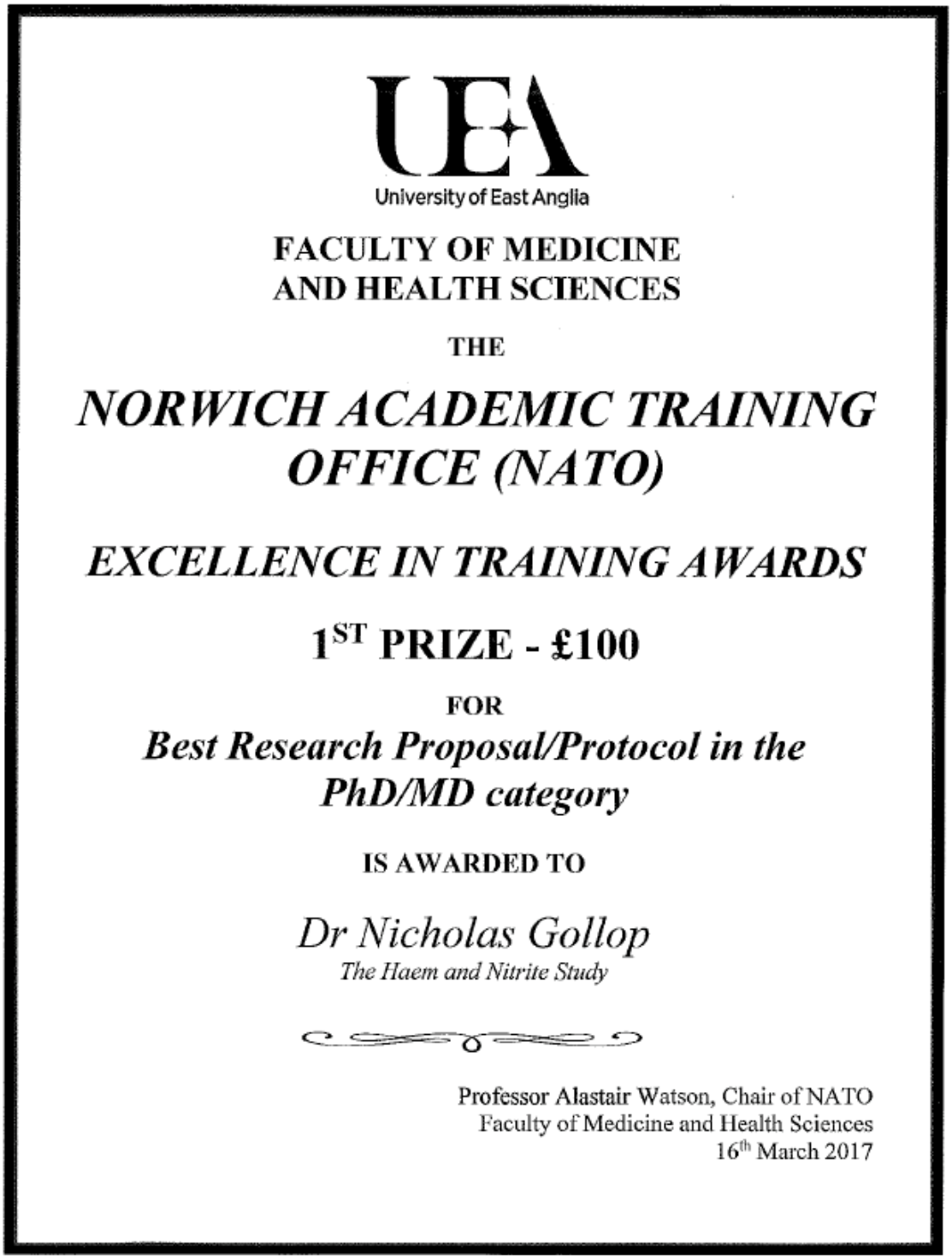

University of East Anglia

FACULTY OF MEDICINE
AND HEALTH SCIENCES

THE

NORWICH ACADEMIC TRAINING OFFICE (NATO)

EXCELLENCE IN TRAINING AWARDS

1ST PRIZE - £100

FOR

Best Research Proposal/Protocol in the PhD/MD category

IS AWARDED TO

Dr Nicholas Gollop

The Haem and Nitrite Study

Professor Alastair Watson, Chair of NATO
Faculty of Medicine and Health Sciences
16th March 2017

Appendix 2: Chapter 3 Publication (131)

ESC European Society of Cardiology

Cardiovascular Research (2020) **116**, 51–62
doi:10.1093/cvr/cvz202

Long-lasting blood pressure lowering effects of nitrite are NO-independent and mediated by hydrogen peroxide, persulfides, and oxidation of protein kinase G1α redox signalling

Martin Feelisch [1†], Takaaki Akaike [2†], Kayleigh Griffiths [3], Tomoaki Ida[2], Oleksandra Prysyazhna[4], Joanna J. Goodwin[3], Nicholas D. Gollop[3,5], Bernadette O. Fernandez [1], Magdalena Minnion[1], Miriam M. Cortese-Krott [6], Alessandra Borgognone[3], Rosie M. Hayes [3], Philip Eaton[4†], Michael P. Frenneaux[5†], and Melanie Madhani [3*†]

[1]Clinical and Experimental Sciences, Faculty of Medicine, University of Southampton, Southampton General Hospital, Southampton, SO16 6YD, UK; [2]Department of Environmental Medicine and Molecular Toxicology, Tohoku University Graduate School of Medicine, Sendai, 980-8575, Japan; [3]Institute of Cardiovascular Sciences, College of Medical and Dental Sciences, University of Birmingham, Birmingham, B15 2TT, UK; [4]King's College of London, School of Cardiovascular Medicine & Sciences, The British Heart Foundation Centre of Excellence, The Rayne Institute, St Thomas' Hospital, London, SE1 7EH, UK; [5]Norwich Medical School, University of East Anglia, Bob Champion Research and Education Building, Norwich Research Park, Norwich, NR4 7UQ, UK; and [6]Division of Cardiology, Pulmonology, and Vascular Medicine, Medical Faculty, Heinrich Heine University, Düsseldorf, 40225, Germany

Received 2 July 2019; revised 17 July 2019; editorial decision 26 July 2019; accepted 29 July 2019; online publish-ahead-of-print 1 August 2019

Time for primary review: 1 day

Aims Under hypoxic conditions, nitrite (NO_2^-) can be reduced to nitric oxide (NO) eliciting vasorelaxation. However, nitrite also exerts vasorelaxant effects of potential therapeutic relevance under normal physiological conditions via undetermined mechanisms. We, therefore, sought to investigate the mechanism(s) by which nitrite regulates the vascular system in normoxia and, specifically, whether the biological effects are a result of NO generation (as in hypoxia) or mediated via alternative mechanisms involving classical downstream targets of NO [e.g. effects on protein kinase G1α (PKG1α)].

Methods and results *Ex vivo* myography revealed that, unlike in thoracic aorta (conduit vessels), the vasorelaxant effects of nitrite in mesenteric resistance vessels from wild-type (WT) mice were NO-independent. Oxidants such as H_2O_2 promote disulfide formation of PKG1α, resulting in NO- cyclic guanosine monophosphate (cGMP) independent kinase activation. To explore whether the microvascular effects of nitrite were associated with PKG1α oxidation, we used a Cys42Ser PKG1α knock-in (C42S PKG1α KI; 'redox-dead') mouse that cannot transduce oxidant signals. Resistance vessels from these C42S PKG1α KI mice were markedly less responsive to nitrite-induced vasodilation. Intraperitoneal (i.p.) bolus application of nitrite in conscious WT mice induced a rapid yet transient increase in plasma nitrite and cGMP concentrations followed by prolonged hypotensive effects, as assessed using *in vivo* telemetry. In the C42S PKG1α KI mice, the blood pressure lowering effects of nitrite were lower compared to WT. Increased H_2O_2 concentrations were detected in WT resistance vessel tissue challenged with nitrite. Consistent with this, increased cysteine and glutathione persulfide levels were detected in these vessels by mass spectrometry, matching the temporal profile of nitrite's effects on H_2O_2 and blood pressure.

Conclusion Under physiological conditions, nitrite induces a delayed and long-lasting blood pressure lowering effect, which is NO-independent and occurs via a new redox mechanism involving H_2O_2, persulfides, and PKG1α oxidation/activation. Targeting this novel pathway may provide new prospects for anti-hypertensive therapy.

* Corresponding author. Tel: +44 (0)121 414 6897; E-mail: m.madhani@bham.ac.uk

† These authors contributed equally to the study.

© The Author(s) 2019. Published by Oxford University Press on behalf of the European Society of Cardiology.
This is an Open Access article distributed under the terms of the Creative Commons Attribution License (http://creativecommons.org/licenses/by/4.0/), which permits unrestricted reuse, distribution, and reproduction in any medium, provided the original work is properly cited.

Keywords Nitrite • Blood pressure • Redox • Hydrogen peroxide • Persulfides

Graphical Abstract

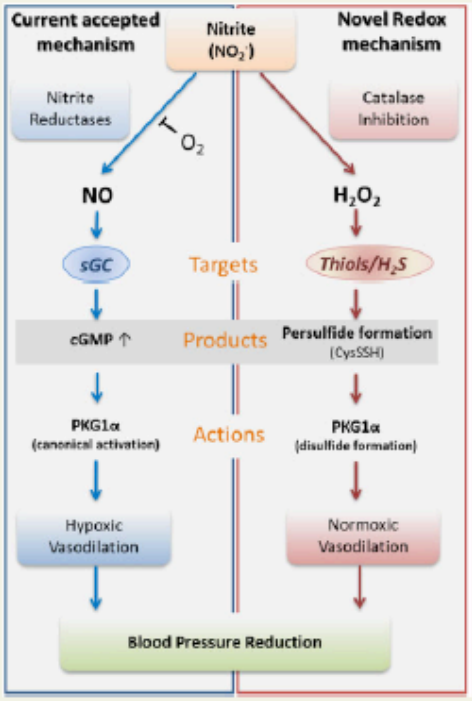

1. Introduction

Despite current pharmacotherapies and interventional procedures, arterial hypertension remains a global health burden and a major risk factor for cardiovascular diseases, dementia, renal failure, and premature death.[1] Inorganic nitrite (NO_2^-) elicits vasorelaxation and lowers blood pressure when infused. Due to the potential beneficial effects and the possible therapeutic utility of NO_2^- in treating hypertension, it becomes essential to understand the mechanism(s) and efficacy by which NO_2^- elicits vasorelaxation under normoxia.[2]

Augmentation of plasma nitrite by oral administration of inorganic nitrate (converted to nitrite by oral/gut bacteria following enterosalivary circulation) has been shown to effectively reduce blood pressure in various animal models and in healthy human subjects.[2–5] It is now clear that at least some of the pharmacological actions of nitrite are mediated via its reduction to nitric oxide (NO) and increased NO/cyclic guanosine monophosphate (cGMP)-signalling under conditions of low pH and oxygen tension.[6,7] Whilst this nitrite-NO pathway offers a conceptually attractive explanation for the blood pressure lowering effect during hypoxia, nitrite also has vasorelaxant and blood pressure lowering effects under normoxic conditions. However, the mechanism(s) responsible for these effects remain incompletely understood. We have shown that under normoxic conditions, the rate of conversion of nitrite to NO is extremely slow,[8] suggesting that these effects may be NO-independent. Using single intraperitoneal (i.p.) injections of nitrite in rats, we previously demonstrated that nitrite was rapidly absorbed and metabolized to nitrate and nitroso/nitrosyl products in all but two tissues studied (brain and aorta)[9]; this was accompanied by cardioprotection and a sustained (48h) increase in ascorbate oxidation in the heart, reflecting persistent changes in tissue redox status.[10]

The mechanism responsible for the vasoactivity of NO (which can be generated from nitrite under hypoxic conditions) is well established and involves activation of the enzyme soluble guanylyl cylase (sGC), resulting in an increase in the generation of the second messenger cGMP with consecutive activation of the cGMP-binding kinase protein kinase G1α (PKG1α), which further transduces the signal associated with vasorelaxation.[11] We have previously shown that PKG1α itself is subject to redox regulation such that the presence of oxidants can result in inter-protein disulfide formation, which translates into an increase in enzyme activity without changes in cGMP.[12,13] Thus, species such as hydrogen peroxide (H_2O_2) that are capable of causing thiol to disulfide oxidation can elicit smooth muscle relaxation, and therefore, lead to vasodilation via oxidative activation of PKG1α in an NO-cGMP-independent fashion. Stubbert *et al.*[14] also reported that polysulfur species derived from hydrogen sulfide (H_2S) oxidation are capable of activating PKG1α via oxidation. The generation of polysulfur species and/or other sulfur oxidants

(e.g. H_2O_2) therefore represents a NO-independent mechanism of PKG1α activation, which could also translate into vasorelaxation. Thus, if nitrite-mediated vasorelaxation under normoxic conditions was found to be NO-independent, it is possible that nitrite is capable of eliciting vasorelaxation via oxidative activation of PKG1α.

Recently, reactive sulfur species known as persulfides (RSSH) and polysulfides (RS_nSR, RSS_nH, $n > 1$) originating from sulfur-containing amino acid metabolism were detected in mammalian tissues and fluids.[15] Specifically, cysteine persulfide (CysSSH), glutathione persulfide (GSSH) and related species may function as potent antioxidants, cytoprotectants, and redox signalling intermediates,[16] and CysSSH appears to be involved in the regulation of mitochondrial biogenesis and bioenergetics.[17] However, the physiological relevance and function of these species is incompletely understood, and whether nitrite has the ability to generate these polysulfur species is unknown.

The significance of nitrite as a redox regulator is not yet widely recognized, and evidence for the possible involvement of these pathways in its blood pressure lowering effects under physiological conditions is lacking. In the present study, we, therefore, sought to explore whether nitrite has the ability to mediate redox signalling and reduce vascular tone under normoxic conditions. We hypothesized that nitrite induces vasodilation and lowers blood pressure by generating endogenous thiol oxidants, such as H_2O_2 and persulfides, to eventually induce oxidation of PKG1α. We integrated *in vitro* and *in vivo* approaches to investigate the redox properties of nitrite. Our studies were further supported by the use of 'redox-dead' Cys42ser PKG1α knock-in (C42S PKG1α KI) mice, which are unable to transduce oxidant signals because the cysteinyl thiol has been replaced by a hydroxyl group, and therefore this mutation prevents the oxidative activation of PKG1α. We demonstrate that a single bolus application of nitrite induces long-lasting blood pressure lowering effects by generating H_2O_2 and persulfide species in the resistance vessels to activate PKG1α in an NO-independent manner.

2. Methods

All experiments were performed under a UK Home Office Licence and conducted according to the Animals Scientific Procedures Act 1986 (UK) and directive 2010/63/EU of the European Parliament guidelines on the protection of animals used for scientific purposes. All experiments were approved by the Institutional Animal Welfare and Ethical Review Body. Male wild-type (PKG1α-WT) or PKG1α Cys42Ser knock-in (C42S PKG1α KI) mice were bred and maintained inhouse.[13] Male C57BL/6 mice (background for the PKG1α Cys42Ser mice) were purchased from Charles River Laboratories (Massachusetts, USA), and all mice were age- and body weight-matched.

2.1 Tissue harvest and blood sampling

C57BL/6 mice were administered a single i.p. injection of sodium nitrite (Sigma-Aldrich, Missouri, USA) dissolved in sterile saline (Baxter Healthcare, Deerfield, IL, USA; 0.9%) at various doses [0 (vehicle control), 0.1, 1.0, and 10 mg/kg body weight[9,10]]. Following nitrite treatment 1 or 24 h previously, mice were terminally anaesthetized [i.p. injection of pentobarbital sodium (300 mg/kg) mixed 50:50 with anticoagulant heparin (150 units)] and biological specimens were harvested. Blood was collected and supplemented with *N*-ethylmaleimide (NEM) and EDTA from a 10× stock in phosphate buffered saline to yield final concentrations of 10 mM NEM/1 mM EDTA and centrifuged for 10 min at 1000 *g* to separate plasma from blood cells. Plasma was then aliquoted, snap frozen in liquid nitrogen, and stored at -80°C until further analysis for nitrite/nitrate and cGMP. Thoracic aorta (conduit) and mesenteric resistance vessels were immediately isolated, dissected in ice-cold Krebs Henseleit buffer (KHB),[12,18] divided into aliquots, snap frozen, and stored at -80°C until analysis for persulfides and H_2O_2. The liver was isolated *in situ*, perfused free of blood, snap frozen, and stored at -80°C for *in vitro* investigations of nitrite's effects on catalase activity. Mice were euthanized by cervical dislocation.

2.2 Functional studies on isolated blood vessels

Conduit vessel rings were isolated from the thoracic aorta, and second-order mesenteric arteries (resistance vessels) from PKG1α WT and C42S PKG1α KI mice. Blood vessels were mounted in a tension myograph (Danish Myo Technology, Hinnerup, Denmark) containing KHB (37°C, pH 7.4) and gassed with 95% O_2/5% CO_2. After equilibration, vascular reactivity was normalized as previously described.[12,18] Submaximal vasocontraction in both vessel types was induced by addition of phenylephrine (PE; Sigma-Aldrich, Missouri, USA) or U46619 (Cambridge Biosciences, Cambridge, UK), respectively, to the organ bath. Relaxation-response curves to sodium nitrite were constructed in the absence or presence of the selective soluble guanylate cyclase inhibitor, 1H-[1,2,4] oxadiazolo[4,3,-a]quinoxalin-1-one (ODQ; Sigma-Aldrich, Missouri, USA; 10 μM[19]) or the NO scavenger, 2-4-carboxyphenyl-4,4,5,5-tetramethylimidazoline-1-oxyl-3-oxide (CPTIO; Enzo Life Sciences, Exeter, UK; 1 mM[19]), and results expressed as a percentage of stable precontractile tone achieved.

2.3 Telemetric blood pressure monitoring *in vivo*

Mean arterial pressure (MAP) in conscious, freely moving PKG1α WT and C42S PKG1α KI mice was assessed using telemetry, as previously described.[13] Briefly, mice were anaesthetized with 2% isoflurane in 0.5 l of oxygen per minute, and a TA11PA-C10 probe catheter (Data Science International, Minnesota, USA) was implanted in the aortic arch via the left aortic carotid artery. Pre- and post-operative analgesia (buprenorphine, subcutaneous injection of 0.1 mg/kg of body weight; Abbot Laboratories, Illinois, USA) was also provided, and the wellbeing of mice monitored daily. After 1 week recovery, mice were placed on the telemetric receivers, and MAP was recorded every 5 min. Blood pressures were measured throughout the day for 72 h before the start of the experiment. Mice then received a single i.p. injection of 0.1 mg/kg sodium nitrite dissolved in sterile saline and their blood pressure was monitored for further 24 h, followed by the administration of a successive 10-fold higher dose of nitrite at the same time on the subsequent 2 days while blood pressure monitoring continued.

2.4 Mass spectrometric analyses of tissue persulfide concentrations

High performance liquid chromatography-electrospray ionization tandem mass spectrometry (LC-ESI-MS/MS) analysis of tissue homogenates following HPE-IAM derivatization was used to determine CysSSH, GSSH, and inorganic persulfide (HSSH; disulfane), as previously described.[17] Briefly, mesenteric and aortic tissues were homogenized with ice-cold 100% methanol solution containing 5 mM HPE-IAM and then incubated at 37°C for 30 min. The homogenates were then centrifuged at 15 000 *g* for 10 min to remove the protein pellet. After centrifugation, the aliquots of the supernatants were diluted with 0.1% formic

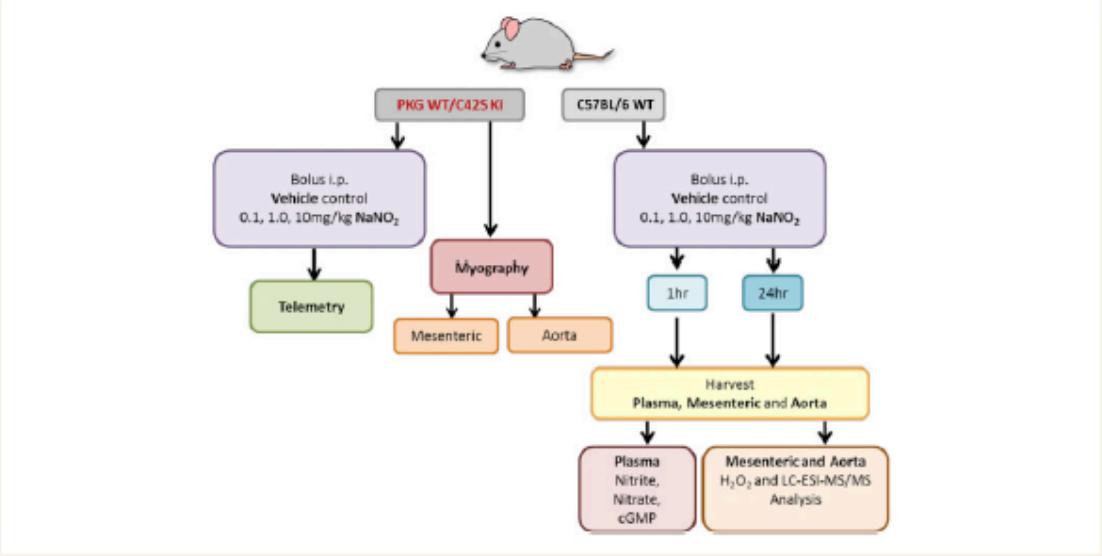

Figure 1 Schematic experimental design to assess nitrite-induced vasodilatory and blood pressure lowering effects as well as biochemical changes during normoxia.

acid containing known amounts of isotope-labelled internal standards. The samples were then analysed for CysSSH, GSSH, and HSSH by LC-ESI-MS/MS.

To assess the potential of H_2O_2 to induce the formation of persulfides from thiols and sulfide under various reaction conditions, L-cysteine (100 μM) or L-glutathione (100 μM), and sodium hydrosulfide (NaHS; 100 μM) was mixed with H_2O_2 (100 μM) in Tris/HCl (pH 7.5 or pH 9) or acetate buffer (pH 5.6) containing 2 mM HPE-IAM. The reaction solutions were incubated at room temperature for 10, 30, 60, 90, or 120 min and subsequently analysed for cysteine (CysSH), CysSSH, HSH, HSSH, GSH, and GSSH.

2.5 Plasma nitrite/nitrate and cyclic GMP determination

Nitrite and nitrate were quantified in plasma as previously described.[19,20] Plasma cGMP was determined using a commercially available assay kit (KGE003 R&D systems, Minneapolis, UK).

2.6 Tissue hydrogen peroxide

Hydrogen peroxide concentrations were measured in tissue (mesenteric and thoracic aorta) using a commercially available assay kit (ab102500 Abcam, Cambridge, UK).

2.7 Tissue catalase activity

Tissue catalase activity was determined by monitoring the rate of H_2O_2 disappearance in the absence and presence of different nitrite concentrations (for order of reagent addition see Supplementary material online, *Figure S1D*). H_2O_2 concentrations were quantified using the horseradish peroxidase-mediated oxidation of phenol red and compared to a calibration curve with absorbance readings taken at 610 nm.[21] For these experiments, frozen mouse liver aliquots were homogenized at 1:4 ratio (w/v) in EDTA-containing phosphate buffer pH 7.4 using a glass–glass Potter-Elvehjem tissue homogenizer immersed in an ice/water bath. The homogenization buffer was supplemented with NEM (10 mM, final concentrations) to minimize potential thiol-mediated metabolic conversion of nitrite to nitroso species. The homogenate was centrifuged (13000 *g*, 15 min, 4°C), and kept on ice in the dark for up to 1 h for measurements of catalase activity, in the absence and presence of nitrite.

3. Results

3.1 Nitrite regulates mesenteric resistance vasorelaxation NO-independently during normoxia

To determine whether in the presence of oxygen nitrite mediates vasorelaxation in an NO-independent or independent fashion, we first constructed cumulative concentration-response curves to nitrite in isolated pre-constricted mesenteric resistance vessels mounted in wire-myographs (*Figure 1*). Pre-incubation of resistance vessels from the wild-type (WT) mice with either the NO-scavenger, carboxy-PTIO or the sGC inhibitor, ODQ failed to abrogate vasorelaxation in the resistance vessels from WT mice (*Figure 2A* and *B*), indicating that the effects of nitrite in this tissue were largely NO/sGC independent. In contrast, when wire-myography was performed in conduit vessels (thoracic aorta) nitrite's vasorelaxant effects were clearly NO/sGC-dependent (*Figure 2C* and *D*).

In light of the above, we hypothesized that nitrite-mediated vasorelaxation may perhaps occur via PKG1α oxidation, independent of the classical NO-cGMP pathway. To explore this possibility, we used a 'redox-dead' genetic variant of PKG1α whereby the important regulatory SH moiety has been mutated to a redox inactive OH group (by replacing a

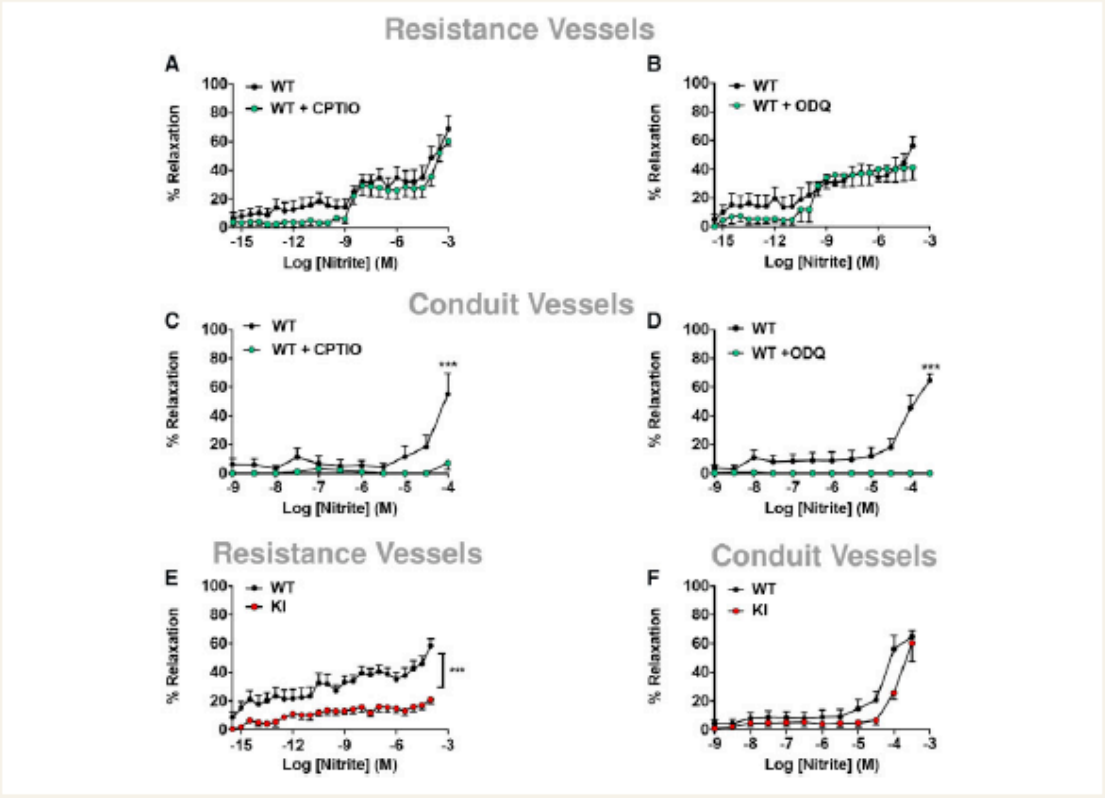

Figure 2 Mesenteric and thoracic blood vessels from PKG-1α WT and C42S PKG1α KI were mounted in myograph and sub-maximally constricted with U46619 and phenylephrine, respectively. Pre-incubation of isolated mesenteric resistance vessels from WT to (*A*) NO scavenger, carboxy-PTIO (CPTIO; 1 mM; $n = 15$) or (*B*) soluble guanylate cyclase inhibitor (sGC), ODQ (10 μM; $n = 14$) did not attenuate the vasodilatory response to nitrite in WT mice. Concentration response curves to nitrite in isolated thoracic aorta. Vasorelaxant effects of nitrite was (*C*) NO-dependent ($n = 7$) and (*D*) sGC-dependent in WT mice ($n = 11$). Concentration response curves to sodium nitrite in (*E*) isolated mesenteric resistance vessels from both genotypes ($n = 19$). Nitrite was significantly less effective as a vasodilator in C42S PKG1α KI mice, but not in the (*F*) thoracic aorta (conduit vessels; $n = 13$–14). Data are expressed as mean ± S.E.M. ***$P \leq 0.001$ as determined by two-way ANOVA with Bonferroni's test (*A*–*F*).

single cysteine, Cys42, against serine).[13] Using this C42S PKG1α knock-in (KI) mouse model and WT littermates as a comparator, we next investigated the molecular target involved in nitrite-mediated vasorelaxation (*Figure 1*). Nitrite-relaxed WT vessels in a concentration-dependent fashion, but did not relax resistance vessels from C42S PGK1α KI mice (*Figure 2E*); whereas in the conduit vessels, nitrite was not mediated through PKG1α oxidation (*Figure 2F*).

To translate our findings into the *in vivo* setting, we administered i.p. injections of sodium nitrite (0.1, 1, and 10 mg/kg) in WT mice on three consecutive days following 72 h continuous telemetric arterial blood pressure monitoring. Compared to the hourly averages for the 3 days baseline blood pressure measurements shown, reductions in blood pressure were not apparent until 4–5 h after the nitrite application (*Figures 1* and *3A*; WT-black trace), but blood pressure remained reduced for almost 24 h, especially during the nocturnal period when the animals were most active (*Figure 3B*, WT-black bars). Unexpectedly, the magnitude of blood pressure lowering by the three doses was similar.

We next assessed the *in vivo* blood pressure lowering effects of nitrite in redox-dead C42S PKG1α KI using the same treatment regime as in their PKG-WT littermates (see above). Of note, the C42S PKG1α KI had modestly, but consistently higher mean blood pressure than the WT.[13] In contrast to the long-lasting hypotensive effects seen with nitrite in WT mice, C42S PKG1α KI animals did not show a blood pressure lowering effect. *Figure 3A* compares the 24 h MAP data in both genotypes following i.p. administration of sodium nitrite (0.1, 1, and 10 mg/kg). *Figure 3B* is further simplified to illustrate the delta difference between baseline and response to nitrite treatment at night. There was a significant difference between the two genotypes (*$P < 0.05$ determined by repeated measures two-way ANOVA). These results are consistent with the notion that the ability of nitrite to elicit persistent hypotension depends on its capacity to oxidatively activate PKG1α.

In a separate group of C57BL/6 mice, the same nitrite injection regime was used and blood samples were taken 1 and 24 h post-treatment for measurement of plasma nitrite, nitrate, and cGMP (*Figures 1* and *3C*–*E*).

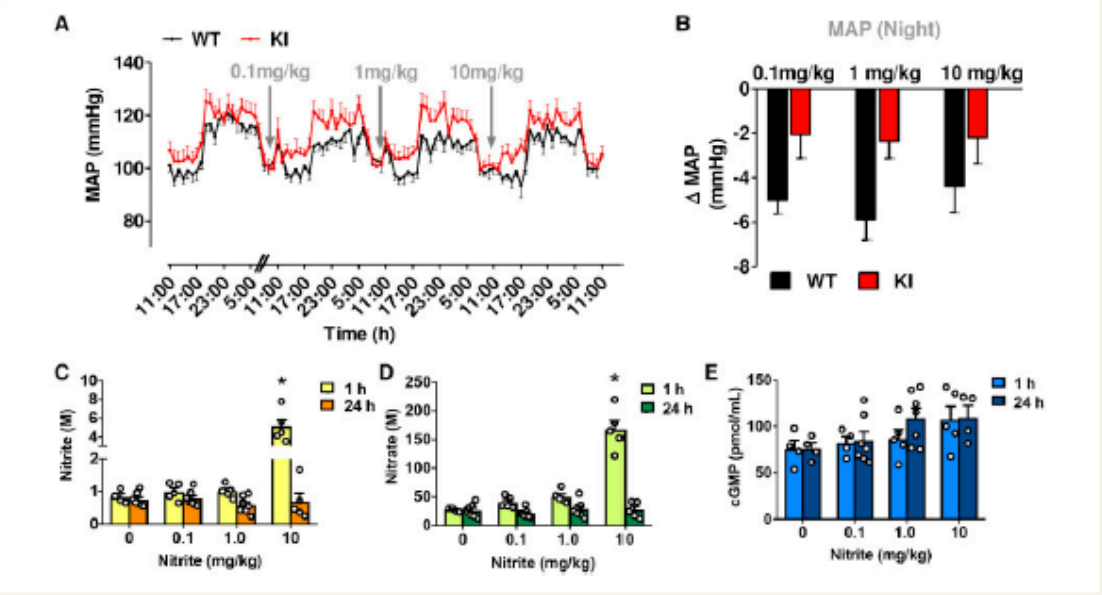

Figure 3 C42S PKG1α KI mice are resistant to nitrite-induced blood pressure lowering compared with age-matched WT littermates, as measured by *in vivo* telemetry ($n = 6$ WT and 7 KI). (*A*) Comparison of the 24 h averaged changes in MAP in both genotypes following bolus administration of sodium nitrite (0.1, 1, and 10 mg/kg). WT mice, but not for KI mice, there was a significant difference in blood pressure lowering effect with each nitrite dose when compared to baseline. (*B*) Delta indicates the difference between baseline and response to treatment at night. In separate group of WT mice (C57BL/6), following bolus i.p. administration with sodium nitrite (vehicle control, 0.1, 1, and 10 mg/kg) for 1 or 24 h treatment, plasma samples were taken (*C*) nitrite, (*D*) nitrate, and (*E*) cGMP ($n = 4$–7 mice/group). Data are represented as mean ± S.E.M. *$P \leq 0.05$ when WT mice compared to each nitrite dose with baseline (repeated measures one-way ANOVA, *A*). *$P \leq 0.05$ between two different genotypes was determined by repeated measures two-way ANOVA (*B*). Significant time and concentration interaction for plasma nitrite and nitrate, as determined by two-way ANOVA. Following Tukey's multiple comparisons test 10 mg/kg sodium nitrite was significant when compared to control vehicle, 0.1 and 1 mg/kg (*$P \leq 0.05$; *C* and *D*). There was no significant difference between nitrite concentration for cGMP levels at either time ($P > 0.05$; two-way ANOVA followed by Tukey's multiple comparisons test; *E*).

Plasma nitrite and nitrate acutely increased in a dose-dependent manner, and this was statistically significant at the highest dose (i.e. 3–4 h before a BP-lowering effect was observed), as determined by two-way ANOVA. Following Tukey's multiple comparisons test 10 mg/kg sodium nitrite, plasma nitrite was significantly higher at 1 h when compared with control vehicle, 0.1 and 1 mg/kg; *$P < 0.05$). However 24 h later plasma nitrite, nitrate, and cGMP were similar to baseline concentrations even at the highest dose (despite persistent BP reduction persisting for almost 24 h); these changes were consistent with our previous results in rats subjected to i.p. nitrite administration, demonstrating that plasma nitrite levels rapidly increased, but returned close to baseline values in ~1 h.[9,10]

3.2 Nitrite increases hydrogen peroxide levels

We next focused on the mechanism of nitrite-mediated vasorelaxation of resistance arteries and blood pressure lowering. Nitrite has the potential to inhibit catalase,[22,23] which may conceivably lead to an increased oxidative tone by reducing the breakdown of endogenously produced H_2O_2. This action was confirmed in complementary studies in which nitrite was found to be capable of inhibiting catalase activity in hepatic tissue *in vitro* (Supplementary material online, *Figure S1*). In order to determine whether this can also occur in vascular tissue, we measured *ex vivo* H_2O_2 concentrations in blood vessels harvested 1 and 24 h after nitrite pre-treatment *in vivo* (*Figure 1*). As depicted in *Figure 4A*, nitrite caused a significant and similar increase in steady-state concentrations of H_2O_2 in mesenteric resistance vessels with both 1 and 10 mg/kg nitrite at 1 h, which persisted at 24 h. Whilst nitrite also triggered an increase of this oxidant in the aorta at 1 h, H_2O_2 concentrations had returned to normal at 24 h (*Figure 4B*), revealing kinetic differences in H_2O_2 handling between these two types of vessels.

3.3 Nitrite increases CysSSHs and GSSH in resistance vessels during normoxia

The results presented thus far indicate that nitrite produces H_2O_2 and induces vasorelaxation by oxidation of PKG1α. We next examined whether there was a possible intermediate that links these effects. We surmised that nitrite may have the ability to oxidatively activate PKG1α via the generation of polysulfur species. To establish whether nitrite generates polysulfur species *in vivo*, mesenteric resistance and thoracic aorta blood vessels were harvested from WT mice (C57BL/6) treated with bolus i.p. administration of vehicle control or sodium nitrite (0.1, 1, and 10 mg/kg) for 1 or 24 h. The levels of persulfides (CysSSH, GSSH, and HSSH) were analysed by LC-ESI-MS/MS following derivation with β-(4-hydroxyphenyl) ethyliodoacetamide (HPE-IAM). We observed

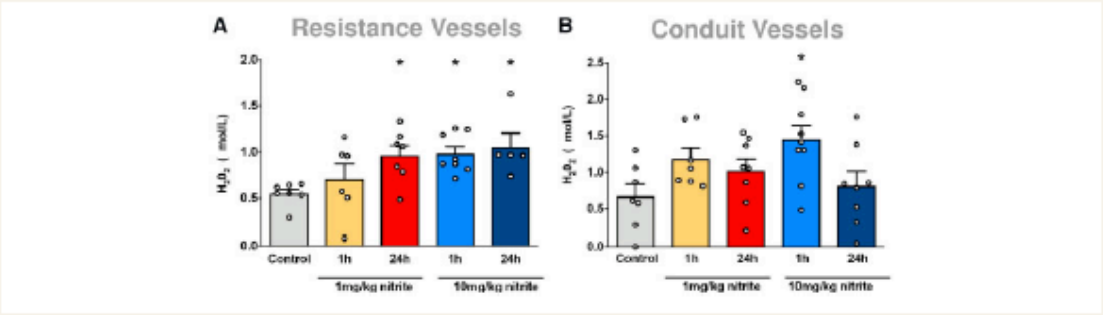

Figure 4 In separate group of mice (C57BL/6), mesenteric resistance and thoracic aorta blood vessels were harvested following bolus i.p. administration of vehicle control or sodium nitrite (1, or 10 mg/kg) in WT mice (C57BL/6) for 1 or 24 h. Hydrogen peroxide (H_2O_2) levels were measured in (*A*) mesenteric resistance vessels ($n = 5–8$) and (*B*) thoracic aorta ($n = 7–9$). Data are expressed as mean ± S.E.M. *$P \leq 0.05$ as determined by one-way ANOVA with Dunnett's test.

dose-dependent increases in CysSSH and GSSH in the resistance vessels (*Figure 5A* and *B*) with progressively lower concentrations of HSSH (*Figure 5C*). In contrast, we observed no changes in CysSSH, GSSH, or HSSH formation in the conduit vessels (*Figure 5D–F*, respectively). In further *in vitro* studies, we sought to confirm experimentally that H_2O_2 is capable of inducing polysulfidation when inorganic sulfide and cysteine are present. This was indeed found to be the case under a variety of pH and H_2O_2 conditions (*Figures 6A–C*), and similar results were observed with glutathione/sulfide/H_2O_2 (*Figure 6D*).

4. Discussion

We have previously shown that the conversion of nitrite to NO is inhibited by oxygen,[8] and the mechanism(s) through which it exerts its pharmacological effects under normoxia remain(s) poorly understood. Whilst blood pressure lowering effects of nitrite have been shown in various animal models and clinical studies, to the best of our knowledge, the impact of long-lasting effects of single bolus application of nitrite during physiological conditions has not been investigated. In the present study, we demonstrate that a single bolus application of nitrite elicits a long-lasting blood pressure lowering effect that is unrelated to the generation of NO. We furthermore show that a marked temporal dissociation exists between plasma nitrite and cGMP concentrations, and the blood pressure lowering effects of i.p. injections of nitrite, with the hypotensive effects being delayed in onset vs. circulating nitrite/cGMP concentrations and persisting despite the return of the latter to baseline values. These observations differ considerably from the short-lived BP-lowering effects of a single intravenous injection of nitrite, thus supporting the role of a non-canonical vasodilator effect via a mechanism that is independent of the NO-cGMP pathway. Our results are consistent with the notion that nitrite has signalling properties in its own right[9] and provides evidence for the notion that nitrite can act as an indirect oxidant. Our next efforts focused on how nitrite might induce vasorelaxation and lower blood pressure. Using a combination of biochemical analytical tools and a genetic KI mouse model, we finally demonstrate that the blood pressure lowering effects of nitrite are mediated by PKG1α oxidation following H_2O_2 and cysteine/glutathione persulfide formation in the resistance vasculature. A conceivable explanation for which evidence exists in the literature is that nitrite acts as an indirect oxidant that mediates oxidation of other biological targets.

We previously demonstrated that oxidants such as H_2O_2 can activate PKG1α independently of the classical NO-sGC-cGMP pathway by forming a disulfide bond at Cys42 to dilate resistance vessels and lower blood pressure.[13] Consistent with this finding, PKG1α-KI mice in which WT kinase has been replaced by a 'redox-dead' serine residue (C42S mutant) cannot transduce oxidant signals because their PKG does not harbour the redox-sensing thiol, rendering these mice unable to lower blood pressure via an oxidative mechanism.[13] Independent of this, we demonstrated that nitrite chemically/functionally interacts with H_2S[24] and that a single bolus application of nitrite triggers long-lasting alterations in myocardial redox status with dramatic alterations in the cardiac mitochondrial proteome.[10] We here sought to integrate these different strands of information and assessed whether nitrite could produce a metabolic signature consistent with a process involving thiol/sulfide oxidation and whether this might be associated with PKG1α dimerization to mediate vasorelaxation and blood pressure reduction.

Whilst the resistance vessels are the primary determinant of diastolic and mean blood pressure, most vascular studies investigated the effects of nitrite in the aorta and have shown NO-dependent effects. Here, we assessed both the aorta and the mesenteric resistance vessels from WT and C42S PKG1α KI mice. Unlike the aorta, it was evident in the isolated resistance vessels from WT mice that nitrite-mediated vasodilatory effects were NO-sGC independent. Moreover, the mesenteries from mice expressing the 'redox-dead' C42S form of PKG1α were relatively insensitive in their vasodilatory response to nitrite compared to WT. Based on these findings, we anticipated that the long-lasting *in vivo* blood pressure lowering effect of nitrite would also be diminished in the KI mice. Indeed, this was found to be the case because nitrite decreased blood pressure via non-canonical oxidative activation of PKG1α, whereas the KI mice were resistant to this hypotensive response.

Nitrite has the ability to reduce the rate of H_2O_2 decomposition by binding to the haem moiety of catalase thereby inhibiting enzyme activity[23,25]; thus we reasoned that nitrite may inhibit catalase activity and possibly increase H_2O_2 levels, especially in resistance vessels, and this may be responsible for the vasoactivity observed. Exploratory studies on the inhibition of catalase activity by nitrite in mouse liver tissue

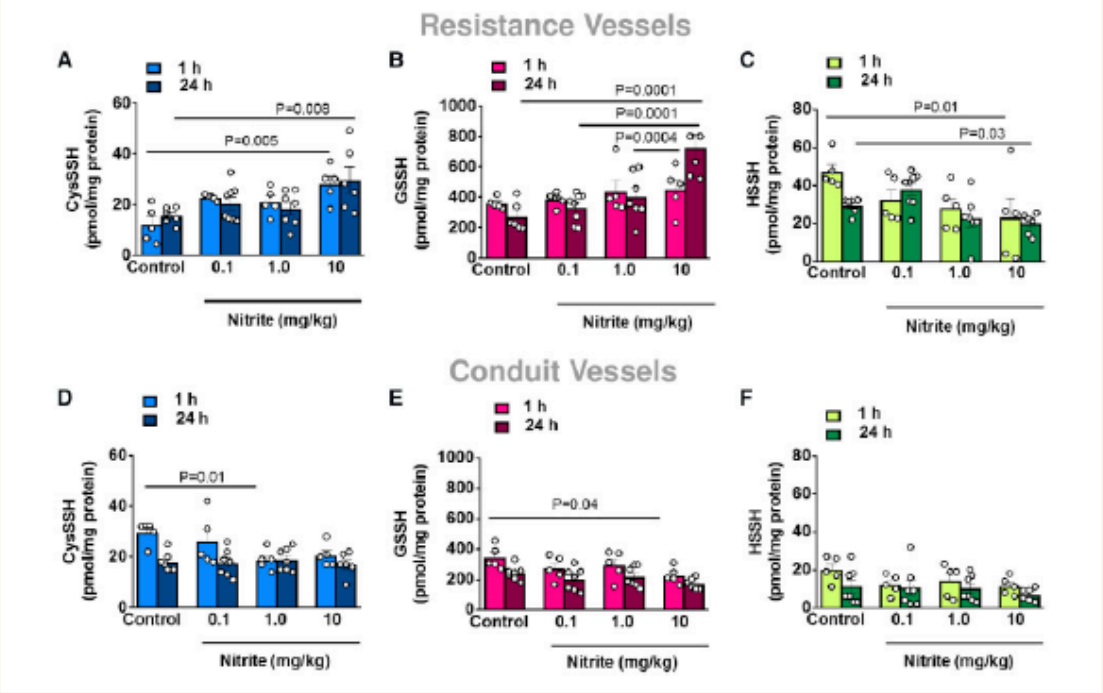

Figure 5 Mesenteric resistance and thoracic aorta blood vessels were harvested from WT mice (C57BL/6) treated with bolus i.p. administration of vehicle control or sodium nitrite (0.1, 1, and 10 mg/kg) for 1 or 24 h. The levels of persulfides (CysSSH, GSSH, and HSSH) were analysed by liquid chromatography-electrospray ionization tandem mass spectrometry (LC-ESI-MS/MS) following derivation with β-(4-hydroxyphenyl)ethyliodoacetamide (HPE-IAM). Data are represented as mean ± S.E.M ($n = 5–8$). *$P \leq 0.05$ as determined by two-way ANOVA with Tukey's test (A–F).

in vitro confirmed that this may be a viable mechanism. In the vasculature, H_2O_2 concentrations were found to remain elevated for prolonged periods of time in the mesenteric resistance vessels when compared with conduit vessels. Although these observations would seem to provide a mechanism that could explain the NO-independent actions of nitrite as a vasorelaxant, previous studies reporting H_2O_2-mediated PKG1α activation required high concentrations of this oxidant,[12] suggesting the effect may not be entirely due to H_2O_2 directly.

Reactive sulfur-containing species, such as CysSSH have been known to exist endogenously, but the physiological relevance of these species remains incompletely understood. CysSSH evidently generates GSSH, and previous work from our group has shown that these reactive species act as potent scavengers of oxidants such as H_2O_2, which contributes to cellular redox signalling.[16] Furthermore, Stubbert *et al.*[14] reported that polysulfur species derived from H_2S oxidation are capable of activating PKG1α via oxidation. Therefore, the generation of polysulfur species may represent an NO-independent mechanism of PKG1α activation, which could mediate vasorelaxation. Thus, the ability for nitrite to oxidatively activate PKG1α may be due to additional generation of polysulfur species. Indeed, there is precedence for the interaction of nitrite with sulfide in forming another reactive sulfur species, nitrosopersulfide, in the literature.[24] Previous reports indicate that analysis of CysSSH, GSSH, and HSSH (disulfane) can serve as detectable surrogates for overall levels of cellular polysulfur species, since they are all in dynamic equilibrium.[26,27] Thus, to test the hypothesis that nitrite generates polysulfur species *in vivo*, the concentrations of all three compounds were determined by mass spectrometry in conduit and mesenteric resistance vessels of WT mice 1 and 24 h after nitrite administration. We observed dose-dependent increases in CysSSH and GSSH in the resistance vessels with progressively lower concentrations of HSSH. Since disulfane is highly reactive, it may immediately react as intracellular disulfide concentrations rise to produce CysSSH and GSSH. In contrast to our findings in resistance vessels, no increases in CysSSH or GSSH were apparent in conduit vessels. These observations demonstrate that bolus applications of nitrite trigger polysulfur species formation through an NO-independent mechanism already at low-to-moderate pharmacological doses with marked differences between vascular beds. Interestingly, persulfide formation from the resistance vessels matched the temporal profile of nitrite effects on H_2O_2 and blood pressure.

Thus far, we demonstrated that nitrite is capable of eliciting increases in H_2O_2 and polysulfur species, with greater propensity for resistance vessels than conduit vessels. It is intriguing to speculate that both events are related and that the source of the polysulfur species is via H_2O_2-mediated oxidation of reduced thiol species. In further *in vitro* studies, we thus sought to confirm experimentally that H_2O_2 is capable of inducing polysulfidation when inorganic sulfide and cysteine are present. This was indeed found to be the case under a variety of conditions (pH

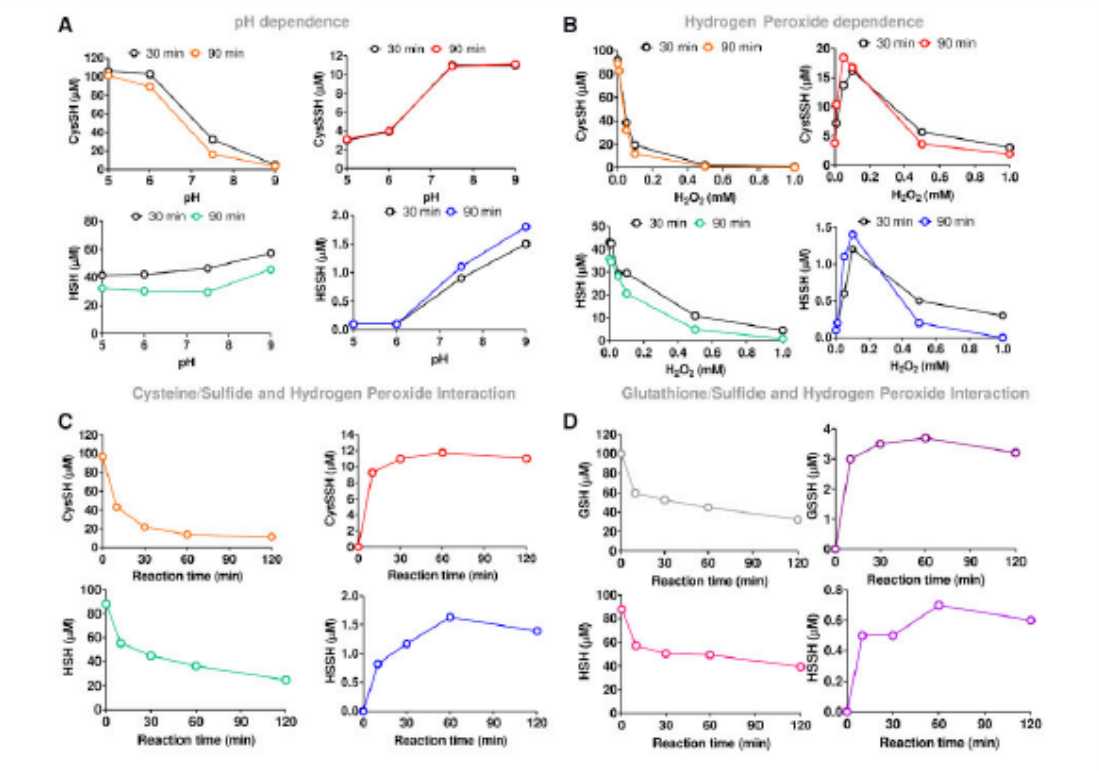

Figure 6 Cysteine persulfide (CysSSH) and polysulfides formation during various reactions. (*A*) pH conditions (5, 6, 7.5, and 9) in the presence of cysteine (100 μM), sulfide (NaHS; 100 μM), hydrogen peroxide (H_2O_2; 100 μM) in 50 mM Acetate buffer (pH 5 and 6), or Tris/HCL (pH 7.5 and 9) or HPEPAM (2 mM). (*B*) H_2O_2 concentrations (0, 0.01, 0.05, 0.1, and 1 mM) in the presence of cysteine (100 μM), NaHS (100 μM) in 50 mM Tris/HCL pH 7.5. Similar results were obtained with glutathione/sulfide mixtures, although final concentrations of GSSH achieved were less compared to the corresponding cysteine analogue. All reactions were also accompanied by the formation of thiosulfate ($S_2O_3^{2-}$) and small concentrations of the corresponding trisulfide (data not shown). (*C*) Interaction of cysteine (100 μM) or (*D*) Glutathione (GSH; 100 μM) in the presence of NaHS (100 μM), H_2O_2 (100 μM) in 50 mM Tris/HCL (pH 7.5). Data presented are from one single independent experiment for each condition.

dependence and H_2O_2 concentrations) and similar results were observed with glutathione/sulfide/H_2O_2. Taken together, these reactions strongly suggest that nitrite can indirectly contribute to polysulfide formation by acting as an amplifier of endogenous H_2O_2 concentrations.

Although it is intriguing to speculate that nitrite may elicit vasorelaxation via its capacity to raise H_2O_2 levels which subsequently give rise to organic persulfides which, in turn, activate PKG1α, it is important to reiterate that detection of CysSSH/GSSH is merely indicative of the general presence of polysulfur species (including protein per- and polysulfides)[26] and that these particular species are not necessarily solely responsible for the biological effects observed herein. What detection of these species does indicate, however, is the presence of an oxidizing environment consistent with the notion of oxidative PKG1α activation. Due to the analytical challenges and rapid interconversion of reactive sulfur species it is currently not possible to disentangle these reaction channels further. Nevertheless, the key findings of this work are that nitrite—when applied i.p.—is capable of creating an oxidizing environment *in vivo*, as evidenced by increases in H_2O_2 and polysulfide concentrations in vascular tissue, favouring PKG1α dimerization, and that these effects occur primarily in resistance vessels. While it has been reported that nitrite is capable of inhibiting catalase (which we confirm to also occur in tissues), and this is a possible pathway through which nitrite creates an oxidizing environment, the exact mechanism(s) by which this occurs are not established. We cannot exclude, for example, that nitrite also increases vascular NADPH oxidase activity[28] and/or up-regulates SOD[29] and/or increases superoxide/H_2O_2 formation by interfering with electron transfer processes in the mitochondria; these possibilities warrant further investigation. Furthermore, increases in resistance vessel H_2O_2 concentration were similar at 1 and 10 mg nitrite, which may explain the absence of dose-response for blood pressure lowering over the range of doses explored.

The ability of nitrite to elicit its vasoactive effects to a greater extent in resistance vs. conduit vessels is intriguing and requires independent confirmation. This mechanism is at odds with nitrite's currently accepted mode of action (*Figure 7*) and represents an unusual case of non-canonical pharmacology whereby a short-lived pro-oxidant elicits long-

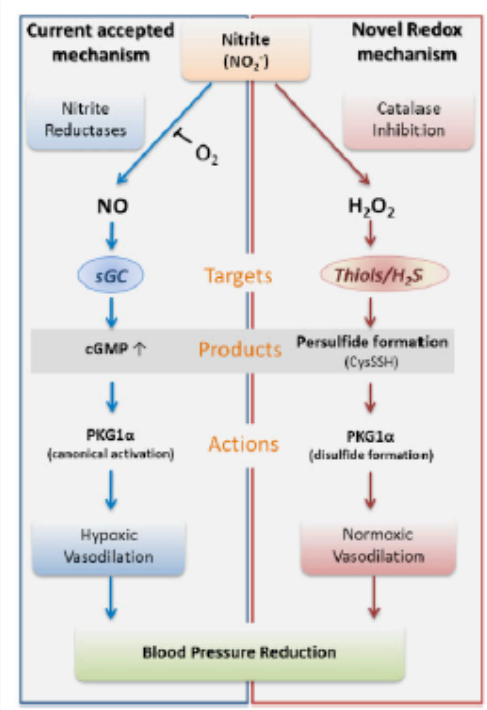

Figure 7 Proposed mechanism of action involved in nitrite-mediated vasorelaxation, including the canonical nitrite reduction pathway (left—blue panel) and the novel nitrite oxidation pathway (right—red panel).

lasting hemodynamic effects *in vivo*. To our knowledge, this is the first report for such a mechanism in resistance vessels *in vivo*.

These findings may potentially be relevant not only to pharmacological, but also to physiological concentrations to nitrite. A previous study reported that antibacterial mouthwash reduced plasma nitrite and increased blood pressure in treated hypertensive patients.[30] Herein, we demonstrated that the delayed but sustained blood pressure lowering effect of nitrite was markedly attenuated in the C42S PKG1α KI vs. the WT mice. Furthermore, we also confirm a previous report that the baseline blood pressure was higher in the C42S PKG1α KI mice.[13] This could potentially be related to effects of physiological concentrations of nitrite on PKG oxidation state or may be consistent with a previous report of impaired acetylcholine mediator effects observed in the C42S PKG1α KI.[13] Mesenteries from KI mice were deficient in their responses to H_2O_2 or acetylcholine, as well as the latter in the presence of L-NAME and indomethacin to remove vasodilation by classical nitric oxide- or prostacyclin-dependent mechanisms.[6] This deficiency in acetylcholine-dependent relaxation in the C42S PKG1α KI is consistent with the endothelium-derived hyperpolarizing factor-dependent component of vasodilation induced by this neurotransmitter being significantly mediated by H_2O_2 generation.[31] Indeed, evidence was presented that C42S PKG1α is deficient in activation by cGMP, although whether this mutation impacts the affinity with cGMP was not determined, and this was suggested to underlie the loss of function observed in C42S PKG1α KI mice.[32] However, the studies comparing the response of isolated resistance vessels of these mutant mice to WT controls, showed their vasodilation to NO donors or a cell-permeable cGMP analogue were the same.[13]

Although oxidation of C42 has been implicated in the targeting and the oxidation of PKG1α, there is additional complexity because of the potential roles of other redox-active cysteines and the interrelationship between cGMP-binding and kinase oxidation. It may be that C42 is more important for targeting the kinase to its substrates, and that cGMP or oxidation of another cysteines is required for kinase competency.[33] For example, nitroxyl donors were shown to induce a disulfide at C42 as well as an intra-disulfide between C117 and 195 in the high-affinity cGMP-binding site of PKG1α—with the latter oxidation mediating most of the activation induced by this nitro-oxidative intervention.[34] C195 was also shown to adduct the electrophile 8-nitro-cGMP, with this S-guanylation modification leading to persistent activation of the kinase.[35] Hyperoxidation of C117 has been implicated as a mechanism of PKG1α activation by H_2O_2,[36] whilst activation by this oxidant was not observed by others.[32] In summary, the redox control of PKG1α is complex, with our understanding continuing to evolve as contemporary studies on the subject emerge. Nevertheless, a casual role for PKG1α C42 oxidation in oxidant or endothelium-derived hyperpolarizing factor-dependent vasodilation is supported by a number of studies.

The generation of polysulfur species is dependent on the presence of cysteine and/or H_2S.[17,37] Thus, if PKG1α activation is polysulfide-mediated (as our *in vivo* experiments suggest) the generation of H_2S in the target tissues becomes an important factor for the action of nitrite and may contribute to the tissue specificity of the observed effects. The overall outcome of these reactions on the effective concentrations of CysSSH and related species (and thus the net effect on physiological function) appears to be complex and tissue/organ-specific, as illustrated by the differences in regulation between resistance and conduit vessels in the present study. The factors contributing to these differences (e.g. oxygen tension, oxidative stress) warrant further investigation.

In summary, this study reports a novel finding, whereby under physiological conditions nitrite induces long-lasting blood pressure lowering effects independent of NO-induced cGMP elevations. We show that nitrite lowers blood pressure by mediating oxidation of PKG1α. This mechanism has been shown by using 'redox-dead' C42S PKG1α KI mice, which cannot activate oxidant signals. We observed dose-dependent vasorelaxant responses to nitrite in the PKG1α WT isolated resistance vessels, but the vasodilatory response to nitrite were blunted in the C42S PKG1α KI mice. These findings were further substantiated by monitoring blood pressure *in vivo*, since nitrite was unable to lower blood pressure in the redox-dead C42S PKG1α KI mice compared with WT littermates. We also identified that the effect of nitrite was mediated via the generation of H_2O_2, with consecutive production of persulfide species (CysSSH and GSSH) in the resistance vessels, which oxidatively activate PKG1α. Our study concludes that a single bolus application of nitrite has the ability to act as a redox regulator during physiological conditions to induce long-lasting blood pressure lowering effects, providing a new prospect for therapeutic strategy in treating the global healthcare burden of hypertension. Future investigations are warranted to address the significance of this redox pathway in hypertensive and other cardiovascular disease models. Furthermore, our findings raise the possibility of identifying other molecules capable of modulating this novel pathway that may have therapeutic potential as hypertensive agents.

Supplementary material

Supplementary material is available at *Cardiovascular Research* online.

Authors' contributions

M.Ma., M.F., and M.P.F designed the studies. M.Ma., P.E, O.P., J.J.G, N.D.G, A.B, R.M.H, K.G. designed, carried out, and analysed the PKG1α and C57BL/6 *in vivo* experiments. M.C.K. contributed pilot data and provided technical guidance for mice telemetry experiments. O.P. carried out and analysed PKG1α telemetry experiments. M.Ma., M.F., and K.G. designed, carried out, and analysed the H_2O_2 experiments. B.O.F. and M.M. contributed to nitrite, nitrate, and cGMP assays and performed exploratory catalase inhibition/polysulfide formation experiments. M.Ma., M.F., T.A., and T.I. designed and carried out *in vitro* polysulfide experiments and analysed *in vivo* tissue samples. All authors interpretated the data. M.Ma., M.F., and M.P.F. wrote the original manuscript and all authors reviewed the revised manuscript.

Acknowledgements

We are grateful for Jon Fukuto's (Sonoma State University, USA) critical reading of the manuscript, the skilful assistance of Monika Mikus-Lelinska (Southampton University, UK) and Peter Nightingale (University Hospitals Birmingham NHS Foundation Trust, Statistician) for his guidance in statistical analysis.

Conflict of interest: none declared.

Funding

This work was funded by the UK Medical Research Council [G1001536] and British Heart Foundation [PG/14/36/30854 to M.Ma., M.P.F., and M.F.]; British Heart Foundation [RG/17/16/33294] and European Research Council Advance Award [339095 to P.E.]; Grants-in-Aid for Scientific Research from the Ministry of Education, Sciences, Sports, and Technology (MEXT), Japan, to T.A. and T.I.

References

1. Forouzanfar MH, Liu P, Roth GA, Ng M, Biryukov S, Marczak L, Alexander L, Estep K, Hassen Abate K, Akinyemiju TF, Ali R, Alvis-Guzman N, Azzopardi P, Banerjee A, Bärnighausen T, Basu A, Bekele T, Bennett DA, Biadgilign S, Catalá-López F, Feigin VL, Fernandes JC, Fischer F, Gebru AA, Gona P, Gupta R, Hankey GJ, Jonas JB, Judd SE, Khang YH, Khosravi A, Kim YJ, Kimokoti RW, Kokubo Y, Kolte D, Lopez A, Lotufo PA, Malekzadeh R, Melaku YA, Mensah GA, Misganaw A, Moldad AH, Moran AE, Nawaz H, Neal B, Ngalesoni FN, Ohkubo T, Pourmalek F, Rafay A, Rai RK, Rojas-Rueda D, Sampson UK, Santos IS, Sawhney M, Schutte AE, Sepanlou SG, Shifa GT, Shiue I, Tedla BA, Thrift AG, Tonelli M, Truelsen T, Tsilimparis N, Ukwaja KN, Uthman OA, Vasankari T, Venketasubramanian N, Vlassov W, Vos T, Westerman R, Yan LL, Yano Y, Yonemoto N, Zaki ME, Murray CJ. Global burden of hypertension and systolic blood pressure of at least 110 to 115 mmHg, 1990–2015. *JAMA* 2017; **317**:165–182.
2. Bailey JC, Feelisch M, Horowitz JD, Frenneaux MP, Madhani M. Pharmacology and therapeutic role of inorganic nitrite and nitrate in vasodilatation. *Pharmacol Ther* 2014;**144**:303–320.
3. Maher AR, Milsom AB, Gunaruwan P, Abozguia K, Ahmed I, Weaver RA, Thomas P, Ashrafian H, Born GV, James PE, Frenneaux MP. Hypoxic modulation of exogenous nitrite-induced vasodilation in humans. *Circulation* 2008;**117**:670–677.
4. Dejam A, Hunter CJ, Tremonti C, Pluta RM, Hon YY, Grimes G, Partovi K, Pelletier MM, Oldfield EH, Cannon RO, Schechter AN, Gladwin MT. Nitrite infusion in humans and nonhuman primates: endocrine effects, pharmacokinetics, and tolerance formation. *Circulation* 2007;**116**:1821–1831.
5. Guimarães DD, Cruz JC, Carvalho-Galvão A, Zhuge Z, Marques SM, Naves LM, Persson AEG, Weitzberg E, Lundberg JO, Balarini CM, Pedrino GR, Braga VA, Carlström M. Dietary nitrate reduces blood pressure in rats with angiotensin II-induced hypertension via mechanisms that involve reduction of sympathetic hyperactivity. *Hypertension* 2019;**73**:839–848.
6. DeMartino AW, Kim-Shapiro DB, Patel RP, Gladwin MT. Nitrite and nitrate chemical biology and signalling. *Br J Pharmacol* 2019;**176**:228–245.
7. Oliveira-Paula GH, Pinheiro LC, Tanus-Santos JE. Mechanisms impairing blood pressure responses to nitrite and nitrate. *Nitric Oxide* 2019;**85**:35–43.
8. Feelisch M, Fernandez BO, Bryan NS, García-Saura MF, Bauer S, Whitlock DR, Ford PC, Janero DR, Rodriguez J, Ashrafian H. Tissue processing of nitrite in hypoxia: an intricate interplay of nitric oxide-generating and -scavenging systems. *J Biol Chem* 2008;**283**:33927–33934.
9. Bryan NS, Fernandez BO, Bauer SM, Garcia-Saura MF, Milsom AB, Rassaf T, Maloney RE, Bharti A, Rodriguez J, Feelisch M. Nitrite is a signaling molecule and regulator of gene expression in mammalian tissues. *Nat Chem Biol* 2005;**1**:290–297.
10. Periman DH, Bauer SM, Ashrafian H, Bryan NS, García-Saura MF, Lim CC, Fernandez BO, Infusini G, McComb ME, Costello CE, Feelisch M. Mechanistic insights into nitrite-induced cardioprotection using an integrated metabolomic/proteomic approach. *Circ Res* 2009;**104**:796–804.
11. Browner NC, Dey NB, Bloch KD, Lincoln TM. Regulation of cGMP-dependent protein kinase expression by soluble guanylyl cyclase in vascular smooth muscle cells. *J Biol Chem* 2004;**279**:46631–46636.
12. Burgoyne JR, Madhani M, Cuello F, Charles RL, Brennan JP, Schröder E, Browning DD, Eaton P. Cysteine redox sensor in PKGIa enables oxidant-induced activation. *Science* 2007;**317**:1393–1397.
13. Prysyazhna O, Rudyk O, Eaton P. Single atom substitution in mouse protein kinase G eliminates oxidant sensing to cause hypertension. *Nat Med* 2012;**18**:286–290.
14. Stubbert D, Prysyazhna O, Rudyk O, Scotcher J, Burgoyne JR, Eaton P. Protein kinase G Iα oxidation paradoxically underlies blood pressure lowering by the reductant hydrogen sulfide. *Hypertension* 2014;**64**:1344–1351.
15. Ida T, Sawa T, Ihara H, Tsuchiya Y, Watanabe Y, Kumagai Y, Suematsu M, Motohashi H, Fujii S, Matsunaga T, Yamamoto M, Ono K, Devarie-Baez NO, Xian M, Fukuto JM, Akaike T. Reactive cysteine persulfides and S-polythiolation regulate oxidative stress and redox signaling. *Proc Natl Acad Sci U S A* 2014;**111**:7606–7611.
16. Fukuto JM, Ignarro LJ, Nagy P, Wink DA, Kevil CG, Feelisch M, Cortese-Krott MM, Bianco CL, Kumagai Y, Hobbs AJ, Lin J, Ida T, Akaike T. Biological hydropersulfides and related polysulfides—a new concept and perspective in redox biology. *FEBS Lett* 2018;**592**:2140.
17. Akaike T, Ida T, Wei FY, Nishida M, Kumagai Y, Alam MM, Ihara H, Sawa T, Matsunaga T, Kasamatsu S, Nishimura A, Morita M, Tomizawa K, Nishimura A, Watanabe S, Inaba K, Shima H, Tanuma N, Jung M, Fujii S, Watanabe Y, Ohmuraya M, Nagy P, Feelisch M, Fukuto JM, Motohashi H. Cysteinyl-tRNA synthetase governs cysteine polysulfidation and mitochondrial bioenergetics. *Nat Commun* 2017;**8**:1177.
18. Madhani M, Scotland RS, MacAllister RJ, Hobbs AJ. Vascular natriuretic peptide receptor-linked particulate guanylate cyclases are modulated by nitric oxide-cyclic GMP signalling. *Br J Pharmacol* 2003;**139**:1289–1296.
19. Pinder AG, Pittaway E, Morris K, James PE. Nitrite directly vasodilates hypoxic vasculature via nitric oxide-dependent and -independent pathways. *Br J Pharmacol* 2009; **157**:1523–1530.
20. Siddiqi N, Neil C, Bruce M, MacLennan G, Cotton S, Papadopoulou S, Feelisch M, Bunce N, Lim PO, Hildick-Smith D, Horowitz J, Madhani M, Boon N, Dawson D, Kaski JC, Frenneaux M, Siddiqi N, Neil C, Bruce M, MacLennan G, Cotton S, Dawson D, Frenneaux M, Singh S, Schwarz K, Jagpal B, Metcalfe M, Stewart A, Hannah A, Awsan N, Broadhurst P, Hogg D, Garg D, Slattery E, Davidson T, McDonald A, McPherson G, Kaski J-C, Lim PO, Brown S, Papadopoulou SA, Gonzalvez F, Roy D, Firoozi S, Bogle R, Roberts E, Rhodes J, Hildick-Smith D, de Belder A, Cooter N, Bennett L, Horowitz J, Rajendran S, Dautov R, Black M, Jansen E, Boon N, Struthers A, Toff W, Dargie H, Lang C, Nightingale P. Intravenous sodium nitrite in acute ST-elevation myocardial infarction: a randomized controlled trial (NIAMI). *Eur Heart J* 2014;**35**:1255–1262.
21. Pick E, Keisari Y. A simple colorimetric method for the measurement of hydrogen peroxide produced by cells in culture. *J Immunol Methods* 1980;**38**:161–170.
22. Krych-Madej J, Gebicka L. Interactions of nitrite with catalase: enzyme activity and reaction kinetics studies. *J Inorg Biochem* 2017;**171**:10–17.
23. Titov VY, Osipov AN. Nitrite and nitroso compounds can serve as specific catalase inhibitors. *Redox Rep* 2017;**22**:91–97.
24. Cortese-Krott MM, Fernandez BO, Kelm M, Butler AR, Feelisch M. On the chemical biology of the nitrite/sulfide interaction. *Nitric Oxide* 2015;**46**:14–24.
25. Titov VY, Petrenko YM. Nitrite-catalase interaction as an important element of nitrite toxicity. *Biochemistry (Mosc)* 2003;**68**:627–633.
26. Bogdandi V, Ida T, Sutton TR, Bianco C, Ditrói T, Koster G, Henthorn HA, Minnion M, Toscano JP, van der Vliet A, Pluth MD, Feelisch M, Fukuto JM, Akaike T, Nagy P. Speciation of reactive sulfur species and their reactions with alkylating agents: do we have any clue about what is present inside the cell? *Br J Pharmacol* 2019;**176**: 646–670.
27. Bianco CL, Akaike T, Ida T, Nagy P, Bogdandi V, Toscano JP, Kumagai Y, Henderson CF, Goddu RN, Lin J, Fukuto JM. The reaction of hydrogen sulfide with disulfides: formation of a stable trisulfide and implications for biological systems. *Br J Pharmacol* 2019;**176**:671–683.
28. Montenegro MF, Amaral JH, Pinheiro LC, Sakamoto EK, Ferreira GC, Reis RI, Marcal DM, Pereira RP, Tanus-Santos JE. Sodium nitrite downregulates vascular NADPH

oxidase and exerts antihypertensive effects in hypertension. *Free Radic Biol Med* 2011; **51**:144–152.
29. Singh M, Arya A, Kumar R, Bhargava K, Sethy NK. Dietary nitrite attenuates oxidative stress and activates antioxidant genes in rat heart during hypobaric hypoxia. *Nitric Oxide* 2012;**26**:61–73.
30. Bondonno CP, Liu AH, Croft KD, Considine MJ, Puddey IB, Woodman RJ, Hodgson JM. Antibacterial mouthwash blunts oral nitrate reduction and increases blood pressure in treated hypertensive men and women. *Am J Hypertens* 2015;**28**:572–575.
31. Shimokawa H, Morikawa K. Hydrogen peroxide is an endothelium-derived hyperpolarizing factor in animals and humans. *J Mol Cell Cardiol* 2005;**39**:725–732.
32. Kalyanaraman H, Zhuang S, Pfitz RB, Casteel DE. The activity of cGMP-dependent protein kinase Ia is not directly regulated by oxidation-induced disulfide formation at cysteine 43. *J Biol Chem* 2017;**292**:8262–8268.
33. Cuello F, Eaton P. Cysteine-based redox sensing and its role in signaling by cyclic nucleotide-dependent kinases in the cardiovascular system. *Annu Rev Physiol* 2019;**81**: 63–87.
34. Donzelli S, Goetz M, Schmidt K, Wolters M, Stathopoulou K, Diering S, Prysyazhna O, Polat V, Scotcher J, Dees C, Subramanian H, Butt E, Kamynina A, Schobesberger S, King SB, Nikolaev VO, de Wit C, Leichert LI, Feil R, Eaton P, Cuello F. Oxidant sensor in the cGMP-binding pocket of PKGIα regulates nitroxyl-mediated kinase activity. *Sci Rep* 2017;**7**:9938.
35. Akashi S, Ahmed KA, Sawa T, Ono K, Tsutsuki H, Burgoyne JR, Ida T, Horio E, Prysyazhna O, Oike Y, Rahaman MM, Eaton P, Fujii S, Akaike T. Persistent activation of cGMP-dependent protein kinase by a nitrated cyclic nucleotide via site specific protein S-guanylation. *Biochemistry* 2016;**55**:751–761.
36. Sheehe JL, Bonev AD, Schmoker AM, Ballif BA, Nelson MT, Moon TM, Dostmann WR. Oxidation of cysteine 117 stimulates constitutive activation of the type Iα cGMP-dependent protein kinase. *J Biol Chem* 2018;**293**:16791–16802.
37. Ono K, Akaike T, Sawa T, Kumagai Y, Wink DA, Tantillo DJ, Hobbs AJ, Nagy P, Xian M, Lin J, Fukuto JM. Redox chemistry and chemical biology of H_2S, hydropersulfides, and derived species: implications of their possible biological activity and utility. *Free Radic Biol Med* 2014;**77**:82–94.

Translational perspective

Despite current pharmacotherapies and interventional procedures, arterial hypertension remains a global health burden. Thus, novel therapeutic interventions are urgently required. Nitrite exerts vasorelaxant effects of potential therapeutic relevance under normal physiological conditions, yet the mechanism of action remain unknown. Here, we present evidence that in normoxia nitrite lowers blood pressure via a novel redox mechanism. This occurs independent of nitric oxide by generating hydrogen peroxide and persulfide, which subsequently activates PKG1α by oxidation. Targeting this novel pathway may provide new prospects for anti-hypertensive therapy and other cardiovascular-related diseases.

Appendix 3: NHSBT Donation Process – Selected documents

i. Donor health check for new and returning donors form (FRM form 421/6)

Donor Health Check for new and returning donors

Please answer the following questions to the best of your knowledge using black or blue ball point ink.
If you are uncertain of any answer or answer yes to any question please call the donor helpline on 0300 123 23 23 or visit www.blood.co.uk to check if you are eligible to donate. Please do not use correction fluid if you make a mistake.

No	Question	RF code	Yes	No	Staff
1	Are you taking any **prescribed** medicines or tablets or other treatments (except HRT for the menopause, the pill or other birth control)?				
2	**In the last 7 days** have you taken any **additional** medicines or tablets including any you have bought yourself?				
3	**In the last 7 days** have you seen a doctor, dentist, dental hygienist or any other healthcare professional or are you waiting to see one?				
4	**In the last 2 weeks** have you had any illness, infection or fever or do you think you have one now?				
5	**In the last 4 weeks** have you been in contact with anyone with an infectious disease?				
6	**In the last 8 weeks** have you had any immunisations, vaccinations or jabs (including smallpox)?				
7	**In the last 8 weeks** have you been in contact with anyone else who has had a smallpox vaccination?				
	In the last 3 months have you...	RF code	Yes	No	Staff
8	...had sex with anyone with Human T Cell Lymphotropic Virus (HTLV), Syphilis or anyone who is HIV positive?				
9	...been given money or drugs for sex?				
10	... had sex with anyone who has ever been given money or drugs for sex?				
11	...had sex with anyone who has ever injected drugs?				
12	...had sex with anyone who may ever have had sex in parts of the world where AIDS/HIV is very common (this includes most countries in Africa)?				
13	**Male donors only:** In the last 3 months have you had oral or anal sex with a man, with or without a condom?				
14	**Female donors only:** In the last 3 months have you had sex with a man who has ever had oral or anal sex with another man, with or without a condom?				
	In the last 12 months have you...	RF code	Yes	No	Staff
15	...had your ears, face or body pierced, had a tattoo or any cosmetic treatment that involved piercing your skin?	S			
16	...had acupuncture?	S			
17	...been exposed to someone else's blood or body fluids eg through a needle prick or bite or broken skin?	S			
18	...shared a home with a person with Hepatitis?	C			
19	...had sex with anyone with Hepatitis?	C			
	Additional information	RF code	Yes	No	Staff
20	Have you ever tested positive for HIV or do you think you may be HIV positive?				
21	Have you ever had Hepatitis or think you may have Hepatitis now?	J			
22	Have you ever injected yourself or been injected with illegal or non-prescribed drugs including body-building drugs or cosmetics or injectable tanning agents (even if this was only once or a long time ago)?				
23	Have you ever had or been treated for Syphilis?				
24	Have you ever been told that you should not give blood?				
25	Have you ever seen a doctor with any complaints about your heart or had any other serious illness?				
26	Have you ever had any hospital investigations, tests, operations or alternative therapies?	S/E			
27	Have you ever had jaundice?	J			
28	Have you ever received a blood or blood product transfusion?	T/R			
29	Have you or anyone in your family had Creutzfeldt-Jakob Disease (CJD)?				
30	Were you treated with growth hormone before 1985?				
31	Did you have brain surgery or an operation for a tumour or cyst in your spine before August 1992?				
32	**Female donors only:** Have you had fertility treatment or had IVF for any other reason since 1980?				
	Travel	RF code	Yes	No	Staff
33	**In the last 12 months** have you been outside the UK (inc. business trips)?	R			
34a.	Were you born or have you ever lived or stayed outside the UK for a continuous period of 6 months or more?	L			
b.	If 'yes' have you been outside the UK since then?	L			
35a.	Have you ever had malaria or an unexplained fever which you could have picked up while travelling or living or working abroad?	M/F			
b.	If 'yes' have you been outside the UK since then?	V			
36	Have you ever visited Central America, South America or Mexico for a continuous period of 4 weeks or more?	R			
37	Were you or your mother born in Central America, South America or Mexico?	L			

(IN CAPITALS)
Forename .....
Surname .....
Your Signature .....
Date ..... /..... /.....

STAFF USE ONLY

Withdraw/suspend until ...../...../.....
☐ Attention Clinical Support Team
☐ Medical Referal ☐ Set Medical Bar ☐ Additional notes

CLINICAL NOTES

☐ Suspend until ...../...../.....
☐ Withdraw
☐ Accept

Date ...../...../.....
CST/Donor Records
Signature .....

Page 1 of 2 DM01/18 FRM421/7

Version 7 08/01/18 **DONATION RECORD - NEW/RETURNING DONOR**

Surname Group

Forenames

Title DOB Gender Donor No

Address

Tel No

Procedure

Tel No. (day)

Outcome of Attendance

01 Donated
02 Low Hb
03 Other samples only
04 No Donation - No numbers
05 No Donation - Numbers issued
06 No Donation - Pack labelled

PACK HOLD CODE

Signature .....

Donation No

Code

BBMR

Total

Award

Attendance Outcome

Date

Panel

Sub Panel

P:
T:

DONATION TYPE: Whole Blood ☐ Apheresis ☐ ..... Autologous Tears ☐

I have completed my tasks in accordance with SOPs	Signatures
Registration	
Health Check	
Hb Pass ☐ Fail ☐	
Session Hb result ..... g/L	
Machine/Pack set up	
CD Second check	
Venepuncture	
Needle Removal	
Dressing/PD advice	
Final Pack/Sample Check	
Reconciliation	

Incident Record

Malaria (MA)

R DD MM YY
L DD MM YY
T DD MM YY

M DD MM YY
V DD MM YY
F DD MM YY

T-Cruzi (TC)

R DD MM YY
L DD MM YY

West Nile Virus (WN)

R DD MM YY
F DD MM YY
W DD MM YY

Sickle Test ☐
Ethnic Code ☐

HBV (AC)

S DD MM YY
J DD MM YY
C DD MM YY
E DD MM YY

Arm used L ☐ R ☐

Needle adjusted Y ☐

Signature

Donor Consent – to be signed in the presence of a member of NHSBT staff

1. I have today read and understood the Welcome Booklet. I have been given the opportunity to ask questions and they have been answered.
2. To the best of my knowledge I am not at risk of infection or of transmitting the infections listed in the Welcome Booklet.
3. I agree that my blood donation may be tested for HIV and other conditions listed in the Welcome Booklet. I understand that if my donation gives a positive result for any of these tests I will be informed and asked to participate in a post-test discussion.
4. I understand and accept the nature of the donation process and the possible risks involved as explained in the risk section on pages 6,7 & 8 of the Welcome Booklet.
5. I agree to NHS Blood and Transplant holding information about me, my health, my attendances and donations, to contacting my doctor for further information and using my information for the purposes explained in the Welcome Booklet and the data protection leaflet.
6. I give my blood to NHS Blood and Transplant to be used for the benefit of patients. This may be by direct transfusion to a patient or for other purposes as explained in the Welcome Booklet.

Donor Signature _____ Date DD MM YY

FOR STAFF USE ONLY

ii. Autologous blood pre-donation assessment form (FRM 1560/4 – cross referenced in primary document MPD 757)

FORM FRM1560/4 Effective: 01/04/14

Affix Unit Address

AUTOLOGOUS BLOOD PRE - DONATION ASSESSMENT

NHS Blood and Transplant

Patient Name:	D.O.B.	Hospital/NHS No:

Please complete section 1 of this form and bring with you to your appointment

(Section 1 – to be completed by the patient)

1	Have you ever been told you that should not give blood or that we could not accept a blood donation from you?	**Yes / No**
If "**Yes**", please give details		
2	Have you ever been a blood donor?	**Yes / No**
3	If "**Yes**", did you ever have any problems when donating or feel unwell afterwards?	**Yes / No**
If "**Yes**", please give details		
4	Are you fit and well?	**Yes / No**
If "**No**", please give details		
5	Do you take any tablets or medicines?	**Yes / No**
If "**Yes**", please list		
6	Have you ever had a serious illness?	**Yes / No**
If "**Yes**", please give details		
7	Have you ever had an operation?	**Yes / No**
If "**Yes**", please give details		
8	Have you ever had or are you prone to fainting or dizzy spells?	**Yes / No**
9	Have you ever had raised blood pressure?	**Yes / No**
10	Do you get breathless after slight exertion?	**Yes / No**
11	Have you ever had or do you suffer from now, chest pain, angina or any other heart problem?	**Yes / No**
If "**Yes**", please give details		
12	Have you ever had a stroke or mini stroke?	**Yes / No**
13	Do you get pains in your legs when walking a short distance?	**Yes / No**
14	Have you ever had a fit?	**Yes / No**
If "**Yes**", please give details		
15	Are you HIV positive or do you think you might be HIV positive?	**Yes / No**
16	Have you ever had Hepatitis B or Hepatitis C or do you think you may have hepatitis now?	**Yes / No**
17	Have you ever had Syphilis or do you think you may have Syphilis now?	**Yes / No**
18	Do you have any infections at the moment?	**Yes / No**
If "**Yes**", please give details		

Patient Name ..... Signature ..... Date.....

(Template Version 01/08)

Cross-Referenced in Primary Document:MPD757 Page 1 of 2

NHS Blood and Transplant

Patient Name:	D.O.B.	Hospital/NHS No:

(Section 2 to be completed by NHSBT staff only)

Comments on patient's answers to healthcheck questions	
Is patient fit for autologous donation?	**Yes / No**
If "**No**", please give specific details	

(Name, Signature and Designation of HCP performing health assessment)

Name..... Signature.....

Designation.....Date .....

PULSE Donor Number	

Details of Consumables

Item	Manufacturer	Lot No:	Expiry Date	Visual Check OK √

iii. Pre-deposit autologous blood donation memorandum (FRM 1563/1.4 – cross referenced in primary document SOP 3968)

FORM FRM1563/1.4

Effective: 02/04/14

NHS
Blood and Transplant

Affix Unit Address label here

PRE-DEPOSIT AUTOLOGOUS BLOOD DONATION MEMORANDUM

Pre-Deposit Autologous Blood Donation

To: ..... (Processing manager) (Issue Manager) (DCM)

Copies: ..... (ASE Lead Consultant)

From: ..... (Blood Donation Consultant)

Date: .....

Re: ..... (Patient's name) **DOB:** .....

Address: .....

.....

.....

Hospital: .....

Hospital/ NHS No: ..... **Consultant:** .....

This patient will attend the ..... (Session venue) on the following dates:

1..... 2 ..... 3..... 4.....

to donate a unit of blood for predeposit autologous use. I enclose a copy of the patient's previous health questionnaire (if applicable).

The normal donation procedure should be followed as usual with the following exceptions:

1. Screen the donor according to SOP3968.
2. The patient's donation must be collected into Machopharma MSG6500LB pack
3. The attached pack label must be fully completed
4. An FBC sample must be collected at time of donation
5. The unit must be placed in a separate transport bag/box clearly labelled "Autologous Blood"
6. FRM410 must be fully completed and placed with pack in transport container

7. Any specific donation instructions .....

Any problems, please contact: .....
(Blood Donation Consultant)

(Template Version 01/04)

Cross-Referenced in Primary Document: SOP3968

Page 1 of 1

iv. SOP3968 (Change Control [6422] Process Flow)

Person/Dept Responsible	**Task**
Research team	FRM1560 at time of study consent to ensure that subjects are fit to donate. FRM1560 then sent to Clinical Support Team (CST) as per SOP3968.
CST	CST forwarded FRM1560 to Donor Records instructing them to register the trial participant as an Autologous Donor (AWB as default procedure).
Planning	Planning create the appropriate panel number so that donors can be slotted into the required session
CST/Donor Records	CST verifies this prior to donation and enters the appropriate Panel Number (created by Planning). Donors registered at least 2 weeks prior to donation date
CST	CST to send FRM1563 to all relevant parties within a week prior to the collection of the unit as per SOP3968
Donor Records	2 USB sticks to be supplied to Thetford Team (responsible for Fakenham and Wymondham donation sites) such that the study donors are inputted on a separate USB to the rest of the session
Blood Donation	Donors bled into Macopharma MSG6500LC pack on the allocated date as coordinated by research team. After a successful donation, FRM410 should be sent with each donation in a plastic wallet. A copy of FRM410 forwarded to CST. CST will cascade this form to Research Team and NNUH Blood bank to inform the donation number of each donor with 3 points of ID
Blood Donation	DHCs for Study donors to be placed in a separate Green Wallet. Also, separate USB stick (provided by Donor records) is to be used for study donors
Hospital Services Cambridge	Wallet and USB received from Transport. HS Cambridge will update the USB stick and segregate the autologous units into easily identifiable crates that will be transported on the BMV transport to Manufacturing Colindale. Hardcopy FRM410 to accompany the units
Manufacturing Colindale	Receive autologous units and follow SOP1157 (PCS20 and PCS22). Hierarchy code (SG0051). Place in labelled cage in Cold Room. Inform Hospital Services Colindale that unit is ready to be sent back to Cambridge, once test results are available
Hospital Services Colindale	Validate the units as per SOP1157. Stock move to Cambridge Hospital Services (PCS80 and PCS81) via BMV transport
Hospital Services Cambridge	Receive autologous units using PCS81. Transfer units to crate in locked cage in Cold Room
Research team/NNUH Blood bank	Request units (fax) as per FRM410 using a non-standard request form requesting date required at NNUH Blood bank
Hospital Services	Create order for NNUH (PCS80) and Issue via PCS81

Appendix 4: The Haem and Nitrite Study – Selected documents

i. The Haem and Nitrite Study – Study specific prescription/drug chart

IRAS NUMBER: 206995
Page 1/2

Norfolk and Norwich University Hospitals NHS
NHS Foundation Trust

Haem Nitrite Study Prescription Chart

E

Admission Date	Ward	Consultant(s)
	CRTU	Fletcher/Frenneaux

Admission Number: 1 ☐ or 2 ☐

Patient Label:

Name:

DOB:

HN:

NORMOXIA COHORT ☐
Dosing: 3umol/min-1 for 30 minutes

HYPOXIA COHORT ☐
1umol/min-1 for 30 minutes

Allergies & Sensitivities:
If none, state "None". Record source of information e.g. "patient", "notes" etc

Latex Allergy ☐ Yes ☐ No

Name	Sign	Date

All Prescribers MUST complete the Signature Record (including signature as used on the prescription chart)

Date	Name (Capitals):	Status	Sign:
	Dr ND Gollop	Clinical Research Fellow	
	Dr BL Loudon	Clinical Research Fellow	

Noticeboard (tick if complete)

Consent ☐
Admitted on PAS ☐
Hospital number issued ☐
Wrist band issued ☐
Clerked ☐
Cross match and group and save sent ☐
Blood Unit tested ☐
Baseline Observations and Bloods ☐

Admission Assessment Completed By:	Name:	Sign:	

Once-only Drugs

Date to be given	Time to be given	Drug (approved name)	Dose	Route	Prescriber's Signature & Bleep	Given by	Time Given	Pharmacy
		Sodium Nitrite		Intra-arterial	/07961716357			
		Sodium Nitrite		Intra-arterial	/07961716357			

Intravenous Fluids

Date	Intravenous Fluids and Blood Products	Volume	Additive & Dose	Duration (hrs) or rate (ml/hr)	Prescriber's Signature and Bleep	Given By	Start Time	End Time
	Normal 0.9% Saline	200ml	None	1ml/min-1	/07961716357			

Blood Products – Use for ALL blood components

Instructions

- Prescribers MUST complete all relevant sections for each blood product prescription.
- Any accompanying medications (e.g. Furosemide must be recorded in the 'Once Only' section of the Prescription Chart

Blood products include:

Obtained from Blood Bank
All products from blood bank must be double checked by 1 person and an electronic bedside check

Guidance: NNUH Trust guidelines CA4029 v3, CA1026 v10, CA1027 v10, CA2057 v5
Care: NNUH Trust guidelines Care Domain 4 v2.1

Obtained from Pharmacy:
All products from pharmacy must be double checked with a 2nd person bedside check

Nurse checked: signature, unit, name, DOB, HN ☐
Research Doctor checked – all above ☐

Date	Blood Product (include any special requirements)	Unique Research Identifiable Number	Volume or Dose	Route	Duration (hrs) or rate (ml/hr)	Prescriber's Signature and Bleep Number	Given By	Start Time	End Time
	Autologous whole blood		470mls/1 unit	Intravenous	2 hours	/07961716357			

IRAS NUMBER: 206995 - Haem Nitrite Study Prescription Chart
Page 2 / 2

Norfolk and Norwich University Hospitals NHS
NHS Foundation Trust

Patient Label:

Name:

DOB:

HN:

NORMOXIA COHORT ☐ HYPOXIA COHORT ☐

Oxygen Therapy

Time of oxygen administration ▼ | Date ▶

Target SpO_2 (%) According to Random Order Sequence

Hypoxia: 83-88% ☐ Normoxia 94-98% ☐

Comments:

Prescriber's Signature | Bleep No

1		
2		
3		
4		

During hypoxia protocol – induce hypoxia at the following times (5 mins of 12% oxygen and check saturations):

1. Baseline FBFR
2. At 5m, 12m, 20m in Nitrite 1
3. 90mins into blood transfusion
4. At 5m, 12m, 20m in Nitrite 2

As Required prescriptions (Anaphylaxis bundle prescription 4-6)

1. Drug (approved name) **LIGNOCAINE HYDROCHLORIDE**		Start Date	Stop Date	Date/ Time				
Dose **1% up to 10mls**	Indication **Local Anaesthesia**	Route **SC**	Frequency	Dose				
Prescriber's Signature – must be present before administering this prescription		Bleep No 07961716357		Given By				
2. Drug (approved name) **PARACETAMOL**		Start Date	Stop Date	Date/ Time				
Dose **1g**	Indication **Pain**	Route **PO**	Frequency **QDS**	Dose				
Prescriber's Signature		Bleep No 07961716357	Pharmacy	Given By				
3. Drug (approved name) **ONDANSETRON**		Start Date	Stop Date	Date/ Time				
Dose **4mg**	Indication **Vomiting**	Route **IV**	Frequency **OD**	Dose				
Prescriber's Signature		Bleep No 07961716357	Pharmacy	Given By				
4. Anaphylaxis Drug (approved name) **ADRENALINE**		Start Date	Stop Date	Date/ Time				
Dose **1:1000, 500micrograms**	Indication **Anaphylaxis**	Route **IM**	Frequency REPEAT AFTER 5 MINUTES IF NO BETTER	Route & Dose				
Prescriber's Signature		Bleep No 07961716357	Pharmacy	Given By				
5. Anaphylaxis Drug (approved name) **CHLORPHENAMINE**		Start Date	Stop Date	Date/ Time				
Dose **10mg**	Indication **Anaphylaxis**	Route **IM or SLOW IV**	Frequency	Route & Dose				
Prescriber's Signature		Bleep No 07961716357	Pharmacy	Given By				
6. Anaphylaxis Drug (approved name) **HYDROCORTISONE**		Start Date	Stop Date	Date/ Time				
Dose **200mg**	Indication **Anaphylaxis**	Route **IM or SLOW IV**	Frequency	Route & Dose				
Prescriber's Signature		Bleep No 07961716357	Pharmacy	Given By				

IRAS NUMBER: 206995 - Haem Nitrite Study Prescription Chart
Additional PRN Prescription Chart

Norfolk and Norwich University Hospitals NHS
NHS Foundation Trust

Patient Label:

Name:

DOB:

HN:

NORMOXIA COHORT ☐ **HYPOXIA COHORT** ☐

As Required prescriptions

1. Supplementary Drug (approved name)		Start Date	Stop Date	Date/ Time				
Dose	Indication	Route	Frequency	Dose				
Prescriber's Signature		**Bleep No**		Given By				
2. Supplementary Drug (approved name)		Start Date	Stop Date	Date/ Time				
Dose	Indication	Route	Frequency	Dose				
Prescriber's Signature		**Bleep No**	Pharmacy	Given By				
3. Supplementary Drug (approved name)		Start Date	Stop Date	Date/ Time				
Dose	Indication	Route	Frequency	Dose				
Prescriber's Signature		**Bleep No**	Pharmacy	Given By				
4. Supplementary Drug (approved name)		Start Date	Stop Date	Date/ Time				
Dose	Indication	Route	Frequency	Route & Dose				
Prescriber's Signature		Bleep No	Pharmacy	Given By				
5. Supplementary Drug (approved name)		Start Date	Stop Date	Date/ Time				
Dose	Indication	Route	Frequency	Route & Dose				
Prescriber's Signature		Bleep No	Pharmacy	Given By				
6. Supplementary Drug (approved name)		Start Date	Stop Date	Date/ Time				
Dose	Indication	Route	Frequency	Route & Dose				
Prescriber's Signature		Bleep No	Pharmacy	Given By				

ii. Autologous whole blood: pre-transfusion safety checklist

'Autologous Whole Blood' check prior to administration for 'Haem and Nitrite' study

Name of participant:_____ Date of birth_____

Name of researcher:_____ Name of nurse:_____

Date of study:_____

ACTION	Yes/ No	Initials of individual confirming
Has the blood been appropriately requested on ICE stating: *"This is a request for one unit of AUTOLOGOUS whole blood for the Haem and nitrite study."*?		
Once the blood request has been received from the research team, have the hospital routine procedures regarding blood transfusion (as identified in NNUH Trust guidelines CA1026 v10, or updated version and CA2057 v5, or updated version been followed), including electronic confirmation, been confirmed?		
Does the allocated unit indicate that it is "Whole blood Autologous" in position A of Figure 1 below?		
Does the allocated unit indicate correctly that it is "Autologous transfusion" and have the signature of the volunteer, as shown in position B of Figure 1 below?		
Can the volunteer confirm their signature on the sticker/sleeve of the autologous blood?		
IF THE ANSWER TO ANY OF THE QUESTIONS IS "NO", DO NOT PROCEED WITH THE TRANSFUSION AND CONTACT THE SENIOR BIOMEDICAL SCIENTIST.		

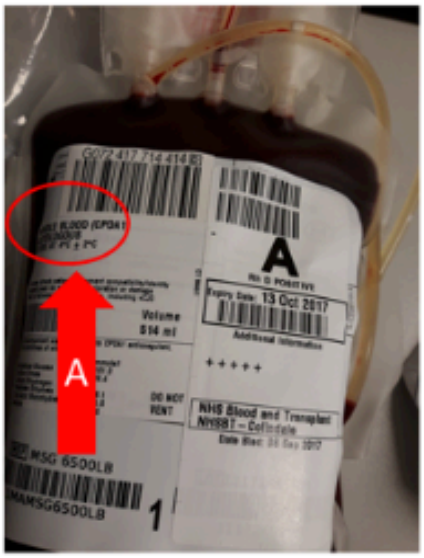

Figure 1: Anonymised sample of 'Whole blood autologous'

This indicates two unique identifiers: **arrow A**, indicating that this is "Whole blood Autologous" and **arrow B**, indicating it is autologous blood and on the sleeve the signature of the volunteer should be identified

Appendix 5: NOx sample processing methodology

The determination of nitrite and nitrate

Apparatus

3.1. Analytical balance measuring down to four or five decimal places.
3.2. Volumetric flask, 2000 mL
3.3. Microcentrifuge tubes of various volumes
3.4. Adjustable volume pipettes
3.5. TissuLyser LT or equivalent
3.6. Vortex-Genie touch mixer or equivalent
3.7. Eppendorf Centrifuge 5415D or equivalent of high speed centrifuge
3.8. Timer/stopwatch
3.9. Fisher Scientific FS30 sonicating bath or equivalent
3.10. Eicom NOx Analyser (ENO-20) with spectrophotometric detector
3.11. Gilson 234 autoinjector or equivalent
3.12. Precolumn NO-PRE
3.13. Separation column NO-PAK
3.14. Reduction column NO-RED

Reagents

4.1. MQ water, ultra-pure, in house
4.2. Sodium nitrite, 99.99% ex Sigma or equivalent
4.3. Sodium nitrate, 99.99% ex Sigma or equivalent
4.4. Methanol, AR (ACS) reagent grade ex Sigma or equivalent
4.5. 10% Methanol Solution
Measure 100mL of methanol and 900mL of MQ water separately and mix them together.
4.6. Methanol, CHROMASOLV, gradient grade, >99.9% or equivalent
4.7. Acetone, AR (ACS) reagent grade ex Sigma or equivalent
4.8. Hydrochloric acid, 37%, AR (ACS) reagent grade ex Sigma
4.9. 2.5% volume of 37% hydrochloric acid (12.1 M) in 10% methanol (0.925% hydrochloric acid in 10% methanol)
Put approximately 400mL of 10% methanol solution into a 500mL volumetric flask. Add 12.5mL of 37% hydrochloric acid and make up to volume with 10% methanol, mix.
4.10. Sodium phosphate dibasic, Na_2HPO_4, AR (ACS) reagent grade ex Sigma or equivalent
4.11. Sodium phosphate monobasic, NaH_2PO_4, AR (ACS) reagent grade ex Sigma or equivalent
4.12. Phospate Buffered Saline (PBS buffer)
Weigh out approximately 1.14 g of Sodium phosphate dibasic (Na_2HPO_4) and 0.24 g of Sodium phosphate monobasic (NaH_2PO_4), and 8.7 g of sodium chloride (NaCl) into the 1L Duran bottle or equivalent. Add approximately 950ml of MQ water and stirring bar and place the bottle on the magnetic stirrer until everything is dissolved. Check pH of the

solution and if required adjust it to pH 7.4. Transfer the contents into the 1L volumetric flask and make up to volume with MQ water.

4.13. N-ethylmaleimide (NEM), ≥98% HPLC ex Sigma or equivalent

4.14. EDTA, 0.5M, pH 8.0, Ultra Pure, Gibco or equivalent

4.15. PBS buffer with NEM/EDTA (homogenisation buffer)

Weigh out approximately 1.14g of Sodium phosphate dibasic, 0.24g of Sodium phosphate monobasic, 8.7 g of sodium chloride, 1.25g of NEM and add 5mL of 0.5M EDTA into the 1L Duran bottle or equivalent. Add approximately 950ml of MQ water and stirring bar and place the bottle on the magnetic stirrer until everything is dissolved. Check pH of the solution and if required adjust it to pH 7.4. Transfer the contents into the 1L volumetric flask and make up to volume with MQ water.

4.16. Carrier Powder EI-NO-CAP3 ex Eicom

4.17. Carrier Solution

Mix the carrier powder with 1000mL of 10% methanol.

4.18. Reactor A Powder EI-NO-RAP3 ex Eicom

4.19. Reactor A solution

Mix the reactor powder A with 500mL of 2.5% volume of 37% hydrochloric acid in 10% methanol. Cover the bottle with aluminium foil.

4.15. Reactor B Powder EI-NO-RBP3 ex Eicom

4.14. Reactor B solution

Mix the reactor powder B with 500mL of 10% methanol. Cover the bottle with aluminium foil.

4.15. Reactor solution

Mix an equal volume of reactor A solution and reactor B solution and cover the bottle with aluminium foil. Only make up the amount needed for the day, plus extra 20%.

Method

Standard

Preparation of stock solution

Dissolve an accurately weighed 0.008 ± 0.0001 g of sodium nitrite and 0.010 ± 0.001 g of sodium nitrate in a 2L volumetric flask with MQ water to obtain a solution of known concentration of approximately 58µM and 59µM nitrite and nitrate respectively.

$$\text{Concentration of nitrite (µM)} = \frac{\text{Weight standard (g)} \times 1000 \times 1000}{69\ \text{(g/mol)} \times 2\ (\text{dm}^3)}$$

$$\text{Concentration of nitrate (µM)} = \frac{\text{Weight standard (g)} \times 1000 \times 1000}{85\ \text{(g/mol)} \times 2\ (\text{dm}^3)}$$

69 g/mol and 85 g/mol are the approximate molecular weights of sodium nitrite and sodium nitrate, respectively.

Calibration curve standards

The linearity of response for nitrite and nitrate has been demonstrated from 0.1 µM to 30 µM. Prepare the standards once a week in buffer (PBS) of the following concentration: 0.1 µM, 0.5 µM, 1.0 µM, 5.0 µM, 10 µM, 20 µM and 30 µM. Please see the Table 1 for the examples of dilutions.

Table 1. Calibration curve standard dilutions

Std code	Volume taken (mL)	Solution used	Volume of buffer solution added (mL)
30µM	0.26	stock solution (58/59 µM)	0.24
20µM	0.17	stock solution (58/59 µM)	0.33
10µM	0.30	20µM	0.30
5.0µM	0.20	10µM	0.20
1.0µM	0.10	10µM	0.90
0.5µM	0.10	5.0µM	0.90
0.1µM	0.10	1.0µM	0.90

The correlation (R^2) should be >0.99.

Note: Once the estimated levels of analytes in the samples are established, the number of standards may be decreased (i.e. if there is a small range, then use less standards within the range). For trace analyses emphasis may need to be placed on the lower concentration end, requiring further dilution down to 10 nM.

Sample preparation

Blood (serum or plasma) sample

If there is sufficient amount of sample for all required analysis, take 100µL of sample and mix it with an equal amount of methanol in a microcentrifuge tube. Vortex the mixture for 1 minute

and then centrifuge it for 20 minutes at the highest speed of the centrifuge (at 4°C). Transfer 100µL of supernatant into a Gilson autosampler vial. This is our 'neat' sample.

If the concentration of NO_2^- or NO_3^- is outside the standard calibration curve dilute the sample with buffer solution and repeat measurement. This is our 'diluted' samples.

Instrument preparation prior to analysis

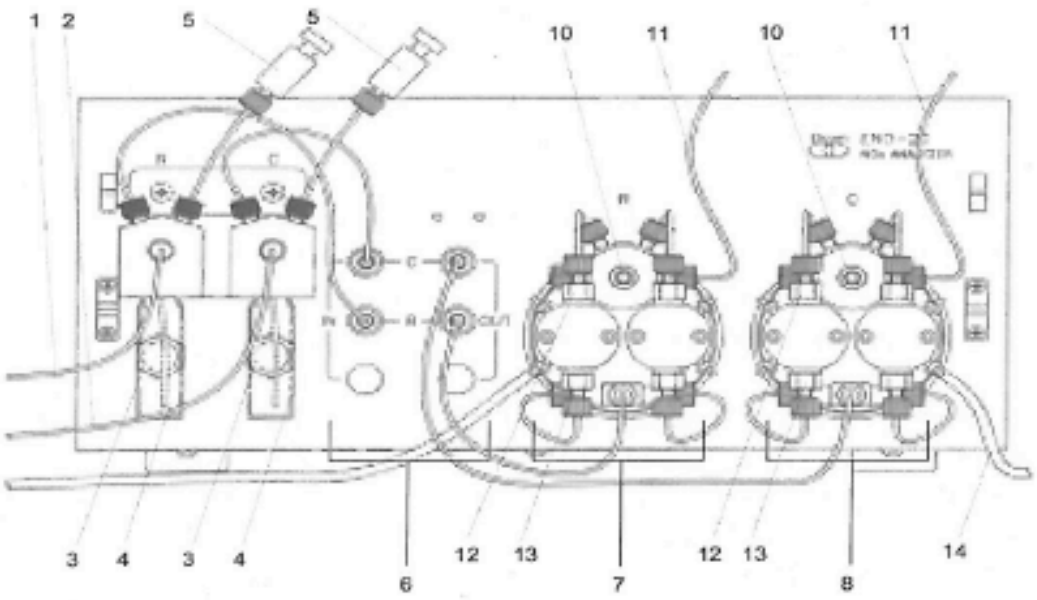

Figure 1. ENO-20 Front lower-body diagram.

1. Reactor Inlet Tube
2. Carrier Inlet Tube
3. Reagents Level Sensor
4. Air Trap Glass Tubes for reactor ('R') and carrier ('C')
5. Air Trap Purge Drain for reactor ('R') and carrier ('C')
6. Degasser
7. Reactor Pumps
8. Carrier Pumps
9. N/A
10. Purge Drain Valves
11. Pump Outlet Tubes
12. Outlet Check Valves
13. Inlet Check Valves
14. Pump Wash Drain

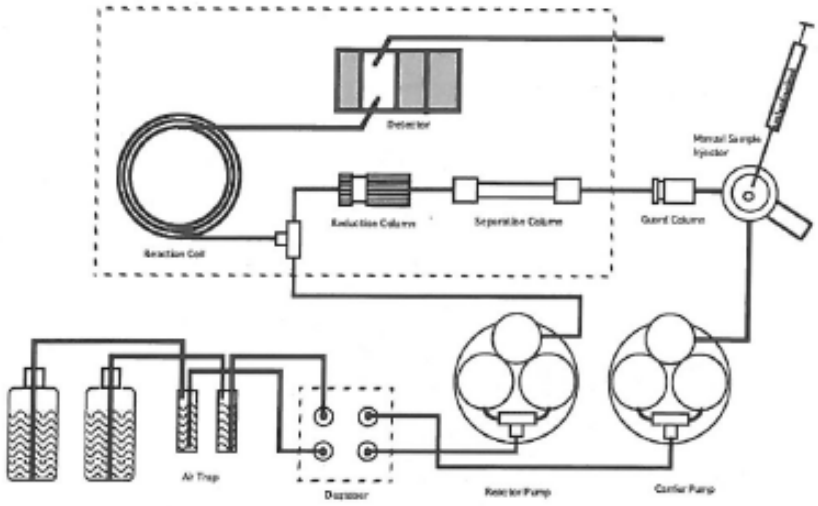

Replacing the carrier and reactor solutions (Figure 1)

- Open shaded dark cover at the front bottom of ENO-20.
- Check if the reactor airtrap glass tube (4) and the tubing line leading to the inlet (1) are stained. If they are, put the end of the reactor inlet tube (1) into the bottom of the bottle with methanol (section 4.2), open the stopper on the air trap purge drain (5) and aspirate methanol into lines and trap using a 10 mL plastic syringe. Repeat until lines and the glass tube are colourless. Cotton tipped applicators dipped in 100% methanol can also be used to scrape off highly stained glass and lines.
- Prepare the fresh carrier and reactor solution as described in section 4.0.
- Put the end of the reactor inlet tube (1) into the bottom of the bottle with fresh reactor solution, open the stopper on the air trap purge drain (5) and aspirate 1-2 ml of reactor solution into the reactor glass tube and discard. Repeat this procedure three times to ensure only fresh reactor solution is present in the lines and the reactor glass trap. Fill the reactor glass tube.
- Put the end of the carrier inlet tube (2) into the bottom of the bottle with fresh carrier solution, open the stopper on the air trap purge drain (5) and aspirate 1-2 ml of carrier solution into the reactor glass tube and discard. Fill the carrier trap glass tube.
- Return shaded dark cover to front bottom of ENO-20.

Preparation of the pre-column

- Turn on power button (blue) at the front of the ENO-20. Allow a few minutes for pumps to power up.
- Shut down pumps by manually pressing 'PUMP' button of reactor and carrier before opening the unit from the top

- Open the top of ENO-20 and detach the guard column. Put the stop fit (closed-end ferrule) at the inlet of the separation column to avoid drying out and close off any other open tubings at all ends.
- Open the guard column with supplied spanners (see Figure 3) and flush out the old packaging gel using the syringe and connector (see Figure 4). Flush with acetone both sides of guard column (packaging gel container end and the filter end). Clean the internal surface of the column with a cotton tipped applicator to remove residual packing gel.
- Check the pressure through both parts of the guard column to check for any blockages on the filter

- Pour 30 ml of acetone into the glass bottle containing dry packaging gel and shake the bottle until the powder is suspended in the acetone. (You may use pre-made packing gel material, if available)
- Connect the aspiration adapter to the downstream side of the column and attach the syringe containing about 0.5 ml of acetone (as shown on Figure 4).
- Slowly fill guard column with packaging gel using 200 µl pipette while simultaneously aspirating acetone from packaging gel (see Figure 5). DO NOT allow the gel to dry out.

Repeat this procedure several times until the pre-column is filled with the gel. Connect the upstream side and fasten the nut.

- Using the arrow on the guard column as a guide, flush the packed guard column with 2-3 ml of methanol in the same direction as the arrow (see Figure 6) and repeat the same procedure with 2-3 ml of MQ water.

Note: If significant pressure is required to flush the packaging gel with MeOH it is likely that the pre-column upstream filter is blocked and need replacing. The filter can be removed using the filter screw shown on Figure 7.

- Reattach the guard column to carrier line keeping the left side of the guard column open and turn on the carrier pump to flush the guard column with carrier solution for 3-5 min (collecting in either a beaker or folded Kimwipe for any excess liquid).
- Connect guard column with the separation column.

Turn on the reactor pump and ensure there are no leaks from connections/column before closing the upper cover

Preparation of the autosampler

- Visually check if there are no obstructions in the path of the syringe to avoid potential problems
- Press Manual on autosampler display and prime the lines to remove bubbles from coiled line, syringe and lines leading to 10% methanol reservoir. Keep it active until all lines are devoid of bubbles and then press stop.
- Press Manual on autosampler display and rinse injection port 3 times prior the analysis.

Running samples

- Open **Powerchrom** on the attached computer
- Click **File** and then **Open** and choose any recent method file (usually saved in the following format: initials_colllaborator project.pfwseq). It opens the sequence list and the method (the method should have a runtime of 5.7 to 10 min, depending on analyses performed)
- Modify the sequence list to specify blanks, standards and samples.
- Place the appropriate samples into the matching positions of the autosampler.
- **Save** new method file and **close** it.
- Click **File** and **Run** chosen method file and assign a location and a new name for data collection. A new Powerchrom file will begin and will wait for the trigger to collect the data.
- Begin the autosampler by selecting **Run** on the display and assigning the start of the samples (usually at position '1') then **Enter** on display. Assign the total number of samples and then click **Enter** to input the value. Click **Next** until the option to **Start** appears.
- Pressing Start will begin the program for the Autosampler and the Powerchrom will receive the trigger to start.
- Data will automatically begin saving.
- Allow the run to complete.
- Once completed, a new box will appear on the upper right saying 'Finished'.
- Select **OK** on the computer and shut down ENO-20 by pressing blue power button.

Integration of peaks

- Open the first run of file
- Click on the **Add** icon (↔)
- Position the mouse at the start of the peak and hold onto left button of the mouse to signify the start of the peak for integration, drag the mouse to the end of the peak and release the left button of the mouse.
- Repeat the steps above for other samples in the same run.
- Type integration values (peak areas) into Excel (or equivalent) file to facilitate final calculations

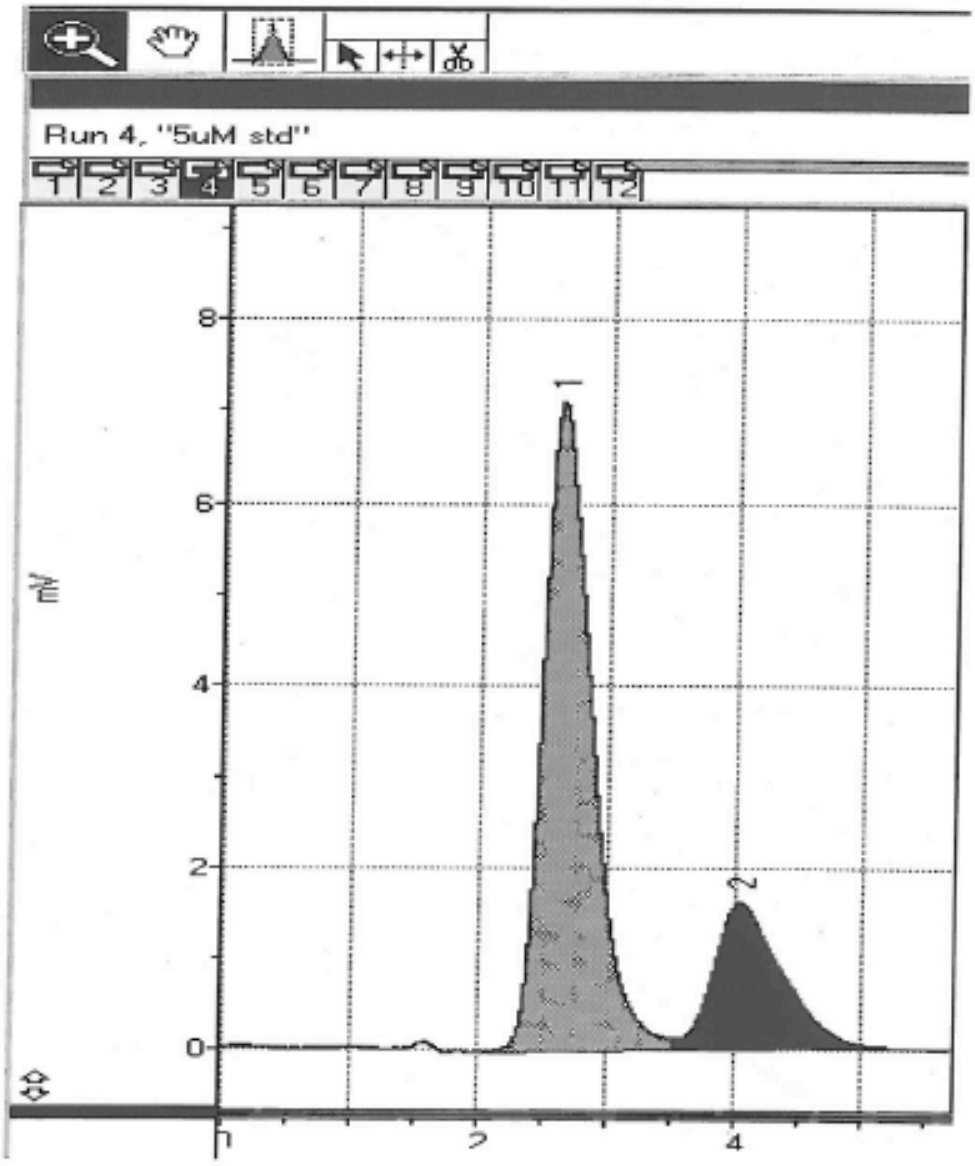

Calculation of final peaks

- Generate regression lines of concentrations versus peak areas for nitrite and nitrate standards and force it through zero (see Figure 9 and 10).
- Using the generated equations calculate the 'on column' concentrations of nitrite and nitrate in the analysed samples

Area = slope * Concentration

$$\text{'On column' Concentration (µM)} = \frac{\text{Area}}{\text{slope}}$$

- To obtain final concentration on nitrite and nitrate in the sample, multiply the 'on column' concentration by the dilution factor.

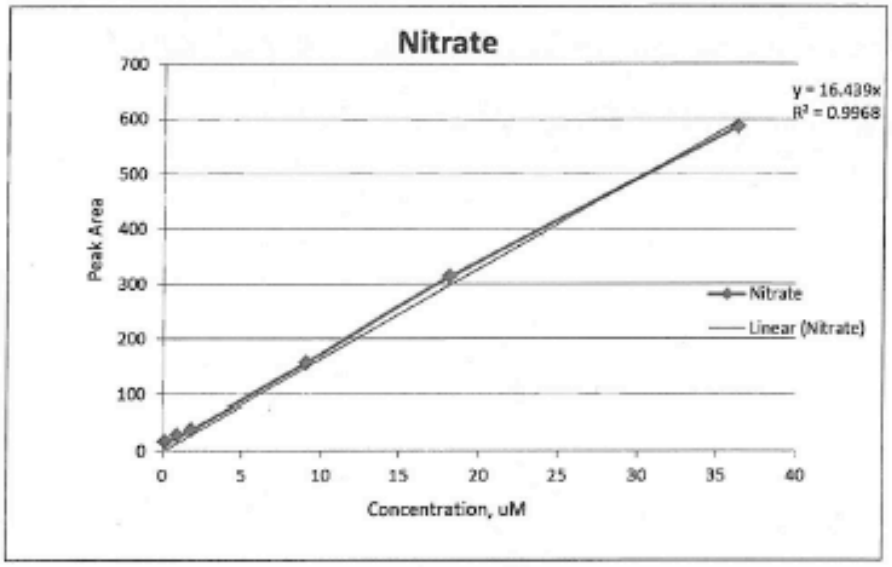

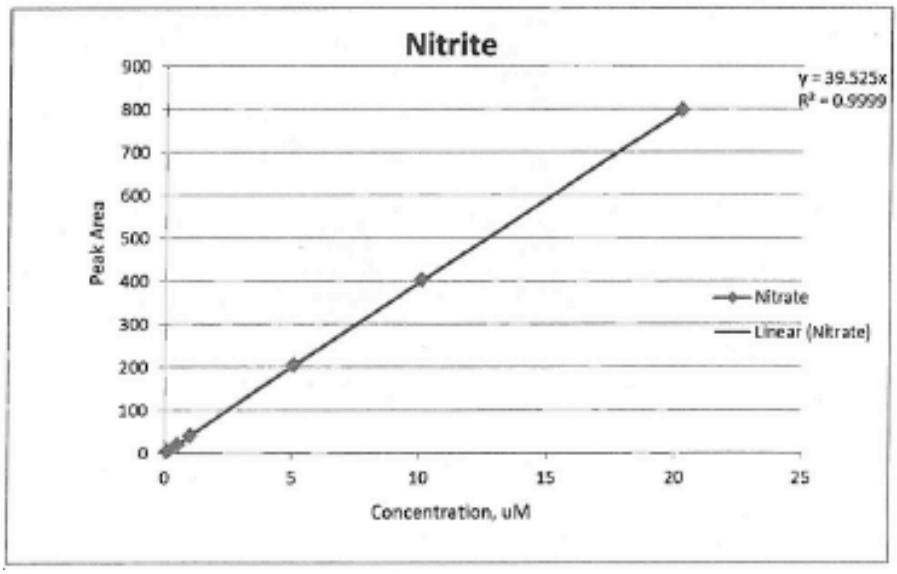

Determination

Analyse the standards and samples under listed conditions by HPLC.

Run blank samples at the beginning of the run and then inject standards and samples. Standard positions should be spread out to span the entire run (for example: one or two standards at the beginning, in the middle and at the end).

The typical retention time of nitrite is 2.8 min and nitrate 4.4 min for a 5.7 min method run (4.7 min for nitrite and 7.0 for a 10 min method run).

5.4. HPLC CONDITIONS

Injection volume:	20µl
Total volume aspirated by autosampler :	35 uL
Columns:	Precolumn NO-PRE Separation column NO-PAK Reduction column NO-RED
Columns temperature:	35°C
Flow rates:	Shorter Method (5-6 min): Carrier pump: 0.6 ml/min Reactor pump: 0.2 ml/min Routine Method (8-10 min) – manufacturer suggestion: Carrier pump: 0.33 ml/min Reactor pump: 0.11 ml/min
Detection wavelength:	540 nm (fixed)
Run time:	5.75 minutes or 10 min

Appendix 6: RXNO sample processing methodology

The determination of S-, N-, and heme-nitros(yl)ated species

Apparatus:

- Analytical balance weighing to four or five decimal places
- Volumetric flask, 2000 mL
- Microcentrifuge tubes of varies volumes
- Adjustable volume pipettes
- Gas-tight Hamilton syringes of varies volumes
- TissuLyser LT or equivalent
- Vortex-Geni touch mixer or equivalent
- Eppendorf Centrifuge 5415D or equivalent of high-speed centrifuge
- Timer/stopwatch
- Fisher Scientific FS30 sonicating bath or equivalent
- Chemiluminescence detector CLD88 Eco Medics or equivalent
- Water bath able to heat water to 37°C
- Water bath able to heat water to 60°C
- Cooling water bath
- Glass reaction chambers
- Reflux condensers
- Scrubbing bottle

Reagents

- MQ water, ultra-pure, in house
- Sodium nitrite, 99.99% ex Sigma or equivalent
- Sodium nitrate, 99.99% ex Sigma or equivalent
- Sodium hydroxide, ACS reagent, ≥97% pellets ex Sigma or equivalent
- 1M Sodium hydroxide. Pour approximately 500mL of MQ water into the beaker and put the magnetic stirring bar inside. Place the beaker onto the magnetic stirrer and slowly add 40g of sodium hydroxide pellets. Once everything is dissolved, transfer the content of the beaker into the 1L measuring cylinder and make up to volume with MQ water. Solution stable for 6 months when stored in air tight container at room temperature.
- Hydrochloric acid, 37%, AR (ACS) reagent grade ex Sigma or equivalent
- 1M hydrochloric acid. Pour approximately 50ml of MQ water into a 100ml volumetric flask and add 830μL of 37% hydrochloric acid. Make up to volume with MQ water and mix. Solution stable for 6 months when stored in air tight container at room temperature.
- Sodium phosphate dibasic, Na_2HPO_4, AR (ACS) reagent grade ex Sigma or equivalent
- Sodium phosphate monobasic, NaH_2PO_4 AR (ACS) reagent grade ex Sigma or equivalent
- PBS buffer. Weigh out approximately 1.14 g of Sodium phosphate dibasic (Na_2HPO_4) and 0.24 g of Sodium phosphate monobasic (NaH_2PO_4), and 8.7 g of sodium chloride

(NaCl) into the 1L Duran bottle or equivalent. Add approximately 950ml of MQ water and stirring bar and place the bottle on the magnetic stirrer until everything is dissolved. Check pH of the solution and if required adjust it to pH 7.4. Transfer the content into the 1L volumetric flask and make up to volume with MQ water. Solution stable for 4 weeks when stored in air tight container at room temperature.

- N-ethylmaleimide (NEM), ≥98% HPLC ex Sigma or equivalent
- EDTA, 0.5M, pH 8.0, Ultra Pure, Gibco or equivalent
- PBS buffer with NEM/EDTA (homogenisation buffer). Weigh out approximately 1.14g of Sodium phosphate dibasic, 0.24g of Sodium phosphate monobasic, 8.7 g of sodium chloride, 1.25g of NEM and add 5mL of 0.5M EDTA into the 1L Duran bottle or equivalent. Add approximately 950ml of MQ water and stirring bar and place the bottle on the magnetic stirrer until everything is dissolved. Check pH of the solution and if required adjust it to pH 7.4. Transfer the contents into the 1L volumetric flask and make up to volume with MQ water. Solution stable for 4 weeks when stored in air tight container at room temperature.
- Glacial Acetic Acid, Analytical Reagent Grade ex Fisher or equivalent
- Potassium Iodide, ≥99.5% ex Sigma or equivalent
- Iodine, ≥99.8% ex Sigma or equivalent
- Iodine/Iodide solution. Dissolve 1.08g of potassium iodide into 10mL of MQ water. Add 0.38g iodine to the solution and place the container on the rocker until dissolve. After adding iodine, the container should be covered in kitchen foil. Prepare solution fresh daily.
- Potassium ferricyanide (III), <10μm 99% ex Sigma or equivalent
- 0.05M Potassium Ferricyanide in PBS at pH 7.5. Dissolve 1.646g of potassium ferricyanide (III) in PBS buffer and adjust pH to 7.5 with 1M sodium hydroxide. Prepare solution fresh daily.
- Mercury (II) chloride, ≥99.5% ex Sigma or equivalent
- 2% Mercury(II) chloride. Dissolve 0.2g of mercury (II) chloride in MQ water. Solution stable for 12 months if stored at 4°C.
- Sulfanilamide, ≥99% ex Sigma or equivalent
- 5% Sulfanilamide in 1M HCl. Dissolve 0.5g of sulphanilamide in 10mL of 1M HCl. Solution stable for 1 week if stored at 4°C.
- Nitrogen or argon gas, ex BOC or equivalent
- Antifoam SE-15, ex Sigma

Method

Standard

Preparation of stock solution

Dissolve an accurately weighed 0.008 ± 0.0001 g of sodium nitrite in a 2L volumetric flask with water to obtain a solution of known concentration of approximately 58μM.

$$\text{Concentration of nitrite } (\mu M) = \frac{\text{Weight standard (g) x 1000 x 1000}}{\text{69 (g/mol) x 2 (dm}^3\text{)}}$$

69 g/mol is the approximate molecular weight of sodium nitrite.

Note: If the samples are to be analysed for nitrite/nitrate using HPLC method too, prepare the standards as described in SOP 'THE DETERMINATION OF NITRITE AND NITRATE' (Appendix 5).

Standard solution

Solution of approximately 1 μM nitrite is used as a standard solution.
Prepare the standard solution as described in the Table 1.

Table 1. Standard solution preparation

Std code	**Volume taken (mL)**	**Solution used**	**Volume of PBS buffer added (mL)**
10μM	0.17	58μM	0.83
1μM	0.10	10μM	0.90

Sample preparation

All samples should be treated with 100mM NEM solution (1:10 v/v to the sample) at the point of sample collection. If the above had not been done, the sample has to be treated with NEM straight after the sample is thawed.

Blood (serum or plasma) sample

Total nitroso species (RXNO)
Add 10% (v/v) of 5% sulphanilamide in 1M HCl solution to the sample (for example: add 15μL of sulphanilamide to 150μL of sample) and incubate for 15 min in room temperature (RT).
After incubation, inject the sample using a gas-tight Hamilton syringe into the reaction chamber containing Iodine/Iodide solution (see section 5.3.1.1)

Instrument preparation prior to analysis

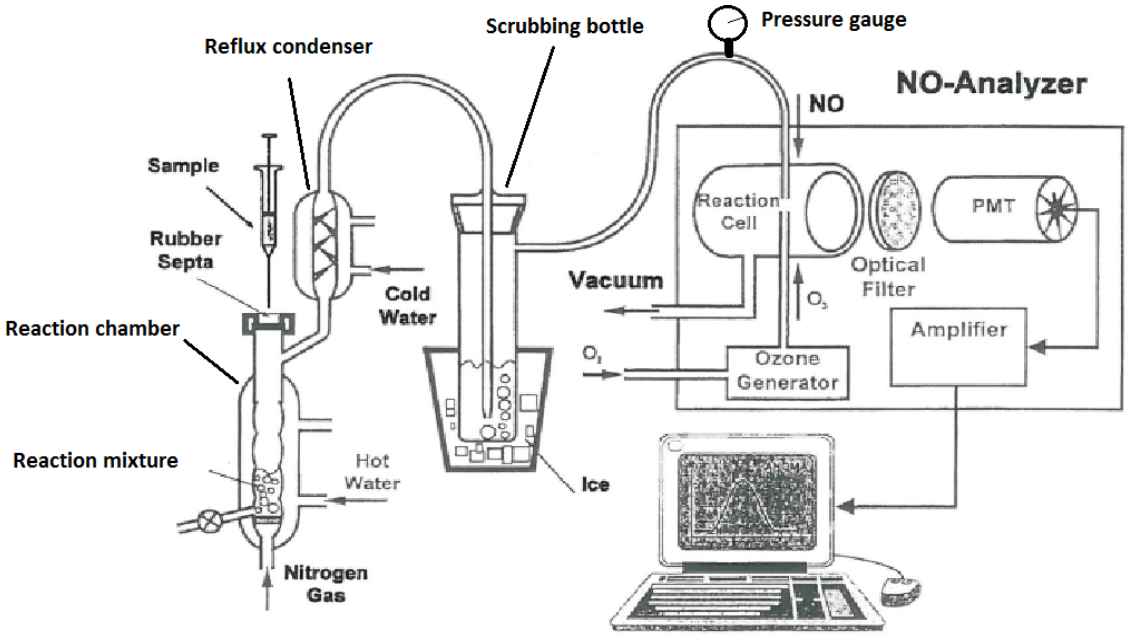

Figure 1. Chemilminescene Detection System Schemat

Reaction chamber set up

Total nitroso species (RXNO)

Add 13.5mL of glacial acetic acid into a rubber septum-sealed, water jacked reaction chamber and add 1mL of Iodine/Iodide solution. The reaction mixture is kept at the constant temperature of 60^{0}C and continuously bubbled with nitrogen. The temperature of the reaction chamber is controlled by the heating water bath.

Reflux condenser

The reaction chambers are connected to efficient reflux condensers that are kept below 0^{0}C. The antifreeze coolant is added to the cooling bath to enable the cooling temperature to be below freezing point.

Scrubbing bottle

Add sufficient volume of 1M sodium hydroxide into the scrubbing bottle, connect it with the reaction chamber through reflux condenser and place it in the plastic beaker filled up with ice. The outlet of the gas from the reaction chamber is passed through the scrubbing bottle in order to trap traces of acetic acid and iodine before transfer into the detector (NO-Analyser).

Pressure gauge

A pressure gauge is placed between the outlet of the scrubbing bottle and the detector inlet for continues pressure monitoring and adjustment of purging gas (nitrogen or argon) flow.
Note: To keep baseline noise at a minimum and achieve consistent results, nitrogen flow must be kept constant throughout the entire measurement cycle.
Note: Do not connect the detector inlet with scrubbing bottle before the cooling bath shows the temperature below 0^{0}C.

Sample gas tube

The sample tube is connected to the inlet fitting on the rear panel of the analyser. The sample tube that is routinely used is sample tube number 1, which gives a flow rate of 100 ml/min. Check if the flow rate is OK before the analysis. Disconnect the sample gas tube from the pressure gauge and press **Test** on the CLD's display and choose **Flow**. The instrument will carry on the test and give the result on the display. If the test result is OK, carry on using the tube, however change to new one if the test came out negative.

Measurement range

The measurement range can be change depending on the levels of analytes in the sample. The range can be selected by pressing the **Range** key when the analyser is in normal measuring mode. The available ranges are as follow:

- 10ppb – D1
- 100ppb – D2
- 1000ppb – D3

Note: For most of the routinely run samples Range D2 is appropriate.

Cleaning reaction chamber and replacing the reaction mixture

The reaction mixture should be replaced after approximately 3 or 8 to 10 injections of lysed red blood cell (RBC) or other sample matrix respectively. To clean the reaction chamber and replace the reaction mixture follow the following steps:

- Drained off the old mixture.
- Rinse the chamber three times with MQ water.
- Add a small amount of soapy water and scrape the inside of the chamber with a brush
- Rinse out all the soapy water with MQ water
- Condition the chamber with 10mL of either acetic acid or 0.05M Potassium Ferricyanide in PBS at pH 7.5 (depending on the analysis).
- Replace the conditioning solution with the appropriate mixtures as described in section 5.3.1. and let it equilibrate and monitor the baseline.
- Once baseline is flat and stable, the standard or sample can be injected.

Note: After cleaning of the chamber and replacement of the reaction mixture new injection of the standard should be performed.

Determination

5% sulphanilamide in 1M HCl solution check

Add 10% (v/v) of 5% sulphanilamide in 1M HCl solution to the 1μM standard (for example: add 5μL of sulphanilamide to 50μL of standarsd) and incubate for 15 min in room temperature (RT).

After incubation, inject the standard using a gas-tight Hamilton syringe into the reaction chamber containing Iodine/Iodide solution (see section 5.3.1.1).

Note: There should be **no** peak present on the chromatogram. If the detector gives response (peak appears) the preparation of 5% sulphanilamide in 1M HCl solution should be repeated.

Running samples

Injection volume

Note: The injection volume and the range set up on the instrument depends on the levels of analytes of interest in the samples. It is impossible to give the exact injection volumes; the suggestions below are just for the guidance:

- The usual injection volume of standard is 50μL for the range D2.
- The usual injection volume for human blood (plasma, serum or red blood cell) is 300μL.
- The usual injection volume for mice blood (plasma, serum or red blood cell) is between 10 and 100μL.
- The usual injection volume for urine samples is 100μL.

Note: After injection of the sample always wipe the syringe needle clean with a tissue and rinse the syringe at least three time with MQ water to avoid contamination.

Analysis time

Note: Shape of the peak depends on the content of the analytes in the sample (see Figures 2-6). It is important to keep the timing consistent for all the samples from the same project to ensure that the comparison of results obtained is possible.

Switch on the timer on the count up setting straight after injection of the sample into the reaction chamber. After the required time has passed, detach the detector inlet from the pressure gauge. This will cause the detector signal to go down to the baseline level and allow the consistent integration of the samples.

Running instrumentation

NO-Analyser (Chemiluminescence detector CLD88 Eco Medics)

- Switch on the CLD pump and leave it equilibration for approximately 20 minutes
- After 20 minutes, switch on the power button on the CLD. The display on the detector will show 'power up'.
- Once the 'power up' is replaced by 'single' and the temperature of cooling bath is below 0^{o}C the detector is ready to be used.
- Connect the detector inlet tube with the scrubbing bottle outlet and monitor the pressure gauge, adjust the gas flow accordingly.

PowerChrom software

- Open Powerchrom.
- Click on 'manual run' and choose the length of time of the analysis (usually kept at 120 min).
- Save the file with the name of the project and date.

- Click ‘inject’ when everything is ready for the first standard to be injected.
- After injection of the standard/samples with little delay the signal of the detector will change. The change of the signal and the shape of the peak depend on the nature of the sample (the levels of the analytes and the sample matrix).
- Once you inject all your samples click ‘stop’ the run and save it.

Integration of peaks

- Open the file
- Click on the Add icon
- Position the mouse at the start of the peak and hold onto left button of the mouse to signify the start of the peak for integration, drag the mouse to the end of the peak and release the left button of the mouse.
  Note: Ensure all the samples are integrated over the same time duration (see section 5.4.1.2)
- Repeat the steps above for all the samples in the same run
- Type integration values (peak areas) into Excel (or equivalent) file to facilitate final calculations

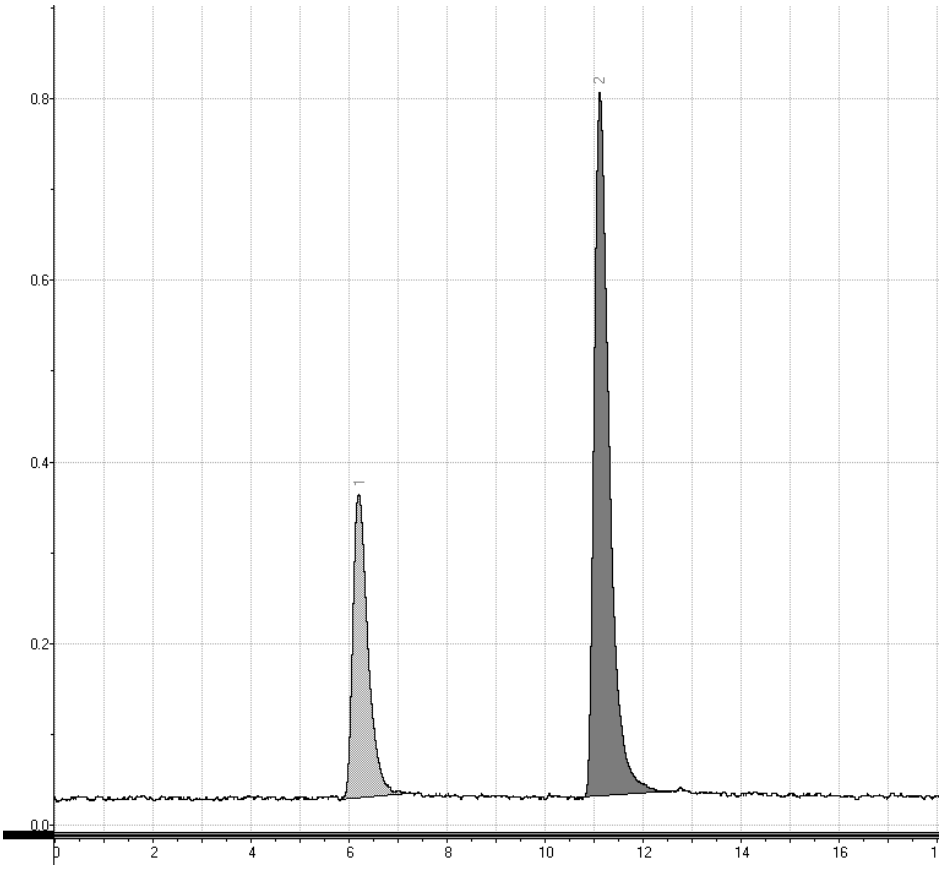

Figure 2. Narrow, sharp and symmetrical peaks (1- 1uM nitrite standard, 2- mice plasma sample)

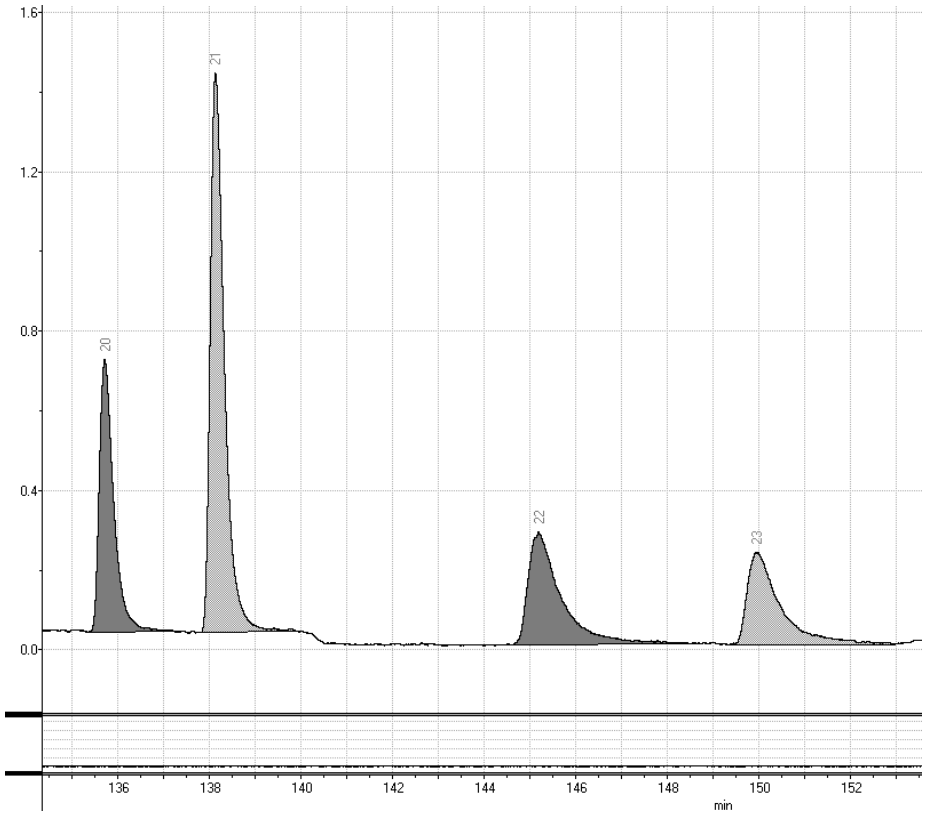

Figure 3. Wide, sharp and asymmetrical peaks (22 and 23- mice plasma sample)

Calculation of final results

Calculation of mean value, standard deviation (SD) and relative standard deviation %RSD of the peak area of standard

Type peak area values for 1uM nitrite standard from the whole run into the Excel spreadsheet. Calculate the peak area mean value, standard deviation (SD) and relative standard deviation %RSD of the peak area.

$$\text{Mean (M)} = \frac{A_1 + A_2 + \ldots + A_N}{N}$$

$A_1, A_2, \ldots A_N$ – Peak areas of the injected standard

N – number of injected standards

$$\text{Standard Deviation (SD)} = \sqrt{\frac{(A_1 - M)^2 + (A_2 - M)^2 + \ldots + (A_N - M)^2}{N - 1}}$$

$$\%\text{RSD} = \frac{\text{SD}}{\text{Mean (M)}} \times 100\%$$

Note: %RSD should be below 10%.

Calculation of response factor (RF)

Calculate the response factor (RF) for the run for standard using the below equation:

$$\text{Response factor (RF)} = \frac{\text{Standard Concentration } [\mu M]}{\text{Mean Peak Area (M)}}$$

5.4.4.3 Serum, plasma and urine samples

Calculate the concentration of analyte in the sample using the equations below:

$$\text{Con. } [\mu M] = \frac{\text{Peak Area in sample x RF x Injection volume of standard}}{\text{Injection volume of sample}} \times DF_1$$

DF_1 – Dilution Factor

$$DF_1 = \frac{\text{Volume of sample with added NEM/sulphanilamide/HgCL}_2}{\text{Volume of sample taken for analysis}}$$

Note: Concentration results should be reported in [nM], therefore multiply obtained concentration in [μM] by 1000.

5.4.4.4 Red Blood Cell (RBC) and tissue homogenate samples

Calculate the concentration of analyte in the sample using the equations below:

$$\text{Con. } [\mu M] = \frac{\text{Peak Area in lysed or homogenate sample x RF x Injection volume of standard}}{\text{Injection volume of lysed or homogenate sample}} \times DF_1 \times DF_2$$

DF_1 and DF_2 – Dilution Factors

$$DF_1 = \frac{\text{Volume of in lysed or homogenate sample with added NEM/ sulphanilamide/HgCL}_2}{\text{Volume of lysed or homogenate sample taken for analysis}}$$

$$DF_2 = \frac{\text{Volume of lysed or homogenate sample with added lysing mixture}}{\text{Volume of RBC sample taken for analysis}}$$

Note: Concentration results should be reported in [nM], therefore multiply obtained concentration in [μM] by 1000.

Appendix 7: The Nitrite and Coronary Artery Study – MRI safety checklist

Clinical MRI Safety Screening Form

Magnetic Resonance Imaging (MRI): Patient Safety Screening Questionnaire

To assess whether it is safe for you to have an MRI scan. Please **complete** the following questionnaire:

Name:		
Weight: **Height:**		
	YES	**NO**
1. Do you have or have you **EVER** had a cardiac pacemaker or implantable cardioverter defibrillator (ICD)?		
2. Have you **EVER** had any heart operations?		
3. Have you **EVER** had any operations on your head, brain, eye(s), ear(s) or spine?		
4. Do you have a hydrocephalus shunt?		
If **YES**, is it a programmable shunt?		
5. Do you have or have you **EVER** had any type of electronic, mechanical or magnetic implant or device (e.g. cochlear implant, neurostimulators, drug infusion pump)?		
6. Have you **EVER** had any operations involving the use of metal implants, plates, pins, clips, stents, gastric bands or breast tissue expanders?		
7. Do you have any aneurysm clip(s) in your head?		
8. Have you **EVER** had metal dust/fragments go into your eye(s)?		
9. Have you **EVER** sustained any metal injuries to any other part of your body (e.g. shrapnel, bullets, pellets)?		
10. Have you had any operations in the last 8 weeks?		
11. Do you have any kidney problems?		
12. Have you had or are you waiting for a liver transplant?		
13. Have you ever had a previous reaction to an MRI contrast agent?		
14. Do you suffer from fits, blackouts or epilepsy?		
15. Do you have **ANY** piercing, hearing aids, coloured contact lenses or dentures? If **YES**, please remove them.		
16. Do you have any medication patches, tattoos or permanent eyeliner?		
Female only:		
17. Are you, or is there any chance you might be, pregnant?		
18. Are you breast-feeding?		
19. Do you have a contraceptive coil (IUD)?		

Important Note: If you answer **YES** to questions 1 to 10 or 17 to 19 you **MUST** provide details in the box below.

Details:

DECLARATION: **I take full responsibility for the information above and confirm that it is correct.**

Signature……..…….. Date……

Thank you

Appendix 8: Root cause analysis for blood transfusion incident and corrective actions

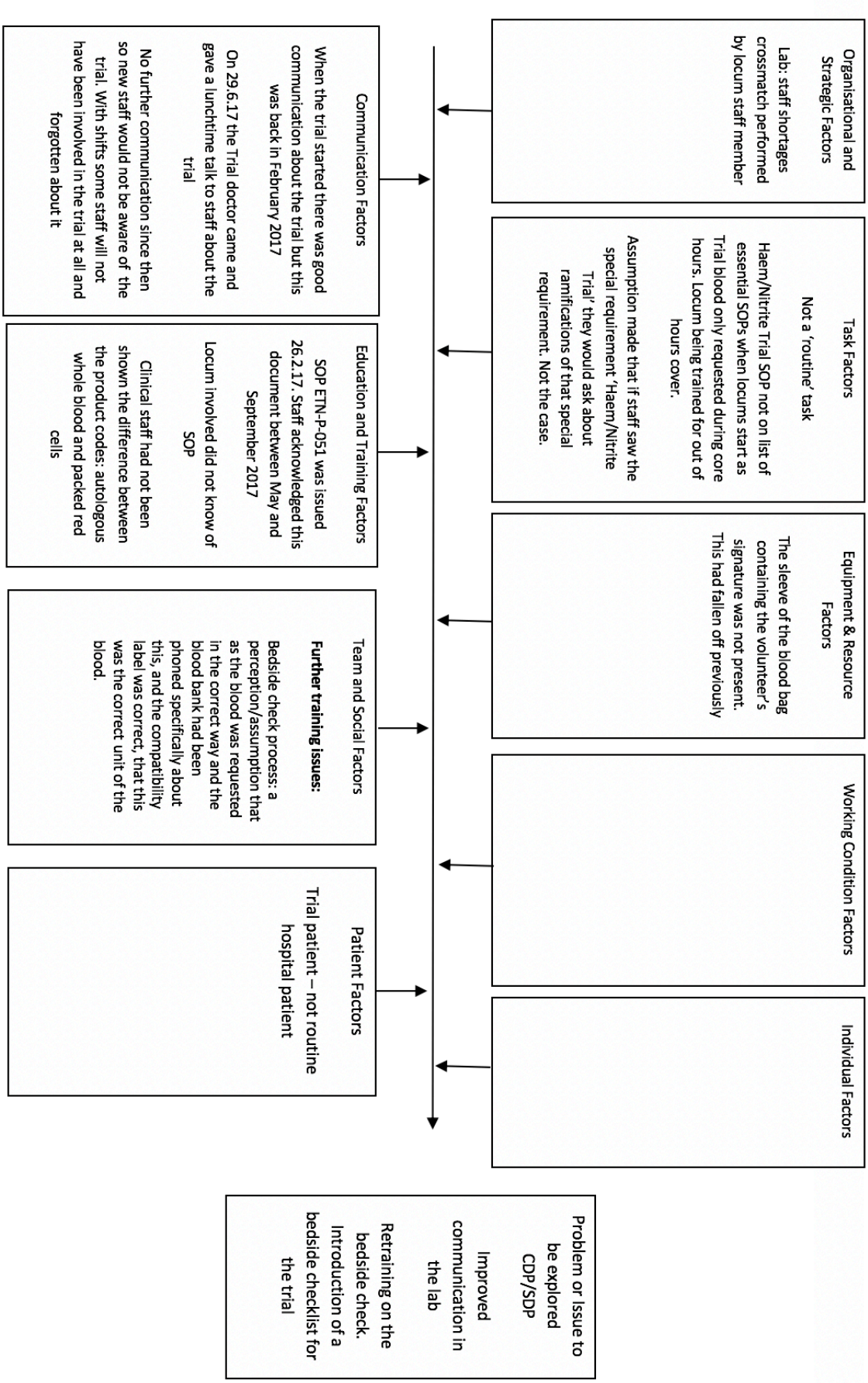

Actions following error BT/17/313 Datix numbers W117884 and W117979: (actions tracked on QPulse) SABRE 2017/010/003/HV1/009

Action:	By whom:	Date completed:
Laboratory **Communication:** Locum involved to read SOP ETN-P-051	E.Lee	3.10.17
Inform all staff of the error through the 'huddle' and send minutes to all staff not present at the 'huddle'	T.McConnell	29.09.17
E-mail all staff a reminder of the trial at the time the autologous units are requested from NHSBT.	D.Asher	5.10.17, 23.10.17 and ongoing
Laboratory: **Education and training:** Check that the distribution list for SOP ETN-P-051 is current and, if not, add new staff to the distribution list	D.Asher	3.10.17
Following meeting with Clinical Trials team 5.10.17: Update SOP ETN-P-051 to match new Requesting Details implemented by Trials Team. This clearly requests Autologous Whole Blood rather than blood for Haem/Nitrite Trial.	D. Asher	6.10.17
All staff to acknowledge revised SOP	D.Asher	31.10.17 Checked 23.10.17 and reminder sent to staff. Checked 3.11.17 and reminder sent to staff
Clinical Area: **Education and Training:** Protocol checked and triangular bedside check clear in protocol (nurse, doctor and volunteer)	D.Asher	9.10.17
Change request for blood for the trial from 'blood for the Haem and Nitrite Study' to 'one unit of autologous whole blood for the Haem and Nitrite Study	N. Gollop	12.10.17
New bedside checklist for trial patients that makes clear the requirement to check for the product code: Autologous Whole Blood, the handwritten volunteer identifiers and volunteer signature on the sleeve of the pack.	V. Vassilou	7.10.17
Clinical trial lead doctor trained on bedside checklist	V. Vassilou	7.10.17
Bedside check observed by Transfusion Practitioner	A.Rudd	9.10.17
NHSBT: Complaint raised with NHSBT re adhesiveness of autologous label on the autologous unit sleeve	D.Asher	26.10.17

Appendix 9: The Nitrite and Coronary Artery Study prescription/drug chart

Royal Brompton & Harefield NHS
NHS Foundation Trust

Time and date required for	

CLINICAL TRIAL PRESCRIPTION

Trial Name	The vascular effect of nitrite on coronary flow under normoxia and hypoxia
Short Title	Nitrite and Coronary Flow Study
Consultant	Dr Sanjay Prasad
Study Doctor	Dr Nicholas Gollop

Subject Name	**Subject Number**
Hospital Number	**Date of Birth**
Allergies	

Please dispense the following medication(s) for the above patient:

Visit Date			
Study Drug	**Direction**		
Sodium Nitrite	Inject the contents of ONE ampoule (17.5mg) by intravenous infusion over 5 minutes as directed per research protocol		
Please supply ONE ampoule of Sodium Nitrite 17.5mg in 5ml Injection in 0.9% Sodium Chloride			
Batch Number		**Expiry Date**	

Prescribed by (Sign and print)		**Date**	

For Pharmacy Use Only

Dispensed by (Sign and print)	**Date**	**Checked by (Sign and print)**	**Date**

Collected by: PRINT _____ SIGN _____ DATE _____

RBH Specific Prescription V1 21/08/18

Appendix 10: Letter from supervisor regarding RXNO samples in The Haem and Nitrite Study

To PhD examiners

I write to confirm that Professor Martin Feelisch contacted me to indicate that he did not have the manpower resource to conduct all of the NO metabolite measurements requested on Nicholas Gollop's samples and that we needed to prioritize. He indicated that he believed the RXNO samples were the lowest priority and therefore he proposed that these be omitted. Given these circumstances I agreed.

Yours Sincerely

Michael Frenneaux